

Thèse présentée en vue de l'obtention du titre de  
Docteur en Neurosciences  
Université Aix-Marseille  
Ecole doctorale 62: Sciences de la Vie et de la Terre  
INMED - INSERM U1249

# SPATIAL RESOLUTION OF THE COGNITIVE MAP

INVESTIGATION ON THE INFLUENCE OF PROXIMAL VISUAL CUES  
ON SPATIAL CODING RESOLUTION IN AREA CA1 OF THE DORSAL  
HIPPOCAMPUS USING VIRTUAL REALITY



Bourboulou Romain

Présentée et soutenue publiquement le 15 Octobre 2019.  
Devant une commission d'examen composée de:

R. Monasson	Directeur de recherche, Paris	Rapporteur
M. Zugaro	Directeur de recherche, Paris	Rapporteur
K. Jeffery	Professeure, Londres	Examinaterice
V. Hok	Maître de conférence, Marseille	Examinateur
J. Koenig	Maître de conférence, Marseille	Invitée
J. Epsztein	Chargé de recherche, Marseille	Co-directeur de thèse
A. Represa	Directeur de recherche, Marseille	Co-directeur de thèse



## ACKNOWLEDGMENTS

---

Ce travail de thèse a été réalisé au sein l’Institut de Neurobiologie de la Méditerranée, INSERM U1249 actuellement dirigé par le Dr. Rosa Cossart et anciennement par le Dr. Alfonso Represa. Je les remercie de m’avoir permis de travailler dans un lieu exceptionnel autant par des aspects scientifiques qu’humains.

J’adresse tout d’abord mes remerciements aux membres du jury ayant accepté de lire et/ou d’examiner cette thèse. Merci à Michaël Zugaro et Rémi Monasson de consacrer leur temps à la relecture et l’examen de ce manuscrit. Je suis également très honoré de la participation de Kate Jeffery et Vincent Hok comme membres du jury de ce travail.

Pour commencer j’aimerais remercier le duo de choc qui s’est consacré à l’encadrement de cette thèse, Jérôme et Julie. Je me souviendrai toujours de notre première rencontre à Luminy, où lors d’un jour de canicule, je me suis perdu dans le campus en suivant les indications de votre mail pour trouver l’INMED. Etait-ce à cause de la chaleur ou une différence de référence frame ? En tout cas, cet égarement a très fortement suggéré que j’aurais quelques petites choses à apprendre en étudiant la cognition spatiale à vos côtés. Des choses, j’en ai apprises lors de cette thèse, aussi bien humainement que scientifiquement. Jérôme, je te suis reconnaissant de m’avoir accueilli dans ton équipe, pour ta confiance et ta rigueur. Mais aussi pour m’avoir poussé dans les congrès, les winter schools et présentations en tout genre. Merci à Julie, pour m’avoir laissé ma liberté mais aussi avoir toujours été présente quand le besoin se présentait. J’ai énormément appris de nos discussions psychologico-philosophiques sur des notions de codage, représentation ou cellules aux corrélats comportementaux exotiques. Pour finir, merci à tous les deux pour ces dernières semaines très intenses d’écriture presque à six mains pour rendre ce manuscrit plus juste et digeste.

Après ce duo, j’aimerais remercier l’équipe qui m’a entouré, aidé, soutenu, fait rire et qui a souffert quotidiennement pendant 4 ans (pour certains) du meilleur comme du pire de mes calembours. Vous allez énormément me manquer. Je voudrais dire un grand merci à : FX, la personne qui m’a ignoré dès le premier bonjour mais qui s’est ensuite bien rattrapé. Merci pour ta présence, tes idées, ton soutien et pour ces longues discussions sur nos intérêts communs. Caroline, une force tranquille, droite (mais pas très haute), attentive, toujours présente ne serait-ce que par un de tes hochements de tête après 1 blag pa taupe... Le plus gros kéké de Marseille, Geogeo, merci pour m’avoir appris les maths et à trouver des noms de variables créatifs, mais surtout pour ces discussions informelles sur le balcon de l’IN-

MED. Mamen, pour nos partages de galères murines, informatiques, électrophysio(pas)logiques. Tes montages, ta subtilité et surtout ton pouf vont grandement me manquer. Laminou, car tu te souviens de notre première rencontre. Pour ton amour partagé des mots dérivés et parce que tu es un mec sympa. A Peter, pour nos agréables échanges et tes conseils.

Je souhaiterais également remercier des personnes plus récemment arrivées dans l'équipe : Rojin, Lexi, Alla pour les échanges bien trop courts que nous avons eus. Merci aussi aux étudiants qui ont rendu cette thèse plus riche : Aurore, Emna, Elissa, Livia, Tom, Maxime, Diane, Nikita et Myriam.

Parmi les personnes qui ont le plus animé ce parcours, il y a la fine équipe du midi. Nos débats de haut vol, notre curiosité insatiable sur des mystères de la vie, notre amour des chansons de qualité et des clairs de lune vont me manquer au plus haut point. Robinou, merci pour ta collaboration blaguistique, videoludique, informatique, geekique et de m'avoir ouvert pour la première fois les portes de l'INMED. Manue, merci pour tes fous rires déclenchés par le plus mauvais des jeux de mots, ta gentillesse. Cacá, merci pour avoir supporté une partie de la rédaction de cette thèse (mais bien avant aussi), de m'avoir affiché lors de la tienne. Fanny, merci de soutenir mon humour mais surtout de corriger mon arabe balbutiant. Erwanito, merci pour tes mails amoureux et d'être venu vérifier régulièrement si j'étais toujours en vie dans ma grotte de thèse. Jordane, pour la meilleure parodie de Carglass du monde. Je remercie également des acteurs plus ponctuels de ces repas, Elise, Popo, Thomas, Nico, Arnaud.

Pendant ces années de thèse, j'ai pu croiser le chemin de personnes formidables : Susanne, Claire, Macu, Laeti, Laura, Yannick, Davide, Manalou, Anissa, Tonia, Olive, Titi, Mostafa, Carola, Laurène, Robin, Julien, Laura, Shu, Lucie, Alex, Morgane, Thomas, Popo, Michel, Marco. Vous avez fait en sorte que ce séjour à l'INMED soit des plus mémorables par des discussions dans le patio, des conseils d'électro-nique, un éclat de rire fulgurant, ou simplement par votre présence. Merci à David, Agnès, Pierre-Pascal, pour vos conseils ponctuels scientifiques, de vie et de vie scientifique. Je remercie également le personnel administratif de l'INMED qui ont apporté un soutien de fond à cette thèse, notamment : Bahija (pour ton sourire et ton efficacité ), Christine, Robert, Gwendoline, Marie.

Mon deuxième institut préféré à Luminy, c'est sans aucun doute le CIML. Cette fois ci pas grâce à la science qu'il s'y fait mais plutôt aux gens qui s'y trouvent. Merci à Marcello, Stefi, Elias, Magda, Marcos, Cynthia, Gabi, Tom, Cricri pour les moments hors du labo, passés à vos côtés. Merci tout particulièrement à Raphael et Lisienna, que le destin a aussi dirigé à Marseille. Si nos chemins se sont suivis jusqu'ici c'est sans aucun doute pour qu'ils se recroisent très bientôt.

En dehors du labo, il y a aussi les colocs : Amandine, Quentin, Laeti, Le, Sethu. Je vous remercie pour tous ces moments de partage au quotidien. Je remercie aussi des « colocs ponctuels » Iole et Romain de Iole pour vos conseils jardinage, bricolage et salsa.

Cette thèse n'aurait pas été possible sans le soutien inconditionnel de mes parents, Marine, Yaya, mes grands-parents et Pascale. Merci de m'avoir écouté, supporté, aidé, aimé. Merci tout simplement pour votre présence malgré mes bien trop fréquentes absences. Je vous aime.

Algunas cosas toman tiempo, pero lo más importante es que otras se fortalecen. Tuve suerte de que un día decidieras viajar por el mundo para venir aquí. Ven conmigo y hazme sentir mejor cada día. Ahora soy muy afortunado de poder viajar por el mundo, pero esta vez a tu lado.

Pour finir, j'aimerais remercier, mes petites souris...



## ABSTRACT

---

To flexibly and efficiently navigate in their natural habitat, mammals can rely on an internal representation of space, also called a cognitive map. The hippocampus is thought to be important for the elaboration of this map. It contains a peculiar type of cells: the place cells, which are active in specific parts of the environment (called their place fields) and virtually silent elsewhere. Place cell spatial coding can be more or less precise depending on the scale of the environment, the availability of sensory cues or the location of their cell body along the septo-temporal axis of the hippocampus. However, whether and how place cells' spatial coding resolution can adapt to local features of the same environment remains unclear. In this thesis work, we explored this possibility by recording the activity of hippocampal neurons in the dorsal hippocampal area CA1 of mice navigating a virtual linear track. We used several types of visual information, unevenly distributed in the environment, such as 3D visual objects and 2D patterns on the walls or their combination to investigate their impact on spatial coding resolution. We observed that virtual objects improved spatial coding resolution in their vicinity. Place fields were more numerous, smaller, with better spatial information and stability. This effect was highly dynamic upon objects manipulations. On the other hand, patterns on the wall led to an enhancement of spatial coding resolution, but to a lesser extent. These results were confirmed at the population level using a Bayesian decoder. Objects also strengthened temporal coding resolution through improved theta phase precession. We propose that the hippocampal place cells representation can have a heterogenous resolution, which could be used to improve coding or inference notably in large-scale environments.

*Key words: Hippocampus, spatial cognition, place cells, virtual reality, object, resolution, CA1*



## RÉSUMÉ

---

Pour naviguer de manière flexible et efficace dans leur habitat naturel, les mammifères peuvent s'appuyer sur une représentation interne du monde qui les entoure. L'hippocampe est considéré comme l'un des acteurs prenant part à l'élaboration de cette représentation notamment parce qu'il contient un type particulier de cellules : les cellules de lieu. Lorsque l'animal se déplace, chacune de ces cellules s'active dans une partie spécifique de l'environnement qui lui est propre, son champ de lieu, et reste silencieuse ailleurs. Par conséquent, ces cellules sont supposées coder pour un endroit spécifique d'un environnement. Néanmoins, la précision de leur patron de décharge peut être plus ou moins importante en fonction de la taille de l'environnement, de la disponibilité d'indices sensoriels ou de la localisation de leur corps cellulaire le long de l'axe septo-temporal de l'hippocampe. Une question importante est de savoir si et comment la résolution spatiale de l'hippocampe dorsal peut s'adapter aux caractéristiques locales d'un même environnement. Dans ce travail de thèse, nous avons exploré cette question en enregistrant l'activité de neurones de la région CA1 de l'hippocampe chez des souris effectuant des allers-retours dans un couloir virtuel. L'utilisation de la réalité virtuelle nous a permis de finement manipuler les indices visuels disponibles pour l'animal. Plusieurs sortes d'indices visuels ont été utilisées, distribuées de façon non homogène dans l'environnement, comme des objets visuels 3D, de motifs sur les murs ou leur combinaison pour étudier leur impact sur la résolution du codage de l'information spatiale. Nous avons observé que les objets virtuels améliorent la résolution du codage spatial dans leur voisinage. Les champs de lieu étaient plus nombreux, plus petits, avec une meilleure information spatiale et une meilleure stabilité. Ces effets étaient également observables instantanément suite à une manipulation des indices visuels. D'autre part, les motifs sur les parois ont également permis d'améliorer la résolution du codage spatial, mais dans une moindre mesure. Ces résultats ont été confirmés au niveau de la population à l'aide d'un décodeur bayésien. Les objets ont également renforcé la résolution du codage temporel en améliorant la précession de phase. Nous proposons que la carte cognitive portée par les cellules de lieu de l'hippocampe pourrait avoir une résolution hétérogène pouvant être utilisée pour améliorer le codage et les inférences, notamment lors de la navigation dans de grands environnements.

*Mots clés : Hippocampe, cognition spatiale, cellules de lieu, réalité virtuelle, objet, résolution, CA1*



## CONTENTS

---

ACKNOWLEDGMENTS	ii
ABSTRACT	vi
RÉSUMÉ	viii
List of figures	xiv
List of acronyms	xv
<b>I INTRODUCTION</b>	
1 THEORY OF SPATIAL COGNITION	1
1.1 Taxon and praxic navigation	2
1.1.1 Taxis	2
1.1.2 Praxis	3
1.1.3 Taxon system	4
1.2 Path Integration	5
1.3 Map based navigation	7
2 NEUROANATOMY OF THE HIPPOCAMPAL FORMATION	11
2.1 Anatomical Definition of the Hippocampal Formation	11
2.2 Intrinsic connectivity of the hippocampus	13
2.2.1 Dentate Gyrus	13
2.2.2 Hippocampus proper	15
2.2.3 Subiculum	19
2.3 Two parallel streams converging to the hippocampus	19
2.3.1 Entorhinal Cortex	20
2.3.2 Afferences and efferences of Entorhinal Cortex	20
3 NEUROPHYSIOLOGICAL CORRELATES OF SPACE	25
3.1 Rate coding of space	25
3.1.1 Neuronal doctrine of space coding	25
3.1.2 Place cells	26
3.1.3 Head direction cells	28
3.1.4 Grid cells	30
3.2 Phase coding of space	32
4 RESOLUTION OF SPACE CODING	35
4.1 Accuracy of the coding at the single cell level	36
4.1.1 Classical metrics of tuning curve quality	36
4.1.2 Information theory for place cells coding	37
4.1.3 Short term variability of place cells activity	38
4.1.4 Place cells activation and spatial resolution	40
4.2 How do sensory cues modify the precision of space coding in the Hippocampus	42
4.2.1 Self-generated cues	42
4.2.2 Distal cues	43
4.2.3 Proximal cues	45
4.2.4 Borders	51

4.2.5	Boundary vector cells model	51
4.2.6	Scaling the hippocampal code to a bigger environment	53
4.3	Non sensory modulation of spatial resolution	55
4.3.1	Representation of goal	55
4.3.2	Modulation of resolution by attention	57
4.4	Anatomical differences in spatial resolution	60
4.4.1	Transverse axis	60
4.4.2	Radial axis	62
4.4.3	Longitudinal axis	63
4.5	Space coding at the population level	64
4.5.1	Decoding population activity	65
4.5.2	Limitation of population decoding	67
5	OBJECTS PERCEPTION FOR NAVIGATION	69
5.1	What is an object and do rodents perceive them?	69
5.2	Are objects used for navigation ?	71
5.3	From objects to landmarks	73
5.3.1	Landmark stability	74
5.3.2	Landmark position	75
5.3.3	Dimensionality	77
5.4	Neuronal correlates of objects for navigation	79
5.4.1	Object coding in perirhinal cortex	79
5.4.2	Object coding in the entorhinal cortex	80
5.4.3	Object coding in the hippocampus	82
<b>II EXPERIMENTAL CONTRIBUTION</b>		
	Preamble	87
	Dynamic control of hippocampal spatial coding resolution by local visual cues	89
<b>III DISCUSSION</b>		
6	DISCUSSION	133
6.1	Comparison with previous studies using physical objects	133
6.2	Could the local change in resolution be due to object-responsive cells?	134
6.3	Comparison with previous reports of heterogenous coding in place cells	135
6.4	Toward a better understanding of place cells coding in virtual reality	136
6.5	Influence of visual information on phase precession	138
6.6	Are 3D virtual objects really that important?	140
6.7	Is more really better and broader worse?	141
6.8	Directionality of place cells in virtual reality	143
6.9	Effect of attention on place cell coding	144
6.10	Put landmarks back in the cognitive map	145
6.11	Conclusion	146

**IV APPENDIX**

Intracellular determinants of CA1 pyramidal cells activation or silencing during locomotion    **151**

**V BIBLIOGRAPHY**

## LIST OF FIGURES

---

Figure 1.1	Taxic and praxic navigation system	2
Figure 1.2	Path integration	6
Figure 1.3	Different model of cognitive maps	8
Figure 2.1	Rodent Hippocampal Formation	12
Figure 2.2	Different axis of the Hippocampus	14
Figure 2.3	Layers of the hippocampus	15
Figure 2.4	Intrinsic connectivity of neurons in the rodent hippocampus	17
Figure 2.5	Entorhinal Cortex	21
Figure 2.6	Main connections between rodent Entorhinal Cortex and the hippocampal formation	23
Figure 3.1	Illustration of an hippocampal place cell	27
Figure 3.2	Head Direction cell	29
Figure 3.3	Grid cells	31
Figure 3.4	Phase coding in place cells	33
Figure 4.1	Properties of place cells tuning curve	36
Figure 4.2	Effect of internal cues on hippocampal spatial scale	42
Figure 4.3	Effect of local sensory cues on hippocampal spatial scale	47
Figure 4.4	Boundary Vector Cell (BVC) model of place field formation	52
Figure 5.1	How do rodents use an array of landmarks to locate a goal?	72
Figure 5.2	Influence of object position	76
Figure 5.3	Do rodents use 2D object to navigate	77
Figure 5.4	Neuronal correlates of object in the hippocampal formation	82

## ACRONYMS

---

RW	Real World
VR	Virtual Reality
EC	Entorhinal Cortex
DG	Dentate Gyrus
MEC	Medial Entorhinal Cortex
LEC	Lateral Entorhinal Cortex
PER	Perirhinal Cortex
POR	Postrhinal Cortex
BVC	Boundary Vector Cell
SI	Spatial Information
LFP	Local Field Potential



Part I  
INTRODUCTION



## THEORY OF SPATIAL COGNITION

---

No animal lives isolated. Even the most solitary creature will, at some point in its life, interact with another organism in order to promote its survival. Animals have to hunt preys, hide from predators or find mates for their reproduction. In addition to these interactions with living things, the survival of an animal also depends on the maintenance of suitable relation with its non living environment. For example, swallows fly thousands of kilometers south during winter to seek a more bearable climate. Animals base their actions on acquired knowledge of their surrounding and act outside of the reach imposed by their body, they are mobile [Dethier and Stellar 1961]. These movements are necessary to find nutriments, congeners or avoid danger. These abilities can be optimized by acquiring knowledge on the environment through active exploration. Indeed, animals developed various strategies in order to find their way to a goal with diverse availability of sensory information and different levels of knowledge about the environment. According to Gallistel [1990], "*Navigation is the process of determining and maintaining a course or trajectory from one place to another*" [Gallistel 1990, p. 35]. As opposed to exploration, which consists in moving from a starting point to an unknown location, navigation implies the existence of a goal directing the movement. The implementation of navigation can be more or less complex and a large body of orientation behaviors can support the process of getting from one place to another. First, some "simple" strategies involve moving towards a perceived goal using direct external sensory information. Other strategies can often be summarized by stereotyped series of actions initiated by internal or external stimuli. Also, numerous organisms have developed more refined navigational methods allowing flexible and efficient navigation. They are able to bypass this sequential stimulus-response strategy by the integration of multiple stimuli to construct an internal representation of the external world [Tolman 1948; O'Keefe and Nadel 1978; Benhamou 2010]. *Spatial cognition* can thus be defined as the acquisition, the organization, the use (potentially through various strategies) and the update of spatial knowledge about an organism's environment in order to flexibly navigate in it.

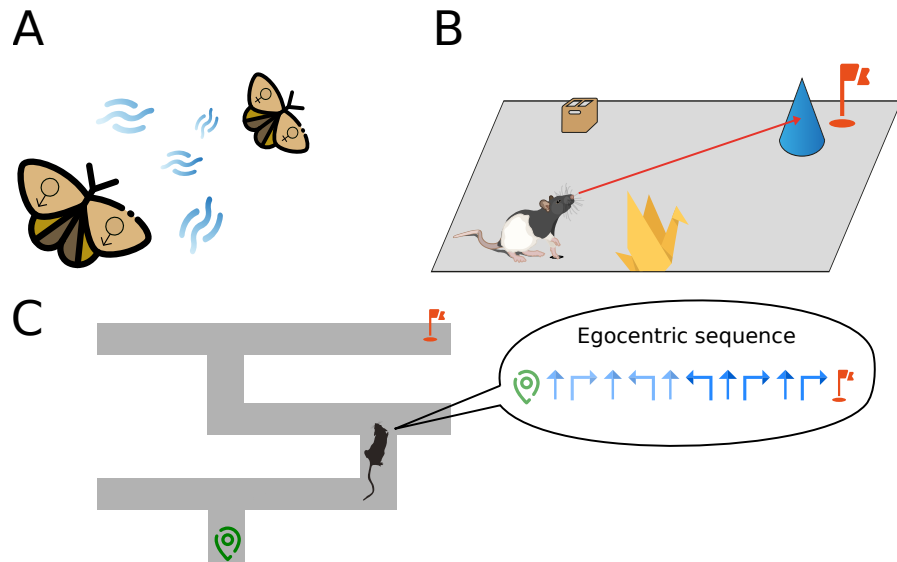


**Figure 1.1:** Illustration of taxic and praxic navigation system. A: a male moth follows the odorant plume of a female congener. B: a rat searching for a particular reward can use an object as a "beacon" to find it. C: a mouse in a multiple T-maze has to perform the adequate egocentric sequence in order to find its goal.

## 1.1 TAXON AND PRAXIC NAVIGATION

### 1.1.1 *Taxis*

Numerous mobile organisms have developed innate behavioral responses: *taxis*, that allow them to move toward or away from a stimulus such as light or chemical gradient [Jacobs 2012]. These *taxis*, consist in following the augmentation or reduction of a stimulus intensity and can be performed by low-level sensory processing<sup>1</sup>. In this form of taxic navigation the stimulus is used as a "beacon" towards which the animal moves. Classical examples of such kind of behavior can be a bacteria reaching a place with high concentration of nutrients or a male moth following pheromone plume of a female congener or even you, chasing the origin of a pleasing "croissant" perfume while going to work in the morning (Figure 1.1 -A). This kind of strategy has been shown to be used by rodents in order to locate single odorant sources in an arena [Wallace et al. 2002; Khan et al. 2012; Gire et al. 2016; Liu et al. 2019].

Beaconing is essentially a stimulus-response strategy and need the constant perception of the beacon or goal landmark [O'Keefe and Nadel 1978](Figure 1.1 -B). It is computationally very simple to learn and to use, because it only requires the association of a single landmark with a goal. However it comes at a cost of a lack of flexibility. If the beacon disappears or moves, the animal will unfortunately be lost and unable to reach its goal.

<sup>1</sup> This process is even performed without a nervous system in some cells of our body or some unicellular organisms.

### 1.1.2 Praxis

Praxic navigation, sometimes called *kinetic strategies*<sup>2</sup>, consists in reaching a goal using a sequence of stereotyped movements. These strategies rely solely on information about the position and displacement of the limbs, independently from a starting position<sup>3</sup> (Figure 1.1 -C). This method is nevertheless useful only if the starting point is kept at a constant location. Imagine yourself for a moment in your room in total darkness. Your bedside lamp no longer works, but you want to turn on the ceiling light. You could then get up from your bed, step forward, turn 90 degrees and then take two more steps to reach the wall switch. The success of this sequence of actions requires the precise execution of each of the movements, in a specific order, and can therefore take a long time to be learned. But above all, you will have to start at the right place on the bed to hope to reach the switch rather than a wall... Evidence of the use of kinetic strategies have been provided in rats. In the Morris water maze, if they are introduced in the pool under full darkness, always at the same location and orientation, they can learn a stereotyped trajectory to reach the platform location [Eichenbaum et al. 1990; Packard and McGaugh 1996; Save and Moghaddam 1996].

Early studies on rodent navigation suggested that rats could perform praxic navigation in complex mazes [Watson 1907; Carr and Watson 1908; Carr 1917; Honzik 1936]. In these experiments, rats submitted to different levels of sensory deprivation, were trained to navigate in complex mazes characterized by multiple paths and choice points.

Watson [1907] demonstrated that rats could solve a complex maze, named "Hampton-Court maze" [Small 1901], after several types of sensory deprivation (vision, smell, vibrissae removal). Even a rat simultaneously blind, deaf, anosmic<sup>4</sup> and lacking vibrissae was able to solve the maze but needed a longer training period<sup>5</sup>. In a later study, Honzik [1936] confirmed that rats could find the goal in a maze with 14-junctions even after being blinded or made anosmic.

---

<sup>2</sup> *kinesthesia* is the sense that detects body position, orientation or movements of muscles, tendons and joints.

<sup>3</sup> kinaesthetic strategy is sometimes used in the literature to describe a navigational process solely relying on internal cues like path integration [see: Save and Moghaddam 1996; Redish 1997]. It will not be the case in the present section.

<sup>4</sup> *anosmia* is the absence or the loss of smell.

<sup>5</sup> "Believing that the proof of the establishment of the maze association in an animal deprived of the possibility of receiving most of the important extra-organic sensory stimulations would add the needed confirmation to our previous work, we removed the eyes, the olfactory bulbs, and the vibrissa simultaneously from a young male rat on September 6, 1906. There is no need to describe the operations. Naturally recovery was slow in this animal. A certain lack of tonicity was observable. [...] The animal finally completely recovered and is still alive (March 1, 1907) and in absolutely perfect condition. [...] He began at once to learn the maze and finally became the usual automaton. The elimination of errors went on more slowly, however, than in the case of the normal animals and consequently the number of trials is greater in his case than in the former." [Watson 1907, p.98]

Even if the removal of one to most of the external sensory cues did not affect rats ability to find the goal location in a complex maze, it does not rule out the possibility that they compensated the loss of some external sensory cues, using spared ones (e.g.: tactile cues for the rat blind, deaf, anosmic and lacking vibrissae of Watson [1907]). Thus, in a follow up study Carr and Watson [1908] addressed this problem by interfering with the kinaesthetic sequence itself either by changing the starting position or by shortening/lengthening some corridors once "*the reactions to the maze became automatic*". If placed at a new starting point, rats were first confused but were then able to reinstate their sequence of movements. For the second type of manipulation, the animal's behavior was deeply disrupted, to the detriment of the rat itself: "*the rats frequently ran full speed into the end of the alley.*" [Carr and Watson 1908]. Similarly, Dorcus and Gray [1932] reported that even with physical alteration of the limbs or muscles of the rats, in order to perturb their motor sequence, rats managed to perform with similar degree of accuracy than before their lesion. Thus kinaesthetic information were not the sole information used to guide the behavior of the animals. Altogether, these experiments show that kinaesthetic information can be used to solve navigation tasks. Nevertheless, they also revealed that some adaptations following experimental manipulations could not entirely be explained by the use of such information. On the other hand, the combination and/or succession of the aforementioned taxis and praxis could also allow the animals to catch up their behavioral sequence after a perturbation. This strategy, called a *route*, will be described in the next section. Also, complex mazes navigation might imply the use of an internal map of the environment, an hypothesis that was developed years after the aforementioned experimental studies (see § 1.3).

### 1.1.3 Taxon system

Remember the last time a tourist approached you to ask you for the nearest location of a good restaurant. After a short period of reflection, your answer certainly consisted in indicating a sequence of instructions to be carried out in order to eat a delicious dinner: "continue to the end of street A, then take left and walk 100 meters. Once you reach the panel C the restaurant will be on your right". In this strategy, the instructions are a list of stimulus-response-stimulus commands (e.g.: street A (stimulus), take left and continue walking (response) until the panel C (stimulus)) that can also be interpreted as a sequence of taxis (guidance to a beacon) or praxis (motor sequence). The use of this type of sequences of instructions is called a route-based navigation, also referred to *taxon system* in O'Keefe and Nadel [1978]. These sequences are coded in egocentric space (in reference to the animal's body) and are triggered by a particular stimulus. In this system, each cue will

determine the next phase of the locomotion sequence. It differs from a simple taxic strategy by its serial nature, and from a praxic strategy by the independence of a given step to the previous ones<sup>6</sup>. Sequences of actions can be constrained by a physical path or route up to the next decision point where the movements should be adjusted. For example, foraging ants can follow the pheromone trace left by previous exploration by their congeners. Nevertheless, different olfactory paths can cross, overlap or terminate and the ant will have to define its sequence of actions according to another set of cues (e.g. visual cues) [Harris et al. 2005; Collett et al. 2006]. Pigeons have also been shown to follow physical routes or railways and use landmarks as turning points during homing [Lipp et al. 2004]. The use of this strategy has also been described in mammals like rodents or bats flying along forest paths [Jones and Holderied 2007; Geva-Sagiv et al. 2015]. In rodents, for example, such kind of navigation strategy can be used in a maze with multiple choice points [Carr and Watson 1908; Honzik 1936].

A particular case in line with the taxon system can be called: "piloting" [O'Keefe and Nadel 1978]. This strategy requires successive tracking or conservation of a particular bearing in relation to one or several landmarks on the way to the goal. This strategy allows the location of the goal if it is not directly accessible, thanks to one or several intermediary beacons. The successive beacons can be tracked using different sensory modalities.

## 1.2 PATH INTEGRATION

Another strategy, which is phylogenetically widespread and yet based on a relatively more complex mechanism, is the path integration. This process has been coined by Darwin [1873] in a letter to *Nature* where he described the "dead reckoning" of a native siberian tribe passing through hummocky ice. Despite ceaseless changes of direction they managed to reach a particular place "*with no guide in the heavens or on the frozen sea*". Hence, Darwin proposed that they could navigate relying on vision but also with proprioceptive information [Darwin 1873]. At the end of this letter Darwin questioned the fact that this ability could be exclusive to men, but did not discuss an analogous process used by animals<sup>7</sup>. In his response to Darwin, Murphy [1873] explained that animals were indeed capable of similar performance. In this letter, he also proposed that path integration could be computed from the

---

<sup>6</sup> A praxis dependent of the previous one can be considered as a motor sequence in itself, a bigger praxis composed of the current and the previous ones. Conversely, a praxis "divided" in two motor sequences will be a route.

<sup>7</sup> "*This is effected chiefly, no doubt, by eyesight, but partly, perhaps, by the sense of muscular movement, in the same manner as a man with his eyes blinded can proceed (and some men much better than others) for a short distance in a nearly straight line, or turn at right angles, or back again.*" [Murphy 1873]

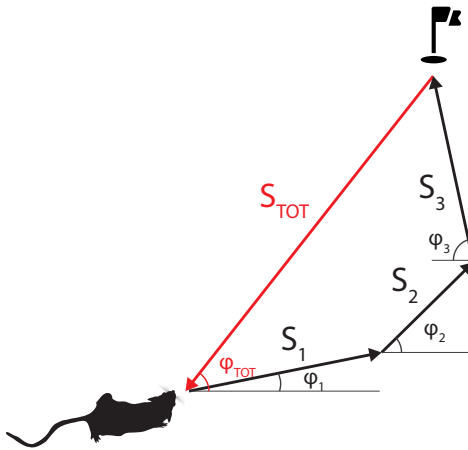


**Figure 1.2:** Depiction of an example of path integration. The animal can add the successive vectors of its inbound path to the goal.  $S_{1-3}$  refer to the length (time elapsed multiplied by speed) of each vector associated with a movement and  $\varphi_{1-3}$  to their corresponding head direction. Once the goal is reached, the animal can compute a "homing vector" to return at its starting position  $S_{TOT}$ .

addition of vectors representing the direction and the magnitude of each movement<sup>8</sup>. This vector summation allows the computation of another vector giving the direction and distance to the starting point of the journey, a homing vector<sup>9</sup> (Figure 1.2). Thus path integration is the ability to track one's position in relation to a reference point, such as a nest, solely relying on internal signal derived from locomotion [Barlow 1964; Gallistel 1990; Etienne and Jeffery 2004; Savelli and Knierim 2019]. One of the most illustrated case of path integration is "dead reckoning": the ability to return directly to a starting or "homing point" from any location in an environment, even in the dark or after a long circuitous route (see § 1.3 for a more general case of path integrator). Since then, this ability has been observed in many species ranging from gerbils, hamsters, rats, mice of even birds and insects [Tolman 1948; Mittelstaedt and Mittelstaedt 1980; Mittelstaedt and Mittelstaedt 1982; Etienne 1987; Gil et al. 2018]. The original observation of this ability by Darwin [1873] and Murphy [1873], did not scrupulously demonstrated the creation and use of a "homing vector". Let's take the example of a small mammal leaving its nest at night to collect some food to a feeding place. Once its goal is reached, the animal could use multiple strategies in order to return to its granary. It could certainly perform path integration, but could to an equal extent use external cues (escaping the experimenter scope) or reverse the sequence of

<sup>8</sup> "If a ball is freely suspended from the roof of a railway carriage, it will receive a shock sufficient to move it, when the carriage is set in motion: and the magnitude and direction of the shock thus given to the ball will depend on the magnitude and direction of the force with which the carriage begins to move." [Murphy 1873].

<sup>9</sup> "Further, it is possible to conceive the apparatus as so integrating its results as to enable the distance and direction of the point where the journey began to the point it has reached" [Murphy 1873].

actions that it did on its inbound route. Thus, the question of the existence of a "true" dead reckoning was still open and the subject of debates during many years.

It was only recently that, Mittelstaedt and Mittelstaedt [1980] and Etienne [1987], demonstrated that (respectively) gerbils or hamsters could deduce their homing vector from the integration of internal cues such as vestibular signal and motor efferent copy. Mittelstaedt and Mittelstaedt [1980] observed that a female gerbil in search of a displaced pup could make a direct path to its nest once the pup was found. The authors ruled out the use of external cues by performing the task in the dark. More importantly, they demonstrated the use of a homing vector by showing that a displacement of the animal, below vestibular detection threshold, during the search phase led to an offset in the return path by a similar amount (thus ruling out the use of a sequence of stereotyped actions or the use of external non-visual cues). In a similar manner, Etienne [1987] showed that golden hamsters used path integration to return to their nest after a rotation of the arena during the inbound route.

By repeatedly adding small movement vectors to an integrated homing vector, path integration will become increasingly inaccurate because of cumulative errors. Nevertheless, animals can compensate this accumulation bias by resetting this path integrator using external cues [Hardcastle et al. 2015; Keinath et al. 2018; Savelli and Knierim 2019].

### 1.3 MAP BASED NAVIGATION

Despite their simplicity and their effectiveness in many scenarios, taxon behaviors described previously can not explain the use of a covert variable in the environment. Hunter [1913] was one of the first scholars who coined the notion of mental representation ("symbolic process") of an external stimulus, when it was not directly accessible to the animal senses but necessary for the completion of a task<sup>10</sup>. This idea of an internal representation of external stimuli in animal was then significantly developed by Tolman [1948]. In this seminal paper, Tolman postulated that a map like representation of the external world could be constructed in rats' brains:

*"We believe that in the course of learning something like a field map of the environment gets established in the rat's brain. [...] The stimuli, which are allowed in, are not connected by just*

<sup>10</sup> "Over against this genetically simple learning, may be placed a more complex form of behavior which involves a representative function. This ideational or representative process arises out of a genetically prior sensorimotor level of behavior. [...] According to the law of parsimony, the only conclusive evidence in favor of the existence of such a representative element is the case where successful adaptations occur when that part of the sensorimotor process assumed to be represented is known to be absent at the moment of response." [Hunter 1913, p.73]

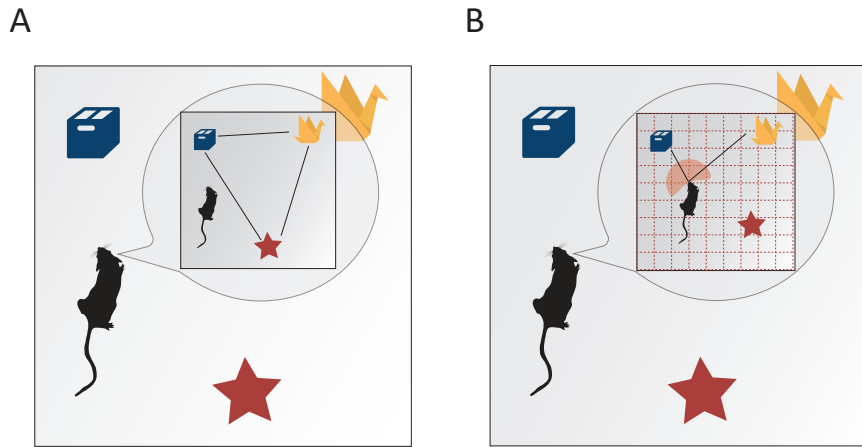


**Figure 1.3:** **A:** Illustration of a map based navigation. A navigating animal can rely on its knowledge about the allocentric relations between external landmarks to find its way in an environment. **(B):** The animal can also use a map consisting in local views of external landmarks in a given position that are then linked to a global coordinate system, a 'path integrator' (red superimposed grid). The integration of the direction and the length of each movement of the animal will update the position of the animal in this preconfigured coordinate system. The allocentric position of the animal is thus deduced from the transformation of egocentric movements.

*simple one-to-one switches to the outgoing responses. Rather, the incoming impulses are usually worked over and elaborated in the central control room into a tentative, cognitive-like map of the environment. And it is this tentative map, indicating routes and paths and environmental relationships, which finally determines what responses, if any, the animal will finally release."* [Tolman 1948]

In this paper, Tolman suggested that the relation between the cognitive map could have an indirect relation with the external world. He proposed that this map could be learnt in a "*latent*" manner and involve information not related to a goal. Contrarily, in the stimulus-response theory only rewarded actions will be stored. This latent knowledge, "*tentative map*", can potentially be useful later in case of changes in the environment, to take a shortcut, avoid dead ends or obstacles. Also, it is worth mentioning that Tolman did not described his theory of the cognitive map solely in a spatial frame. In the discussion of his paper he applied this perspective to social representation or human behavior like: "regression", "fixation" and "displacement of aggression onto outgroups". For example, he used this theory to explain the behavior of a woman, described in an article of Time Magazine, who regressed to a childish behavior after the loss of her husband: "*Time's middle-aged woman was presented by too frustrating an emotional situation at her husband's death and she regressed, I would wager, to too narrow adolescent and childhood maps ...*" [Tolman 1948, p.207]. Tolman's definition of a cognitive map is thus close to the modern definition

of the notion of "schema" in psychology<sup>11</sup> introduced by Jean Piaget [Piaget 1952].

Later, O'Keefe and Nadel [1978] developed this theory of a cognitive map by proposing that the spatial properties of the external world could be carried internally by a cognitive structure (Figure 1.3 - A). This model is not necessarily isomorphic to a strict physical map of the world but will contain enough information about the external world to be able to make useful inference about it. This cognitive representation is nevertheless analogous to a "map" in the sense that it provides a simultaneous access to all the mapped relations in a reference frame depending on external stimulus: "*allocentric*". Such structure allows to deduce the relation of different sets of overlapping relations. In other words, if the relations from A to B and from B to C are mapped, then the relation from A to C can be deduced from the model even if the path (A-C) has never been experienced [O'Keefe and Nadel 1978; Poucet 1993] (but see: Simon [1996] and Jensen [2006]).

A decade after, Leonard and McNaughton [1990] developed another theory of navigation relying on "local views" of space (Figure 1.3 - B). Their initial motivation was that: "*A location is nothing more than a set or a constellation of sensory/perceptual experiences joined to others by specific movements*" [Leonard and McNaughton 1990, p. 366]. In their model, position in an environment could be deduced from the perceived set of cues or "local views" (that are not necessary visual despite the use of the term "view"). These "local views" are then linked during behavior to a general coordinate system: a preconfigured path integrator. Consequently, the position and direction of the animal can be updated solely on the basis of idiothetic information. The integration of the angular and linear components of each movements results in the displacement of a bump of activity in a preconfigured coordinate system. Landmark cues are then used to define a relevant reference frame and to correct potential drift of the path integrator. The map in allocentric space is thus deduced from egocentric perceptions [Leonard and McNaughton 1990; McNaughton et al. 1996].

The differences between these two theories can be attributed mainly to their implementation. In the O'Keefe and Nadel [1978] model, an allocentric map of the environment stores relationships among a set of landmarks. Consequently it requires time to be formed in a new environment. Furthermore, as pointed out by McNaughton et al. [1991], the storage of such kind of map would need to increase supralinearly ( $n^2$ ) its storage capacity to cope for a higher number of external cues (n). This will not be the case in the Leonard and McNaughton [1990] model, where relations between landmarks are associated to a preconfigured coordinate system. In this case, storage requirements will increase only linearly with the number of landmarks.

---

<sup>11</sup> Schema: An expertise-dependent representation of the structure of the world, identifying the important parameters over which the world varies. [from: Redish 2016]

Also, in the first case, the accuracy of the position estimate of the model will be dependent on the number of cues in the environment whereas in the second it depend on the preconfigured coordinate system.

In the frame of the Marr's level of analysis [Marr 1982], these models serve the same purpose (computational level). Nevertheless, they are not mutually exclusive and can complement each other depending on the environmental conditions favouring an externally or internally driven navigation strategy [Gothard et al. 1996a; Savelli and Knierim 2019]. These two theories propose different implementation, or algorithm in order to explain how an animal forms a map of its environment. Nowadays, the current state of these two models is still unclear and requires further investigations. However, one of the main factor that contributed to the emergence and development of these theories is the discovery of neural correlates of space: place cells, head direction cells, grids cells and a variety of other spatially modulated cells [O'Keefe and Dostrovsky 1971; Ranck 1984; Hafting et al. 2005]. I will detail briefly these complementary neuronal correlates of space in a following chapter (§ 3). But first, in the next chapter I will present the anatomy of a set of structures crucial for spatial cognition, the hippocampal formation.

# 2

## NEUROANATOMY OF THE HIPPOCAMPAL FORMATION

---

"¡Como el entomólogo a caza de mariposas de vistosos matices, mi atención perseguía, en el verjel de la substancia gris, células de formas delicadas y elegantes, las misteriosas mariposas del alma, cuyo batir de alas quién sabe si esclarecerá algún día el secreto de la vida mental!"

---

Ramon y Cajal [1917]

Tolman [1948] proposed the existence of a "cognitive map" in order to navigate in a flexible and efficient way in a constantly changing world. An important discovery which contributed to the development of this theory was the discovery of spatially modulated cells in the hippocampus and the adjacent cortical regions [O'Keefe and Dostrovsky 1971; Ranck 1973; Hafting et al. 2005]. A description of this space modulated neuron will be developed in the next section § 3. First, I will focus on an anatomical description of the hippocampal and parahippocampal regions. In parallel, I will describe their connectivity as it could be involved in the way spatial information flows and is processed in the hippocampal formation.

### 2.1 ANATOMICAL DEFINITION OF THE HIPPOCAMPAL FORMATION

The hippocampus is a brain structure belonging to the limbic system located in the middle of the temporal lobe beneath the cerebral cortex. This region is often referred to as an archicortex, a type of cortex characterized by three or four layers, phylogenically older and more primitive than the surrounding neocortex. The hippocampal formation can be decomposed in the hippocampus (archicortex) and the parahippocampal formation (neocortex) that differ in respect to their general connectivity and their number of layers (Figure 2.1 - A). Indeed, regions functionally homologous to the hippocampus can be traced to the earliest vertebrates where the neocortex is absent or extremely small: medial pallium in teleosts such as goldfish and medial cortex in modern reptiles such as turtles and lizards [Murray et al. 2018].

The hippocampus is a bilateral medial temporal lobe structure first described in human by Julius Caesar Arantius, a student of Andreas Vesalius, in *De Humano Foetu Liber* in 1587 [Aranzi 1587; Bir et al. 2015]. This pioneer anatomist and surgeon coined the term hippocampus from the combination of the greek words for seahorse: ἵππος (hippos, "horse") and κάμπος (kampos, "sea monster"). This term was chosen due to the similarity of the 3-dimensional shape of the human hippocampus with this sea creature. In humans, the hippocampus is located deeply in the brain as it lies within the medial temporal lobe, in the floor of the inferior horn of the lateral ventricle. In rodents however, the hippocampus has a banana-shape that occupies a much larger fraction of the telencephalon inside its caudal pole (Figure 2.1 - A).

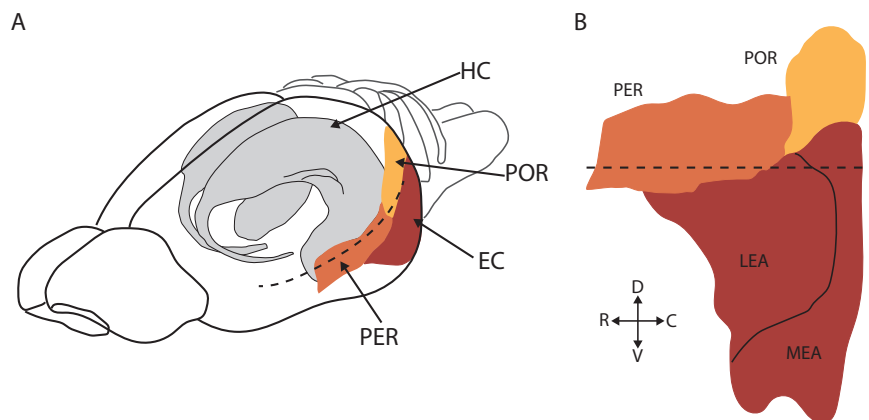


**Figure 2.1:** A Schema illustrating the location of the Hippocampus (gray, HC), and the parahippocampal regions: perirhinal (PER), entorhinal (EC), and postrhinal (POR) cortices. B Planar projection of parahippocampal regions. The dotted line depicts the rhinal sulcus. Other abbreviations: C, caudal; D, dorsal; R, rostral; V, ventral. (Modified from [Furtak et al. 2007])

In rodents, the superior portion, at the rostro-dorsal extremity, is known as the "dorsal hippocampus" and is also called "the septal pole" due to its proximity to the septum, a subcortical structure located at the midline of the brain, between the lateral ventricles [Amaral 1989]. The inferior portion is called the ventral hippocampus and has a caudo-ventral localization so that, along this long axis, the hippocampus has a C-shape (or a banana-shape) (Figure 2.1 - A). The long axis of the hippocampus is generally designated as the septo-temporal axis and the orthogonal axis is referred to as the transverse axis. Along its transverse axis, the hippocampus proper can clearly be divided into two major regions, a large-celled region and a smaller-celled region. Santiago Ramón y Cajal (1852-1934), a neuroanatomist famous for his pioneer works describing the organization of the central nervous system, respectively called these two regions *regio inferior* and *regio superior*. However, the terminology of one of his disciples, Rafael Lorente de Nò (1902-1990) known notably for the first description

of the columnar organization of the cortex, has achieved more common usage. He divided the hippocampus proper into three fields (CA<sub>1</sub>, CA<sub>2</sub> and CA<sub>3</sub>). His CA<sub>3</sub> and CA<sub>2</sub> fields are equivalent to the large-celled *regio inferior* of Ramon y Cajal, and his CA<sub>1</sub> corresponds to the *regio superior* [Ramon y Cajal 1909; Witter 2012]. Most anatomists use the term "hippocampus proper" to designate the three CA subregions (CA<sub>1</sub>, CA<sub>2</sub> and CA<sub>3</sub>), and hippocampus to refer to the hippocampus proper plus dentate gyrus [Amaral and Lavenex 2006]. The dentate gyrus and hippocampus proper forms two opposed "C" that interlock. The parahippocampal region includes the Entorhinal Cortex (EC), the Perirhinal Cortex (PER), the Postrhinal Cortex (POR) and Pre- and Parasubiculum [Witter and Amaral 2004]. The location of some parahippocampal regions in comparison to the hippocampus is shown in Figure 2.1.

The hippocampus presents a remarkable organization along its transverse axis. Along this axis, information flowing through the hippocampus passes through three successive groups of neurons, from granule cells in the dentate gyrus to CA<sub>3</sub> and then CA<sub>1</sub> pyramidal cells (Figure 2.2). Dentate granule cells receive inputs from the adjacent entorhinal cortex through fibers named collectively the perforant path, then project their axons, the mossy fibers, on CA<sub>3</sub> pyramidal cells. CA<sub>3</sub> pyramidal cells then contact CA<sub>1</sub> via the Schaffer collaterals. This simple circuit is often referred to as the "trisynaptic loop". The output of this loop is made by CA<sub>1</sub> pyramidal cells that project outside of the hippocampus proper, to the subiculum and entorhinal cortex. The description of this trisynaptic loop led to believe that the CA subfields, particularly the CA<sub>1</sub> and CA<sub>3</sub> regions, corresponded to successive processing stages in a major feed-forward loop through the transverse axis of the hippocampus [Andersen et al. 1971]. In the following section I will follow this flow of information to describe successively the intrinsic hippocampal connectivity.

## 2.2 INTRINSIC CONNECTIVITY OF THE HIPPOCAMPUS

### 2.2.1 Dentate Gyrus

The dentate gyrus is regarded as the "entry point" for information into the hippocampus via the perforant path. It is organized in a superposition of three *Strata* in the dorso-ventral axis: *Stratum Moleculare* containing few neuronal cell bodies, *Stratum Granulosum*: composed largely by neuronal cell bodies of dentate granule cells and the polymorphic layer [Amaral et al. 2007] (Figure 2.3). The polymorphic layer is often referred to as *hilus* and was defined as CA<sub>4</sub> by Lorente de Nó [Lorente De Nó 1934]. Granule cells of the *Stratum Granulosum* have a small diameter (8-12  $\mu\text{m}$ ) and form a fairly dense layer of cellular bodies. The entire dendritic tree of granule cells is confined in the

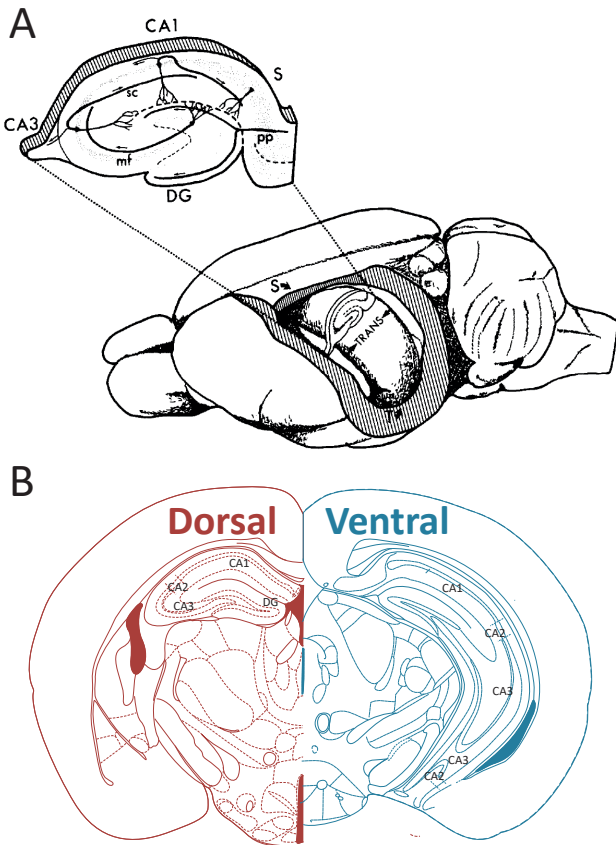


**Figure 2.2: A Bottom:** Illustration of the position of the hippocampus in a rat brain. The drawing shows a preparation where the cortex overlying the hippocampus has been removed. S and T indicate the septal/dorsal and the temporal/ventral pole respectively. **top:** a zoom on a transverse slice (TRANS), cut perpendicularly to the longitudinal axis, illustrate the major fields of the hippocampus and its intrinsic connectivity. Abbreviations: DG, dentate gyrus; mf, mossy fibers; pp, perforant path; sc, Schaffer collaterals (from Amaral 1989) **B** Transversal slices of a rodent brain illustrating the change in the organization of the major hippocampal subfields along the longitudinal axis of the hippocampus. The slices through the right and left hemisphere were made at two different antero-posterior levels: left red, dorsal level (-1.82 from Bregma), right blue ventral level (-2.80 from Bregma) (Modified from [Franklin and Paxinos 2013]).

molecular layer bordering the granular layer. Between the *Stratum Granulosum* and the hilus lays the subgranular zone which is one of the few stem-cell-containing niches in the adult mammalian brain. Neural progenitors in this region have the ability to differentiate into mature granule cells that will integrate the pre-existing adult network [see Gonçalves et al. 2016, for review]. The axons of granule cells, called mossy fibers, reach the hilus in which they divide into many axon collaterals [Claiborne et al. 1986]. In the hilus, these collaterals contact cellular bodies and dendrites of inhibitory interneurons and mossy cells [Ribak and Peterson 1991].

Mossy cells of the hilus are excitatory cells covered with thorny excrescences on both the cell body and proximal dendritic shafts. These excrescences are large spine complexes that are contacted by very large

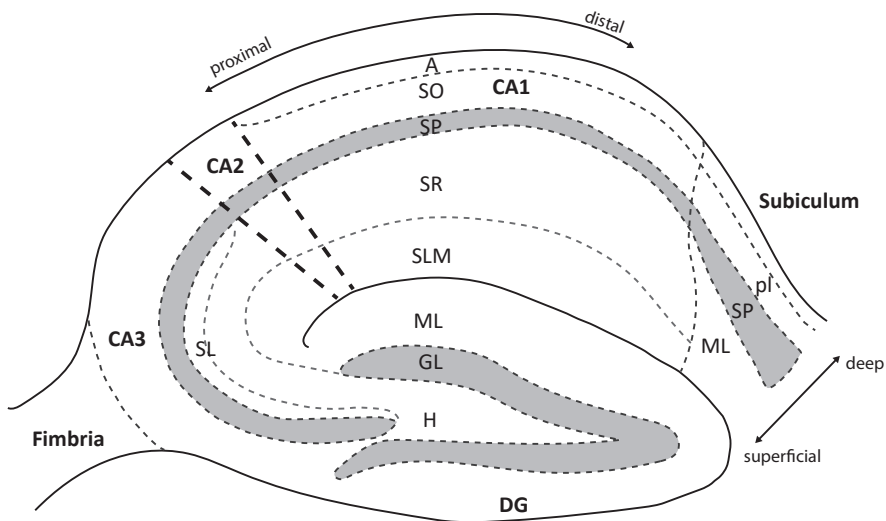


**Figure 2.3:** Schema illustrating the different layers of the hippocampus in a transverse slice.  
A: alveus, SO: Stratum Oriens, SP: Stratum Pyramide, SR: Stratum Radiatum, SLM: Stratum Lacunosum Moleculare, GL: Stratum Granulosum, ML: Stratum Moleculare, H: Hilus, SL: Stratum Lucidum, pl: polymorphic layer

synaptic boutons from the mossy fibers (the so-called giant mossy fiber boutons)[Amaral 1978]. Mossy cells project their axons widely along the septo-temporal axis on the granule cells layer, suggesting that these cells integrate information from a local set of granule cells to redistribute them to more distant granule cells [Buckmaster et al. 1996; Scharfman and Myers 2013].

Granule cells project outside of the dentate gyrus onto CA3. The main axon of the granule cells leaves the hilus and continues its path towards the CA3 region in *Stratum Lucidum*. There, it contacts several pyramidal cells via giant "en passant" boutons on the proximal dendrites of the pyramidal cell and several interneurons via associated *filopodia* [Freund and Buzsaki 1996; Acsády et al. 1998].

### 2.2.2 Hippocampus proper

The hippocampus proper follows a clear cytoarchitectonic organization defined by Ramon y Cajal from the observation of Golgi stained hippocampal slices [Ramon y Cajal 1909]. The laminar structure as seen in Figure 2.3 is organized dorso-ventrally into five layers: the *Alveus*, *Stratum Oriens*, *Stratum Pyramide*, *Stratum Radiatum* and *Stratum Lacunosum Moleculare*. *Stratum Pyramide* contains most of the neuronal cell bodies, mostly composed of excitatory pyramidal cells. The other layers mostly contain fibers and the cell bodies of inhibitory interneurons. An additional layer, *Stratum Lucidum*, is present above the pyramidal layer of CA3 only. It receives the axonal projections of the mossy fibers coming from the dentate gyrus. In the following section, the dentate gyrus will serve as a reference point in order to describe

different regions along the transverse axis of the hippocampus. For example, the portion of CA1 adjacent to CA2, closer to the DG, will be considered proximal, while the portion closer to the subiculum will be called the distal portion.

#### 2.2.2.1 CA<sub>3</sub>

The CA<sub>3</sub> region is the second stage of the tri-synaptic loop. As described previously, pyramidal cells of CA<sub>3</sub> are targeted in their most apical portion, *Stratum Lucidum*, by mossy fibers originating from dentate gyrus. This Ammonic subfield can be subdivided in three other subregions along its proximo-distal axis [Lorente De Nô 1934]. The most proximal subregion, CA<sub>3c</sub> penetrates the hilus. It is then followed by CA<sub>3b</sub> and finally CA<sub>3a</sub> corresponding to the curved portion adjacent to CA2. Between these three regions, pyramidal neurons differ in their morphology but also connectivity [Lu et al. 2015]. Mossy fiber inputs from the dentate gyrus taper off along this proximo-distal axis [Ishizuka et al. 1995]. In addition to these inputs, CA<sub>3</sub> pyramidal cells are contacted at the level of their *Strata Oriens* and *Radiatum* by collaterals originating from other CA<sub>3</sub> pyramidal cells. Before going out of CA<sub>3</sub>, 30 to 70% of CA<sub>3</sub> synapses contact other CA<sub>3</sub> pyramidal cells [Li et al. 1994]. The recurrent projections of a single axon can extend to ~70% of the septo-temporal axis of the hippocampus [Sik et al. 1993; Li et al. 1994; Le Duigou et al. 2014].

The strong recurrent circuitry of CA<sub>3</sub> pyramidal cells can be computationally seen as an auto-associative network [Marr 1971; McNaughton and Morris 1987; Rolls 2007]. Such networks have been suggested to perform pattern completion, the ability to retrieve a stored pattern of activity based on incomplete inputs. This mechanism could allow to retrieve a particular memory with the help of partial or degraded cues.

In 1892, a Hungarian anatomist, Károly Schaffer (1864–1939) described projections of CA<sub>3</sub> pyramidal cells to CA1 [Schaffer 1892; Szirmai et al. 2012]. These Schaffer collaterals are organized topologically along the proximo-distal axis [Li et al. 1994]. Briefly, CA<sub>3a</sub> (close to CA2) principally innervates proximal CA1 (close to CA2) while CA<sub>3c</sub> (close to DG) contacts principally distant segment of CA1 close to the subiculum (distal CA1). These collaterals are also organized along the CA1 radial axis as CA<sub>3a</sub> neurons target predominantly the basal dendrites, whereas neurons located close to the hilus (CA<sub>3c</sub>) terminate predominantly on the apical dendrites of both CA1 and CA<sub>3</sub> cells [Li et al. 1994].

CA<sub>3</sub> collaterals originate either from ipsilateral or contralateral pyramidal cells. A population of inter-hemispheric fibers crosses the midline via the hippocampal commissure and contacts the contralateral hippocampus (CA<sub>3</sub>, CA<sub>2</sub>, CA1) [Amaral 1989; Swanson and Sawchenko 1981; Andersen et al. 2006].

Finally, CA3 pyramidal cells projections are widely distributed along the longitudinal axis so that a single CA3 cell distributes its collaterals to much of the full septo-temporal extent of CA1 [Li et al. 1994; Andersen et al. 2006; Wittner et al. 2007]. The divergence of CA3 projections to CA1 could be used to distribute CA3 activity to a larger pyramidal cells population and distribute it along different axes of the hippocampus.

#### 2.2.2.2 CA2

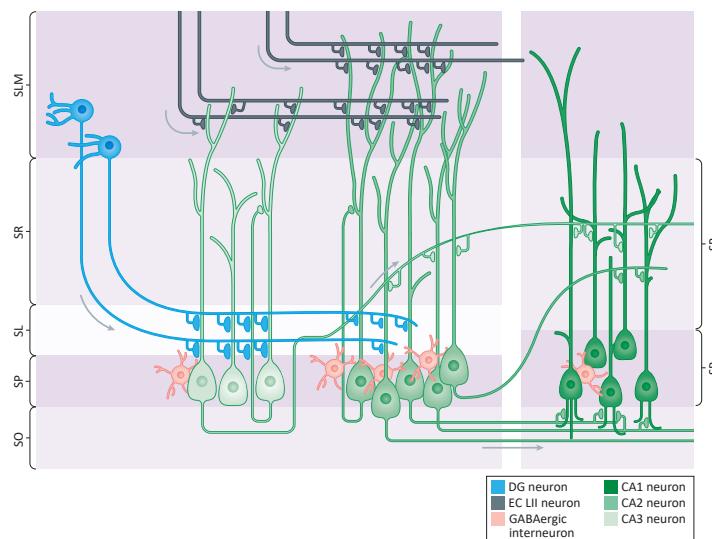


**Figure 2.4:** Intrinsic connectivity of the hippocampal neurons in rodents. Dentate Gyrus (DG) granule cells (blue), contact CA3 neurons (light green) in *Stratum Lucidum* and weakly CA2 cells (medium green). Both CA3 and CA2 receive projections from medial and lateral entorhinal cortex layer II (EC LII) neurons (grey) that target the *Stratum Lacunosum-Moleculare* (SLM). In rodents, CA2 neurons receive projections from CA3 neurons that target the *Stratum Radiatum* (SR). CA1 neurons (dark green) are targeted by CA3 projections from Schaffer collaterals in *Stratum Radiatum* and to a lesser extent by CA2 projections in the same layer. The main efferent projections of CA2 pyramidal target the basal dendrites (*Stratum Orien(s)SO*) of ‘deep’ calbindin-negative CA1 neurons. The density of reelin- and parvalbumin-positive interneurons (pink) is several-fold higher in area CA2 *Stratum Pyramidale* than in CA1 SP and CA3 SP (Modified from [Dudek et al. 2016])

CA2 is an Ammonic region that attracted attention only belatedly compared to its neighbors. It is not considered as a part of the tri-synaptic loop, but recent discoveries on its composition and connectivity reinforce the idea that CA2 has a singular but underappreciated role in the processing of the information flow transiting in the hippocampus [Zhao et al. 2001; Lein et al. 2005; Jones and McHugh 2011; Dudek et al. 2016]. The cellular composition of CA2 is also distinct;

in rats, it contains the highest concentration of different classes of interneurons present in all three regions of the *Corns Ammonis*, including parvalbumin, reelin, calbindin and calretinin expressing cells [Mercer et al. 2007; Dudek et al. 2016].

When Rafael Lorente de Nô defined the different subfields of the *Cornus Ammonis*, he described that the cell bodies of the CA2 region, akin to those in CA3, were larger than the one found in CA1 [Lorente De Nô 1934]. However, he noted that CA2 pyramidal cell dendrites lack the specialized thorny excrescences associated with inputs from mossy fibers from the DG, which are characteristic of CA3 pyramidal neurons [Ishizuka et al. 1995]. Albeit the absence of these excrescences, CA2 receives tapering inputs from mossy fibers in rats and mice<sup>1</sup> [Kohara et al. 2014]. CA2 neurons also receive Schaffer collateral inputs from CA3 neurons, much like the cells of area CA1 [Lorente De Nô 1934; Chevaleyre and Piskorowski 2016; Dudek et al. 2016].

The axonal arborization of CA2 pyramidal cells is rather important and divergent. Indeed, the axons of these cells send projections at the intra-hippocampal level mainly on CA1 *Stratum Oriens*, but also on *Stratum Radiatum* of the ipsi and contralateral CA2 and CA3. CA2 pyramidal cells contact different extra-hippocampal targets such as the supramammillary nucleus, medial septum and diagonal bands of Broca [Cui et al. 2013]. Recent evidence also suggest a physiological and functional proximo-distal organization of CA2 [Lu et al. 2015; Fernandez-Lamo et al. 2019].

#### 2.2.2.3 CA1

The CA1 region is the last stage of the tri-synaptic circuit and receives mostly CA3 axons via the Schaffer collaterals, though it is also contacted by the entorhinal cortex (see Figure 2.6). The pyramidal cell layer of CA1 is much more compact than in CA3, and the cells have a more regular morphology [Ishizuka et al. 1995]. Cellular bodies are thinner than in the CA3 region and mostly emit a single dendrite, subsequently splitting into the *Stratum Radiatum*. These dendrites usually end in a fine arborization in the *Stratum Lacunosum Moleculare* and commonly reach the hippocampal fissure. Basal dendrites grow strongly in the *Stratum Oriens* and often reach the alveus. CA1 pyramidal cells do not appear to be segregated in distinct layers at first sight, but they are organized along a gradient of distinct morphological, molecular and physiological features along the radial axis [Geiller et al. 2017b; Soltesz and Losonczy 2018; Valero and Prida 2018]. This gradient unfolds from the deep CA1 cells located more dorsally, close to *Stratum Oriens*, to the superficial cells located beneath this deep layer along the border of *Stratum Radiatum*. Like CA2 cells, pyramidal CA1 neurons do not have thorny excrescences [Ishizuka et al. 1995].

---

<sup>1</sup> The extent of the dentate gyrus projections to CA2 is species specific, see Dudek et al. [2016] for review.

CA<sub>1</sub> projections mostly target the subiculum in a topological manner. Briefly, proximal CA<sub>1</sub> cells project towards the distal part of the subiculum, while distal CA<sub>1</sub> cells project onto the proximal part [Amaral et al. 1991]. Also, CA<sub>1</sub> cells receive a low input from the subiculum [Commins et al. 2002; Sun et al. 2014]. Together with the subiculum, CA<sub>1</sub> is the most prominent output of the hippocampus to entorhinal cortex and other neocortical areas [Freund and Buzsaki 1996].

Unlike CA<sub>3</sub>, CA<sub>1</sub> cells do not have recurrent collaterals. Also, contrarily to CA<sub>3</sub>, CA<sub>1</sub> neurons send very few commissural projections. These major differences in intrinsic connectivity suggest a strong functional dichotomy between these two ammonic regions.

### 2.2.3 Subiculum

The subiculum is composed of three principal layers. Its most superficial layer, the molecular layer, is continuous with *Strata Lacunosum-Moleculare* and radiatum of the adjacent hippocampal area CA<sub>1</sub> field. Its enlarged pyramidal cell layer contains the soma of principal neurons. The polymorphic layer is located deeper (i.e., closer to the alveus) than the pyramidal cell layer and is continuous with the *Stratum Oriens* of the CA<sub>1</sub> area [O'Mara et al. 2001; O'Mara 2005; Matsumoto et al. 2019]. Recent investigations revealed that the cytoarchitecture and immunoreactivity of the subicular region could allow the division of this region in proximal (closer to CA<sub>1</sub> area) and distal (further from CA<sub>1</sub> area) subfields [Ishihara and Fukuda 2016].

The subiculum is in majority contacted by CA<sub>1</sub> and the entorhinal region [Amaral et al. 1991; O'Mara 2005; Matsumoto et al. 2019]. Reciprocally, proximal CA<sub>1</sub> cells project to the distal subiculum close to the parasubiculum [Amaral et al. 1991; O'Mara 2005]. The subiculum also receives major inputs from the layer 3 of the medial and lateral entorhinal cortices [Honda et al. 2012].

The subicular region sends numerous projections to various areas of the hippocampal and parahippocampal formation: entorhinal, perirhinal and postrhinal cortices [O'Mara 2005; Matsumoto et al. 2019]. Furthermore, recent evidences showed that the subiculum also sends backward projections to the CA<sub>1</sub> region [Commins et al. 2002; Sun et al. 2014]. Moreover, the dorsal subiculum innervates adult-born dentate granule cells [Deshpande et al. 2013; Matsumoto et al. 2019].

## 2.3 TWO PARALLEL STREAMS CONVERGING TO THE HIPPOCAMPUS

The hippocampus receives most of its cortical inputs through the entorhinal cortex via the perforant path. Entorhinal cortex also constitutes the main output cortical structure of the hippocampus directly from CA<sub>1</sub> or indirectly via the subiculum. In the following

sections, I will describe how hippocampal-entorhinal connections are anatomically organized along the longitudinal and transverse axis of the hippocampus. One key aspect in this organization resides in the anatomical dichotomy within the entorhinal cortex that can be divided in lateral and medial parts. Numerous anatomical studies reported a segregation of the cortical inputs to the medial and lateral areas of the entorhinal cortex [Burwell and Amaral 1998; Furtak et al. 2007; Kerr et al. 2007]. Medial Entorhinal Cortex (**MEC**) receives strong visuo-spatial inputs while Lateral Entorhinal Cortex (**LEC**) is contacted by non-spatial, contextual areas. This suggests that information transiting through this area is segregated and processed in a parallel fashion to then leads to functional diversity in the hippocampus [Brandon et al. 2014; Igarashi et al. 2014a; Knierim et al. 2014].

### 2.3.1 *Entorhinal Cortex*

The entorhinal cortex is the major input and output region of the hippocampal formation [Knierim et al. 2014; Witter et al. 2017]. Its name comes from the fact that it is partially enclosed in the rhinal sulcus. A particular interest to this cortex has been initiated by Santiago Ramón y Cajal when he observed its strong projections to the hippocampus through the perforant path [Ramon y Cajal 1909]. The entorhinal cortex can be divided, based on cyto-architectonic differences, into two regions generally referred to as lateral and medial entorhinal cortex or Brodmann's areas 28a and 28b respectively [Brodmann 1909]. In rodents, the difference between these two regions was first very strikingly observed at the level of their projections on the dentate gyrus as axons originating in the LEC terminate in the outer one-third of the molecular layer and axons from the MEC terminate in the middle one-third of the molecular layer [Hjorth-Simonsen and Jeune 1972; Hjorth-Simonsen 1972]. The medial vs lateral entorhinal cortex dichotomy was later completed by studies demonstrating differences in connectivity patterns and functional roles between these two regions. I will first highlight the main differences in connectivity patterns between the medial and lateral entorhinal cortex before presenting the organization of the projections between the entorhinal cortex and the hippocampus.

### 2.3.2 *Afferences and efferences of Entorhinal Cortex*

**MEC** and **LEC** exhibit important differences regarding the brain structures with which they are anatomically connected. In this section, we will focus on the main differences in inputs/outputs between **LEC** and **MEC** independently of their distinct pattern of connectivity along the longitudinal axis of the hippocampus [see: Kerr et al. 2007; Agster et al. 2016; Tomás Pereira et al. 2016, details on subregions connectivity].

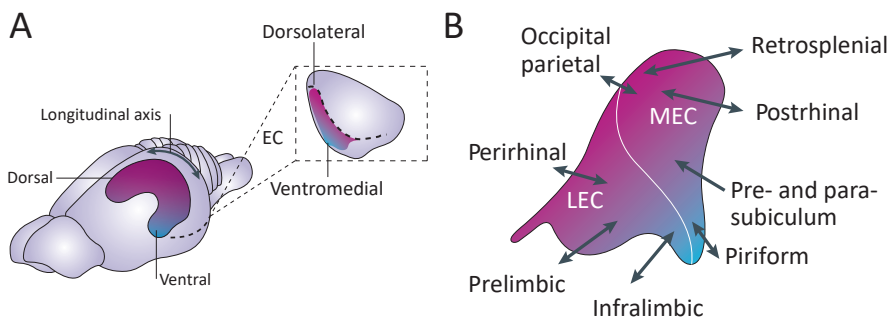


**Figure 2.5:** A Schematic representation of the gradient in connectivity between hippocampus and entorhinal cortex in rodents. The dorsolateral band of the entorhinal cortex (EC) (magenta) preferentially contacts the dorsal hippocampus. Increasingly more ventral and medial bands of the EC (purple to blue) are connected to increasingly more ventral levels of the hippocampus. B Planar projection of the entorhinal cortex depicted with a color gradient corresponding to the hippocampal gradient displayed in A. Arrows show the topology of the major cortical projections to the entorhinal cortex. The white line symbolize the border between medial and lateral entorhinal cortex. (Modified from [Strange et al. 2014])

### 2.3.2.1 Afferences of the Entorhinal Cortex

Despite their close anatomical proximity, **MEC** and **LEC**, strikingly differ based on their afferent connectivity with their cortical, subcortical or parahippocampal partners [Kerr et al. 2007; Agster et al. 2016; Tomás Pereira et al. 2016]. **LEC** receives stronger cortical projections than its medial counterpart: one third versus one fifth of the total afferent input [Kerr et al. 2007]. The main afferences to the **LEC** mostly come from olfactory structures comprising the piriform cortex and the olfactory bulb [Kerr et al. 2007; Chapuis et al. 2013; Agster et al. 2016]. The piriform cortex also accounts for the strongest cortical inputs to the **MEC**. However, while the frontal and insular cortex contact more heavily the **LEC**, the **MEC** is more strongly innervated by the temporal, parietal and occipital cortices.

Subcortical structures provide one third of the total number of afferences received by **LEC** or **MEC** [Kerr et al. 2007; Tomás Pereira et al. 2016]. In accordance with the strong projections from the piriform cortex to the **LEC**, this region is also strongly innervated by the amygdala or subcortical olfactory nuclei such as the endopiriform nucleus [Tomás Pereira et al. 2016]. While these nuclei also project to the **MEC**, subcortical inputs to the **MEC** are dominated by the dorsal thalamus, particularly the lateral posterior nucleus, a region implicated in visuospatial attention. The medial septum, a structure important for the generation of the theta rhythm, also projects more strongly to the **MEC** than to the **LEC** [Burwell and Agster 2008; Canto et al. 2008; Gonzalez-Sulser et al. 2014].

The major afferences to the **MEC** come from the hippocampal formation (hippocampus, pre- and parasubiculum, subiculum, post- and perirhinal cortices) as such structures account for 50% of its total afferent input (versus one third for the **LEC**) [Kerr et al. 2007; Tomás Pereira

et al. 2016]. The two main hippocampal afferences to the LEC come from the ventral hippocampus and the PER while the MEC is more strongly innervated by the pre- and parasubiculum as well as by the hippocampus proper. While the projections from the PER is heavier on the LEC, the MEC receives projections equally from both the PER and the POR [Naber et al. 1999; Witter et al. 2017; Nilssen et al. 2019].

### 2.3.2.2 *Efferences of the Entorhinal Cortex*

Both subdivisions of the entorhinal cortex project strongly to the hippocampus proper. This close anatomical relationship will be described in details in the following section. The efferent projections of LEC and MEC into cortical areas are largely reciprocal with their afferent cortical regions but this reciprocity is not well respected for subcortical structures [Kerr et al. 2007; Agster et al. 2016; Tomás Pereira et al. 2016]. Notably, LEC and MEC project strongly to the basal ganglia but are only weakly contacted back by these structures. It is worth mentioning that the basal ganglia represents more than 90% of the total subcortical efferences from the grid cells area (dorsolateral pole of the MEC) [Kerr et al. 2007]. Reciprocal connections are however present between the olfactory nuclei/amygdala and LEC but also between the septal nuclei and the MEC.

### 2.3.2.3 *Intrinsic organization of the Entorhinal Cortex*

MEC and LEC are composed of six layers [Moser et al. 2010]. Schematically, superficial layers II and III of the entorhinal cortex project to the hippocampus, while the output from the hippocampus is sent back to deep layers V and VI of the EC. The first layer (Layer I) is a plexiform layer embedding few GABAergic interneurons. Layer II is mostly composed of large multipolar cells called stellate cells in MEC and fan cells in LEC. Layer II contains a second category of principal glutamatergic cells: pyramidal cells that are morphologically and functionally distinct from stellate/fan cells. Additionally, stellate/fan cells are reelin positive while pyramidal cells are calbindin positive. In the MEC, pyramidal cells are grouped into small clusters (islands) arranged in an hexagonal grid aligned to layer I axons [Kitamura et al. 2014; Ray et al. 2014] but this striking arrangement is not present in the LEC where pyramidal cells tend instead to be segregated into sublayers [Witter et al. 2017]. Layer III is populated by pyramidal cells with similar morphology and electrophysiological characteristics in MEC and LEC. Layer IV is an other plexiform layer, containing very few neuronal cell bodies and interneurons. It is nevertheless considered as a transition between superficial I-III and deep V-VI layers. Layer V contains superficially pyramidal cells (layer Va) while its deep part (layer Vb) is composed of smaller neurons. In mice, layers Va and b were recently identified based on the expression pattern of the transcription factors Etv1 and Ctip2 respectively [Ramsden et al. 2015].

The particularity of layer V is that it contacts superficial layers of the EC with its apical dendrites. Layer VI has a heterogeneous neuronal population whose density decreases in depth. Occasionally, its axon collaterals contact the surface layers.

Intrinsic connections of the EC provides microcircuits where afferences from the deep layers can influence the information incoming to the surface layers, and vice versa, though these microcircuits are still not well understood. These intrinsic projections are more important in the medial than in the lateral part.

#### 2.3.2.4 Projections of the Entorhinal Cortex to the hippocampus

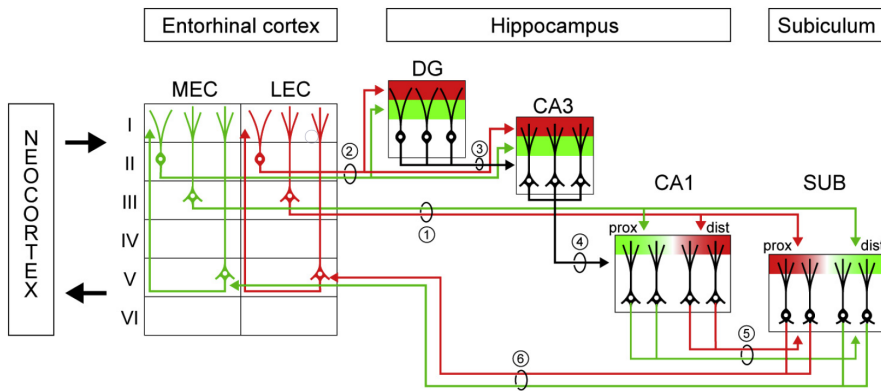


**Figure 2.6:** Schematic representation of the main connections between rodent Entorhinal Cortex and the hippocampal formation. The hippocampus is strongly interconnected with the entorhinal cortex. The arrows indicate strong to moderate connections between regions of the hippocampal (dentate gyrus, CA3, CA1, subiculum) and the medial and lateral areas of the entorhinal cortex. MEC and LEC send projections to CA1 through two major pathways: direct (1) and indirect (2). In the direct pathway (1), layer III neurons of MEC largely project to the proximal part of CA1 subfield (close to CA2). Conversely, layer III cells of LEC contact the distal part of CA1 (close to subiculum). However, in the indirect pathway (2), axons of layer II neurons of both MEC and LEC converge on the same population of cells in the dentate gyrus and CA3. This combined information in DG and CA3 is then transmitted to CA1 via mossy fibers (3) and Schaffer collaterals (4). The output from CA1 is then brought to the Entorhinal Cortex mostly through subiculum. Once in subiculum, information from proximal CA1 is conveyed to MEC via distal subiculum, whereas distal CA1 sends information to LEC via proximal subiculum (5 and 6). (Adapted from Igarashi et al. [2014b])

The CA1 region is contacted by the EC by two major routes, the direct and indirect pathways. In the direct pathway, layer III of the EC projects directly on CA1 neurons. In the indirect pathway, layer II cells from the EC synapse on the dentate gyrus and CA3, to then finish in CA1 via the *Schaffer collaterals*. In the indirect pathway, reelin positive cells from layer II (stellate cells in the MEC and fan cells in LEC) project to the dentate gyrus and CA3. In layer II of the MEC, an additional direct pathway has been described as calbindin positive pyramidal cells project to CA1 as well as to the contralateral MEC [Varga et al. 2010; Kitamura et al. 2014; Witter et al. 2017].

The indirect and direct pathways originating from the **MEC** and **LEC** present some important anatomical differences regarding the hippocampal subfields that they target. As noted above, the indirect **MEC** and **LEC** pathways converge to the same population of neurons in the dentate gyrus and CA3 at different level of the dendritic trees [Witter and Amaral 2004] (Figure 2.6).

In the direct pathway however, **MEC** and **LEC** projections contact distinct population of neurons segregated along the proximo-distal axis of CA1. **MEC** preferentially targets proximal CA1 (close to subiculum) while **LEC** synapses on distal CA1 (close to CA2). Interestingly, this separation of entorhinal projection is mirrored for subicular projections as **MEC** and **LEC** respectively target distal and proximal subiculum (Figure 2.6).

In rodents, entorhinal projections to the hippocampal formation are also anatomically organized along a dorsolateral to ventromedial axis (see Figure 2.5 - A). In other words, the dorsolateral band of the entorhinal cortex is preferentially connected to the dorsal hippocampus. Gradually, more ventral and medial bands of the **EC** are connected to increasingly more ventral levels of the hippocampus [Dolorfo and Amaral 1998; Witter et al. 2000].

Numerous evidences now support the hypothesis of functional gradients along the proximo-distal [Henriksen et al. 2010; Burke et al. 2011; Igarashi et al. 2014a], longitudinal [Kjelstrup et al. 2008; Strien et al. 2009] or radial axis [Mizuseki et al. 2011; Geiller et al. 2017a,b; Soltesz and Losonczy 2018; Valero and Prida 2018] of the hippocampus. Interestingly, these functional gradients are correlated to differences in **EC** projections. A pure segregation of spatial and non-spatial information stream is now attenuated because of multiple convergences of these two streams in the hippocampal formation. Also backpropagation of information from the hippocampus to the deep layers of the entorhinal cortex could allow the integration of spatial and contextual information. Nevertheless, the connectivity of the entorhinal cortex strongly implies that it constitutes a cortical hub, separating and pre-processing spatial and non-spatial information and subsequently disseminating it to its hippocampal and cortical partners [Brandon et al. 2014; Witter et al. 2017].

# 3

## NEUROPHYSIOLOGICAL CORRELATES OF SPACE

---

"It is the response properties of the last class of units which has led us to postulate that the rat hippocampus functions as a spatial map. These 8 units responded solely or maximally when the rat was situated *in a particular part of the testing platform facing in a particular direction.*"

---

O'Keefe and Dostrovsky  
[1971]

### 3.1 RATE CODING OF SPACE

#### 3.1.1 *Neuronal doctrine of space coding*

The nervous system is constantly receiving sensory inputs from which it extracts a multitude of features. These features are assembled from primary sensory neurons to more integrative cortices in order to form representations of increasing complexity, specificity and invariance. This idea of the neuron as a functional unit of the nervous system originated from seminal works by Sherrington [1906] and Ramon y Cajal [1909]. In this paper, Sherrington described for the first time "*receptive fields*": the area of the body surface that could elicit a reflex when stimulated. Decades later, and thanks to technical advances allowing the recording of single nerve fibers, scientists discovered that different neurons could specifically respond to distinct stimuli [Hartline 1938]. The notion of receptive field was then applied to a neuron as the specific feature of the sensory space activating it and thus defining its function. This "neuron doctrine" [Yuste 2015; Eichenbaum 2018], is not directly applicable to more integrative areas of the brain like the hippocampus. However, early electrophysiological works on hippocampal formation and its behavioral correlates acknowledged the influence of previous works on visual and somatosensory systems on their approach: "... *the analog of a receptive field will be the behavioral correlate of a neuron, ...*"<sup>1</sup> [Ranck 1973].

---

<sup>1</sup> Interestingly, Ranck [1973] even used the term "microphrenology" when referring to this approach that defines functional types of neurons based on their behavioral

### 3.1.2 Place cells

In 1971, O'Keefe and Dostrovsky recorded the extracellular activity of cells from the dorsal hippocampus of rats while they were freely foraging in an arena [O'Keefe and Dostrovsky 1971]. They observed that some cells were activated in a particular location in the environment and virtually silent elsewhere. This specificity of their firing in relation to space endowed them the name of *place cells* (Figure 3.1 - A-B). The similarity of the receptive field of place cells and of cells in sensory cortices is at first sight striking, but they importantly differ for some crucial particularities. Early investigations of these neurons showed that hippocampal place cells were not only activated in relation to one sensory modality (sight, sound, touch,...), but by a combination of external and internal cues. External cues represent the characteristics of the environment and internal cues refers to the information provided by the animal's own movements. Later works confirmed that the spatial firing of place cells was triggered by multiple sensory cues [Ranck 1973; O'Keefe and Conway 1978] and that their activity changed depending on the set of cues available during exploration [Muller and Kubie 1987; Bostock et al. 1991]<sup>2</sup>. The receptive fields in sensory structures are thought to be "hardwired" so that the same response will be observed for the same stimulus from birth to death. Nevertheless, place cells are "softwired". Their activity can change from one context to the other: "remap" [Muller and Kubie 1987; Latuske et al. 2018] in order to form orthogonal representations of different environments [Leutgeb et al. 2005b] (Figure 3.1 - C). This variability and level of integration of sensory information make place cells incompatible with a strict definition of the "neuron doctrine". Nevertheless, this perspective influenced place cells works, certainly until this day.

*By design the term "place cell" suggests that such cells (anatomically, hippocampal pyramidal cells) signal only the position of the head in the environment. A perfect place cell would discharge if and only if the rat's head were in a single place in the world. Such a cell would discharge purely as a function of proximity to the place, regardless of the rat's activity (running, eating, grooming, etc.) and regardless of any aspect of the spatial relationship between the animal and the environment (e.g., running speed or acceleration) other than head position. [Muller et al. 1994]*

---

correlates : "For a neuron many synapses removed from sensory receptors or motor effectors, the analog of receptive field will be the behavioral correlate of a neuron, i.e., the sensory inputs and motor outputs of a rat which are associated with a given frequency or pattern of firing of a single neuron. Let us call this search for the behavioral correlates of single neurons "microphrenology." [Ranck 1973]

<sup>2</sup> An extensive review of the sensory cues influencing place cells coding will be detailed in § 4.

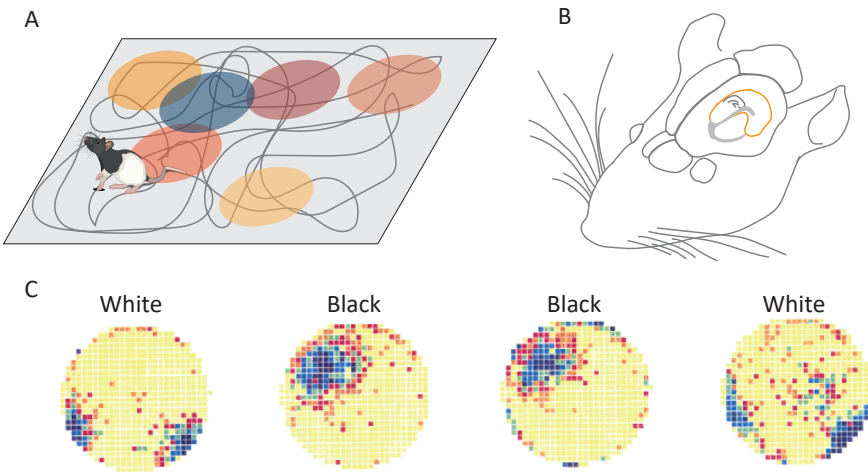


**Figure 3.1:** A: Schema illustrating the activity of different place cells while a rat forage in an environment. The path of the animal is depicted with a grey line. A place field is the region where a place cell fires in the environment. They are illustrated with colored oval zones. B: Schema illustrating the position of the hippocampus (orange), in a rodent's brain. C: Color coded firing rate maps of one hippocampal place cell (yellow: low rate; purple: high rate). The same place cell is depicted in different conditions. The place field of this cell changed its location following a modification of the color (black or white) of a wall mounted cue card. (Adapted from [Bostock et al. 1991])

This common interpretation of place cells coding suggests that they directly code for a place in an environment (its place field) and that their firing could be interpreted as a detector informing if the animal is located at a particular place or not. This activity is classically studied on time-averaged firing activity of the cell in relation to the position of the animal. This average activity is then considered as the *tuning curve* of the neuron for space and called a *rate map* [McNaughton et al. 1983].

In a given environment, each place cell fires at distinct positions so that the simultaneous activity of a population of place cells can be used to reliably infer the position of the animal [Wilson and McNaughton 1993; Brown et al. 1998]. Place cells are not topographically organized [O'Keefe et al. 1998; Redish et al. 2001] [but see: Hampson et al. 1999] in the sense that anatomically close place cells can either code for distant or nearby regions of an environment [O'Keefe 1979; Redish et al. 2001]. Despite this lack of topographical organization, the size of the place field progressively increases from the dorsal to the ventral pole of the hippocampus [Jung et al. 1994; Kjelstrup et al. 2008]. Similarly, a difference in place field size can be observed along the proximo-distal axis of CA1 [Henriksen et al. 2010](see § 4.4). These gradients of place field size suggest that space is coded at different scales along the longitudinal or transverse axis of the hippocampus. This difference in scale could be linked to the distinct pattern of connectivity with the medial and lateral entorhinal cortex along these axes (see § 2.3).

The spatial firing of place cells is generated and shaped by a myriad of external and internal factors that I will review in a later section of this manuscript (§ 4). The role of place cells as a building block of a neuronal spatial map is now corroborated by a large body of work initiated by O'Keefe and Dostrovsky [1971]. Since then, place cells activity have been shown to contribute to the animal's spatial behavior [Lenck-Santini et al. 2001; Girardeau et al. 2009; De Lavilleon et al. 2013; Trouche et al. 2016]. Despite their strong spatial modulation, place cells are influenced by various spatial and non-spatial factors (see § 4) such that the "perfect place" portrayed above by Muller et al. [1994] might not exist. Furthermore, the fact that "place-cell like" activity has been found for numerous non-spatial variables [Pastalkova et al. 2008; Aronov et al. 2017; Radvansky and Dombeck 2018] and outside of the hippocampus [Jankowski et al. 2015; Hok et al. 2018; Saleem et al. 2018] casts some doubts on a purely spatial function of this region. Consequently, no consensus on the function and nature of the coding supported by the hippocampus is currently commonly accepted [Eichenbaum 2017].

### 3.1.3 Head direction cells

In January of 1984, Dr James Ranck Jr. implanted electrodes in a group of rats attempting to record the activity of neurons in the subiculum [Ranck 2005]. In reality, he later realized that his electrodes deviated from their original goal to end up in a neighboring region, the postsubiculum. The morning of the January 15th, he lowered an electrode in one of his rat and encountered the striking activity of an head direction cell [Ranck 2005; Dudchenko et al. 2019]. The firing of this cell was modulated by the absolute direction in the horizontal plane (yaw), independent of pitch, roll, and location of the animal. Also, he noticed that the firing was extremely robust and independent of the behaviors observed the afternoon of the recording<sup>3</sup>. Head direction cells were then more carefully described and quantified in recordings from rats dorsal presubiculum [Ranck 1984; Taube et al. 1990a,b]. Since its discovery in rats, they have been reported in other mammals like monkeys, mice or bats [Rolls et al. 1999; Yoder and Taube 2009; Finkelstein et al. 2015] and even some invertebrates [Seelig and Jayaraman 2015; Kim et al. 2017]. These cells are thought to provide directional information akin to those of a compass. Head direction cells fire in a particular direction no matter where the animal

---

<sup>3</sup> Interestingly, James Rank later reported that this cell encountered serendipitously was certainly not the "first" head direction cell recorded in his lab. When he talked to his colleagues the day after, John Kubie remembered that someone uncovered a similar cell before. *"I had no recollection of the cell, but when we played the tape, lo and behold, it was a head direction cell, unappreciated at the time. This cell was in stratum oriens of CA1. If we had picked up on it, we would not have gotten anywhere (since such cells have only rarely been found there since). I guess we were lucky to let it slip by."* [Ranck 2005]

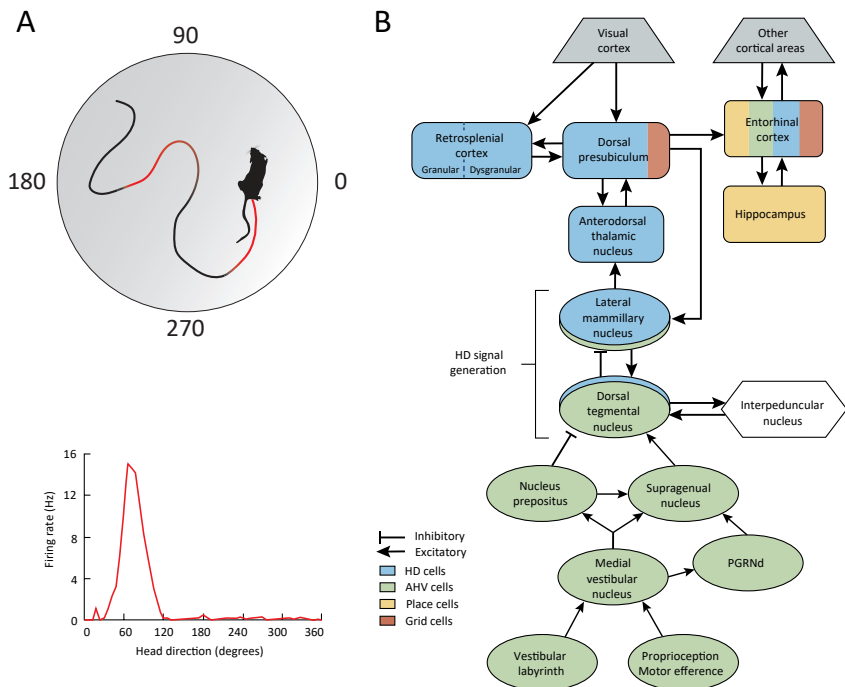


**Figure 3.2:** Schematic illustration of a rodent foraging in a circular arena. **A:** While doing so, a particular type of cells is activated when the animal is facing a specific direction in the environment. The path of the animal is depicted with a black line becoming red when the head direction cell is activated (**top**). The activity of this cell during the whole recording session can be represented with a tuning curve as a function of the direction faced by the animal (**bottom**). **B:** Diagram representing the connections between the main areas containing head direction, angular head velocity, place and grid cells. (part B is adapted from [Cullen and Taube 2017])

is located (Figure 3.2 - A ). Contrarily to a compass these cells do not seem to be modulated by the earth magnetic field but rather by landmark cues [Taube 2007]. Each HD cell is tuned to a different direction, and a population of such cells uniformly represents all directions [Taube et al. 1990a]. Their firing is thought to provide a continuous representation of the animal's heading angle.

Although head direction cells were initially uncovered in the presubiculum, they have now been recorded in several other areas of the limbic system as: the thalamus (the anterior dorsal [Taube 1995] and the lateral dorsal [Mizumori and Williams 1993] thalamic nuclei), entorhinal cortex [Sargolini et al. 2006; Giocomo et al. 2014], retrosplenial cortex [Chen et al. 1994; Cho and Sharp 2001; Chen et al. 2004] and lateral mammillary nuclei [Stackman and Taube 1998] (Figure 3.2 - B ). The head direction signal is mostly generated by two complementary pathways. The first relies on self-movement cues integrated from brainstem areas to the anterodorsal thalamus, dorsal presubiculum, and entorhinal cortex [Taube 2007](Figure 3.2 - B ). In addition, visual landmarks information is integrated into this circuit from the visual cortex directly projecting to the dorsal presubiculum (and to a lesser extent, the retrosplenial cortex), which then exerts

top-down control with projections to the lateral mammillary nuclei [Yoder et al. 2011](Figure 3.2 - B ).

Theoretically, the generation of the head direction signal can be explained by a "ring" attractor network [Skaggs et al. 1995; Redish et al. 1996; Zhang 1996]. In this model, neurons are virtually arranged in a circular fashion, sorted according to the value of their preferred direction. The position of a neuron in the ring will impact the connectivity of each neuron. While adjacent cells with close preferred head direction excite each other, distant cells tend to inhibit each other (indirectly through global feedback inhibition). This connectivity pattern will lead to the emergence of an instantaneous activity of the network reflecting the head direction of the animal. According to this model, the relative difference of preferred direction between pairs of cells is hardwired, and thus should not change between brain state or behaviors. Interestingly, experimental studies have provided evidence in favor of these hypothesis [Peyrache et al. 2015; Seelig and Jayaraman 2015; Kim et al. 2017; Chaudhuri et al. 2019]. Nevertheless, more "softwired" activity patterns of head direction cells have also been reported [Knight et al. 2014; Jeffery et al. 2016; Jacob et al. 2017; Kornienko et al. 2018] suggesting that fine mechanisms of head direction signal processing could subserves multiple functions [Taube 2007; Cullen and Taube 2017; Peyrache et al. 2017].

### 3.1.4 Grid cells

In 2004 Fyhn et al. [2004] discovered that some neurons of the medial entorhinal cortex exhibited a spatially modulated firing characterized by multiple firing fields. In a follow up study Hafting et al. [2005], described that the spatial firing of these neurons was organized in a periodic triangular array tilling the entire surface of the available space, thus endowing these cells the name of *grid cells*. After this discovery in rats, grid cells were also recorded in mice [Fyhn et al. 2008], Egyptian fruit bats <sup>4</sup>[Yartsev et al. 2011] and humans [Doeller et al. 2010; Jacobs et al. 2013]. Since their discovery in the superficial layers of the MEC, grid cells have also been recorded in presubiculum [Boccara et al. 2010]. In superficial layers of MEC, grid cells are present in both categories of principal cells (stellate and pyramidal cells)[Sun et al. 2015] [but see; Tang et al. 2014]. In deeper layers of the MEC, as well as in the presubiculum, grid cells co-localize with head direction cells and "conjunctive" cells, which combine grid spatial firing with a directional tuning [Sargolini et al. 2006](Figure 3.3 - D ).

The periodic firing of grid cells can be characterized by three main characteristics: scale, orientation and offset (Figure 3.3 - A ). Grid cells are organized in modules with increasing scale from dorsal to ventral MEC [Barry et al. 2007; Mathis et al. 2012; Stensola et al. 2012](Figure

---

<sup>4</sup> In Yartsev et al. [2011] bats were crawling for food pellets on a planar arena.

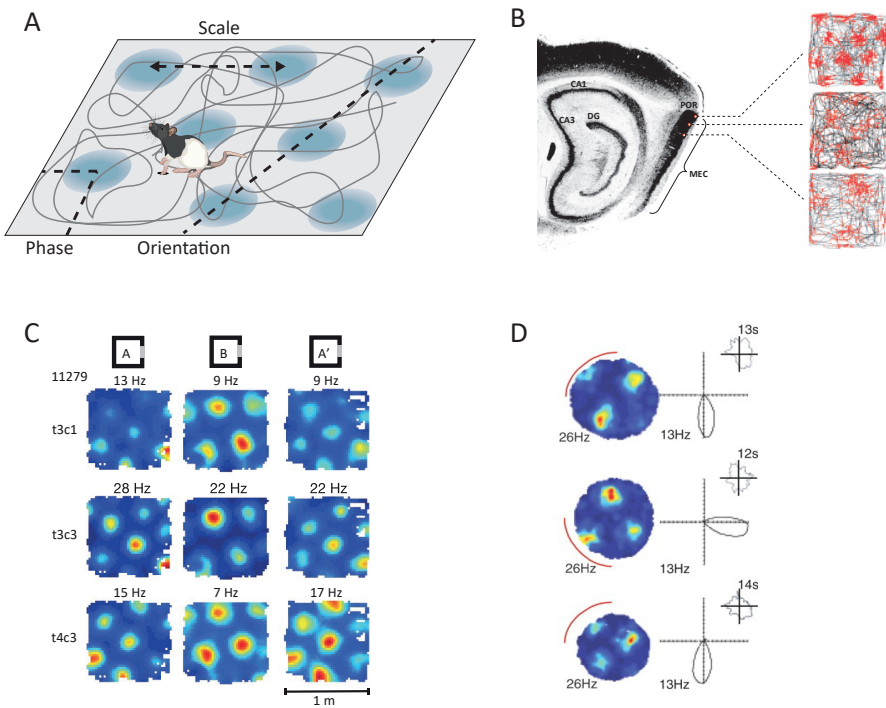


**Figure 3.3:** A: Illustration of a rat foraging in a square arena. While the animal forages in this arena (path in grey line), some cells of its entorhinal cortex are activated at multiple locations that form a grid pattern. Grid cells can be characterized by three parameters. The scale is the spacing between field. Orientation is the angle of the grid pattern. The phase measures the offset between a reference point and the grid pattern. B: Grid cells are organized in modules with increasing scales from dorsal to ventral MEC (Adapted from [Stensola et al. 2012]). C: If exposed to a new environment, grid cells remap in a coherent way (Adapted from [McNaughton et al. 2006]) D: Some cells from deep layers of the entorhinal cortex manifest a head direction signal in addition to their grid pattern. In this experiment, when the cue card was rotated by 90°, both the grid map and the head direction vector rotated accordingly, suggesting that both were anchored to the external cues. (Adapted from [Sargolini et al. 2006]).

3.3 - B ). Within a module, neighboring grid cells will share the same scale and orientation. Additionally, recent work using calcium imaging during virtual navigation uncovered a topographical organization of grid cells phases within modules as the anatomical distribution of grid cells matched their spatial tuning phases [Gu et al. 2018].

Unlike hippocampal place cells, entorhinal grid cells remap in a coherent way [Fyhn et al. 2007](Figure 3.3 - C ). The relation between the firing of pairs of cells is conserved in novel environment and even during sleep [Gardner et al. 2019; Trettel et al. 2019]. This suggests that grid cells are embedded in a low dimensional continuous attractor network [Burak and Fiete 2009; Yoon et al. 2013; Burak 2014] mostly governed by recurrent connectivity between grid cells [Almog et al. 2019; Gardner et al. 2019]. However, principal cells (at least stellate cells in layer II) do not interact directly with one another but indirectly via inhibitory interneurons, so that stable grid firing patterns are likely to emerge from an inhibitory recurrent network [Couey et al. 2013;

Pastoll et al. 2013]. The apparent rigidity of the grid pattern instigated multiple theories of grid cells function. The first was that grid cells could be used for self-location similarly to place cells [Fiete et al. 2008; Mathis et al. 2012]. Also, they could provide a substrate for a metric of space, a preconfigured path integrator used to link multiple locations in an environment [McNaughton et al. 2006; Burak and Fiete 2009; Gil et al. 2018] or to compute vector-based navigation [Kubie and Fenton 2012; Bush et al. 2015; Banino et al. 2018].

However, recent works have highlighted that the grid code was not as rigid as previously thought. First, the grid pattern can change over time. In a novel arena, the grid pattern is initially irregular and expanded (increased scale) and several exposures are needed for this pattern to regain a spatial selectivity and scale similar to baseline sessions in a familiar environment [Barry et al. 2007; Keinath et al. 2018]. Second, environmental cues, in particular boundaries, can influence the regularity of the grid cell pattern [Krupic et al. 2015; Stensola et al. 2015; Krupic et al. 2018; Hägglund et al. 2019]. Also, grid cells appear to be highly sensitive to external cues as they are strongly disrupted in the dark in mice and even each grid field can have distinct properties and be influenced differentially by external cues [Reifenstein et al. 2012; Chen et al. 2016; Pérez-Escobar et al. 2016; Ismakov et al. 2017; Gerlei et al. 2019]. Recent works also showed a sensitivity to non-metric cues [Marozzi et al. 2015], and an embedding of object related [Høydal et al. 2019] or goal related activity in grid firing [Boccara et al. 2019; Butler and Hardcastle 2019].

Thus, albeit their apparent regularity and the striking correspondence of their firing with seminal models of spatial navigation [McNaughton et al. 1996], the role of grid cells is still unclear. Their regularity is now being challenged by studies highlighting functional differences in the population of grid cells, contextual sensitivity or inhomogeneous spatial firing [Reifenstein et al. 2012; Pérez-Escobar et al. 2016; Ismakov et al. 2017; Miao et al. 2017]. Recent works comfort their involvement in path integration [Parron and Save 2004; Gil et al. 2018; Jacob et al. 2019] while other suggest that their role could extend beyond pure spatial cognition to support navigation functions in abstract or conceptual space [Constantinescu et al. 2016; Aronov et al. 2017; Behrens et al. 2018; Bellmund et al. 2018].

### 3.2 PHASE CODING OF SPACE

A fascinating rhythm animates the hippocampus as much as its literature since early electrophysiological recordings in this area [Green and Arduini 1954; Vanderwolf 1969]. "Theta" rhythm is a slow oscillatory activity around 8 Hz (more broadly 5 – 12 Hz) which dominates the Local Field Potential (LFP)<sup>5</sup> during locomotion and during periods of active engagement in the environment, such as rearing, exploring

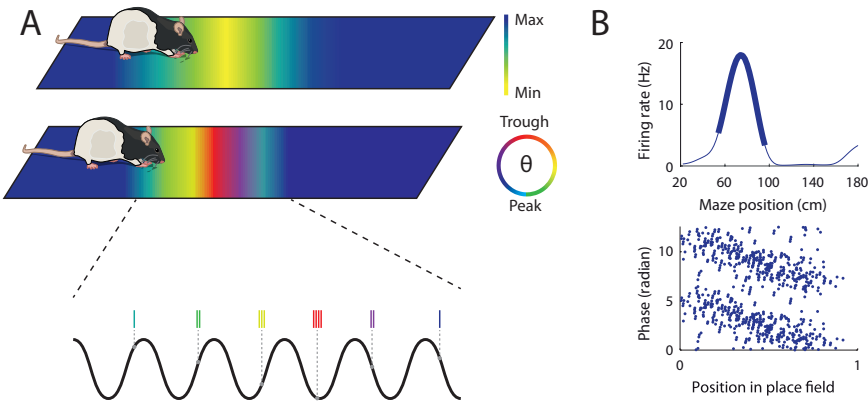


**Figure 3.4:** **A-top:** Depiction of a place cell increasing its firing rate at a specific location in the environment: its place field (the intensity of the firing is represented from blue, minimal firing, to yellow, maximal firing). **A-bottom:** While the rat crosses the place field, the place cell fires at earlier theta phases as the animal progresses though the place field. **B-top:** The activity of the place cell can be averaged for the whole recording session into a rate map. Here the place cell fires significantly more than noise, forms a place field, between 60 and 100 cm on the linear maze. **bottom:** The theta-phase of each spike (in radian) plotted against the normalized progression through the place field show a negative correlation between these two variables. This phenomenon is called theta phase precession [Bourboulou et al. 2019].

objects, and preparation for movement [Green and Arduini 1954; Vanderwolf 1969; Foster et al. 1989]. A large body of work uncovered its crucial role in synchronizing and organizing information processing in the hippocampus [Buzsáki 2002; Malhotra et al. 2012; Colgin 2013; Lisman and Jensen 2013; Jaramillo and Kempter 2017]. One of the most curious theta-related phenomenon was discovered by O'Keefe and Recce [1993]. They observed that the firing of action potentials of individual hippocampal neurons was correlated to the phase of the ongoing theta oscillation. They noticed that the burst of activity elicited when the rat entered a place field was out of synchrony with the theta oscillation (contrarily to out of field spikes). As the rat traverses the place field, the cell would fire progressively at earlier phases of the theta cycle (Figure 3.4 - A-B ). O'Keefe and Recce named this advancement of spike phase relative to the progression through the place field: "phase precession". This phenomenon is present in dorsal CA1 while animal foraged in linear tracks but also in open arenas [O'Keefe and Recce 1993; Huxter et al. 2008] and in hippocampal interneurons [Maurer et al. 2006; Ego-Stengel and Wilson 2007]. Furthermore, it is not exclusive to the hippocampus and has been observed in several areas of the hippocampal formation like the subiculum [Kim et al. 2012] and entorhinal cortex [Jeewajee et al. 2008; Mizuseki et al. 2009]. Perturbation experiments suggest that it could have an extrahippocam-

<sup>5</sup> LFPs are intra cerebral recordings of extra cellular electrical activity up to 40 kHz thanks to microelectrodes. It reflects the summed contributions of synaptic inputs, membrane potentials, and synchronous spiking recorded from a very small neuronal volume. Its generation is also influenced by the neuronal arrangement and morphology. See Buzsáki et al. [2012] for a detailed review.

pal origin [Zugaro et al. 2005]. It has also been described outside of this formation in dorsal lateral geniculate nucleus [Hok et al. 2018], prefrontal cortex [Jones and Wilson 2005] and striatum [Meer and Redish 2011].

This correlate of the animal position inside a place field with theta phase directly suggested the existence of a spatial phase code [O'Keefe and Recce 1993]. Simultaneous use of rate and phase codes can lead to a more accurate estimation of the current position of the animal [Brown et al. 1998; Jensen and Lisman 2000; Reifenstein et al. 2012]. Taking into account phase information allow to disambiguate entry and exit through a place field, even if the animal is engaged in backward travel movements [Cei et al. 2014; Drieu and Zugaro 2019]. This rate code is often studied on time averaged data but can also be observed during individual run through a place field [Schmidt et al. 2009]. At this single-lap level, phase precession exhibited a large trial-to-trial variability but was stronger than in pooled data. Most of this variability could not be explained by behavioral factors and remains to be elucidated. However these results suggest a robust phase code at each traversal of a place field. One implication of this single-lap phase precession robustness despite potential speed variation, is that the frequency of the cell's intrinsic oscillation should adapt to the time spent by the animal inside the place field. Phase precession occurs over a limited range of the theta rhythm (few theta cycles), but place fields can have different sizes or the animal's speed can change through successive passes through the place field [Jung et al. 1994; Geisler et al. 2007; Schmidt et al. 2009]. A mechanism is necessary to conserve the rate of phase precession despite changes in field's size or speed. Experimental studies have shown that such mechanism is given by a modification of the cellular intrinsic oscillation frequency, such that at faster running speeds or for smaller place fields, place cells oscillate at a higher frequency and emit more spikes per cycle [Geisler et al. 2007; Diba and Buzsaki 2008]. Thus, phase precession allows a robust coding of place information independently of rate or behavioral variation at the single lap level. Nevertheless, its role supporting the coding of information inside or outside the hippocampus is still unclear [Malhotra et al. 2012; Jaramillo and Kempter 2017].

# 4

## RESOLUTION OF SPACE CODING

---

"Our brain is mapping the world. Often that map is distorted, but it's a map with constant immediate sensory input."

*E. O. Wilson*

We introduced in the previous chapters the notions that animals could use an internal representation of their surrounding space in order to navigate in their environment. This cognitive map can then be used by the animal to locate itself but also to make inferences about its environment: plan trajectories, shortcuts or find hidden goals [Tolman 1948; O'Keefe and Nadel 1978; Redish 2016]. In order to perform these inferences, this "cognitive map" should reflect different components of the external world like the multitude of borders or landmarks populating the environment. Nevertheless, the link between the internal and external world does not need to be a one to one relation [Leonard and McNaughton 1990]. Numerous investigations suggest that the brain minimizes the metabolical resources used to encode a stimulus while maximizing the amount of information encoded about it [Attneave 1954; Barlow 1961; Laughlin et al. 1998; Laughlin and Sejnowski 2003]. This efficient organization of relevant sensory information could allow an easier formation, maintenance and use of this internal model [Barlow 1961; Simoncelli and Olshausen 2001; Simoncelli 2003; Mathis et al. 2012; Mlynarski and Hermundstad 2018].

For place cells, we could thus wonder if the number of activated cells and the way they are coding for space could be modulated by the amount and type of external cues present in the environment. For example, will you represent the room you are currently in with the same resolution than if it was empty? If this is the case, how your internal representation of space will adapt to the introduction of a new objects or furniture inside this room?

Defining spatial resolution is nevertheless a complex question notably because of the different levels at which we can approach it. In order to study the fidelity of an internal representation, an observer could either focus his attention on its individual building blocks or on the whole population of coding cells. To make an analogy, imagine a conductor trying to find out why his ensemble does not play a piece of music perfectly on a particular day. Discordance could emerge from the fact that many musicians have not tuned their instruments or have neglected their practice. However, even a "perfect" musical collective

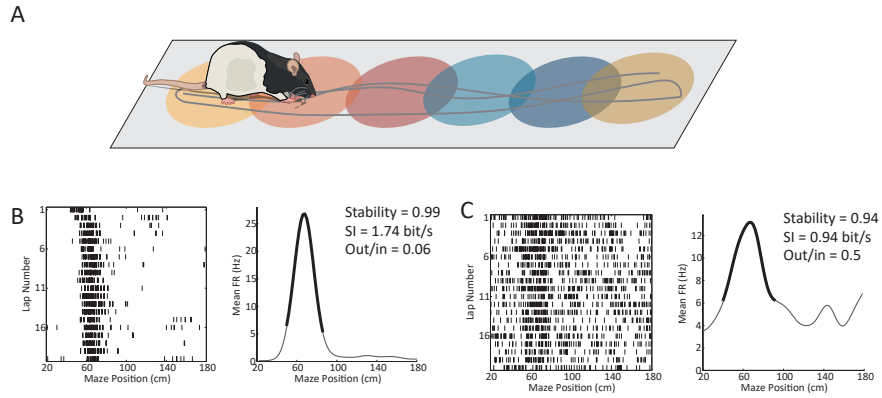


**Figure 4.1:** A Schema illustrating the activity of different place cells while a rat forages in a linear environment. The path of the animal is depicted with a grey line. Different place fields are illustrated with colored oval zones. **B-C;** Left: Lap per lap raster plot of two place cells Right: time averaged mean tuning curve of the place cells. The bold part of the tuning curve depict the location of the place field. The place cells in **B** has more Spatial Information (Spatial Information (**SI**)), and a better Out of field versus In field firing Ratio (Out/In) than the cell represented in **C**

could perform poorly because of the fact that they do not play in a coherent way. Consequently, the resolution of space coding can be defined at two complementary levels, considering cells individually or collectively. In the next chapter I will first describe what are the different ways to study the resolution at an individual cell level by characterizing its spatial modulation. Next I will describe the sensory or non-sensory factors influencing the spatial tuning of place cells. And finally, I will conclude this chapter by developing why and how population decoding can help us to study spatial resolution at the population level.

#### 4.1 ACCURACY OF THE CODING AT THE SINGLE CELL LEVEL

##### 4.1.1 *Classical metrics of tuning curve quality*

In order to analyze the precision with which an environmental feature (such as the animal position) is coded by neurons, scientists can focus on the properties of time-averaged or trials-averaged spiking data. In Figure 4.1, we can observe two place cells recorded in an animal running in a linear corridor. These two cells exhibit a clear space modulation of their firing, in both cases they exhibit a clear increase of their firing rate at a specific location in the corridor. Nevertheless, we can also observe that these cells are not equally tuned to space. The cell in Figure 4.1 - B has a sharper tuning, with a higher peak firing and a better signal to noise ratio than the cell depicted in C. In the place cells literature, classical metrics of place cells firing quality are:

- **selectivity:** the width range in sensory space where the cell fires significantly more than the noise. For place cells, a change in selectivity is related to a change in place field width.
- **peak height:** amplitude of the firing rate peak inside the place field.
- **signal to noise ratio:** measured by dividing the mean firing rate outside the place field by the firing inside the place field. This measure informs how much the place field is dissociated from noise.

Albeit informative, these metrics are heavily dependent on the detection method of the place field<sup>1</sup>. Furthermore, we only focused here on the most used metrics to place cells quality estimation. A more detailed description of neuronal encoding of information in the brain can be found in the following comprehensive review [Rolls and Treves 2011]. We will nevertheless, in the next sections detail quality measures that take into account the whole tuning of the cell in relation to space (§ 4.1.2) and the reproducibility of the firing pattern between the different presentation of the same stimuli (§ 4.1.3).

#### 4.1.2 Information theory for place cells coding

A common information measure used to quantify the information content of a place cells is the *Spatial Information* (SI; in bit/spike) introduced by Skaggs et al. [1993, 1996]:

$$SI_{spike} = \sum_{i=1}^N \left( \frac{FR_i}{FR} * \frac{OT_i}{OT} * \log_2 \left( \frac{FR_i}{FR} \right) \right) \quad (4.1)$$

where N is the number of spatial bins,  $FR_i$  is the mean firing rate determined in the  $i^{th}$  spatial bin, FR is the mean firing rate,  $OT_i$  is the mean occupancy time determined in the  $i^{th}$  spatial bin, OT is the total occupancy time based on the mean occupancy time vector.

This measure reflects the amount of information conveyed by a spike about the position of the animal in the maze [Shannon 1948]. This metric is not dependent on the detection of the place field and includes the whole firing rate of the cell as a function of space. Although very valuable, this measure has some drawbacks. First it only considers the time-averaged firing rate as a function of space (tuning curve). Consequently, two cells with the same mean firing rate but a different distribution of spike trains across laps (firing during all the laps or half of them) will carry the same amount of spatial information. Second, this metric is sensitive to background activity. A cell with

---

<sup>1</sup> It exists no consensus on a standard way to detect place cells. This could lead to difference in quality reported by different laboratories.

a clearly defined place field will be disadvantaged if it has a high baseline activity. Thus, this index has to be used alongside other quantification of the coding quality as seen in section 3.1. To overcome these potential bias, Souza et al. [2018] adapted the original Spatial Information measure to consider lap-per-lap variation of firing and basal firing rate. This adaptation of the original *Mutual Information* by Shannon [1948] is more consistently correlated with the capacity of decoding the animal position, which directly relates to the amount of spatial information conveyed by the cells [Quian Quiroga and Panzeri 2009].

#### 4.1.3 Short term variability of place cells activity

Firing rate maps and consequently place fields, as discussed in the sections above, are usually constructed by accumulating neuronal activity over several minutes [McNaughton et al. 1983]. They give an impression of a rigid space coding in a particular environment, each pass through the same location giving the same population activity. Even if the hippocampal spatial code can be stable across days [Muller et al. 1987; Ziv et al. 2013; Rubin et al. 2015; Hayashi 2019] or weeks [Thompson and Best 1990; Kinsky et al. 2018], it is in reality, highly variable at a short time scale. These variations can be due to random noise (introduced by one or multiple uncontrolled factors) or could reflect more subtle temporal dynamics of place cells coding [Johnson et al. 2009; Poucet et al. 2012; Poucet et al. 2015]. Though Muller et al. [1987] already noticed that a place cell could be silent when passing through its place field, the first study investigating the "*excess variance*" of firing through place fields was done by Fenton and Muller [1998]. In this study, they compared the firing rate observed through each individual pass inside the place field with a firing rate expected from an inhomogeneous Poisson process. Remarkably, they observed that in a random foraging task, place cells fired with more variability than expected in their place field. For example, during two passes through a place field with the same trajectory, a place cell could emit ten spikes for the first and none for the second. This phenomenon called "*overdispersion*" was later interpreted as a phenomenon reflecting a switch between different reference frames. In a follow up study Fenton et al. [2010] trained rats in different behavioral tasks that could be solved using one or several reference frames (distal / local cues and/or self-motion). They showed that overdispersion was decreased when the animal performed the task using only one reference frame (distal cues) while it was increased when the animal performed the task using several reference frames. Interestingly, by analyzing population activity of place cells at each time point, they could identify different uncorrelated ensemble states (that could correspond to distinct reference frames) alternatively switched on and off within a period of about one

second [Lánský and Vaillant 2000; Lánský et al. 2001; Olypher et al. 2002; Fenton et al. 2010]. This study, as others, supports the hypothesis that the hippocampus could maintain and dynamically switch between multiple maps (sub-maps or reference frames) of the same environment [Worley 1992; Harris et al. 2003; Harris 2005; Jackson and Redish 2007; Kelemen and Fenton 2010; Kay et al. 2019]. This process could alter the apparent spatial coding resolution if the existence of multiple reference frames is not taken into account.

Analogous short term alternation of hippocampal coding has also been described by Jezek et al. [2011] in a study investigating how an animal switched between distinct maps of two environments after a "teleportation" in a new arena. In this study, the animal was heavily trained in two similar arenas (A and B) that were characterized by different visual cues (light patterns on the walls). In CA3, this behavioral assay was able to generate two distinct, minimally overlapping (nearly orthogonal) maps of both environments. The set of place cells active in A was different than the one active in B<sup>2</sup>. During the test session performed while the rat was foraging in arena A, the light patterns were switched from the A to the B configuration in order to artificially "teleport" the rat in arena B. After each teleportation, Jezek et al. observed a "flickering" between the A and B spatial maps. These flickers alternated between the A and B neuronal populations and were paced by the theta rhythm. Recently, Posani et al. [2018] showed that the position of the animal could be reconstructed at any time with an accuracy comparable to fixed-context periods, even during flickering periods. This was made possible thanks to the decoding of the spatial context, at each time step, before applying the position decoder. In other words, position decoding can be accurate even during flickering if it is done in the right reference frame.

Besides this hypothesis explaining overdispersion as a switch between distinct reference frames or spatial maps, it has also been proposed that single lap variability of place cells' firing rate could code for trial-related information through single lap rate remapping [Allen et al. 2012]. In this study, the authors showed that task-related information was represented via firing rate modulation of spatially stable place cells without modification of the location of their place field. Altogether these studies highlight the fact that the place cells code is highly dynamic on a short time scale so that it is important to take into account the behaviorally relevant reference frames and/or task specific information to avoid mistaking refined information processing for random noise [Johnson et al. 2009].

---

<sup>2</sup> Cells firing in both A and B conditions had uncorrelated spatial firing.

#### 4.1.4 Place cells activation and spatial resolution

Early reports of extracellular recordings in the hippocampus stated that a large majority of CA1 neurons were place cells [O'Keefe and Conway 1978]. Thompson and Best [1989] were the first to address extensively the problematic of "silent cells" in the hippocampus. Silent cells are normally not accessible through classical extracellular recordings because this technique can only record spiking cells with a sufficient level of activity to be detected and dissociated from noise. In this study, Thompson and Best notably used barbiturate anesthesia (among other techniques) to maximize the activity of CA1 cells in order to identify them. From their pool of spiking cells, they observed that only two third were active during subsequent behavior. Recent technological developments such as intracellular patch-clamp recordings or two-photon microscopy in navigating animals, allowed a better estimation of the true percentage of silent cells as they are not biased towards the recording of firing cells [Lee et al. 2006; Harvey et al. 2009; Lee et al. 2009; Dombeck et al. 2010; Villette et al. 2015]. Using intracellular recordings of neurons, it was even possible to study the subthreshold activity of silent neurons in freely moving animals [Chorev et al. 2009; Lee et al. 2009; Epsztein et al. 2011]. Through this method, it has been shown that intrinsically more excitable pyramidal cells (*e.g.*: having a lower spike threshold or increased burstiness; assessed before exploration) would be more likely to form a place field in a new environment than silent less excitable cells [Epsztein et al. 2011]. Recent works in the team further showed that during movement or immobility, the membrane potential of CA1 hippocampal cells was differently modulated in two populations of cells in mice foraging in a familiar virtual linear track (see iv).

The increased excitability in a particular population of cells suggests that only a portion of the neuronal ensemble is primed in a particular moment. If the animal had to form two spatial maps in a time period where the same population is primed, then the spatial maps might overlap more than if it was formed at very different time points. Interestingly, Cai et al. [2016] showed that this overlap was particularly efficient to link distinct contextual memories that occurred close in time. This was demonstrated by showing that fear conditioning in an environment A could be transferred to a neutral environment B only if the spatial maps of A and B were formed the same day but not if they were formed one week apart. In CA3, Alme et al. [2014] recorded the activity of the same population of place cells in eleven different rooms. They showed that neuronal ensembles activated in the different environments were minimally overlapping, possibly to maximize the storing capacity of the network. Only a small proportion of cells were active in many rooms while a majority fired only in one environment and thus allowed the orthogonalization of the neuronal substrate

active in each room [Alme et al. 2014]. At the sight of these studies, the partial priming of a population of cells to code for new environments could link different experiences close in time with highly active cells while distinguishing them with cells only firing in one environment.

The fact that at each moment, the hippocampal network contains a pool of neurons with a higher excitability could increase the proportion of spatially modulated neurons in order to cope with a more complex environment. We have observed such increase in the proportion of spatially modulated cells in a virtual linear track enriched with local visual cues in comparison to a linear track impoverished in visual cues (see § ii ). This increase in place cells recruitment has also been observed in rats exploring a new very large environment [Rich et al. 2014]. In this experiment, some cells that were originally silent in a small environment became active when this environment was enlarged. In the large environment, the distribution of field propensity<sup>3</sup> followed a gamma distribution. Briefly, a vast population of cells will have a low activation level and form one or few place fields while a minority will have a high number of place fields in the large environment [see also: Buzsáki and Mizuseki 2014; Rich et al. 2014; Lee et al. 2019]. Recent evidence also suggest that the intrinsic properties of hippocampal neurons could be linked to their activation but also to their spatial selectivity [Epsztein et al. 2011; Schmidt-Hieber and Nolan 2017]. Grosmark and Buzsáki [2016] described that a minority of neurons with a high propensity also exhibited a high firing rate and a low spatial selectivity in a new environment. These cells were called "rigid cells" as they participated with a high probability in hippocampal neuronal sequences during both preplay (during the sleep before the new environment exposure) and replay (during the sleep after the new environment) [Lee and Wilson 2002; Karlsson and Frank 2009; Dragoi 2013]. These rigid cells differed from "plastic cells" with lower firing rate that acquired progressively a high spatial selectivity during exploration and that were recruited more during neuronal sequences after environmental exposure (replay)[also see Ven et al. 2016]. These two subgroups of cells could be the building blocks of a nested coding by hippocampal CA1 neurons by coarse grained rigid cells and finer grained plastic cells [Mizuseki and Buzsáki 2013; Buzsáki and Mizuseki 2014].

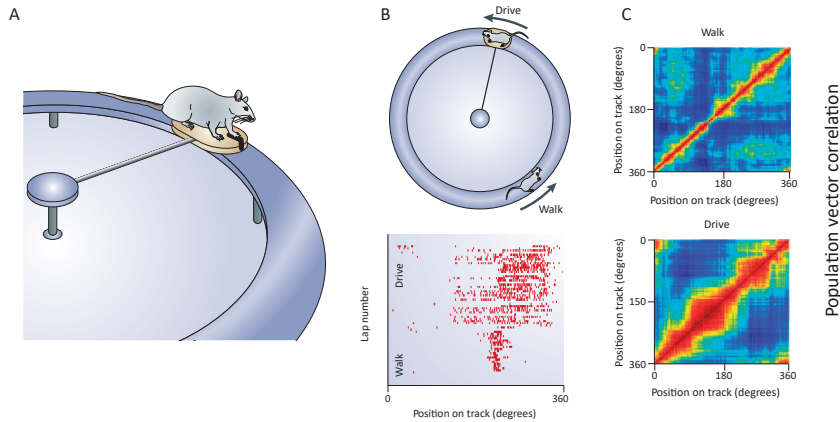


**Figure 4.2:** A: Schematic representation of the apparatus used in Terrazas et al. [2005]. Rats were trained to press a lever in order to move a mobile platform around a circular track and stop at a specific location to obtain a reward. B: Laps of driving were interspersed with laps of walking (top). When the rat was driving the platform, the place fields were approximately three times bigger than during walking laps (top). C: Population vector correlation matrices highlighting the fact that during walk population vectors became decorrelated more quickly as a function of space than during driving. (Adapted from Terrazas et al. [2005] and McNaughton et al. [2006])

## 4.2 HOW DO SENSORY CUES MODIFY THE PRECISION OF SPACE CODING IN THE HIPPOCAMPUS

### 4.2.1 *Self-generated cues*

One of the simplest strategies to navigate in an environment is to rely only on self-generated information, by integrating the length and the angle of each animal's movements. This process called, *path integration* derived only from the computation of cues generated by an animal's own movements, also called idiothetic cues: proprioception, optic flow, vestibular information and efference copy of motor commands [McNaughton et al. 2006]. Navigating exclusively relying on idiothetic cues is prone to cumulative errors that can be corrected by the use of allocentric information [Gallistel 1990; Hardcastle et al. 2015; Jayakumar et al. 2019]. Despite this, path integration could be very useful in a new environment where the spatial relationships between external sensory information have not yet been learnt. An early theory postulated that the hippocampus was part of a preconfigured path integrator network that could represent position using place cells linked by self-motion information [McNaughton et al. 1996]. According to this path integrator model, the size of the place fields, and by extension the scale at which space is represented in dorsal hippocampus, was thought to be controlled by self-generated sensory information. Experimental investigations performed to test this theory first showed that idiothetic

<sup>3</sup> **Propensity:** probability of a cell to form a place field in an environment. A cell with a high propensity will be more active and tend to form multiple fields in an environment.

information appeared to be important for place cells activation. Indeed, passive exploration of an environment with limb restriction has been shown to dramatically reduce the number of active place cells in dorsal hippocampus [Foster et al. 1989]. A later study conducted by Quirk et al. [1990] has shown that in addition to being necessary, idiothetic information was sufficient to form place fields in rats placed in total darkness in circular arena. These fields were maintained at a similar scale during subsequent illumination of the arena. Subsequently, a deeper insight into place cell coding in the dark was brought by Markus et al. [1994]. In this work they showed that place cells in the dark had similar spatial scale but a decreased "selectivity"<sup>4</sup> (signal to noise ratio) and "reliability"<sup>5</sup> (stability). This decrease in place cells coding quality was conjointly observed for "theta cells" (likely putative interneurons). Interestingly, in this study, rats with more stable place fields also made fewer error (re-entry in the same arm in a eight-arm radial maze), suggesting a link between place cells quality and task performance. In Terrazas et al. [2005], the authors demonstrated that a systematic alteration of self-motion information affected the scale of dorsal CA1 place fields. In this study, rats were trained to move forward in a circular track by pressing a lever to activate a mobile platform in order to find a reward location. Laps of assisted movement (driving the platform) were interspersed with laps of walking. In comparison to the walking condition, the proportion of place cells and their peak firing rates were reduced during the driving condition. Strikingly, place fields were also approximately three times larger than in the walking condition. The driving condition allowed the reduction of ambulatory signals while preserving a normal optic flow and vestibular input. Further reduction of vestibular signals by rotating the entire environment around the animal sitting on the stationary car reinforced the scale augmentation of the place fields. This additional increase in scale was more modest than the change of scale driven by the suppression of self-ambulatory signals. These results have been corroborated by other studies using totally passive navigation on mobile platforms or motorized robots [Gavrillov et al. 1996; Song et al. 2005]. Altogether, these studies suggest that self-motion plays a crucial part in the definition of the scale at which space is represented in the hippocampus.

#### 4.2.2 *Distal cues*

Distal sensory cues are known to be used by rodents to guide navigation [Morris 1981; Morris 1984]. Numerous studies have also shown that they could control the spatial configuration of place fields and the

---

<sup>4</sup> Maximal firing rate/mean firing rate.

<sup>5</sup> Mean Pearson correlation coefficient of standardized firing patterns between pairs of trials.

orientation of the hippocampal spatial map [Muller and Kubie 1987; Bostock et al. 1991; Knierim and Rao 2003; Knierim and Hamilton 2011]. Distal cues are by definition far from the animal and located outside of the explored environment. Their stability in relation to proximal indices gives them an important ability to anchor and orient the cognitive map. However, their impact on hippocampal spatial coding on a quantitative and qualitative aspect is still unclear considering their low sensory resolution<sup>6</sup>. Early works on the impact of distal cues on place cells coding have mainly used comparison between light and dark conditions [Markus et al. 1994; Lee et al. 2012]. Indeed, in these behavioral assays, the landmarks cues available in the light condition were distal<sup>7</sup>. As mentioned in the previous section, stability and spatial information were significantly reduced when the distal cues were removed. In Lee et al. [2012], they also showed that the effects of distal visual cues on place cells stability and selectivity was blocked in *Bax* knock-out mice in which dentate gyrus neural circuitry was selectively disrupted. These results suggest that the Dentate Gyrus might be important in order to align internally generated spatial representation to distal cues.

One problem with the previously described approaches is that in the dark, the animals are deprived of visual cues in general. This drastic manipulation will affect distal visual cues outside of the apparatus as much as more local visual cues such as the borders of the arena. A recent study by Ravassard et al. [2013] used Virtual Reality (VR) in rats to allow finer control of external cues that could carry spatial information about the animal's position in the environment. In their VR system, only distal visual and some self-motion cues<sup>8</sup> provided spatial information to the animal. Their approach was to compare place cells coding in two visually distinct real and VR 1D environments (linear tracks) in order to identify the contributions of different types of cues to CA1 place cells coding. While the percentage of place cells among the active cells was very similar in VR and real environment (96% in VR vs 99% in Real World (RW) ), VR was less efficient to mobilize hippocampal neurons as in VR, only 20% of the CA1 cells were active compared to 45% in the real environment. Their study also reported a weaker spatial information content of place cells in VR against RW. These results proposed that distal and self-motion cues available in VR were sufficient for spatial selectivity but additional sensory information, absent in VR, was important to fully mobilize place cells population. In a follow up study Aghajan et al. [2015] studied the spatial firing of dorsal CA1 cells during a 2D random foraging task in virtual reality. In this work, they showed that distal visual cues alone had a very poor ability to stabilize place cells. Despite this apparent

---

<sup>6</sup> Distal cues are mostly apprehended through vision only and at some points of view.

<sup>7</sup> Visual cues located at 2-3 meters from a 8-arm radial maze in Markus et al. [1994] or two cue cards attached to the curtain that surrounded a circular arena in Lee et al. [2012].

lack of spatial selectivity, place cells in VR were activated during short periods of approximately 2 seconds. These "motifs" exhibited similar temporal structures between RW and VR (duration, firing rate, phase precession), but their location was diffuse in VR, partially explaining the spatial instability of cells firing. Interestingly, in this study a partial improvement of place cells selectivity was triggered by the introduction of proximal visual cues inside the arena. When the animal was trained to locate the position of one or several proximal visual cues (floating pillars) associated to a reward, place cells code was stabilized at the reward location and between reward locations. Nevertheless, this condition does not rule out the possibility that the change in spatial coding could be caused by the use of a distinct navigational strategy (beaconing, stereotyped or goal directed) or by a goal related activity of the place cells. Parallel studies conducted by other groups showed no or little quality differences between a RW and VR environment [Chen et al. 2013; Aronov and Tank 2014]. The inconsistencies in VR studies could be explained by particularities of the VR apparatus used in each studies. The way the animal is fixed could deeply affect the use of vestibular inputs. The animals are body-fixed in Ravassard et al. [2013] and Aghajan et al. [2015] (rats) and head-fixed in Chen et al. [2013] (mice), without the possibility to physically turn their body in the VR apparatus. Conversely, in Aronov and Tank [2014], the authors used a light body fixation enabling the animal to turn physically and in the virtual environment. Likewise, the availability of proximal visual information in the different apparatus could explain the previously described discrepancies between VR and RW. Aronov and Tank [2014] positioned complex visual shapes inside the 2D arena and Chen et al. [2013] used discrete patterns on the sides of the walls. But hitherto, no studies scrupulously compared the effect of distal versus proximal cues on place cells activity in VR. Bourboulou et al. [2019] showed that the introduction of proximal visual cues in virtual reality could strongly activate CA1's spatially modulated cells and their coding quality. This study and the importance of proximal cues on place cells coding will be detailed in the Results section (§ ii).

#### 4.2.3 Proximal cues

##### 4.2.3.1 Visuo-spatial cues

In addition to internal (idiothetic) and distant external information, an animal can use cues in its immediate proximity to navigate in an environment. Proximal cues encompass borders, textures of the floor, intra-maze cues, self-generated odors beyond various others cues. Intrinsically, these information are close to the navigating subject, they

---

<sup>8</sup> In this study [Ravassard et al. 2013] the rat was body harnessed thus restricting its body motion. Idiothetic cues available to the animal were proprioceptive and optic flow.

can be sensorially rich, experienced with multiple sensory modalities and perspectives. However, their perceived orientation and size will change in relation to a moving subject. At first sight, proximal cues seem less suited than distal cues to orient the hippocampal representation [Knierim and Hamilton 2011; Yoder et al. 2011] but they could be very efficient to disentangle nearby locations. In a seminal study, Collett et al. evidenced that gerbils were able to locate a buried seed in the sand in relation to intra-arena landmarks (*e.g.*: two cylinders) in an otherwise impoverished environment [Collett et al. 1986]. Gerbils were able to use one or several intra-maze cues in order to navigate to their goal<sup>9</sup>. A decade later, Gothard et al. recorded place cells activity while animals foraged in a cylindrical arena where the food location was defined by two cylinders [Gothard et al. 1996b]. During successive exploration of the arena, these landmarks were moved inside the apparatus while keeping their relative distance constant. Thanks to this task, it was possible to dissociate the participation of distal and proximal cues on place cells firing. The authors evidenced that place cells could entirely or partially ("*disjunctive cells*") fire in a reference frame defined by proximal landmarks. Numerous ensuing studies even reported that the presence of objects could control place cells firing in the hippocampus [Deshmukh and Knierim 2013; Geiller et al. 2017a; Fattah et al. 2018]. As an example, Deshmukh and Knierim [2013] described a category of cells that developed multiple place fields with the same distance and bearing from objects inside the arena: "landmark vector cells". Other studies reported that objects located at the periphery, but not at the center, of a circular arena exerted a strong influence on place cells map orientation [Cressant et al. 1997, 1999]. A follow up study showed that objects located at the periphery of the arena had a stronger control over place cell firing than distal cues [Renaudineau et al. 2007]. Aforementioned results highlight a key role of proximal cues on the control of the hippocampal spatial map.

Additional studies showed that local cues could also affect the scale of the hippocampal space representation. Battaglia et al. [2004] studied this question in a task where rats were trained to shuttle in a linear track entirely enriched with or deprived of local sensory cues (cue-rich and cue-poor condition, respectively), or in a linear track divided in two cue-rich and cue-poor half (combined cue-rich/cue-poor) (Figure 4.3 - A). Population vector of place cells active in the cue-rich track decorrelated more quickly in comparison to the cue-poor condition (Figure 4.3 - B), which indicated that the presence of intra maze cues (cue rich condition) decreased the scale of the spatial representation. Interestingly, this effect was not observed in the combined track between the cue rich and the cue poor regions of the same track (Figure 4.3 - C). The authors explained this absence of

---

<sup>9</sup> See § 5.2 for a more detailed description of the study by Collett et al. [1986]

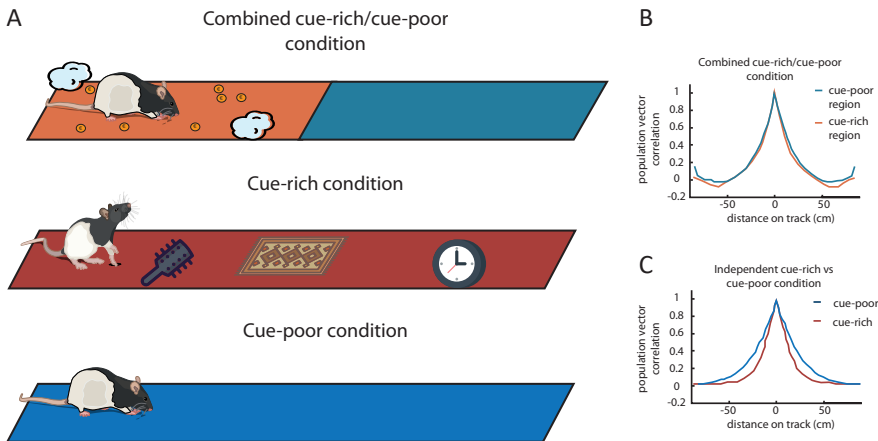


**Figure 4.3:** Effect of local sensory cues on hippocampal spatial scale: **A:** Schema of the three experimental conditions used in Battaglia et al. [2004] study. Animals foraged in a combined cue-rich/cue-poor condition (top), a cue-rich (middle) or a cue-poor linear track (bottom). **B-C:** The mean population vector correlation as a function of the distance between the locations at which the two population vectors were computed for the combined cue-rich/cue-poor condition (**B**, light blue: poor side, light-red: rich side) and for the cue-rich (**C**, dark red) vs cue-poor (**C**, dark blue) condition (Adapted from Battaglia et al. [2004])

effect by a possible "*low statistical power*" or more notably by the fact that "*the cues in [the combined condition] were relatively small compared with those in [the cue-rich condition] and did not require large changes in locomotor pattern*". This absence of difference could thus be explained by the modest saliency of intra maze cues but could also result from the presence of other types of proximal cues as self-generated odors. It is also worth noting that they did not observe any difference in the number of detected place cells between the cue-rich and cue-poor tracks. Proximal cues appeared to affect the scale but not the pool of cells coding for space in this experiment. A complementary study conducted by Burke et al. investigated the contribution of objects on place cells coding in rats circumnavigating in a circular linear track with several intra-maze objects [Burke et al. 2011]. This time, the authors wanted to focus on the distal region of the dorsal hippocampus known to receive extensive projections from the lateral entorhinal cortex (see § 2.3). This cortical area has been shown to process object-related information [Deshmukh and Knierim 2011; Van Cauter et al. 2013; Knierim et al. 2014; Burke and Barnes 2015]. Conversely to the Battaglia et al. [2004] paper, they found that local cues increased the number of place cells and their propensity to form a place field. In addition, they observed a decrease of the place field size in the presence of object. Nevertheless, this shift to smaller place fields was concomitant with an increase in the number of place fields. Hence these phenomena suggest a conservation of the hippocampal spatial scale with or without objects: "*Thus, there was a conservation of the amount of space over which a given CA1 neuron fired. A possible consequence*

*of this property is that it may serve to maintain a constant level of excitation in the CA1 neuron population when behavioral conditions change” [Burke et al. 2011].*

Together, these studies demonstrate a strong influence of proximal visuo-spatial cues on place cells coding scale. However, at a short range visuo-spatial stimuli are likely to be intermingled with other sensory cues. Further studies are needed to clearly identify the relative participation of vision and other sensory modalities on hippocampal spatial coding scale.

#### 4.2.3.2 Local olfactory cues

Previously mentioned studies focused on visuo-spatial cues, but it is known that other proximal sensory cues can complement visual information or replace them in their absence [Lavenex and Schenk 1995]. For example, blind rats are able to form place fields comparable in sighted rats [Save et al. 1998]. This is certainly possible thanks to a compensation with tactile information and more frequent tactile objects exploration. In a subsequent study, Save et al. [2000], compared the impact of visual and/or olfactory cues on spatial firing of hippocampal cells while rats randomly searched for scattered food in a circular polarized arena. After an initial exploratory session in light with a polarizing cue, the animal was confronted to three sessions without the cue-card in light or dark conditions and with the arena cleaned or not (cleaning condition): dark/cleaning, dark/no cleaning, light/cleaning, and light/no cleaning. Most place fields expanded and place cells were unstable in both light/cleaning and dark/cleaning condition in comparison to the dark and light condition without removing olfactory cues (cleaning). Also, half of the cells in the dark/-cleaned condition turned off following the experimental manipulation. These results highlight the importance of self-generated olfactory cues in presence or absence or visual information for the activation and stabilization of hippocampal place cells. These results may seem surprising taking into account that olfactory cues, due to their volatile nature and the way they are perceived (through their intensity), can be useful to determine the proximity of the odor source but less to locate its direction [see: Jacobs 2012, for more details on the use of olfaction for navigation]. Consequently, it is unclear how much spatial information can be provided by self-generated olfactory cues. To address this issue, Aikath et al. [2014] investigated the influence of these self-generated olfactory cues in presence or absence of visual cues and when both sets of cues were put in conflict (rotation of one set of cues). This experimental protocol allowed the maintenance of local olfactory cues between sessions, by re-using the same animal-specific paperboard on the floor of the arena, with the same relation with visual cues. The authors familiarized mice to the configuration of a set of visual and/or self-generated olfactory cues, before a rotation

of one or both type of cues. As expected, a rotation of the visual set of cues led to an according rotation of place fields in animals trained without self-generated olfactory cues. Remarkably, in presence of both visual and olfactory cues, place cells followed essentially the rotation of visual cues and ignored the counter-rotated olfactory information. Accordingly, self-generated olfactory cues were not sufficient to anchor place fields on their own. These results suggest that visual cues dominate self-generated olfactory cues for the control of place cells orientation. Supplementary manipulation showed that the absence of the self-generated olfactory cues during the exploration of a novel environment strongly disrupted the stability of newly generated place cells across successive sessions. Other spatial properties of place cells (such as spatial information) were however largely similar in the novel environment with and without olfactory cues. These results suggest that in a novel environment, olfactory cues are incorporated in the spatial representation and participate to its stabilization. With further familiarization of the environment their importance, however, decreased. A final experiment was done to study whether hippocampal spatial maps could be expressed and formed only in the presence of olfactory cues. In a featureless environment, these cues failed to generate stable fields and to guide spatial maps rotation. Altogether, these results suggest that olfactory cues alone do not provide spatially discriminative signals to anchor place cells firing.

In a subsequent experiment, Zhang and Manahan-Vaughan [2015], found contradictory results to the aforementioned one. In their study, olfactory cues were shown to be very efficient to elicit stable and selective place cells and to control place fields rotation. In their protocol, rats had first to forage in an empty circular arena in complete darkness. Then, four different odors were placed underneath pinholes organized in square in the arena's floor. Coherently with Aikath et al. [2014] observation, the introduction of odors in the arena stabilized hippocampal spatial firing. In their case, however, odors only were able to support the formation of a stable hippocampal map. A rotation of the odor source rotated the map accordingly and a shuffling of the odors led to place cells remapping. The discrepancies between these two studies could be species dependent (rat: Zhang and Manahan-Vaughan [2015] vs mouse: Aikath et al. [2014]), but could also depend on the type and the amount of olfactory cues provided. In Aikath et al. [2014] self-generated odors are likely to be less salient, potentially mixed or disturbed by daily manipulation of the absorbent paper. The constant addition of new odorant sources to the absorbent paper could make them too numerous to be accurately spatially informative. Zhang and Manahan-Vaughan [2015], on the contrary, used four distinct synthetic odors evenly spaced in the arena that could constitute a more stable, anisotropic spatial framework.

The formation of a cognitive map based solely on olfactory information has recently been shown using a task where mice had to shuttle in the dark while "navigating" in an odor space [Radvansky and Dombeck 2018]. In this task, head-fixed mice were first trained in a virtual linear track in presence of two monotonically increasing odor gradients for the upward and downward directions<sup>10</sup>. After a successful learning in presence of the odor gradient and visual information in the virtual corridor (*e.g.*: when the mouse licked at the extremities of the corridor), the authors showed that the animal was able to complete the task in the dark, relying exclusively on the two odors gradients. With the help of two-photon calcium imaging, they monitored the activity of hippocampal pyramidal cells and found a proportion of place modulated neurons in the "odor space" (in the dark). Nevertheless, this population only represented  $10\% \pm 7\%$  of their recorded neurons<sup>11</sup>, a lower number than reported in VR studies with visual information [Dombeck et al. 2010; Bourboulou et al. 2019]. Interestingly, they showed that the number of cells with a significant place modulation dropped drastically (88%) when the odor were made uninformative (flat odor concentration along the track). This result strongly implies that, in the dark-odor condition, hippocampal representation was largely odor-dependent.

The close link between the olfactory system and the hippocampus in mammals has long been known; in fact, olfaction was once considered to be the main function of the hippocampus [Vanderwolf 1992, 2001]. From the aforementioned studies we can clearly conclude that olfaction plays a crucial role for spatial context definition [Jeffery and Anderson 2003]. We also saw that olfaction was incorporated in the spatial representation in use to define and refine it [Save et al. 2000; Aikath et al. 2014; Zhang and Manahan-Vaughan 2015]. The existence of a complementary or intertwined olfactory map is nevertheless uncertain. Animals appear to use olfactory sources in some particularly controlled experiments [Zhang and Manahan-Vaughan 2015; Radvansky and Dombeck 2018]. It is likely that such level of odorant control can only be achieved inside the walls of a laboratory. In reality, olfactory cues are volatile and subject to turbulences created by the behavior of the animal or external causes. Simple navigational strategies are compatible with such conditions [Wallace et al. 2002; Khan et al. 2012; Gire et al. 2016; Liu et al. 2019] but their involvement in map formation is still unclear [Theories about olfactory navigation are reviewed in the following extensive review Jacobs 2012]. However, it would be of great interest to study the role of olfactory cues in long distance navigation as in such condition, their volatility might be more an advantage than a drawback in comparison to small scale navigation as shown for birds [Papi 2001; Gagliardo 2013].

<sup>10</sup> Visual information were first provided to guide the animal's learning of the task

<sup>11</sup> The total number of cells corresponded to the number of ROIs (regions of interest) identified by the cell-identification algorithm.

#### 4.2.4 *Borders*

Physical boundaries of an environment, such as walls or corners, provide strong sensory (visual, tactile,...) cues, while also defining the geometry of an environment. This geometry can be very informative in itself to generate space or directional information<sup>12</sup>. In a seminal study, Cheng [1986] found that the arena geometry dominated over local cues in guiding navigation to a reward location. Place fields also maintain their positions relative to the edges of a raised holding platform [O'Keefe 1979] while it was moved in the laboratory frame, suggesting that a drop which impedes movement, the limits of a raised platform, also constitutes a boundary. Nevertheless, in order to be spatially relevant, non-physical border should be at fixed location in relation to the environment. If it is not the case, as with the fuzzy-boundaries used in Hayman et al. [2008], then the animal can not use them as a spatial localizing cue<sup>13</sup>. Recording studies showed that place cells were sensitive to the geometric features of an environment as they scaled their place fields if the animal was exposed to an identical larger one [Muller and Kubie 1987]. They also showed that introduction of walls inside the arena bisected the firing of some place fields<sup>14</sup>. The walls also caused a duplication or deletion of place fields nearby them while letting distant fields intact. Later work by Rivard et al. [2004], showed that a small proportion of CA1 place cells were firing in relation to a barrier inside the arena independently of external landmarks (and the context). It is of interest to note that the extend of the barrier is of a crucial importance to affect place field location. For instance, Cressant et al. [1997] showed that small objects placed inside a cylindrical arena did not affect the location of firing fields when they were separated, but did so when aligned to form an extended barrier. Altogether these results show a deep influence of borders and geometry of an environment in place cells firing.

#### 4.2.5 *Boundary vector cells model*

In 1996, John O'Keefe and Neil Burgess showed how dorsal CA1 place cells remodeled their place fields when a small square box was extended in one dimension into a rectangle, and then into a large square arena [O'Keefe and Burgess 1996] (Figure 4.4-A). The place field of

<sup>12</sup> A rectangle-shaped environment is an anisotropic geometric space, providing directional information inherent to its structure. In contrast, a circular arena will constitute an isotropic space. However, a certain anisotropy can be artificially created by the introduction other environmental features (objects [Cressant et al. 1997], polarizing cues[Muller and Kubie 1987], slope of the floor [Jeffery et al. 2006]...) that will break its structural symmetry.

<sup>13</sup> In Hayman et al. [2008] the "fuzzy" barrier consisted in a imaginary "wall" that triggered an aversive noise if it was crossed by the animal. The path of the animal was reliably constrained within the thus defined limits.

<sup>14</sup> A transparent barrier worked equally well

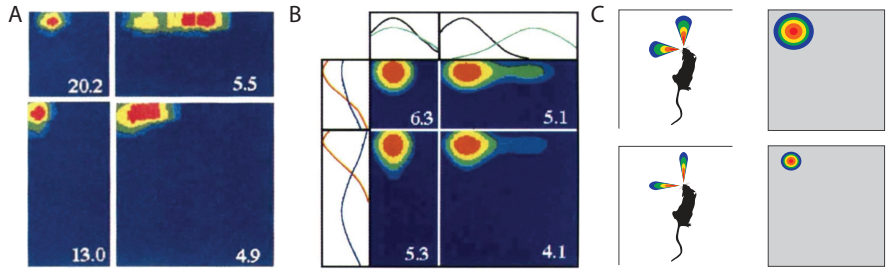


**Figure 4.4:** **A** Example of place cells showing how the summation of separate gaussian tuning curves locked to distinct walls in the environment can lead to the formation of place fields. Stretching the environment into a **HR** (Horizontal Rectangle) leads to a stretching of the place field in this direction and the emergence of two separate sub-peaks. A change in the opposite direction into a **VR** (vertical rectangle) moderately extends the place field in this direction. **B** BVC model of place field formation explaining the firing modification observed in A. The main characteristics (shape and location) of the place field seen in A can be decomposed as a thresholded linear sum of multiple gaussian wall-distance tuning curves. (Firing rate is color coded from high firing rate: hot colors, to low firing rate: cold colors) **C** Schema of the generalization proposed in Hartley et al. [2000]. Boundary Vector components can be modeled by components tuned to the distance from a wall and an allocentric direction to the animal. **Top row** shows broadly tuning components (**left**) leading to a wide place field (**right**). **Bottom row** A sharpening of the angular and distance tuning **left** can lead to smaller place fields (**right**). Adapted from O'Keefe and Burgess [1996] and Hartley et al. [2000]

some of the recorded cells appeared to be anchored to one or two walls. When an expansion in one direction was observed, the position of this place field was still determined by its distance from the wall. Another population of cells revealed a secondary place field along the direction of the extended box. The modulation of the place fields according to these geometrical deformations suggested that a place field could result from the thresholded summation of one or several putative wall-distance components (Figure 4.4-B). These components are tuned to respond maximally when there is a wall at a particular distance along a specific direction. Hartley et al. [2000] generalized this description by proposing components tuned to the distance from a wall and an allocentric direction to the animal. These theorized boundary vector cells were later found in a number of brain regions including the subiculum [Sharp 1999; Barry et al. 2006; Lever et al. 2009; Stewart et al. 2014], parasubiculum [Boccaro et al. 2010], medial entorhinal cortex Savelli et al. [2008] and Solstad et al. [2008] and recently the rostral thalamus and anterior claustrum [Jankowski et al. 2015]. Most of the cells recorded in the aforementioned studies were more numerous closer to the wall than further apart. According to this model, a study by Barry et al. [2006] showed that the successive removal of borders, profoundly affected the spatial representation. Place fields became broader and less coherent as the number of borders in the environment decreased. In the frame of the BVC model, scale of the spatial representation could be globally modulated by a change in either the angular or distance tuning of the boundary vectors (Figure 4.4-B). Global change could also be observed following a decrease in

the threshold value of the summed components. Indeed a lower global threshold could lead to a broadening of the place fields and even trigger the generation of secondary place fields. Nevertheless, this model could allow local variation of the spatial scale representation by the introduction of components tuned to non-geometrical features as distance and/or bearing to landmarks. These non-geometrical components are usually not considered in BVC model [Hartley et al. 2000; Barry et al. 2006; Grieves et al. 2018]. This vectorial activity in relation to landmarks could explain why gerbils searched at different positions when one or several cues were separated in the Collett et al. [1986] study. Furthermore, cells firing in a reference frame defined by a landmark [Gothard et al. 1996b; Barry et al. 2006] or Landmark Vector Cells have later been observed [Deshmukh and Knierim 2013; Geiller et al. 2017a](also see §4.2.3). In parallel, local cues could indirectly influence the variation of BVC tuning by locally modifying the optical flow of the animal. The integration of visual flow estimates has been shown to lead to realistic border cells firing [Raudies and Hasselmo 2012]. Altogether, the previous results highlight a profound impact of borders on the scale and the stability of space coding in the hippocampal formation.

#### 4.2.6 *Scaling the hippocampal code to a bigger environment*

We saw in the previous section that place cells could stretch in relation to the extension of an environment, from 61 to 122 cm, in one or two directions [O'Keefe and Burgess 1996]. In this experiment, a modification of the apparatus geometry also led to a change of scale. Hence, the place fields expanded as a result of this change in the size of the environment. The effects of an isotropic scaling of the environment were first examined by Muller and Kubie [1987] either in circular or squared arenas. Interestingly, they observed that place fields were indeed broadened following the increase in size of the arena but that this scaling was sub-linear. In other words, the ratio of the scaling of the place fields was smaller than the environments' one. Later works confirmed that changing the size of the recording enclosure modified the size of hippocampal place fields [Maurer et al. 2005; Fenton et al. 2008]. Fenton et al. [2008] investigated the effect of a non isotropic scaling, first by recording place cell activity in rats foraging in a cylinder (68 cm diameter) inside a "monkey chamber" (a bigger apparatus usually used for monkey recordings; 150 x 140 cm) and then recording them in the full chamber without the cylinder. In addition to the previously reported scaling of the place fields size they also reported a multiplication of the number of place fields per cell and a remapping<sup>15</sup>. CA1 place cells with a unique place field in the

---

<sup>15</sup> This remapping was potentially caused by the non isotropic change in size and geometry from the circular arena to the monkey chamber Fenton and Muller [1998]

cylinder, formed multiple place fields in the six times larger chamber. At first sight, we could hypothesize that this multiplication of place fields could cause the spatial representation to become ambiguous, as one place cell codes for multiple locations in the chamber. Nevertheless, a population vector-based decoding of simulated cylinder and chamber place cells showed an equivalent small error in reconstructing the animal position<sup>16</sup>. This suggests a homeostatic maintenance of hippocampus activity according to the size of the environment<sup>17</sup>. A follow up study by Park et al. [2011] uncovered that this multiplication of the number of place fields following anisotropic scaling was not a particularity of CA1 as this phenomenon was also observed in CA3 and DG<sup>18</sup>

This body of research proposes that the hippocampal spatial code adapts to a scaling of the environment. More notably, it suggests that this adjustment is not directly proportional to the increase in size of the environment, neither for the increase in propensity nor for the increase in place fields size. This observation raises the question of the statistics that govern the scaling of the hippocampal spatial code in big environments. In order to shed light on this question, Rich et al. [2014] trained animals to forage in linear mazes of increasing size: from 3 to 48 meters. They uncovered that the probability of place cells to form a place field (propensity) followed a gamma-Poisson distribution. Briefly, a minority of cells expressed many fields while most of the others had only few or none. Thus, the recruitment of place cells scaled logarithmically with the track length. Also, as expected from the gamma-Poisson distribution of the place cell propensity, fields were allocated randomly and homogeneously over the environment. They did not report any clustering of the place fields in the large environment ruling out the possibility of a chunking of a global map into several smaller ones [Gupta et al. 2012; Alexander and Nitz 2017].

Altogether, these results suggest that the hippocampal spatial representation adapts to an augmentation in size of the environment. The multiplication of the number of place fields reinforces the hypothesis of a population code of space in dorsal hippocampus. Several locations could be coded by the same neuron but disambiguated at the

---

<sup>16</sup> Here Fenton and Muller used the decoding on simulated data certainly because of a lack of simultaneously recorded cells. Briefly, they used the characteristics of the whole population of place cell recorded in each condition to generate space modulated spike trains from Inhomogeneous Poisson Process. Then, they used a population vector decoding to deduce the position of the animal from the simultaneous activity of the simulated cells [see also: Fenton and Muller 1998]

<sup>17</sup> Such homeostatic processes of hippocampal activity have been proposed elsewhere to compensate for the introduction of barrier, objects or in a new environment [Buzsáki et al. 2002; Lever et al. 2009; Burke et al. 2011]

<sup>18</sup> In the previous study by Fenton and Muller [1998] numerous components of the apparatus were changing in addition to the scaling: the availability of distal cues or stairs allowing 3D movement. Park et al. [2011] confirmed the previous results in CA1 in less complex arenas while also characterizing the properties of spatially modulated cells in CA3 and DG following the scaling.

population level. But most of all, these results revealed an efficient sub-linear mechanisms of place cells scaling (size and number of place fields) or recruitment in large environments.

#### 4.3 NON SENSORY MODULATION OF SPATIAL RESOLUTION

##### 4.3.1 *Representation of goal*

During navigation, animals need to represent their position in the environment as well as the location of goals such as food, water or a safe place [Poucet and Hok 2017]. Behavioral evidences of the implication of the hippocampus in goal localization has long been known [Morris et al. 1982; Morris 1984; Sato et al. 2017]. Indeed, the first studies investigating behavioral correlates of hippocampal cells reported goal-related firing activity. Accordingly, these cells were called "consummatory-approach" [Ranck 1973] or "goal approach" cells [Eichenbaum et al. 1987]. More recent works revealed that this goal representation could also be accompanied by an over-representation of the goal characterized by an accumulation of place fields at the goal location. The first study that showed such accumulation was performed by Hollup et al. in rats swimming in an annular version of the water maze. In a follow up study, the same team showed that this fields' accumulation was following the goal if it was moved to a new location [Fyhn et al. 2002]. These studies suggested that the hippocampal map could be non-uniform by over-representing behaviorally meaningful unmarked locations. Several other studies corroborated the fact that CA1 place cells over-represented reward locations [Dupret et al. 2010; Danielson et al. 2016; Mamad et al. 2017; Zaremba et al. 2017; Gauthier and Tank 2018; Sato et al. 2018; Lee et al. 2019]. This local clustering of place fields at the goal location was later shown to be linked to a place preference behavior [Mamad et al. 2017] or to the memory of the goal location [Zaremba et al. 2017]. Kobayashi et al. [2003] showed a correlation between the performance of an animal to shuttle between reward zones and an increased firing at the reward location. In this study, some hippocampal neurons progressively changed their spatial discharge during learning of a goal. These neurons fired robustly at the reward location once efficient navigation between goals was achieved [Kobayashi et al. 2003]. Altogether, these works demonstrate a clear goal-related activity in the hippocampus in addition to its position-specific activity. Nevertheless, in light of these results, it is still unclear if the two spatial and goal codes coexist or if the goal information is intertwined in a spatial canvas provided by place cells [Eichenbaum 2017].

Two decades ago Burgess and O'Keefe [1996] hypothesized a dedicated population of cells coding for the goal location. In line with this hypothesis, a recent work found that 1-5% of cells in the CA1

and subiculum were context-invariant cells firing at the goal location [Gauthier and Tank 2018]. Additionally, cells coding for a vector to the goal location have been discovered in bats [Sarel et al. 2017]. These works imply that two distinct populations of neurons could code for goal or space in CA1. Nevertheless, additional experiments indicated that goals are not uniquely coded by a dedicated population of hippocampal cells. Indeed, Hok et al. [2007] described that place cells could develop, in addition to their typical place field, a very peculiar goal-related activity [Hok et al. 2007; Hok et al. 2013]. In this study, rats had to enter an unmarked circular goal zone in a cylindrical arena and stay there for two seconds to trigger the release of a food pellet at a random location in the environment. Next, they had to leave the goal zone to find and eat the pellet. Surprisingly, in this goal-directed task, where the goal and the reward were dissociated, the authors did not observe an over-representation of the goal (homogeneous repartition of place fields) but place cells formed a secondary firing field at the goal location. These results show that, in the Hok et al. [2007] task, the same neuronal ensemble in the hippocampus provides a composite coding of both goal and space. In line with this study, Lee et al. [2019], found that goal fields were not specific to a particular population of hippocampal cells. Additionally, they showed that the generation of a place and goal field by a neuron were both a function of the propensity<sup>19</sup> of a cell (with a constant gain for the goal location; see section 4.1.4). They proposed that the dedicated population of goal cells observed in previous work [Gauthier and Tank 2018; Sato et al. 2018] could be explained by the small size of the environment they used. This low proportion of cells exhibiting only a reward field (e.g.: goal cells) is compatible with their model of gamma distribution of neuron propensity and could happen by chance in a small environment. The authors do not however completely reject the existence of a very small population of cells dedicated to goal coding that their model could not detect. Another recent paper by Aghajan et al. [2015] showed that hippocampal neurons with no spatial selectivity during a random foraging task in virtual reality, became place selective after the introduction of fixed cued goals in the arena. This work thus suggested an effect of goal-directed behavior on place cells activity. Also Aoki et al. [2019] found that in-field firing rate of place cells, irrespectively to their relation to the goal location, was more pronounced when rats were running toward the goal location. Despite this apparent mix in goal and space coding, this goal-related activity was specifically affected by medial septum inactivation while the spatial coding was not.

Despite this body of work, it is worth noting that numerous studies did not find over-representation of goal locations [Trullier et al. 1999; Grieves et al. 2016; Duvelle et al. 2019]. These discrepancies could

---

<sup>19</sup> See note 3 on page 42.

be explainable by idiosyncrasies at the behavioral task. For example, no over-representation of the goal location was found if the goal was indicated by cues [Dupret et al. 2010] or if the reward was moved [Speakman and O'Keefe 1990; Kobayashi et al. 2003]. In Fyhn et al. [2002] study, the accumulation of place fields at the goal to a new location vanished rapidly with experience. We could thus hypothesize that this phenomenon is transiently present to learn new location of a goal if a stable reference frame is used throughout the task. This hypothesis does not seem likely as over-representation can be observed after extensive training in some studies [Danielson et al. 2016; Mamad et al. 2017; Lee et al. 2019]. Another possibility would be that in some tasks and/or environments, the goal might be encoded in CA1 in a very sparse way so that goal-related activities could not be directly observable. This hypothesis might explain why goal-related coding was not observed in CA3 [Dupret et al. 2010]. Finally, it is worth noting that in the Gauthier and Tank [2018] paper that described a specific population of goal cells in the hippocampus, they did not rule out the possibility that these cells might be interneurons (and not pyramidal cells) as they use Thy1-GCaMP3 mice that express the fluorescent calcium indicator in all neurons (interneurons included). This could go in line with a recent study by Turi et al. [2019] showing the involvement of Vasoactive Intestinal Polypeptide (VIP) expressing interneurons in dorsal CA1 to learn goal locations.

A last question about goal representation in the hippocampus concerns the origins of such firing (whether or not it is made by a dedicated population of hippocampal cells). Indeed, goal-related activities have been described in prefrontal cortex [Hok et al. 2005; Hok et al. 2013] and more recently in medial entorhinal cortex [Boccaro et al. 2019; Butler and Hardcastle 2019; Sargolini et al. 2019]. These results suggest that the coding of goal locations could be inherited or conjointly supported by parahippocampal regions and/or prefrontal cortex (maybe via the rhomboid/reuniens or the ventral hippocampus that are anatomically connected to the prefrontal cortex).

#### 4.3.2 Modulation of resolution by attention

As we saw in the previous sections, place cells activity is tightly linked to idiothetic and allothetic sensory information. Such modulation of place cells by various types of sensory cues in an environment implies that in the same conditions (in an identical environment) place cells should always keep the same pattern of activation. Nevertheless, depending on the behavioral constraints of the task performed by the animal in the environment, some cues might be more important than others in order to achieve different purposes in the same environment. Can this type of non-sensory, task-related factors, also influence hippocampal space coding? This question was addressed in a seminal

study where hippocampal neurons were recorded either during a goal-directed task or during a random foraging task in the exact same environment [Markus et al. 1995] [but see: Trullier et al. 1999]. Most of the place cells remapped between the two different tasks suggesting that place cells were not only controlled by sensory stimuli. In a later study, Zinyuk et al. [2012] used a similar paradigm to study the effects of the animal behavior on place cells activity. They trained rats in a random foraging or a goal-directed task to obtain food pellets. They used the similar place preference task that in the Hok et al. [2007] study: navigator rats were trained to find an unmarked target area kept at a fixed location in comparison to the room reference frame. Their paradigm differed from Markus et al. [1995] study by the use of a continuously rotating arena in a cue rich room [Rossier et al. 2000]. The day of the recording, rats were exposed alternatively to the stable or rotated arena (stable-rotated-stable). In stable sessions, the quality of place cells was similar in both tasks. However, during the rotated condition, the spatial firing was strongly affected only during the random foraging task. When placed in the rotating area, place fields from the forager rats appeared as if they were not spatially modulated any more : their firing did not follow the rotation of the arena and was not anchored to the stable room frame. Conversely, in the navigators group, a majority of place cells stayed stable and were more likely to be preserved in the stationary frame that defined the goal. Altogether, these results confirm that the hippocampus encodes environmental information in a way that depends not only on the animal's overt behavior but also on the task that the animal is doing.

The aforementioned studies were conducted in rats and reported an influence of the performed task on the control of place field location but did not uncover any qualitative difference in place cells between spatial and non-spatial tasks. On the contrary, Kentros et al. [2004] showed that for mice, place cells coding quality strongly depended on the behavioral task performed by the animal. In their study they used four different tasks, with different behavioral demands, while recording hippocampal neurons in C57B6 mice. First they used a "no task" condition in which animals were placed in a circular arena and could behave freely, without any task contingencies. The three other conditions were 1) a random pellet chasing task 2) the exposition to a novel environment and 3) a spatial task. In this spatial task, the animal were placed five minutes in the arena before the occurrence of an aversive stimulus (bright light and a car alarm). In order to stop this aversive stimulus, the animal had to find an unmarked location and stay there for few seconds. This led to a period of 2-3 minutes when the animal could be safe. Surprisingly, the authors showed that the stability and spatial information of place cells recorded in mice performing the spatial task was higher than in the other conditions. Also, the place fields stability in good performers was comparable to

those observed in rats. Thus, this study highlighted a link between place cell coding quality, the behavioral contingencies of a task, as well as the behavioral performance of the animal. This peculiar stability of spatial coding was potentially explained by an increased attention to the spatial cues, specially in good performer mice. In the previous experimental paradigm, the attention to a particular set of sensory cues was "forced". Nevertheless, we could wonder if animals could willingly redirect its attentional focus on a particular set of cues to optimize its behavior. Such possibility would fit with the original definition of an attentional process by James [1890]: "*Everyone knows what attention is. It is the taking possession by the mind in clear and vivid form, of one out of what seem several simultaneously possible objects or trains of thought ... It implies withdrawal from some things to deal effectively with others ...*" [James 1890; Rowland and Kentros 2008; Fenton et al. 2010]. Such online modulation of place cells coding has been uncovered by Fenton et al. [2010]. In their study they particularly focused on place cells firing variability on short time scales: overdispersion [Fenton and Muller 1998; Fenton et al. 2010] (see: § 4.1.3). This phenomenon is thought to reflect a switch between different reference frames on a very short time scale [Olypher et al. 2002]. In their study they thus wondered if a higher navigational demand, a higher need to pay attention to a specific set of cues, could bias the hippocampal cells to be in a single reference frame and consequently to reduce overdispersion. Indeed, they observed that navigator rats, on a rotating arena, had lower overdispersion than their foraging congeners. Surprisingly, they also uncovered that overdispersion was lower during approach to a goal than during departures. This suggests that attention can generally increase the focus of the animal on external sensory cues and that it directly impacts the short term variability of place cells firing.

In a follow up study, Muzzio et al. [2009b] addressed one of the question opened by the aforementioned papers. In this serie of experiments they asked if the stabilization of the place field map simply depended on an increase in a general form of arousal or could require attention to a particular set of visuo-spatial cues [Muzzio et al. 2009a,b]. To answer this question, they used two goal-directed tasks where the animal had to pay attention to a set of visuo-spatial or olfactory cues to find a reward. During the visuo-spatial task, the mice had to associate a particular location in relation to visual cues, independently of odor cues. In the olfactory version, mice had to associate a specific odor with the food reward, independently of spatial location. Importantly, all sensory cues (olfactory and visuo-spatial) were identical in the two versions of the task and rotation or reorganisation of the cues were performed. If attention leads to an increased general state of arousal, the stability of the representation should be similar in the two conditions. Conversely, a selective modulation of attention could cause a different level of stability in one of the conditions. They found

that the hippocampal spatial representation was only stable in the visuo-spatial group. They thus showed that attention could allow the selection of a particular set of cues, relevant for the completion of the task. This could also be explained by a change in the type of navigation used to locate the goal. In the olfactory task, the animal could use a beaconing strategy and thus only pay attention to the rewarded odor. Altogether, the use of a constellation of visuo-spatial cues is correlated with the maintenance of a stable hippocampal spatial coding. On the other hand, the use of a simpler strategy that does not require the use of the fixed visual cues leads to an unstable hippocampal map.

The definition of attention could also slightly derive from the initial one proposed by [James 1890]. Attention is not only used to select relevant information and to discard irrelevant ones for the task but it can also be focused on a novel, salient stimulus that appears in the environment. Monaco et al. [2014] developed a task leading to an increase in the occurrence of attentive head-scanning behavior while rats foraged in a closed loop track. The rats were first exposed to the familiar track and then two types of manipulation were done to stimulate the curiosity of the animal: either a double cue-rotation, by rotating, in the opposition direction, the distal and proximal cues or a completely new maze. These novel conditions triggered homogeneously, around the track, a unique type of behavior: attentive head-scanning. This behavior is described as "*lateral head-scanning movements*" during pauses that are thought to "*reflect investigation of environmental features and [...] represent an animal's active management of information gathered during exploration*" [Monaco et al. 2014]. The authors found that in numerous cases, attentive head-scannings led to the creation of a place field, on the subsequent lap, at its location. This field was then stable for the rest of the exploration. This demonstrated that attentive behavior could trigger the abrupt formation of place fields, possibly to modify or refine the pre-existing hippocampal representation. This result also reinforces the hypothesis of a "dense" code in the hippocampus where new information are incorporated by the creation of new place fields.

#### 4.4 ANATOMICAL DIFFERENCES IN SPATIAL RESOLUTION

##### 4.4.1 *Transverse axis*

As we saw in the previous sections, the hippocampal pyramidal cells are influenced by a myriad of internal and external sensory information. This information is first processed upstream of the hippocampus, specially in cortical regions that send spatial and non-spatial inputs to the place cells networks. These inputs originate in majority from the entorhinal cortex which is itself functionally divided. The lateral part of the entorhinal cortex is weakly modulated by space [Hargreaves 2005] but carry non spatial activity correlated to object identity, context

or even temporal information [Deshmukh and Knierim 2011; Yoganasimha et al. 2011; Van Cauter et al. 2013; Wilson et al. 2013; Tsao et al. 2018]. Conversely, medial entorhinal cortex is thought to be a key component to the neuronal representation of space [Hafting et al. 2005; Moser et al. 2008]. This region contains a wide variety of specialized cells such as grid, head direction, speed, border or conjunctive cells [Hafting et al. 2005; Sargolini et al. 2006; Solstad et al. 2008; Kropff et al. 2015; Diehl et al. 2017]. In CA1, the lateral and medial entorhinal cortex projections terminate on different population of cells along the proximo-distal axis. MEC inputs contact preferentially the proximal part of CA1 (closer to CA2), while LEC axons terminate primarily on the distal part of CA1 (close to the subiculum) [Witter et al. 2000; Naber et al. 2001] (see § 2). This distinct connectivity suggests a potential difference in information processing along the proximo-distal axis of CA1: proximal CA1 being more spatially modulated (MEC) and distal CA1 preferentially influenced by non spatial information (LEC). Could there be a difference in spatial tuning following this gradient of connectivity from the entorhinal cortex? This question was addressed by Henriksen et al. [2010] by recording hippocampal neurons along the proximo-distal axis of the hippocampus while rats foraged in big circular environments<sup>20</sup>. They showed that, indeed, distal place cells, receiving LEC inputs, had more dispersed place fields, with a lower information content and a higher propensity than place cells in proximal CA1. This decline in spatial coding quality from proximal to distal CA1 mirrors the decrease of spatial coherence in the proximodistal axis of the adjacent subiculum [Sharp and Green 1994]. Additionally, proximal CA1 cells were more strongly phase locked to the MEC theta LFP than distal CA1 cells suggesting a tight link between space processing in these two regions.

Contrary to CA1, entorhinal inputs are not segregated in CA3. Projections from LEC and MEC converge on the same cells but on different dendritic segments [Witter and Amaral 2004; Leutgeb et al. 2005a]. Furthermore, the strong recurrent connections in CA3 could prevent the creation of a functional gradient akin to CA1 [Marr 1971; Witter and Amaral 2004; Igarashi et al. 2014a]. Nevertheless, Lu et al. [2015] investigated if a gradient of spatial coding quality across the CA2 to proximal CA3 (pCA3) could emerge from other factors than the segregation of LEC-MEC projections (see § 2.3) [see also: Lee et al. 2015]. Interestingly, they found several differences in place cells coding quality along this axis. The proportion of active cells increased along the CA3-CA2 axis, together with a broadening of place field size. These gradients were also accompanied by a loss of spatial information and stability from pCA3 to CA2. Altogether, these results suggest the existence of a graded representation of spatial and non-

---

<sup>20</sup> The authors specifically used a big environment to increase the likelihood of having multiple place fields per cell and thus have an indication of the propensity of the cells

spatial information along the CA2-pCA3 axis despite the convergence of LEC and MEC inputs. This gradient could nevertheless originate from differences in the degree of collateral projections, a dampening of DG inputs or cells intrinsic differences (*e.g.*: gene expression) along this proximo-distal axis [Ishizuka et al. 1995; Igarashi et al. 2014a; Lu et al. 2015].

#### 4.4.2 Radial axis

The pyramidal layer of CA1 is composed of two superposed layers of cells: the deep layer which is more dorsal (near *Stratum Oriens*) and the superficial layer that is more ventral (near *Stratum Radiatum*). These two layers are named according to the position of their respective basal and apical dendrites [Lorente De Nô 1934]. The study of the physiological and functional properties of deep and superficial cells was strongly facilitated notably by the development of silicon probes and optical imaging that allow simultaneous recordings at different depths (silicon probes) or a precise targeting and identification of these layers (calcium imaging). Indeed, both technical requirements were impossible using the classical electrophysiological recording with tetrodes [Geiller et al. 2017b; Mallory and Giocomo 2018].

Mizuseki et al. [2011] were the first to show a functional gradient along the radial axis of the hippocampal pyramidal layer thanks to silicon probes recordings in rats performing various behavioral tasks. The fixed spacing between the recording sites of the silicon probe allowed the electrophysiological discrimination of deep and superficial layers. To do so, the site with the highest spike amplitude was first identified as the "location" of the neuronal cell body. Then the middle of the pyramidal layer was deduced from the site with the largest ripple power [Ylinen et al. 1995]. The combination of these two measures determined if a cell was above or under the midline of the pyramidal layer. Interestingly, they found that these two subpopulations of cells had different physiological properties. Notably, deep cells had higher firing rate, bursts frequency and probability to form a place field than their superficial counterparts. Nevertheless, no differences between the stability, place field size, slope of the phase precession or spatial coherence were observed between the two subpopulations. In a follow up experiment, Danielson et al. [2016] performed the first optical simultaneous recordings of deep and superficial CA1 cells. They achieved this by coupling their two-photon imaging system with a piezoelectric crystal allowing them to switch the depth of the field of view quasi instantaneously. Thanks to this strategy, they confirmed previous results showing that deep cells were more active and had longer  $\text{Ca}^{2+}$  transients (likely bursting activity). Also, the deep layer had a higher fraction of place cells with better spatial information in comparison to the superficial layer. Curiously, deep place cells fired

more variably around their place fields ("tuning specificity") but had place fields of comparable size with superficial cells. Altogether, these results suggest that space is coded more strongly in deep than in superficial cells. A later study highlighted that these differences in firing properties entailed distinct potential functions. Geiller et al. [2017a] used silicon probe recordings in head-fixed mice running on a treadmill. The belt of the treadmill was punctually enriched with multiple visuo-tactile cues. Deep cells had their firing fields tightly correlated with the location of landmarks. Meanwhile, superficial cells exhibited mostly a single field less tied to the landmarks, and thus more inclined to code for the global context of the task. Altogether, these results demonstrated a strong radial diversity of CA1 pyramidal cell physiology and function. Deep cells provide a more flexible map influenced by landmarks while superficial cells support a more stable and context-dependent map of the environment.

#### 4.4.3 Longitudinal axis

The dominant view about longitudinal axis is that it functionally divides the hippocampus. This viewpoint states that the dorsal hippocampus is implicated in memory and spatial navigation while the ventral hippocampus mediates anxiety-related behaviors [Strange et al. 2014]. In spite of this dichotomy, numerous studies showed that the place cells maps involve the entire hippocampus and that environments are represented in a topographically graded continuum of spatial scales [Young et al. 1994; Kjelstrup et al. 2008]. Place cells from the dorsal portion of the hippocampus have sparse and small place fields [O'Keefe and Conway 1978] whereas more ventral place cells recording reveal wider and more overlapping place fields [Young et al. 1994; Maurer et al. 2005; Kjelstrup et al. 2008; Royer et al. 2010]<sup>21</sup>. This gradient of place fields size suggests that the scale of the spatial representation increases along the longitudinal axis [Royer et al. 2010]. Furthermore, this multiscale coding of space could also represent a computational advantage to reconcile accuracy and generalization in the same population of neurons. In dorsal hippocampus, population vector activity decorrelate rapidly, within tens of centimeters [Battaglia et al. 2004; Maurer et al. 2005]. Thus, the similarity (high correlation) between different population vectors can only be identified within this range. A nested code with larger spatial scale will allow to extend this proximity relation without losing the accuracy conferred by the fine scale.

---

<sup>21</sup> On the contrary, one study did not report differences in place fields size in ventral or dorsal hippocampus [Poucet et al. 1994]. Only a non significant tendency was reported as place fields in ventral hippocampus tended to be wider than in dorsal hippocampus. This is likely explained by the too short spacing between dorsal and ventral hippocampus electrodes. See the *Discussion* of Maurer et al. [2005] for further details and explanations.

Larger ventral place fields could also reflect a representation of additional non-spatial information by the ventral hippocampus [Royer et al. 2010; Keinath et al. 2014]. This region receives strong inputs from brain areas implicated in emotion and anxiety [Strange et al. 2014]. Royer et al. [2010] provided evidence that ventral place cells incorporated more non-spatial information than dorsal place cells. For example, ventral place cells exhibited different firing patterns in open versus closed arm, or between inbound versus outbound trajectories in a radial maze.

In conclusion, numerous studies have shown that spatial information is coded at different scales along the longitudinal axis of the hippocampus and that this difference is likely explained by the anatomical and functional diversity of incoming projections to the hippocampus. The combination of these different scales could subserve several functions. It could allow the integration of spatial and non spatial information for downstream areas or a refinement of a spatial canvas with non spatial information. Until now, this variety of anatomical scale of space coding brings a plethora of questions that needs further investigations in the future.

#### 4.5 SPACE CODING AT THE POPULATION LEVEL

One of the principal limitation of feature detector theory is that place cells do not consistently code for the same place if some cues are changed in the environment [Muller and Kubie 1987; Bostock et al. 1991]. Place cells can also change their activity depending on the task performed in the arena [Markus et al. 1995; Gothard et al. 1996b]. Thus a place cell can not directly code for a place. One possibility could be that it codes for a place in a "context" signaled by the pattern of activity of its co-active pairs. This hypothesis stating that an ensemble of neurons could jointly represent a concept or an event was coined by Hebb [1949]. In this perspective, an individual neuron does not work alone, it is a part of a neuronal assembly, and thus can not account for a percept or an ability on its own. Much more knowledge about the animal behavior can be extracted using decoding based on population activity than single cells analyses [Quijan Quiroga and Panzeri 2009; Eichenbaum 2018]. Ambiguous information at the single-cell level like multiple or wider place fields could be advantageous when considering the whole population of active cells. In the next section, I will describe the principal methods of population decoding before demonstrating how and why they are very useful tools to study spatial coding resolution.

#### 4.5.1 Decoding population activity

In 1986 Georgopoulos et al. [1986] were the first to provide evidence that an ensemble of cells could coherently represent the direction of an arm movement in a monkey. They developed a decoding algorithm based on population vector activity<sup>22</sup>, to deduce the current arm movement of the monkey from the weighted firing rate of each activated neuron in the motor cortex. Even if motor neurons were broadly tuned to one direction of movement, fine movement was accurately coded at the population level. Few years later, Georgopoulos et al. [1989] demonstrated that it was even possible to decode the movement intention (and not only the current movement) of the monkey with a variation of the task used in their original work. In the following study, the monkey was trained to reach a target selected on each trial from one of eight potential directions around a circle [Georgopoulos et al. 1989]. On a subset of probe trials, a bright target indicated that the rewarded direction would be rotated 90° from the signaled direction. The authors analyzed the correspondence between observed spiking activity in the motor cortex immediately before reaching and the direction of the subsequent reach by computing tuning curves of the cells during the unrotated trials. They observed that, preceding the initiation of the movement in the rotated probe-trials, spiking activity in the ensemble of motor neurons activated, reflected a "mental rotation", such that the orientation represented by this population rotated 90°. This apparent noise in the activity of the motor neurons preceding the movement were actually reflecting the intention of the monkey for a future movement. Although elegant, these experiments required a long and complex training of the primate. Hippocampal multi-units recordings allow the simultaneous recording of hundreds of cells. The strong neurophysiological correlates of space observed in this region makes it a very suitable candidate to decode covert variable from neuronal population activity. In 1993, Wilson and McNaughton showed that population rate vectors of hippocampal cells were a robust predictor of spatial location of the animal [Wilson and McNaughton 1993]. In this study, the authors were able to record dozens of cells simultaneously (73 to 148) thanks to twelve bundles of tetrodes implanted in the dorsal hippocampus of freely moving rats. Using similarity of population vectors calculated over a brief interval of time with the mean population vector calculated over the whole exploration episode, they were able to find that the instantaneous activity of the ensemble of cells could precisely predict the animal position. Although efficient, this algorithm only achieved high accuracy with relatively long times bins (above 1 second) and a high number of cells (several dozens).

<sup>22</sup> **Population vector:** The neuronal population vector is the outcome of a computation by which weighted neural activities of individual elements in a population yield an estimate of the population's functional operation.[Mahan and Georgopoulos 2014]

Later approaches improved hippocampal space decoding using a Bayesian statistical paradigm. This method can be decomposed in two distinct stages. Firstly, the encoding stage uses the biological signal to construct probability of neural spiking in relation to one or several variable of interest. Subsequently, the decoding stage uses Bayes's rule to estimate the most probable value of the variable given the spiking activity [Brown et al. 1998; Zhang et al. 1998; Meer et al. 2017]. Applied to position decoding in the hippocampus, this method provides several advantages compared to previous decoding algorithms. Primarily, it increases the accuracy of the decoding compared to previously mentioned methods [Zhang et al. 1998] during smaller integration time. As well, it allows to integrate a continuity constraint in the decoding and to take into account other variables during the decoding (*e.g.*: speed or theta phase,...).

These population approaches allow to take into account the greatest informativity of a population as a whole [Quian Quiroga and Panzeri 2009]. A broad tuning or single trial instability of a place cell firing can be compensated by other cells in the population. To illustrate this point, Keinath et al. [2014] studied the spatial signal of cells in the ventral portion of the hippocampus. According to previous results, the population of place cells in ventral hippocampus embedded non-spatial information [Strange et al. 2014] and ventral place fields were more broadly tuned in relation to space [Young et al. 1994; Maurer et al. 2005; Kjelstrup et al. 2008; Royer et al. 2010]. Interestingly, they asked if this coarse tuning of space in ventral hippocampus leads to a bad decoding of positional information at the population level. Against the commonly thought notion that a broad tuning meant a bad position decoding, they found that the population activity of ventral place cells provided a reliable decoding of space. Even if spatial information of single ventral place cells did not reach the dorsal place cells values, a comparable reconstruction of the position of the animal was computed from population of equal size from both regions. This accurate representation of space in ventral hippocampus could explain why either dorsal or ventral hippocampal lesions have been shown to affect navigation in large or small scale complex arena [Contreras et al. 2018].

These results highlight that a broad tuning do not directly mean that a variable is badly represented. On the contrary, a broad tuning could support a multidimensional coding of different variables and be advantageous for efficient [Zhang and Sejnowski 1999; Rigotti et al. 2013; Insanally et al. 2019] or more robust coding when stimuli change quickly [Finkelstein et al. 2018]. The population analyses should thus go hand in hand with individual cells analyses. Nevertheless, a disadvantage of population decoding is that it makes some assumptions regarding the variable to decode, the cells that carry the information and the way the variable is represented by the neuronal population.

#### 4.5.2 Limitation of population decoding

While studying the hippocampal formation, it is natural to focus our attention on active coding cells (with spiking activity correlated to one aspect of the environment or the animal's behavior). In 1973, Ranck wrote that "*It may not be possible to find a behavioral correlate of a neuron, for its firing may signal something not directly related to overt behavior, such as drive state, or some idea the rat has, or the blood level of some substance.*". Indeed, when no clear correlate to a neuron activity is found, it is common to conclude that this neuron serves no function in the current behavior of the animal. Nevertheless, advances in recording technics and analysis showed that non-clearly categorized cells could carry information about the current animal's behavior. Harris et al. [2003] showed that hippocampal cells could form "assemblies" of cooperating cells during a spatial behavior. Interestingly, these assemblies included either place and non-place cells (even if non-place cells proportion was really small 2%). In a recent study, other authors corroborated this idea by investigating how the collective behavior of hippocampal cells could give rise to place-modulated activity [Meshulam et al. 2017]. In this paper, the authors fitted a statistical model only reproducing the mean and the peer-correlation activity of all cells in the dorsal hippocampus of mice foraging in a virtual linear track. They found that this model could accurately predict the activity of each neuron from the state of all other place or non-place modulated neurons in the network. This result reinforces the idea that information about the animal behavior is collectively carried by the whole state of the neuronal state independently of the cell "classification".

In addition to the type of cells considered during decoding, a decoder often assumes that a certain kind of information will be encoded in a particular way. Most of the decoding approaches focus on rate coding of neurons and do not consider the temporal code of place cells [O'Keefe and Recce 1993] [but see: Brown et al. 1998]. These two types of code are intermingled but not in direct relation [Huxter et al. 2003; Middleton and McHugh 2016]. For example, some place fields, defined according to their firing rate, can hide several "temporal" fields [Maurer et al. 2006]. Theta rhythm is instrumental in structuring information in the hippocampus [Colgin 2013] and the position of the animal can be extracted from it alone [Agarwal et al. 2014].

A broad review of population encoding and decoding is beyond the scope of this introduction. In this section, I nevertheless highlighted the advantages and some of the major drawbacks of a population decoding approach. Nowadays, population decoding is widely used and regularly improved to open new perspectives to decipher information carried by neuronal ensembles [Meshulam et al. 2017; Maboudi et al. 2018; Stringer et al. 2019a; Tampuu et al. 2019]. To summarize, a better understanding of what and how information is encoded in the

brain will strongly benefit from the combined used of single cell and population analyses.

# 5

## OBJECTS PERCEPTION FOR NAVIGATION

---

" The self thus becomes aware of itself, at least in its practical action, and discovers itself as a cause among other causes and as an object subject to the same laws as other objects. "

---

Piaget [1955]

We saw in previous chapters that the internal representation of space provided by place cells could be influenced notably by a myriad of external stimuli. In "real world", these stimuli are often 3-dimensional objects populating the space surrounding us. In the following chapter, I will intent to give a definition of an objet in the context of spatial navigation, before explaining how they can be used to navigate. Last, I will present the current knowledge about their neuronal correlates across different brain regions.

### 5.1 WHAT IS AN OBJECT AND DO RODENTS PERCEIVE THEM?

An object can be defined as any stimulus within an environment that an animal can explore directly and interact with [Burke and Barnes 2015]. It is generally smaller or of comparable size than the subject and is distinct from boundaries of the environment [Scaplen et al. 2014; Burke and Barnes 2015]. For rodents, spatial cognition was largely dominated in the 50's and 60's by behaviorist approaches using operant chambers and mazes where objects were not useful and thus considered as not suitable for these animals. One of the first use of 3D objects to study animal cognition was performed in a delayed non-matching to sample task. Different variations of this task exist but their general principle is the following. First the animal has to memorize one (or a set of identical objects) during a sample phase. After a delay, the animal is faced with two objects: one familiar (identical to the test phase) and a new one. During this test phase, the goal of the animal is to recognize the new object (non-matching) in order to obtain a reward [Aggleton et al. 1986; Rothblat and Hayes 1987; Burke and Barnes 2015]. Nevertheless, this type of discrimination task has been shown to be solvable with non-configural solution<sup>1</sup>. In other words,

---

<sup>1</sup> A configural process rely on the combination of different types of information (height, width, odor,...), possibly from different modalities, in order to process a complex stimulus

we expect that in this task the animal is combining several dimensions of the object (height, width, color, shape,...) in order to discriminate the new and familiar objects. But some experimental evidences have shown that rats, in some cases simplify the discrimination, only considering one dimension (for example luminance in Minini and Jeffery [2006]). Therefore this type of task does not seem appropriate to ascertain the recognition of an object in rodents [see: Jeffery 2007, for an other example and discussion on this subject]. A later developed task, used the spontaneous tendency of rodents to explore preferentially a stimulus that is novel in order to test their ability to perceive and distinguish 3D objects [Ennaceur and Meliani 1992]. This task consisted in exposing first the animal to an object during a familiarization phase of few minutes (sample phase). After a delay, ranging from few minutes to a day, the animal was exposed to the same object than in the sample phase (familiar object) and another novel object. Naturally, the animal was spending more time investigating the new than the familiar object in the test phase. Note however that, in this behavioral paradigm, if the animal does not show this preference for the novel object, this deficit can reflect either a recognition failure (a false recognition of the novel object as familiar) or a habituation deficit (e.g. : the animal has forgotten the familiar object). A clear characterization of the exploration time during the sample phase as well as a look at the raw exploration time are very important to discriminate between these two possibilities. For example, if the animal does not show a clear familiarization during the sample phase (by exploring the object less and less), then a deficit during the test phase is likely to reflect primarily a habituation deficit. In this task, the exploration is defined as the presence of the animal in an extremely restricted circle around the object, thus providing a multisensory examination composed of a combination of tactile, visual and olfactory information.

We could now expand the previously proposed definition of an object as an entity of comparable size than the subject, to something with which the animal can interact through multiple senses. Consequently, can an object explored with one sensory modality be recognized using another one (a phenomenon called cross-modal recognition)? After an initial development of this question in monkeys [see for review Burke and Barnes 2015], a cross modal object recognition task has been developed in rats [Winters and Reid 2010; Gaynor et al. 2018]. This task used a variation of the spontaneous object recognition previously described. However, in the sample phase, animals were allowed to explore two identical objects in the dark, thus eliminating visual information while preserving tactile and olfactory ones. Then, the test phase was conducted with light, but conversely to the sample phase, the objects were protected behind a Plexiglas screen so that the animal could only use visual information to experience them. In this task, Winters and Reid [2010] showed that rats explored more the novel

object in the test phase, even if the familiar object was previously inspected with a different sensory modality. Rodent can thus extrapolate the knowledge acquired on an object solely from tactile information to vision.

Collectively, these sets of experiments demonstrate that rodents can perceive and distinguish 3D objects in their surrounding. In the next sections, I will focus on their role in spatial navigation.

## 5.2 ARE OBJECTS USED FOR NAVIGATION ?

In a seminal paper Collett et al. [1986] studied how gerbils (*Meriones unguiculatus*) used objects in order to locate and reach a food reward (sunflower seed) buried in the ground. The position of this seed was defined in relation to an array of cylinders placed in an impoverished arena: "*light-tight, black painted room illuminated by a single light bulb hung from the ceiling*" [Collett et al. 1986]. Once the animal learned to locate the seed in relation to one or several objects, the authors elegantly designed a series of test conditions in order to identify the way the animal was using the objects to locate the reward. First, the simplest test they performed was to train the animals to find a seed at a constant direction and distance from a cylinder inside the arena. The fact that gerbils searched at a single location and not in a circle around the landmark showed that the animal could use additional external cues (different from the cylinder) to compute the correct direction. In a second time, the authors wanted to test the hypothesis that gerbils were storing the angle and the distance from the object to the goal. Indeed, a similar search pattern could be obtained if gerbils, akin to bees, learned instead to associate the location of the seed with a specific visual snapshot at this location (characterized specially by how large the object is at this location)[Collett et al. 2006]. Consequently, Collett et al. varied the size of the cylinder during the test phase. If gerbils used a similar strategy than bees, they should search further from the landmark if the cylinder was bigger and closer if it was smaller. Following this manipulation, the search area of the animal became broader, but remained approximately at the same spot. This demonstrated that gerbils were not using a retinal snapshot of the landmark in order to locate the seed but used a vector deduced from external sensory cues.

Then, Collett et al. asked if the gerbil could find the goal location using either the entire array of objects or each landmark individually. In order to answer this question, the authors trained animals to find a goal location between two identical cylinders (Figure 5.1 A-B). Once the animals learned the task, one of the cylinder was removed (Figure 5.1 C). In this condition the gerbils "*behaved as though they had identified the solitary, remaining landmark as first one and then another of the elements of the array*". In other words, the search pattern of the

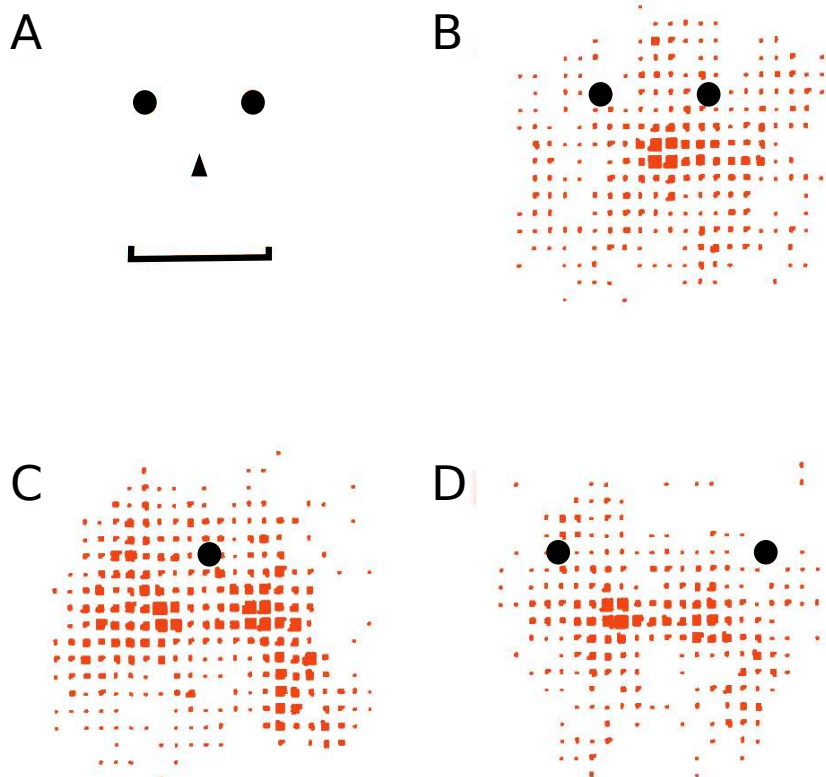


**Figure 5.1:** A: Task description, the animals had to search for a sunflower seed (triangle) positioned in relation to two identical white cylinders (70 cm high and 11 cm in diameter; Black circles). The cumulative search pattern of four animal is displayed with orange squares. The size of the squares reflect the time spent at this location. The depicted calibration bar measures 100cm B-D: Search pattern of gerbils after the training (B), the removal of one landmark (C) or after doubling the distance between the cylinders (D) (Modified from [Collett et al. 1986])

animal was distributed between two zones where the goal should be in relation to each individual cylinder. In a following experiment, the authors doubled the distance between the landmarks (Figure 5.1 D). Interestingly, the same search behavior was observed. The gerbils investigated alternatively the place defined by one or other landmark and did not compute an averaged goal position. Altogether these results demonstrate that rodents use landmarks during navigation in order to construct individual vectors (bearing and distance) from each individual landmarks<sup>2</sup>.

In order to assess how this type of vector-based navigation using individual landmarks is represented in the brain, Gothard et al. [1996b] recorded hippocampal place cells in an experimental design inspired by Collett et al. [1986]. In this task, rats were released from a starting box to search for a reward positioned in relation to two different white cylinders before reaching an end box for additional rewards. From

<sup>2</sup> In the last manipulation described, the fact that gerbils only searched on one side of the landmark array suggested that they combined the information of the landmark array with an orienting cue.

trial to trial, experimenters moved the position of the start / end boxes and the location of the two cylinders. The relative position of the goal in comparison to the cylinders was however maintained to indicate coherently the goal location in this frame. Indeed, analysis of the rats' trajectories indicated that they were able to use the cylinders as spatial cues and not only as beacons as their search focused first at the appropriate goal location. This approach allowed them to uncover cells exhibiting a spatial tuning in the reference frame defined by the landmarks (either cylinders or start/end boxes) as these cells were bound to these landmarks independently of their location in the arena. The firing of other place cells was however anchored to the global fixed room reference frame. This paper is one of the first report of place cells firing in a reference frame defined by an array of objects, with place fields located at the same position relative to intra-maze objects. Nevertheless, a confound with a potential goal related activity remains unclear. Since then, other correlates of landmark-related activity have been described, I will detail them in a later section (§ 5.4).

### 5.3 FROM OBJECTS TO LANDMARKS

Given that our surrounding world contains a multitude of objects, the question of what bestows them their property of navigational landmarks is of utmost importance [Chan et al. 2012]. If you walk in a park you just discovered, you will certainly use unique or easily distinctive objects to guide you, as a fountain or a playground instead of the multitude of resembling bushes and trees [Stankiewicz and Kalia 2007; Bruns and Chamberlain 2019]. For example, humans have been shown to use object landmarks (statues in a virtual environment) easily to locate a goal in a large-scale virtual maze. The statues were unique in the environment and thus were very informative about one's location. Interestingly, participants had a more difficult time using "abstract art" statues for navigation [Ruddle et al. 1997]. These results suggest that the difficulty in distinguishing each abstract statue was explained by the lower informativity of this type of cue. For large scale navigation in cities, building landmarks with strong perceptual features (*e.g.*: unique, size and shape) are better remembered after performing a navigation task [Evans et al. 1982; Miller and Carlson 2011; Bruns and Chamberlain 2019]. However, it is worth noting that the saliency is not necessarily driven by inherent properties of a specific feature as even the most mundane object could be used as a landmark because of contextual particularities (*e.g.*: a water well in the desert). Last, saliency can also depend on the current cognitive state of the navigator that will determine the way it directs its attention in the environment (this state depends on motivation as well as on subject's purposes)[Caduff and Timpf 2008].

In the next sessions, I will briefly illustrate these points by focusing on the critical components of an object that are relevant for its use as a landmark during navigation.

### 5.3.1 Landmark stability

The stability of an object in its environment can influence their use as a landmark. O'Keefe and Nadel [1978] already raised this matter in their book: "*the mapping system is sensitive to constant variability in the environment; such variability makes it difficult, if not impossible, to build a useful map.*" [O'Keefe and Nadel 1978, p.95]. An object needs to be perceived at a stable location to provide meaningful and reliable spatial information. In order to investigate this question, Biegler and Morris [1994], trained rats to find food in a large arena ( $10.89\text{m}^2$ ) oriented by a white curtain on one side and containing two distinct landmarks (objects). Forty centimeters at the south or north of each object was positioned a feeder containing a reward that was accessible in only one of the two feeders. The same object was always associated with the rewarded feeder. Experimenters then varied, across trials, the position of the landmarks in the arena for one group of rodents. Importantly, the feeder and the landmark always kept a fixed relation despite the manipulation. In the stable condition, animals learned to seek the food reward at the appropriate location. On the other hand, the performance of animals trained in the variable condition were impaired. Thus Biegler and Morris [1994] showed that geometric stability was necessary for a landmark to be used to find a goal location.

In a follow up study they showed that if the goal was always at a fixed distance and direction to a single, isolated object in the environment, then the rats in the variable condition could eventually learn the task [Biegler and Morris 1996]. Taken together, these results revealed that in order to be used to find a goal, an object had to maintain stable relations with at least one other landmark or the geometric feature of the environment. Note however that only the first aspect is not hippocampus-dependent as rats with lesions of the dorsal hippocampus were able to learn the location of a platform that was always at the same distance and direction to a landmark independent of its position in the pool [Pearce et al. 1998]. Burgess et al. [2004] later highlighted similar effects of landmark stability in humans. Further evidence of the importance of landmark stability has been brought by experiments showing that the propensity of a salient landmark to control place fields position was lost when the animal experienced that its relative position in comparison to the landmarks is changing (by moving the animal and/or the landmarks) [Jeffery 1998; Jeffery and O'Keefe 1999; Lenck-Santini et al. 2002]. In this case, rats are likely

to trust less visual cues and to rely more on idiothetic information [Knierim et al. 1995].

### 5.3.2 Landmark position

The position of an object inside an arena is an important criteria as it can drastically impact its use for navigation and for place cells control. For example, Biegler and Morris [1996] showed that four objects clustered at the center of the environment were more difficult to use in order to locate a food source than if they were spread apart. Similarly, Cressant et al. [1997] observed that centrally positioned objects did not exert a strong control on hippocampal place cells. A rotation of these clustered objects only affected 2 of 52 place fields. Conversely, if the objects were positioned against the walls of the circular arena, they could take control over the angular position of firing fields [Cressant et al. 1997, 1999; Renaudineau et al. 2007]. Nevertheless, being at the periphery of the environment might not be sufficient to systematically control the orientation of space representation. An illustration of this idea was given by Zugaro et al. [2001] in a study investigating how objects could control thalamic head direction cells. First, in accordance with Cressant et al. [1997], they showed that objects situated at the periphery of a circular arena exerted a strong control on thalamic head direction cells.

Another set of results was however surprising, as the peripheral objects lost their control on head-direction cells if the cylindrical wall was removed to reveal the larger square made of the curtains surrounding the enclosure (1.5m away of the platform). These results suggested that objects were used as orientation landmark only when they were background and not foreground cues.

Considering the results of both Cressant et al. [1997] and Zugaro et al. [2001], animals seemed to select orienting landmark with the lowest optic flow and/or that are more visually stable (more distal) and thus with a low parallax effect<sup>3</sup>.

In human subjects, a fMRI study by Janzen and Van Turennout [2004] found that objects located at decision points strongly activated the para-hippocampal gyrus during a recognition task following the exploration of a virtual museum (Figure 5.2). In this study, healthy adults were passively moved through a virtual museum with objects placed at intersections (*e.g.*: decision points) or at simple corridor turns (non-decision points). Half of these objects were toys and the other half were from other semantic categories (non-toys). These two types of objects were disposed in a random manner at decision and non-decision points. The participants were instructed to pay a particular attention to objects that were toys, to be able to guide children in this virtual mu-

---

<sup>3</sup> Parallax effect: the apparent displacement or apparent modification of an object due to a change in the position of the observer.

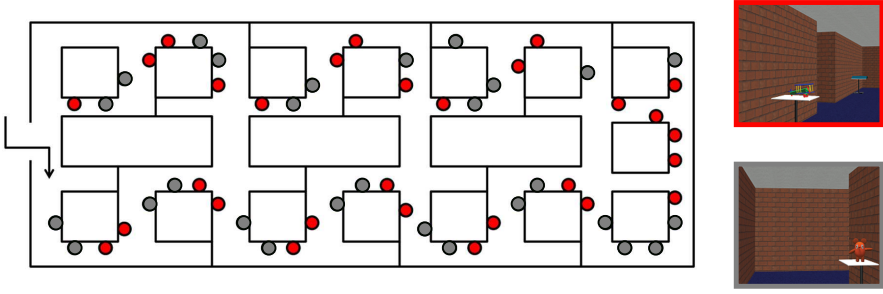


**Figure 5.2:** **left** Schematic of an aerial view of the virtual museum used in Janzen and Van Turennout [2004]. Red circles indicate the location of an object at a decision points, conversely gray circles depict objects at non-decision points. **right:** View of a decision point (**top**) and non-decision point(**bottom**) (Adapted from [Janzen and Van Turennout 2004; Chan et al. 2012])

seum later. This paradigm enabled to discriminate the brains regions activated by objects relevant for navigation (at decision points) or by simply paying attention to one set of objects (toys). Event-related fMRI was then performed during an old (present in the virtual museum) vs new (absent in the museum) object recognition task. Reaction times were faster for toys compared to non-toys highlighting a clear effect of attention. This effect however strongly interacted with the navigational value of these objects as the reaction times for toys located at decision points were higher than for toys located at non decision points. Finally, analyses of fMRI data showed that the parahippocampal region (right and left side) was the only brain region that was significantly more activated at decision points. This effect was independent from attentional demand notably as it was present for both the toys and the non-toys, even if they were not explicitly recognized during the test. Taken together, these results highlighted an important role of the parahippocampal region in processing objects as landmarks to guide navigation. Further studies by this team confirmed that recognition performances were better for landmark objects versus objects placed at non-decision points and interestingly they also showed that this effect was lost in patients with Alzheimer Disease [Janzen and Weststeijn 2007; Kessels et al. 2011]. More recent work by an independent group reproduced such effects in real large scale environment [Schinazi and Epstein 2010]. Briefly, after a 3.8km walk in the university of Pennsylvania, participants manifested a better recall of buildings located at decision points than at non-decision points.

Overall, these studies provide strong evidence that an object is not used as a reference point solely because of its intrinsic attributes. Other factors are important to determine whether or not it will be used as a landmark, specially its position in the environment.

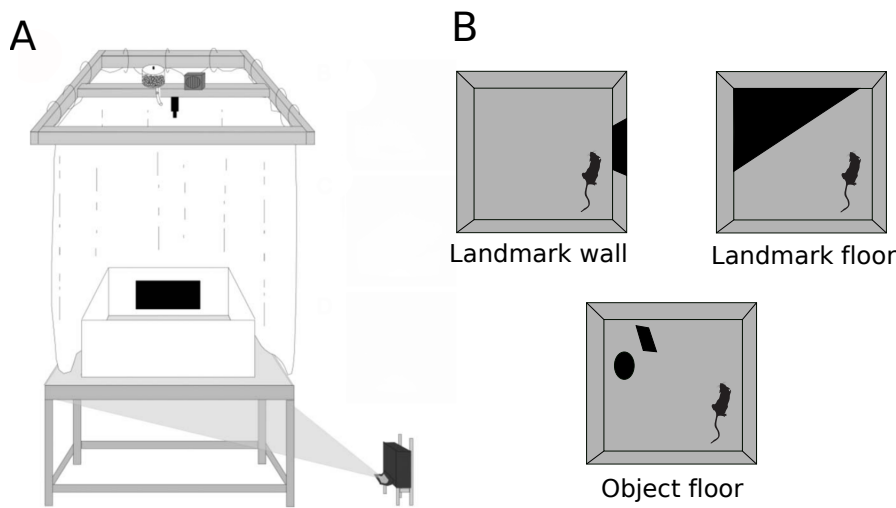


**Figure 5.3:** A: Behavioral apparatus used in the Scaplen et al. [2014] study depicted with the wall cue. The floor cues are projected on a plexiglass floor using a projector. The maze was surrounded by white curtains thus masking extra-maze cues. A speaker was playing a 70db white noise and was positioned close to the food dispenser and the camera above the apparatus. B: Depiction of the different apparatus conditions: **top-left:** Landmark wall condition, **top-right:** Landmark floor condition and **bottom:** object floor condition. (Adapted from [Scaplen et al. 2014])

### 5.3.3 Dimensionality

Virtual reality in rodents is now widely used to study spatial cognition as already mentioned. In this set up, virtual objects are presented in two dimensions raising the question about the way they are perceived and used for navigation.

Early studies on visual discrimination in rodents suggest that they are able to discriminate 2D shapes [Burke and Barnes 2015; Ahn and Lee 2017] [but see: Minini and Jeffery 2006]. Nevertheless, it is still unclear if such shapes will be considered akin to an object in the context of navigation. Scaplen et al. [2014] studied this question using an elegant experimental paradigm. In their task they recorded the activity of hippocampal place cells while rats foraged in a squared arena devoid of physical objects. Instead, they used an ingenious design to project shadows of various shape on the walls or floor of the apparatus. Their goal was to study the influence of small, "object-like" and big "landmark-like" shadows on place cells firing (Figure 5.3 - A). The three conditions they used was: a large vertical cue on one wall, a large floor cue at a corner and a smaller complex floor cue close to a corner (Figure 5.3 - B). A rotation of each type of cues had different impact on the orientation of the place cells map. Rotation of large cues, independently of their position on the wall or the floor, caused concordant rotation of the place fields. Conversely, the rotation of the small object cues led either to local remapping of the place fields (local change in firing rate) or to no change at all. These results indicate that large shadows located at the periphery were more likely to anchor

place cells than local "object-like" shadow. One possibility to explain this difference is that "object-like" shadows were not sufficiently salient and thus likely to be neglected or considered as a contextual cue. In a later study, Scaplen et al. [2017] showed that a muscimol inactivation of the lateral entorhinal cortex increased the effects of visual cues in their paradigm with some differences between the large shadow and the smaller "object" shadow. First, the inactivation increased the proportion of place cells that rotate coherently with the large shadow without affecting spatial coding quality. In the small object shadow condition however, place cells exhibited an increased spatial selectivity under muscimol but no effect of the inactivation was observed after the rotation of this type of cue. These results comfort the hypothesis that these two types of cues could be involved in different spatial information processing and highlight a role of lateral entorhinal cortex in processing visual cues for space representation.

The object cues used in the previously described studies were shadows on the floor that were not necessary in the behavioral paradigm. Recent studies using virtual (see: § ii) and augmented reality [Grosso et al. 2017] suggest that 3D objects influence the hippocampal coding of space. Grosso et al. [2017] developed an augmented reality setup similar to the one used previously by Scaplen et al. [2014, 2017] but with a more sophisticated projection procedure. In their augmented reality task, they tracked in real time the position of the animal in a rectangular area and adjusted the projection of the object to give the impression of 3D (the view of the object was modified according to the view of the animal). This type of objects triggered spontaneous naturalistic exploration comparable to physical 3D objects. Rats investigated newly introduced virtual objects and often adjusted their trajectories to avoid them. This observation suggests that virtual 3D objects, perceived solely using vision are sufficient to drive behaviors similar to physical objects. Further recordings in this paradigm or in virtual reality will be needed to investigate the impact of visual objects on hippocampal spatial coding.

Taken together, these results suggest that the factors that determine the use of an object as a navigational landmark are not strictly intrinsic but involve also extrinsic factors like position or motivation of the subject [Caduff and Timpf 2008]. Subjective impact on saliency of an object is a fascinating question. It is still unclear how a mundane object can reach saliency if it has a particular interest for the navigating subject. For example, a random house, lost in the middle of similar houses can be used as a landmark if it belongs to a close friend or if you have already visited this place [Sanguinett-Scheck2019; Caduff and Timpf 2008].

## 5.4 NEURONAL CORRELATES OF OBJECTS FOR NAVIGATION

### 5.4.1 Object coding in perirhinal cortex

The perirhinal cortex is a parahippocampal region receiving diverse cortical inputs from olfactory, auditory, somatosensory and visual associative cortices [Burwell and Amaral 1998; Furtak et al. 2007], thus making it a suitably positioned area in objects processing that are polymodal in nature. Early investigations of PER neuronal firing correlates have indeed shown that PER neurons exhibited an increase firing rate in response to the presentation of isolated objects in awake and anesthetized rats [Zhu and Brown 1995; Zhu et al. 1995]. This response was not modulated by object identity and only very few neurons exhibited discriminative firing rates in response to distinct objects (3 out of 86 in Zhu and Brown [1995]). However, these two studies showed that PER might be essential to detect the novelty of objects as neuronal activity in this region decreased in response to repeated presentation of the same object. Is the perirhinal cortex only important for novelty detection of objects or does it have a more elaborated function in processing object information in the context of navigation?

Recent investigations of PER neurons activity during navigational tasks in presence of objects brought elements of answer in favor of the last hypothesis. Two different groups showed that PER neurons increased their activity at the locations of objects when rats were running back and forth in a circular track or if they randomly foraged in a square arena (in both cases the environment contained several objects located at the periphery of the track or scattered inside the arena) [Burke et al. 2012; Deshmukh et al. 2012]. In the circular track , more than a third of PER neurons exhibited "object fields", stable across successive sessions, either for familiar or newly introduced objects (Figure 5.4 - A). Importantly, spatial selectivity of PER neurons was low in the absence of objects, and increased only at objects' locations in their presence suggesting that PER process non-spatial information rather than spatial information *per se*. Additionally, in the Burke et al. [2012] study, the authors also showed that this effect was not modulated by the familiarity/novelty of the objects. Contrarily to what was observed in a perceptual task (passive presentation of objects in Zhu et al. [1995]), they did not observed a "repetition suppression" effect on firing rates in response to repeated exposure to objects<sup>4</sup>. Finally, when objects were manipulated (familiar object replaced by new object at the same location in Burke et al. [2012]), the introduction of a new object at a new location or misplacement of a familiar object

---

<sup>4</sup> The absence of "*repetition suppression*" was observed even when the authors controlled for the recognition of the novel versus familiar stimulus: (e.g. the animal spend more time exploring new objects)

in Deshmukh et al. [2012]), analyses brought poor evidence of activity locked to a specific object at a single cells level, suggesting that **PER** is important for object recognition but not discrimination<sup>5</sup>.

Recent works proposed that novelty coding might not have been detected in these previous studies because the attention load on the objects was too low, or because novelty could be subtly coded in **PER** via other neurophysiological correlates. Indeed, Ahn et al. [2019] provided evidence that repetition suppression occurred robustly in an object discrimination task. In this task the animal had to learn to associate two objects (both familiar or both new) to distinct actions in an operant box (push the lever or nose poke). In this task, half of the neurons in the **PER** showed a repetition effect (either a suppression or augmentation) and this effect was more common for single object (one specific object out of the four objects used in the task) than for a groups of objects (new or novel). Interestingly they observed that spikes remaining during repetition suppression were the ones phase-locked to the gamma rhythm peak in **PER** during the whole task. Indeed, the gamma phase variability decreased with familiarity and the eliminated spikes where the ones located outside of the gamma peak ("pruning" effect). Interestingly, they also showed similar effects for hippocampal neurons, but in this brain structure, object-related firing was phase-locked to the theta rhythm. Consequently, these results showed that novelty coding can be robust in a goal-oriented task necessitating objects discrimination. In this type of task, novelty was represented by a very striking temporal code where noisy spikes (out of phase) are pruned from the object neuronal correlates [Ahn et al. 2019]. It would be interesting to know whether such pruning is functionally relevant for the task performance.

This body of work reveals an undeniable object-related activity in **PER** even if the functions of such coding is still unclear. It is important, however, to understand how non-spatial information is processed before it is distributed to downstream regions of the hippocampal formation and in particular to the entorhinal cortex.

#### 5.4.2 Object coding in the entorhinal cortex

Object-related activity was also observed in the Entorhinal Cortex, in both the **LEC** and more recently the **MEC**. The **LEC** is more strongly connected with the **PER** than the **MEC**, suggesting that this structure might contain similar object-related activities. Following [Zhu et al. 1995] observation of **LEC** neurons responding to passive presentation of objects, Deshmukh and Knierim [2011] investigated these neuronal correlates during a foraging task in a square arena containing dis-

---

<sup>5</sup> The implication of **PER** in object discrimination is still a mater of debates, but recent work showed that the **PER** could carry an activity allowing the discrimination of object at the population level [Ahn and Lee 2017]

tinct objects. They reported a population of **LEC** cells exhibiting an "object field" not necessarily at the object location but also at a distance from it (Figure 5.4 - B). Interestingly, the object-related spatial selectivity of LEC neurons vanished in an empty arena. This effect was also reported in an environment enriched with distal cues as no obvious neuronal LEC correlates could be observed [Hargreaves 2005; Yoganarasimha et al. 2011]. Curiously, in the Deshmukh and Knierim [2011] study, despite persistent object fields in successive sessions of the task, some neurons did not always fired at the same object. Furthermore, Deshmukh and Knierim [2011], reported the observation of two **LEC** neurons which fired at a consistent location even after the object was misplaced. Tsao et al. [2013], later investigated these rare "*object trace*" cells and uncovered that such neurons were able to maintain an activity trace of the remembered object for at least 17 days (Figure 5.4 - B). Similar observations of object trace activities have also been reported in hippocampus and anterior cingulate cortex [Weible et al. 2012; Deshmukh and Knierim 2013].

This remanent trace in absence of object strongly suggests that this activity is not linked to the object *per se* but to the object-place relation, to the location that the object had occupied. This hypothesis that the location of objects is represented in the para-hippocampal region is supported by human functional magnetic resonance imaging studies. Kanwisher and Epstein [1998] showed that para-hippocampal region, measured by functional magnetic resonance imaging, was more activated when viewing photographs of a furnished room versus an array of the same furniture on a blank page. This work has led to the idea that human para-hippocampal cortex was involved in the processing of spatial layout within scenes [Epstein 2005, 2008; Epstein et al. 2017]. Recently, Wang et al. [2018] observed that some **LEC** cells exhibited an egocentric tuning to the nearest boundary<sup>6</sup>. In addition to this response to boundaries, some neurons showed an egocentric tuning to 3D objects present in the arena. **LEC** could thus allow the convergence of allocentric and egocentric position of the navigating subject in a landmark based reference frame.

The medial entorhinal cortex is known for its stronger spatial modulation due to the presence of grid, head direction, speed, border or conjunctive cells [Fyhn et al. 2004; Hafting et al. 2005; Sargolini et al. 2006; Kropff et al. 2015; Diehl et al. 2017]. Surprisingly, recent recordings of **MEC** in freely moving mice uncovered the presence of object-vector cells among this multitude of spatially modulated cells [Høydal et al. 2019]. This small proportion of cells fired when the mice was at a given distance and direction of an object present in the arena. Interestingly, these cells were not specific to the object identity and location but fired with a similar relation to any discrete object in the

<sup>6</sup> Similar observations of egocentric tuning to borders have also been made in retrosplenial cortex by Alexander et al. [2019]

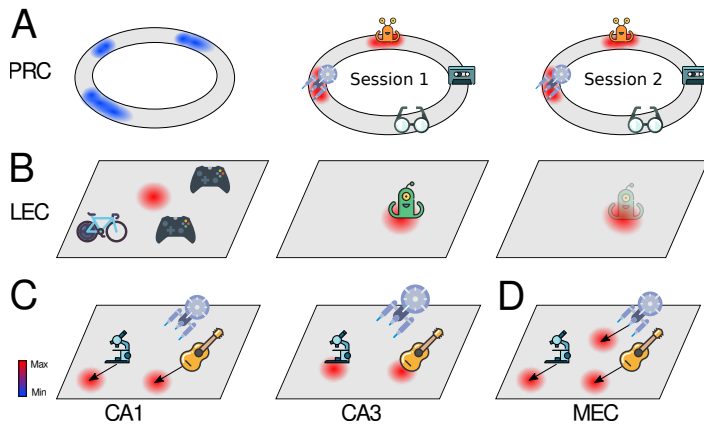


**Figure 5.4:** Single unity activity associated with the presence of objects. **A:** Schematic representation of the firing pattern of a Perirhinal Cortex neuron recorded while a rat runs in a circular maze. In an empty track, a proportion of **PER** neurons show a dispersed low intensity firing all around the maze, (left). If objects are introduced in the track, previously non-selective cells will fire coherently for successive sessions near objects (right). **B:** Unlike **PER** neurons, some **LEC** principal cells fire at a particular distance and orientation in relation to local objects (left). In absence of object **LEC** neurons are weakly spatially modulated. **LEC** neurons also form objects fields at the location of object and in certain instance maintain an “*object-trace*” activity, sometimes for several days, after the object is removed from the arena (middle-right). **C:** Schematic example of hippocampal object-related activity. In an open arena containing objects, **CA1** cells will exhibit landmark vector activity (right). In parallel, **CA3** fields will be more likely to manifest object related activity near the location of the objects. **D:** Schematic of object related neuronal activity in **MEC**. After the introduction of intra-maze objects, object vector cells will be tuned equally to discrete objects in the arena irrespectively to their position in the arena. (Adapted from [Burke and Barnes 2015])

maze. Additionally, this object-vector coding was preserved across environments (different rooms) and was weakly overlapping with grid-like or border-like firing patterns. The fact that these cells were firing irrespectively to the object identity but that they maintained their relative alignment across environment suggest that they could provide a low dimensional allocentric scaffold coding for the location of objects.

#### 5.4.3 Object coding in the hippocampus

Both lateral and medial entorhinal cortex project to the hippocampus. Although the most striking behavioral correlate in the hippocampus is space, numerous studies reported firing activity in relation to the current or remembered location of an object in principal cells of **CA1** and **CA3** [O’Keefe and Nadel 1978; Gothard et al. 1996b; Lenck-Santini et al. 2005; Manns and Eichenbaum 2009; Burke et al. 2011; Deshmukh and Knierim 2013; Geiller et al. 2017b; Omer et al. 2018]. An early report of hippocampal recording described “*misplace unit*” characterized as “*complex place units fir[ing] maximally during myostatial sniffing elicited in a place, either by the absence of an expected object or by*

*the presence of an unexpected one.*" [O'Keefe and Nadel 1978, p. 202]<sup>7</sup>. Later, Gothard et al. [1996b], recorded place cells firing in a reference frame defined by an array of cylinders. Despite a coherent activity in relation to these objects, the activation of these cells could still be tainted by the reward that the animal had to seek, also defined in relation to the array of objects. A complementary study by Deshmukh and Knierim [2013], recorded in the hippocampus, a small proportion of landmark-vector cells firing when the rat was located at the same distance and orientation from multiple landmarks<sup>8</sup> (Figure 5.4 - C). These units revealed a fascinating multitude of behaviors. Some fired at the same orientation and distance from several objects, while other neurons first fired in relation to one landmark and then developed a secondary field matching the preexistent landmark vector in relation to a second landmark. Also, the authors reported "*object trace*" cells in both CA1 and CA3 that fired where an object was previously as described in LEC or cingulate cortex (see § 5.4.2) [Deshmukh and Knierim 2011; Weible et al. 2012; Tsao et al. 2013]. In a parallel study, Burke et al. [2011] recorded the activity of neurons located in the distal part of CA1, an area known to receive direct input from LEC. They showed that, in a circular linear track, the presence of objects increased the number of place fields and reduced the size of the place fields, such that the probability of activation of a place cell was homogenous along the whole track<sup>9</sup>. The linearity of the maze and the close proximity between adjacent objects did not allow to uncover undoubted landmark-vector cells. Nevertheless, the changes in spatial coding following the introduction of objects suggest the incorporation of non-spatial information in the hippocampus (as also seen in Manns and Eichenbaum [2009]).

Now, one of the question emerging at the view of this body of work is whether these object-responsive cells constitute a particular class of neurons. To investigate this question Geiller et al. [2017a] recorded the activity of dorsal hippocampal neurons while a mouse was running on a treadmill enriched with visuo-tactile landmarks at multiple locations on the belt. They provided evidence that cells located in the deep section of the pyramidal layer were more strongly tied to landmarks than their superficial counterparts. Deep CA1 cells fired at several locations, in accordance with the position of landmarks, and thus likely represented the position of the landmark. Among their landmark cells, 19% encoded landmark identity as they were firing preferentially at a specific type of landmark. Conversely, superficial cells appeared more contextual, as they had in majority a single field

<sup>7</sup> Misplace units were in reality first reported in O'Keefe [1976]

<sup>8</sup> It is worth precising that a landmark-vector cell with a unique field can not be distinguished from a classical place cell. A landmark cell need to fire in relation to several objects (multiple fields) or to follow the displacement of the landmark

<sup>9</sup> see § 4.2.3 for a more detailed description of this study

and responded more slowly to landmarks manipulation [Geiller et al. 2017a; Fattah et al. 2018].

Hitherto, we described static objects but our world is also made of moving objects. As cited in the epigraph of this chapter, Jean Piaget highlighted the fact that, in a way, individuals are "*object subject to the same laws as other objects*" [Piaget 1955]. Wondering if the hippocampus carried signals related to the position of other congeners, Omer et al. [2018] recorded neurons in the hippocampus of flying bats observing a moving congener. The authors successfully found that some cells were activated in relation to others, and named them "*social cells*". As a control they also performed the same recordings but replaced the moving bat by an object. Surprisingly, Omer et al. [2018] some cells were also correlated to the activity of a moving object. The population of "social" and "moving object" neurons were distinct but overlapping, thus ruling out a purely segregated information processing for objects and others. At the sight of this result a comparison between a static and mobile landmark would need further investigation to be reconciled with previous results in the literature [Biegler and Morris 1994; Biegler and Morris 1996; Jeffery 1998; Jeffery and O'Keefe 1999; Lenck-Santini et al. 2002].

Three-dimensional objects are a widespread correlate of neuronal activity from early visual sensory cortex to parahippocampal and hippocampal areas [Burke and Barnes 2015; Zoccolan 2015; Connor and Knierim 2017]. This is undoubtedly the case because of the ubiquity of objects in many aspects of an animal's sensory experience and memory. This variety of aspects comes at a cost of complexity. Many fine aspects of object information processing and memory are yet to uncover.

Part II

EXPERIMENTAL CONTRIBUTION



## PREAMBLE

---

Animals move in their natural habitat in order to find food, congeners or to avoid dangers like predators or unsuitable environmental conditions. In order to reach their goal during navigation animals can use a plethora of strategies. One of the most efficient method to navigate flexibly and dynamically (*e.g.*: find shortcuts or avoid obstacles) is to construct and use an internal representation of space, a cognitive map [Tolman 1948; O'Keefe and Nadel 1978]. The hippocampus is known to be important for the elaboration of this map. It contains a peculiar type of cells: the *place cells*, which are active in specific parts of the environment, their *place fields*, and virtually silent elsewhere. The scale at which these cells code for space can vary across different axis of the hippocampus. For example, place fields increase in size dorso-ventrally along the longitudinal hippocampal axis [Poucet et al. 1994; Young et al. 1994; Kjelstrup et al. 2008]. Similar gradients can be observed along the transverse and radial axes [Henriksen et al. 2010; Lu et al. 2015; Geiller et al. 2017a]. However, whether and how place cells' spatial coding resolution can adapt to local features of the same environment remains unclear [Battaglia et al. 2004; Burke et al. 2011].

In this thesis work, we explored the possibility of an adaptation of the hippocampal spatial coding resolution in a single environment by recording the activity of hippocampal neurons in the dorsal hippocampal area CA1 of mice navigating a virtual linear track. We used several types of visual information, unevenly distributed in the environment, to investigate the relative contribution of 3D visual objects, patterns on the walls or a combination of both. We observed that virtual objects improved spatial coding resolution in their vicinity. Place fields were more numerous, smaller, with better spatial information and stability. A population decoding analysis confirmed these results at the single cells level by showing a better decoding accuracy close to the objects. These effects were observable almost instantly after the online addition or removal of objects during the recording sessions. Thereafter, we tested the effect of patterns on the wall on the quality of the hippocampal spatial coding. Indeed, we uncovered that it led to an enhancement of spatial coding resolution, but to a lesser extent than objects. Visual objects also strengthened temporal coding resolution through improved theta phase precession. We propose that the hippocampal place cells representation can have a heterogenous resolution, which could be used to improve coding or inference notably in large-scale environments.





# Dynamic control of hippocampal spatial coding resolution by local visual cues

Romain Bourboulou<sup>1†</sup>, Geoffrey Marti<sup>1†</sup>, François-Xavier Michon<sup>1</sup>,  
Elissa El Feghaly<sup>1</sup>, Morgane Nouguier<sup>1</sup>, David Robbe<sup>1</sup>, Julie Koenig<sup>1,2\*\*</sup>,  
Jerome Epsztein<sup>1\*</sup>

<sup>1</sup>Institute of Neurobiology of the Mediterranean Sea (INMED), Turing Center for Living Systems, Aix-Marseille Université, INSERM, Marseille, France; <sup>2</sup>Institut Universitaire de France, Paris, France

**Abstract** The ability to flexibly navigate an environment relies on a hippocampal-dependent cognitive map. External space can be internally mapped at different spatial resolutions. However, whether hippocampal spatial coding resolution can rapidly adapt to local features of an environment remains unclear. To explore this possibility, we recorded the firing of hippocampal neurons in mice navigating virtual reality environments, embedding or not local visual cues (virtual 3D objects) in specific locations. Virtual objects enhanced spatial coding resolution in their vicinity with a higher proportion of place cells, smaller place fields, increased spatial selectivity and stability. This effect was highly dynamic upon objects manipulations. Objects also improved temporal coding resolution through improved theta phase precession and theta timescale spike coordination. We propose that the fast adaptation of hippocampal spatial coding resolution to local features of an environment could be relevant for large-scale navigation.

DOI: <https://doi.org/10.7554/eLife.44487.001>

\*For correspondence:

julie.koenig@inserm.fr (JK);  
jerome.epsztein@inserm.fr (JE)

†These authors contributed equally to this work

\*\*These authors also contributed equally to this work

**Competing interests:** The authors declare that no competing interests exist.

**Funding:** See page 26

**Received:** 18 December 2018

**Accepted:** 04 February 2019

**Published:** 01 March 2019

**Reviewing editor:** Neil Burgess,  
University College London,  
United Kingdom

© Copyright Bourboulou et al.  
This article is distributed under  
the terms of the [Creative Commons Attribution License](#),  
which permits unrestricted use  
and redistribution provided that  
the original author and source are  
credited.

## Introduction

Animals can flexibly navigate their environment. In mammals such as rodents and humans, this ability is thought to rely on an internal cognitive map ([Tolman, 1948](#); [O'Keefe and Nadel, 1978](#); [Epstein et al., 2017](#)). When animals move in their environment, hippocampal place cells fire in specific locations (their place fields) and this spatial tuning is believed to provide a neuronal substrate to the cognitive map. To be useful for navigation, such internal representation should be properly oriented and positioned in reference to the external world ([Knierim and Hamilton, 2011](#)). A dynamic control of hippocampal spatial coding resolution between different regions of the same environment could be important for spatial navigation ([Geva-Sagiv et al., 2015](#)). Wild animals, including rodents, often travel kilometers away from their home through empty space to specific food locations ([Taylor, 1978](#)). Mapping all traveled space at similar spatial resolution would require a huge neuronal and computational investment. Alternatively, mapping different parts of the same environment at different spatial resolutions could be advantageous.

In rodents, hippocampal place cell coding can vary both qualitatively and quantitatively. Qualitatively, place cells can code more or less accurately for space depending on several behavioral/experimental manipulations such as passive vs active movements ([Terrazas et al., 2005](#)) or light vs dark conditions ([Lee et al., 2012](#)). A better accuracy is generally associated with decreased place field size, increased spatial and temporal place field stability upon repeated visits of the same location and low out-of-field firing rate. Quantitatively, the number of spatially selective cells and place fields' density can increase globally in the presence of objects ([Burke et al., 2011](#)) and locally near rewarded locations ([O'Keefe and Conway, 1978](#); [Hollup et al., 2001](#); [Dupret et al., 2010](#); [Danielson et al., 2016](#); [Gauthier and Tank, 2018](#); [Sato et al., 2018](#)), salient sensory cues

(Wiener et al., 1989; Hetherington and Shapiro, 1997; Sato et al., 2018) or connecting parts in multi-compartment environments (Spiers et al., 2015). Whether these overrepresentations correspond to position coding at higher spatial resolution (i.e. the resolution of the ‘where’ information) or the coding of nonspatial information associated with these particular locations (also referred to as ‘what’ information) is, however, difficult to disentangle. If they would represent increased spatial resolution, then place fields should not only be more numerous but they should also more accurately code for space in terms of spatial selectivity, spatial information content and stability. Furthermore, in the context of navigation, spatial coding resolution should be rapidly adjustable within different parts of the same environment or upon specific experimental manipulations. Finally, improved spatial coding resolution should extend to the temporal coding domain.

The factors controlling spatial coding resolution are still poorly understood. While distal visual cues play an important role in map orientation and environmental boundaries in map anchoring (O’Keefe and Burgess, 1996; Knierim and Rao, 2003; Knierim and Hamilton, 2011), local sensory cues, with a high sensory resolution, could be instrumental in setting spatial coding resolution (Hartley et al., 2000; Strösslin et al., 2005; Barry et al., 2006; Sheynikhovich et al., 2009; Geva-Sagiv et al., 2015). Here, we took advantage of virtual reality (Hölscher et al., 2005; Harvey et al., 2009; Youngstrom and Strowbridge, 2012; Ravassard et al., 2013; Aronov and Tank, 2014; Cohen et al., 2017; Thurley and Ayaz, 2017; Gauthier and Tank, 2018) to specifically control and quickly manipulate local sensory cues and test their impact on hippocampal spatial coding resolution. We recorded a large number of hippocampal cells in area CA1 to be able to use decoding strategies to decipher the functional impact of the changes observed. Our results are consistent with a rapid adaptation of hippocampal spatial coding resolution to local features of the environment. We propose that this mechanism could be important for large-scale navigation.

## Results

### Effects of local visual cues on spatial coding resolution

To investigate the effect of local visual cues on hippocampal coding resolution, head-fixed mice were trained to run on a wheel and to shuttle back and forth on a 2 m-long virtual linear track to collect liquid rewards at its extremities (**Figure 1A**). The lateral walls of the virtual track displayed distinct visual patterns to provide directional information. To investigate the contribution of local cues to hippocampal spatial representation, mice were trained either in the presence or absence of 3D visual cues (hereafter called virtual objects; Objects Track, OT: n = 3 mice; No Objects Track, ØT: n = 3 mice), which were virtually positioned on the floor of the track between the animal trajectory and the walls (**Figure 1B**). The running wheel forced the animals to run in a unidirectional manner so that they repetitively ran along the virtual objects without the possibility to orient toward them or explore them with any sensory modality but vision. Animals received a reward (sucrose in water 5%) each time they reached one of the extremities of the linear track. After licking, the mice were ‘teleported’ in the same position but facing the opposite direction of the track (**Figure 1C**), allowing them to run back and forth in the same environment. Once animals reached a stable and proficient behavior (at least one reward/min during a 60-min-long session), we recorded spiking activity in the pyramidal cell layer of the CA1 hippocampal region using either 4-shanks or 8-shanks silicon probes (**Figure 1A**, **Figure 1—figure supplement 1**) in the right and/or left hemispheres over the course of 2–3 days. A total of 1021 neurons were recorded in the CA1 pyramidal cell layer in OT and ØT (**Supplementary file 1**). Mice trained in ØT performed the task with similar proficiency than mice trained in OT, as shown by similar rate of reward collections (ØT:  $1.86 \pm 0.31$  rewards/minute, n = 9 sessions in three mice; OT:  $1.44 \pm 0.12$  rewards/minute, n = 8 sessions in three mice; Z = 0.52, p=0.59, two-tailed Wilcoxon rank sum (WRS) test; all values expressed as mean  $\pm$ SEM) and average running speed (ØT:  $14.1 \pm 2.12$  cm/s, n = 9 recording sessions in three mice; OT:  $15.3 \pm 1.28$  cm/s, n = 8 recording sessions in three mice;  $t_{15} = -0.47$ , p=0.64, two-tailed unpaired t-test).

We first assessed possible effects of local visual cues on overall hippocampal excitability by comparing the percentage of track-active putative pyramidal cells among all recorded cells in ØT and OT. The percentage of track active cells was comparable between the track without and with virtual objects (ØT:  $66.4 \pm 5.8\%$ , n = 7 sessions in three mice; OT:  $54.6 \pm 4.8\%$ , n = 8 sessions in three mice;  $t_{13} = 1.58$ , p=0.14, two-tailed unpaired t-test; **Figure 1D**). We next started to assess spatial coding

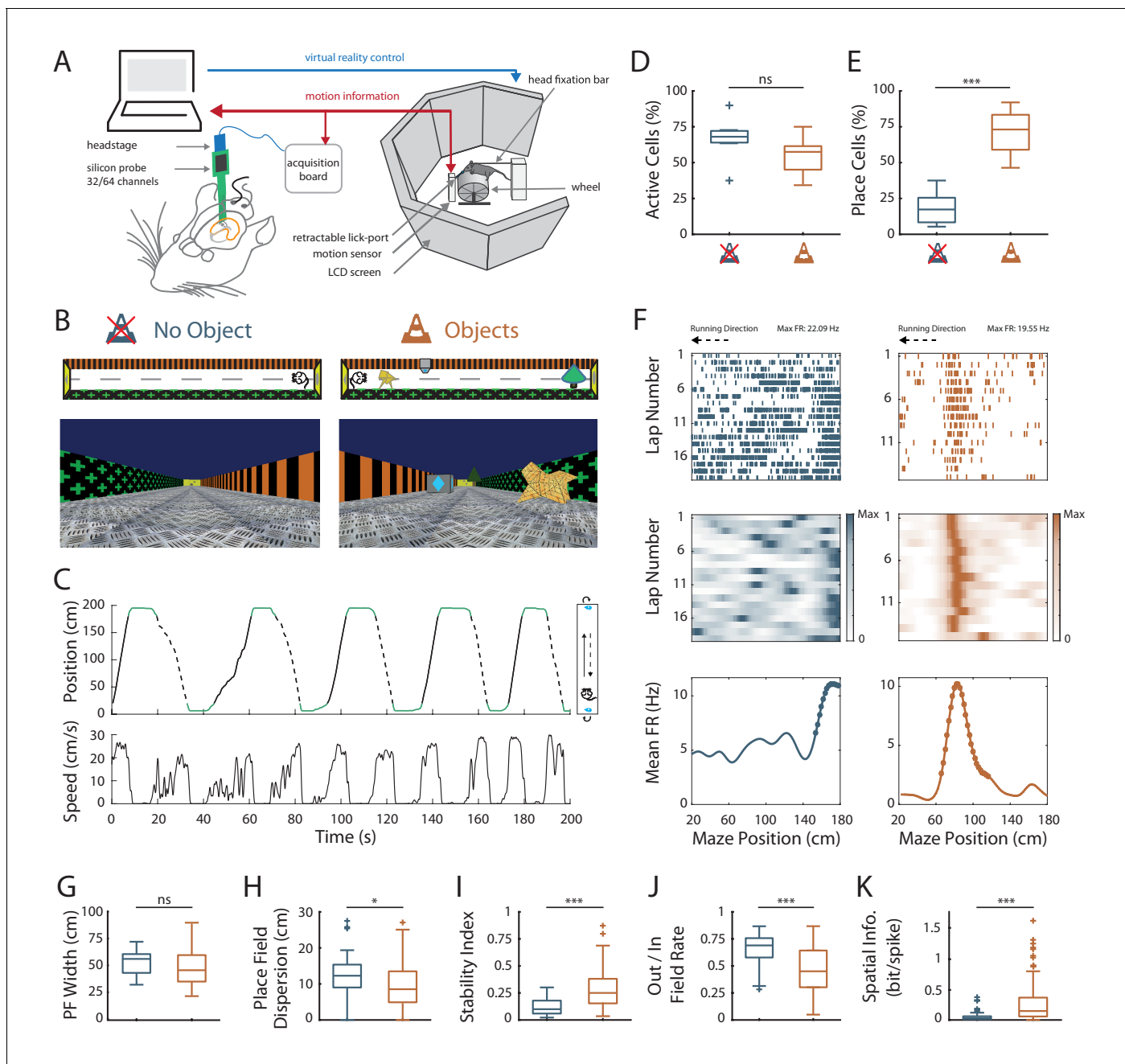


**Figure 1.** Effects of local visual cues on spatial coding resolution. (A) Schema of the virtual reality set up. The mouse is head-fixed and located on a wheel surrounded by LCD screens where a virtual environment is displayed. (B) Top and first person views of virtual linear tracks used. Left: track without objects (OT) and right: track with virtual 3D objects (OT). (C) Top: Animal's position in the virtual track as a function of time. Green lines indicate times when animal was in a reward zone location. These locations were not considered for further analysis. Solid and dotted black lines indicate back and forth trials respectively. Top view of animal in the maze is depicted on the right. Arrows indicate teleportation in the same position but facing opposite direction after reward consumption. Bottom: Animal's speed as a function of time. (D,E) Box plots of the percentage of active cells (D) and place cells (E) in the maze without (blue) and with (orange) objects (same color code throughout the figures). (F) Spike raster plots (top) and color-coded firing rate map (middle) for successive trials in one direction (arrow) as a function of the position in the maze. Bottom: corresponding mean firing rate by positions. Dots indicate positions of the detected place field (see Materials and methods). (G–K) Box plots of the place field width (G), the place field dispersion (H), the stability index (I), the out/in field firing rate (J) and the spatial information (K). For box plots in this and subsequent figures, box extends from the first (Q1) to the third quartile (Q3) with the band inside showing the median and the extremities of the whiskers include values greater than  $Q1 + 1.5 \times (Q3 - Q1)$  and smaller than  $Q3 + 1.5 \times (Q3 - Q1)$ .

DOI: <https://doi.org/10.7554/eLife.44487.002>

Figure 1 continued on next page

Figure 1 continued

The following source data and figure supplements are available for figure 1:

**Source data 1.** Source data for **Figure 1**.

DOI: <https://doi.org/10.7554/eLife.44487.005>

**Figure supplement 1.** Histology and spike sorting.

DOI: <https://doi.org/10.7554/eLife.44487.003>

**Figure supplement 2.** Effects of local visual cues on spatial coding resolution across different recording sessions.

DOI: <https://doi.org/10.7554/eLife.44487.004>

resolution by comparing the proportion of place cells among active cells in the presence and absence of local visual cues. While only 19% of track active cells had at least one place field (place cells) in the empty track ( $n = 48$  place cells), 71% of track active cells were place cells when virtual objects were present ( $n = 193$  place cells;  $t_{13} = -7.3$ ,  $p < 10^{-5}$ , two-tailed unpaired t-test; **Figure 1E**). In  $\emptyset$ T, place fields were relatively sparse in the middle of the track with a large proportion of them aligned either to the beginning or to the end of the track (End-Track fields:  $53.1 \pm 9.95\%$ ,  $n = 7$  sessions in three mice; **Figure 2A**). In the maze with objects, however, the majority of fields were located in the central part of the track (On-Track fields:  $79 \pm 3.52\%$ ;  $n = 8$  sessions in three mice;  $Z = 2.84$ ,  $p = 0.0045$ , two-tailed WRS test; **Figure 2A**). These results indicate that local visual cues can strongly increase the proportion of place cells among active cells notably to code the central part of the maze. Another factor influencing spatial resolution is place field size. There was a small, non-significant, tendency for place field width (calculated on complete fields) to be lower in the track with objects ( $\emptyset$ T:  $51.5 \pm 3.33$  cm,  $n = 15$  place fields; OT:  $48.7 \pm 1.29$  cm,  $n = 157$  place fields;  $Z = 0.93$ ,  $p = 0.35$ , two-tailed WRS test; **Figure 1G**), in agreement with a higher spatial coding resolution. The size of place fields based on single-trial detection was also not significantly different between the two conditions ( $\emptyset$ T:  $34.4 \pm 1.2$  cm,  $n = 15$  place fields; OT:  $34.2 \pm 0.47$  cm,  $n = 156$  place fields;  $Z = 0.51$ ,  $p = 0.61$ , two-tailed WRS test). On the other hand, the spatial dispersion of single-trial detected place fields was significantly reduced in the presence of 3D objects ( $\emptyset$ T:  $11.9 \pm 0.90$  cm,  $n = 48$  place cells; OT:  $9.70 \pm 0.44$  cm,  $n = 193$  place cells;  $Z = 2.56$ ,  $p = 0.01$ , two-tailed WRS test; **Figure 1H**). To further assess inter-trial place field stability, independently from place field detection, we calculated a stability index (based on spatial correlations between all pairs of firing rate vectors, see Materials and methods section). This stability index was significantly lower in the track without objects ( $\emptyset$ T:  $0.12 \pm 0.01$ ,  $n = 48$  place cells; OT:  $0.28 \pm 0.01$ ,  $n = 193$  place cells;  $Z = -6.64$ ,  $p < 10^{-10}$ , two-tailed WRS test; **Figure 1I**). Altogether, these results demonstrate that local visual cues can improve inter-trial spatial and temporal stability.

An increase in spatial coding resolution would also be associated with higher spatial selectivity and information content. Spatial selectivity was assessed by comparing the in-field versus out-of-field firing rates (i.e. signal-to-noise ratio) for place fields recorded in OT and  $\emptyset$ T. In the track without objects, place cells increased their firing rate inside the place field ( $7.44 \pm 0.75$  Hz,  $n = 48$  place cells) but also discharged at high rate outside the field ( $5.23 \pm 0.62$  Hz; **Figure 1F and J**; ratio:  $0.65 \pm 0.02$ ). In comparison, place cells recorded in the track with objects had comparable firing rates inside the place field ( $6.80 \pm 0.43$  Hz,  $n = 193$  place cells;  $Z = 1.5$ ,  $p = 0.13$ , two-tailed WRS test) but fired significantly less outside the field ( $3.79 \pm 0.34$  Hz; ratio:  $0.46 \pm 0.01$ ; **Figure 1F and J**;  $Z = 5.48$ ,  $p < 10^{-7}$ , two-tailed WRS test). Accordingly, spatial information (in bit/spike), a measure independent of place fields' detection (Skaggs et al., 1993) was very low in the track without objects ( $0.06 \pm 0.01$  bit/spike,  $n = 48$  place cells) and significantly higher in the presence of objects ( $0.25 \pm 0.02$  bit/spike,  $n = 193$  place cells;  $Z = -5.67$ ,  $p < 10^{-7}$ , two-tailed WRS test; **Figure 1K**). Similar results were obtained with a different method to estimate spatial information content based on the original mutual information metric with a normalization to correct possible bias due to differences in basal firing rates between conditions (Souza et al., 2018) ( $\emptyset$ T:  $1.67 \pm 0.21$ ,  $n = 48$  place cells; OT:  $5.62 \pm 0.29$ ,  $n = 193$  place cells;  $Z = -7.57$ ,  $p < 10^{-13}$ , two-tailed WRS test). The effects of objects on spatial coding resolution were also observed when comparisons were performed across recording sessions (**Figure 1—figure supplement 2** and **Supplementary file 2**).

Altogether these results indicate that local visual cues can strongly enhance the proportion of place cells among active cells but also place cell's coding accuracy in agreement with an improved spatial coding resolution.

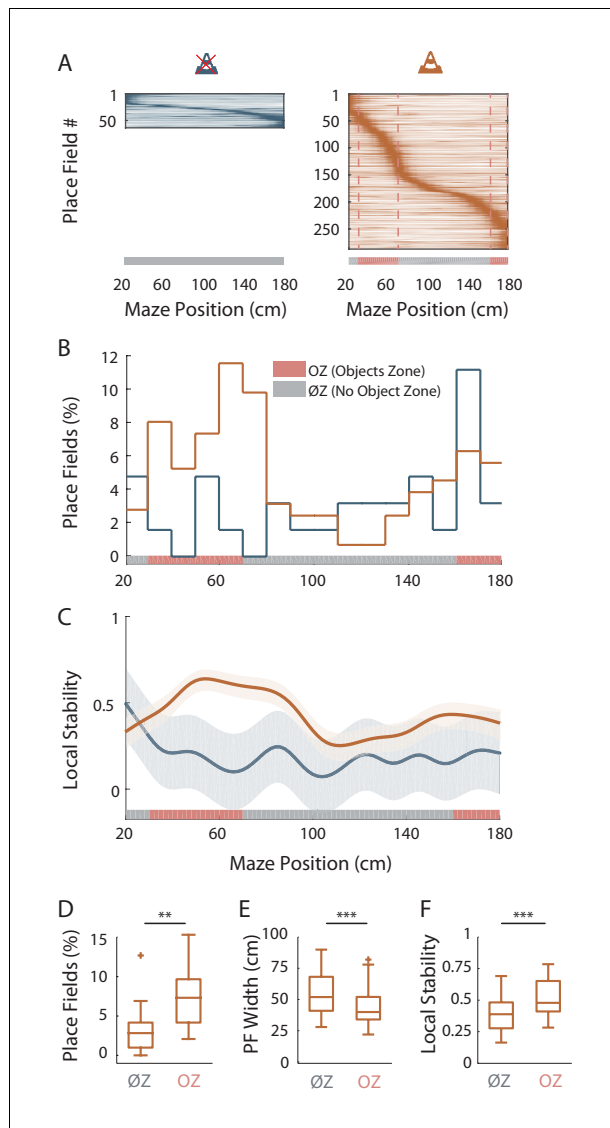


**Figure 2.** Virtual 3D objects improve spatial coding resolution locally. (A) Color-coded mean firing rate maps of all place fields recorded in the maze without objects (left) or with objects (right). The color codes for the intensity of the bin's mean firing rate normalized on the maximal mean firing rate (peak rate) in the recording session. The place cells are ordered according to the position of their peak rate in the track (reward zones excluded). Bottom: The tracks were divided into Objects Zones (OZ, in red on the x-axis) around the objects and No Object Zones ( $\emptyset$ Z, in grey on the x-axis) deprived of objects. Red dotted lines depict the boundaries of the OZ in the track with objects. (B) Percentage of On-Track place fields at each spatial bin (10 cm) in the maze with (orange line) and without objects (blue line). (C) Mean local stability index (solid lines)  $\pm$  SEM (shaded bands) for place cells with On-Track fields at each spatial bin in the track with (orange) or without (blue) objects. (D–F) Box plots depicting the mean percentage of place fields per spatial bin (D), the place field width (E) and the local stability index (F) in OZ and  $\emptyset$ Z in the maze with objects. **Figure 2—source data 1.** Source data for **Figure 2**.

DOI: <https://doi.org/10.7554/eLife.44487.006>

The following source data and figure supplement are available for figure 2:

**Source data 1.** Source data for **Figure 2**.

DOI: <https://doi.org/10.7554/eLife.44487.008>

**Figure supplement 1.** Virtual 3D objects improve spatial coding resolution locally across different recording sessions.

DOI: <https://doi.org/10.7554/eLife.44487.007>

## Virtual 3D objects improve spatial coding resolution locally

We then wondered whether spatial resolution could be adjusted locally, within the same environment. To address this question, we focused our analysis on On-Track fields recorded in the OT. We first noticed that the distribution of these fields was non-uniform ( $p=0.017$ , test of non-uniformity). To quantify more precisely this effect, we divided the linear track in Objects Zones (OZ) and No Objects Zones ( $\emptyset$ Z), depending if a given track zone contained an object or not, respectively (*Figure 2A*, right). The density of place fields was significantly higher in OZ (OZ:  $7.31 \pm 1.09\%$ /10 cm,  $n = 12$  spatial bins of 10 cm, six in each direction;  $\emptyset$ Z:  $3.28 \pm 0.65\%$ /10 cm,  $n = 20$  spatial bins of 10 cm, 10 in each direction;  $t_{30} = -3.38$ ,  $p=0.002$ , two-tailed unpaired t-test; *Figure 2B and D*). Furthermore, in the maze with objects, place fields were significantly smaller in OZ ( $42.3 \pm 1.43$  cm,  $n = 77$  fields) compared to  $\emptyset$ Z ( $54.8 \pm 1.89$  cm,  $n = 80$  fields;  $Z = 4.60$ ,  $p < 10^{-5}$ , two-tailed WRS test; *Figure 2E*). Accordingly, place field dispersion was also significantly reduced in OZ ( $8.33 \pm 0.50$  cm,  $n = 130$  fields) compared to  $\emptyset$ Z ( $11.8 \pm 0.71$  cm,  $n = 90$  fields;  $Z = 3.90$ ,  $p < 10^{-4}$ , two-tailed WRS test). A local stability index (see Materials and methods section) was significantly increased in OZ ( $0.52 \pm 0.02$ ,  $n = 60$  bins of 2 cm, 30 in each direction) compared to  $\emptyset$ Z ( $0.39 \pm 0.01$ ,  $n = 100$  bins of 2 cm, 50 in each direction;  $Z = -5.21$ ,  $p < 10^{-6}$ , two-tailed WRS test; *Figure 2C and F*). Spatial information was also significantly higher in OZ ( $0.32 \pm 0.03$  bit/spike,  $n = 130$  fields) compared to  $\emptyset$ Z ( $0.20 \pm 0.03$  bit/spike,  $n = 90$  fields;  $Z = -2.16$ ,  $p=0.03$ , two-tailed WRS test). Finally, we found no significant difference in the out-of-field versus in-field firing ratio between fields located in OZ or  $\emptyset$ Z (OZ:  $0.46 \pm 0.02$ ,  $n = 130$  fields;  $\emptyset$ Z:  $0.49 \pm 0.02$ ,  $n = 90$  fields;  $Z = 1.03$ ,  $p=0.30$ , two-tailed unpaired t test). The local effects of objects on spatial coding resolution were also observed when comparisons were performed across recording sessions (*Figure 2—figure supplement 1*).

These results indicate that 3D objects can locally improve spatial coding resolution through a local increase in place field number, a local reduction in place field size, a higher local stability and spatial information content while their effect on the out-of-field versus in-field firing ratio is more global.

We next wondered whether similar local effects on spatial coding resolution could be observed in  $\emptyset$ T. In this track, place fields were also non-uniformly distributed ( $p=0$ ; test of non-uniformity) with a higher density of fields at the ends of the track (i.e. End-Track fields; *Figure 2A*). However, we found no significant difference between End-Track and On-Track fields in terms of out-of-field versus in-field firing ratio (End-Track:  $0.65 \pm 0.02$ ,  $n = 32$  fields; On-Track:  $0.62 \pm 0.03$ ,  $n = 31$  fields;  $Z = 0.21$ ,  $p=0.83$ , two-tailed WRS test) and stability (End-Track:  $0.17 \pm 0.01$ ,  $n = 32$  fields; On-Track:  $0.15 \pm 0.02$ ,  $n = 31$  fields;  $t_{61} = 1.14$ ,  $p=0.26$ , two-tailed unpaired t-test). Spatial information was low for both types of fields but paradoxically lower for End-Track fields (End-Track:  $0.04 \pm 0.01$  bit/spike,  $n = 32$  fields; On-Track:  $0.1 \pm 0.02$  bit/spike,  $n = 31$  fields;  $Z = -2.66$ ,  $p=0.008$ , two-tailed WRS test). We conclude that overrepresentation of the ends of the  $\emptyset$ T is not associated with increased spatial coding accuracy and is unlikely to represent increased spatial coding resolution at these locations.

## Effect of local visual cues on spatial coding resolution at the population level

The results so far suggest that hippocampal spatial coding resolution can be locally adjusted. To assess this at the population level, we next performed position-decoding analysis (*Brown et al., 1998; Zhang et al., 1998*) (*Figure 3A*). We used the spike trains from all pyramidal cells recorded (i.e. both the spatially modulated and nonspatially modulated cells) and compared decoded positions with actual positions of the animal in the virtual linear tracks. Overall, the effect of objects on hippocampal spatial coding was obvious because the decoding error across trials was nearly two-fold larger in the track without objects compared to the track with objects ( $\emptyset$ T:  $46.3 \pm 0.73$  cm,  $n = 180$  trials; OT:  $27.1 \pm 0.94$  cm,  $n = 249$  trials;  $Z = 13.6$ ,  $p < 10^{-36}$ , two-tailed WRS test; *Figure 3A and B*). Accordingly, the decoding accuracy (*van der Meer et al., 2010*) was three fold lower in the empty track compared to the track with objects ( $\emptyset$ T:  $0.017 \pm 3.8 \times 10^{-4}$ ,  $n = 180$  trials; OT:  $0.048 \pm 1.49 \times 10^{-3}$ ,  $n = 249$  trials; chance level 0.01;  $Z = -15.68$ ,  $p < 10^{-54}$ , two-tailed WRS test; *Figure 3A and C*). In both cases, downsampling was performed to equalize the number of cells used for decoding between the two conditions (20 active cells). The effects of objects on population coding accuracy were also observed when comparisons were performed across recording sessions (*Figure 3—figure supplement 1*).

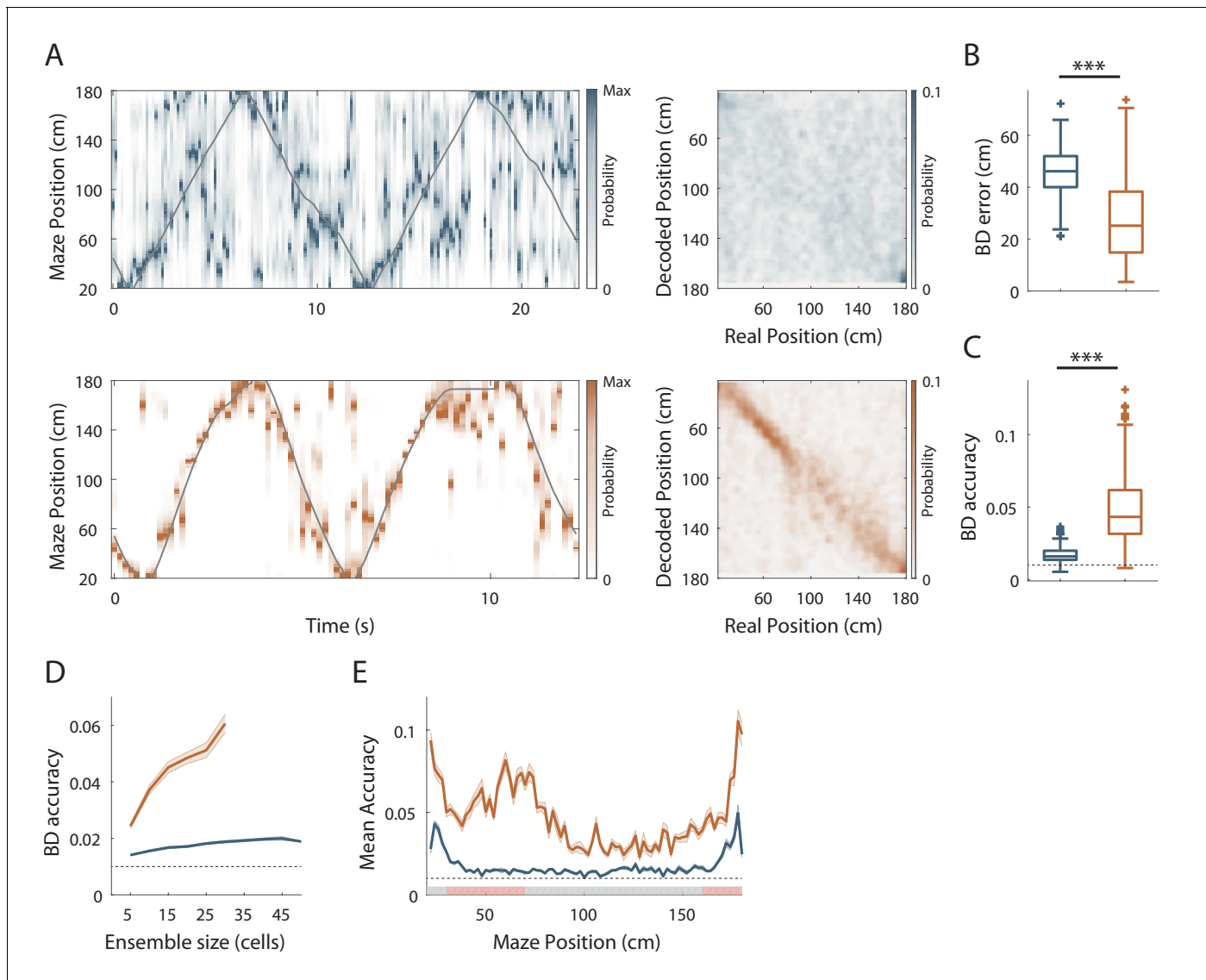


**Figure 3.** Effect of visual cues on spatial coding resolution at the population level. **(A)** Left: Color-coded distribution of the animal position's probability in the virtual track (the reward zones are excluded) computed using a Bayesian decoder (see Materials and methods) at each time window (500 ms) illustrated during four trials in the maze without (top) and with (bottom) objects. Spike trains of active cells were used to compute the animal position's probability. For visualization purpose, position probability is normalized by its maximum at each time bin. The real position is indicated with a solid grey line. Right: Confusion matrix between the real (x-axis) and the decoded position (y-axis) for all recording sessions performed on the track without objects (top) or with objects (bottom). **(B)** Box plots depicting the Bayesian decoding error (BD error) in the maze with and without objects. The BD error was significantly higher in the maze deprived of objects. **(C)** Box plots depicting the Bayesian decoding accuracy (BD accuracy) in the maze with and without objects. The BD accuracy was significantly higher in the maze with objects. **(D)** Mean BD accuracy (solid lines)  $\pm$  SEM (shaded bands) as a function of a subset of active cells in the maze with and without objects. **(E)** Mean BD accuracy (solid lines)  $\pm$  SEM (shaded bands) at each position in the maze with and without objects. The track was divided in two zones: Objects Zone (OZ, in red on the x axis) around the objects and No Object Zone ( $\emptyset$ Z, in grey on the x axis) deprived of objects. Note that the decoding accuracy was specifically improved in OZ in comparison to  $\emptyset$ Z in the maze with objects.

DOI: <https://doi.org/10.7554/eLife.44487.009>

The following source data and figure supplements are available for figure 3:

**Source data 1.** Source data for **Figure 3**.

DOI: <https://doi.org/10.7554/eLife.44487.012>

**Figure supplement 1.** Virtual 3D objects improve hippocampal population coding accuracy across different recording sessions Box plots of the Bayesian decoding error.

Figure 3 continued on next page

Figure 3 continued

DOI: <https://doi.org/10.7554/eLife.44487.010>

**Figure supplement 2.** Firing Rate vector decoding in familiar conditions.

DOI: <https://doi.org/10.7554/eLife.44487.011>

These effects were independent of the decoding method used because similar results were observed using a Firing Rate Vector (FRV) method (**Figure 3—figure supplement 2**; **Wilson and McNaughton, 1993; Middleton and McHugh, 2016**). Correlation values were lower in the empty track ( $\emptyset T$ :  $0.63 \pm 0.008$ ,  $n = 180$  trials;  $T$ :  $0.74 \pm 6.69 \times 10^{-3}$ ,  $n = 249$  trials;  $Z = -10.27$ ,  $p < 10^{-24}$ , two-tailed WRS test) and decoding errors were higher ( $\emptyset T$ :  $49.12 \pm 0.68$  cm,  $n = 180$  trials;  $T$ :  $31.31 \pm 1.09$  cm,  $n = 249$  trials;  $Z = 11.21$ ,  $p < 10^{-29}$ , two-tailed WRS test). Because Bayesian decoding was performed using a drop cell approach, we could measure decoding accuracy for different sample sizes of active cells (**van der Meer et al., 2010**) (**Figure 3D**). Decoding accuracy was positively correlated with sample size in the track with objects but not in the track without objects (**Figure 3D**). Importantly, decoding accuracy was better in  $T$  even if the sample size of active cells used was three time lower than in  $\emptyset T$  (to compensate for the three time lower proportion of place cells in this condition;  $\emptyset T$   $n = 15$  vs  $T$   $n = 5$ ,  $Z = -2.26$ ,  $p = 0.02$ , two-tailed WRS test;  $\emptyset T$   $n = 30$  vs  $T$   $n = 10$ ,  $Z = -2.85$ ,  $p = 0.004$ , two-tailed WRS test;  $\emptyset T$   $n = 45$  vs  $T$   $n = 15$ ,  $Z = -2.55$ ,  $p = 0.01$ , two-tailed WRS test). To see if objects could locally increase spatial decoding accuracy, we compared decoding accuracy between  $OZ$  and  $\emptyset Z$ . While decoding accuracy was uniformly low in the track without objects ( $OZ$ :  $0.02 \pm 1.48 \times 10^{-3}$ ,  $n = 30$  spatial bins of 2 cm;  $\emptyset Z$ :  $0.02 \pm 8.98 \times 10^{-4}$ ,  $n = 50$  spatial bins of 2 cm;  $Z = -1.64$ ,  $p = 0.1$ , two-tailed WRS test; **Figure 3E**), it was increased in every part of the track with objects but significantly more in  $OZ$  compared to  $\emptyset Z$  ( $OZ$ :  $0.06 \pm 0.003$ ,  $n = 30$  spatial bins of 2 cm;  $\emptyset Z$ :  $0.04 \pm 2.3 \times 10^{-3}$ ,  $n = 50$  spatial bins of 2 cm;  $Z = -5.21$ ,  $p < 10^{-6}$ , two-tailed WRS test; **Figure 3E**). We concluded that local visual cues can globally and locally improve spatial coding accuracy at the population level.

## Fast dynamics of spatial coding resolution tuning upon objects manipulation

Place cells usually appear instantaneously upon exploration of a new environment in area CA1 (**Wilson and McNaughton, 1993; Epsztain et al., 2011**). To see if similar dynamics could be observed for the effects of virtual objects on spatial resolution, we manipulated objects online while recording the same ensemble of cells in area CA1. For mice trained in an empty track, we instantaneously added the three objects (which were thus new to the mice) after 20 back and forth trials. Conversely, for mice trained in the track with objects we instantaneously removed the three objects. Objects manipulation had no effect on the proportion of active cells (**Figure 4B**) but a strong impact on the proportion of place cells (**Figure 4A and C**). For mice trained in an empty track, adding objects instantaneously increased the proportion of place cells (from  $21.6 \pm 5.3\%$  to  $75.0 \pm 4.1\%$ ;  $n = 5$  sessions in three mice;  $t_4 = -35.8$ ,  $p < 10^{-5}$ , two-tailed paired t-test; **Figure 4A and C**). Thus, a large proportion of cells initially silent or active but nonspatially modulated in the familiar empty track became spatially modulated (40.3%). Most of these cells had on-track fields (81.3%; **Figure 4H**). A majority of cells initially spatially modulated remained place cells (75.7%), while the others became nonspatially modulated or silent. Adding objects also increased place cells' stability ( $Z = -4.68$ ,  $p < 10^{-5}$ , two-tailed WRS test; **Figure 4E**) and spatial information ( $Z = -3.20$ ,  $p = 0.0014$ , two-tailed WRS test; **Figure 4G**). Local stability was significantly higher in  $OZ$  when objects were added ( $OZ$ :  $0.56 \pm 0.02$ ,  $n = 60$  bins of 2 cm, 30 in each direction;  $\emptyset Z$ :  $0.25 \pm 0.02$ ,  $n = 100$  bins of 2 cm, 50 in each direction;  $Z = -8.57$ ,  $p < 10^{-16}$ , two-tailed WRS test; **Figure 4I**) but not before ( $Z = 1.25$ ,  $p = 0.21$ , two-tailed WRS test). Place fields' spatial dispersion and out/in field firing ratio were decreased ( $Z = 3.55$ ,  $p = 0.0004$  and  $Z = 1.87$ ,  $p = 0.06$ , respectively, two-tailed WRS test; **Figure 4D and F**).

On the other hand, removing objects decreased the proportion of place cells (from  $71.1 \pm 5.54\%$  to  $34.9 \pm 10.9\%$ ,  $n = 8$  sessions in three mice;  $t_5 = 5.54$ ,  $p = 0.001$ , two-tailed paired t-test; **Figure 4A and C**). The spatial information and stability were decreased by this manipulation ( $Z = 2.27$ ,  $p = 0.02$  and  $Z = 4.51$ ,  $p < 10^{-5}$ , respectively, two-tailed WRS test; **Figure 4E and G**), while place field out/in

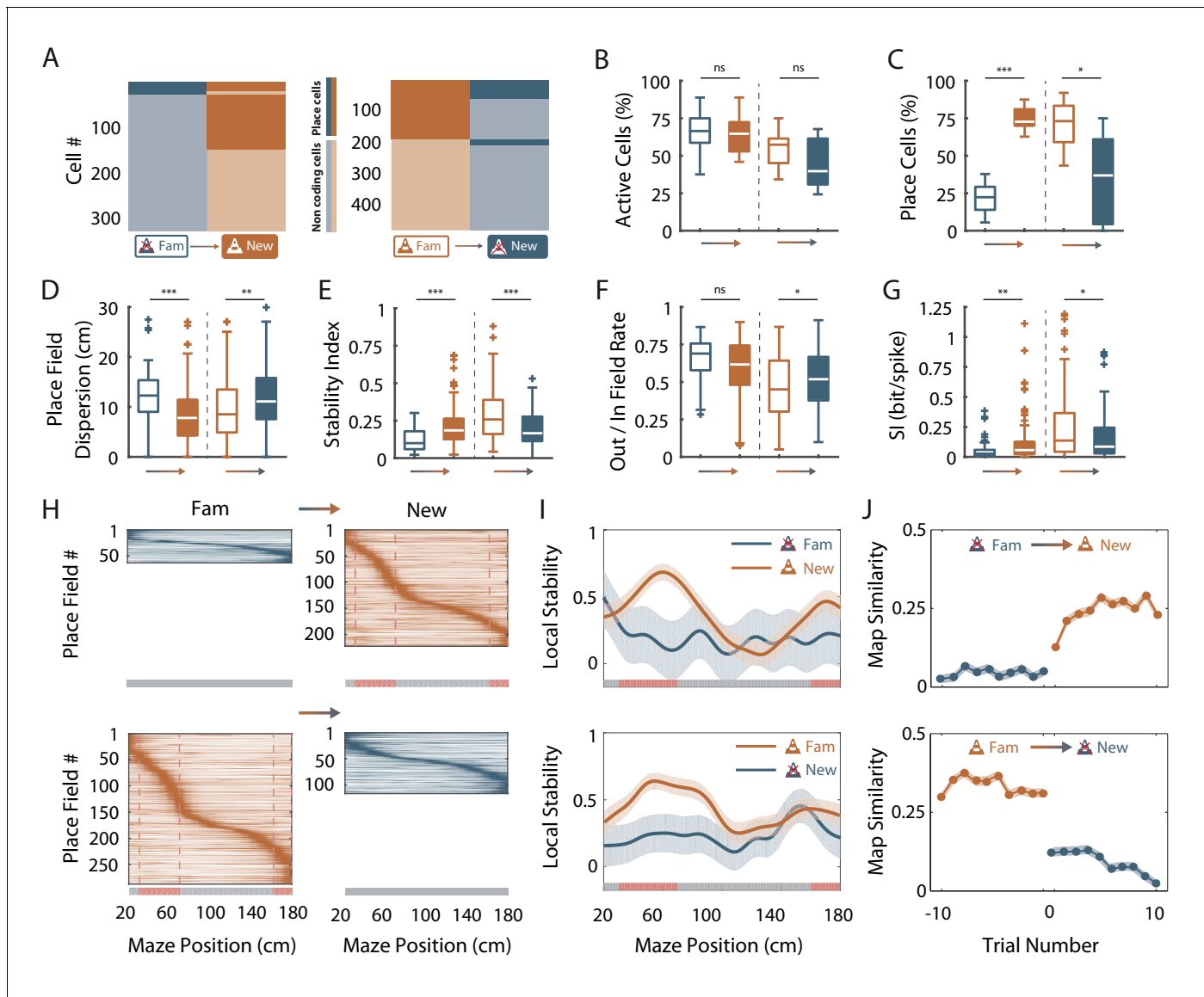


**Figure 4.** Fast dynamics of spatial coding resolution tuning upon objects manipulation. (A) Mosaic plots representing the cells classified as place cells (darker orange and blue) or non-coding cells (i.e. silent or active non-coding, lighter orange and blue) in the familiar and the new mazes. (B–G) Box plots comparing familiar (empty box) and new mazes (filled box) conditions. Two pairs of box plots are illustrated; Left: comparison between the familiar maze without objects (blue,  $\emptyset T_{fam}$ ) and the new maze with objects (orange,  $OT_{new}$ ). Right: comparison between the familiar maze with objects (orange,  $OT_{fam}$ ) and the new maze without objects (blue,  $\emptyset T_{new}$ ). A gradient color arrow shows the way of the transition. Plots show the percentage of active cells (B), the percentage of place cells (C), the Out/In field firing rate (D), the spatial information (SI; E) and the stability index (G). (H) Color-coded mean firing rate maps of place fields recorded in the familiar and new mazes. The color codes for the intensity of the firing rate normalized by the peak rate. The place fields are ordered according to the position of their peak rate in each track (the reward zones are excluded). The tracks were divided into Objects Zones (OZ, in red on the x-axis) around the objects and No Object Zones ( $\emptyset Z$ , in grey on the x-axis) deprived of objects. Red dotted lines depict the boundaries of the OZ in the track with objects. (I) Mean local stability index (solid orange or blue lines)  $\pm$  SEM (blue or orange shaded areas) at each spatial bin in the familiar and new mazes (top: from  $\emptyset T_{fam}$  to  $OT_{new}$ ; bottom: from  $OT_{fam}$  to  $\emptyset T_{new}$ ). (J) Map similarity (see Materials and methods) for 10 trials before and 10 trials after the experimental manipulation (indicated by 0) for  $\emptyset T_{fam}$  to  $OT_{new}$  (top) and for  $OT_{fam}$  to  $\emptyset T_{new}$  condition (bottom).

DOI: <https://doi.org/10.7554/eLife.44487.013>

The following source data and figure supplements are available for figure 4:

**Source data 1.** Source data for **Figure 4**.

DOI: <https://doi.org/10.7554/eLife.44487.016>

Figure 4 continued on next page

Figure 4 continued

**Figure supplement 1.** Spatial coding resolution adaptation upon objects manipulations is already visible during the first session in the new condition Box plots comparing familiar (empty boxes, all recording sessions) and new (filled boxes, first recording session) conditions upon objects manipulation.

DOI: <https://doi.org/10.7554/eLife.44487.014>

**Figure supplement 2.** Virtual 3D objects modulation of hippocampal population coding accuracy upon objects manipulation.

DOI: <https://doi.org/10.7554/eLife.44487.015>

field firing ratio and dispersion were increased ( $Z = -2.01$ ,  $p=0.04$  and  $Z = -3.06$ ,  $p=0.002$ , respectively, two-tailed WRS test; **Figure 4D and F**). After object removal, local stability was not significantly higher in OZ (OZ:  $0.24 \pm 0.02$ ,  $n = 60$  bins of 2 cm, 30 in each direction) compared to ØZ ( $0.24 \pm 0.02$ ,  $n = 100$  bins of 2 cm, 50 in each direction;  $Z = 0.19$ ,  $p=0.85$ , two-tailed WRS test; **Figure 4I**). Importantly, these effects were already observed during the first recording sessions following objects manipulation (**Figure 4—figure supplement 1**). Furthermore, objects manipulations were associated with significant changes of spatial coding resolution at the population level (**Figure 4—figure supplement 2**). We conclude that the effects of local visual cues on place cells' coding observed between familiar tracks can be reproduced with instantaneous objects manipulation.

We next investigated the dynamic of these changes by first calculating the correlation of the firing rate maps of each back and forth trial with the corresponding average firing rate map in the condition with objects (the most stable condition) for 10 trials before ( $t-1$  to  $t-10$ ) and 10 trials after ( $t + 1$  to  $t + 10$ ) the manipulation (**Figure 4J**) then comparing the correlation values before and after the manipulation. When objects were added in the empty track, map similarity was significantly higher for the second trial in the new condition ( $t-1$  vs  $t + 2$ ,  $n = 598$  and  $n = 608$  pyramidal cells, respectively;  $n = 5$  sessions in three mice;  $Z = 7.18$ ,  $p<10^{-9}$ ; Kruskall-Wallis one-way test with post-hoc Bonferroni correction) and then stayed higher from this second trial on ( $t + 2$  vs  $t + 3$ ,  $n = 608$  and  $n = 612$  pyramidal cells, respectively;  $n = 5$  sessions in three mice;  $Z = 1.10$ ,  $p=1$ , Kruskall-Wallis one-way test with post-hoc Bonferroni correction). Conversely, when objects were removed from the familiar track with objects, map similarity dropped already for the first trial in the new condition ( $t-1$  vs  $t + 1$ ,  $n = 744$  and  $n = 743$  pyramidal cells, respectively;  $n = 8$  sessions in three mice;  $Z = 8.80$ ,  $p<10^{-15}$ , Kruskall-Wallis one-way test with post-hoc Bonferroni correction) and stayed lower from this first trial on ( $t + 1$  vs  $t + 2$ ,  $n = 743$  and  $n = 720$  pyramidal cells, respectively;  $Z = 0.17$ ,  $p=1$ , Kruskall-Wallis one-way test with post-hoc Bonferroni correction). Thus, the hippocampus can rapidly adapt its spatial coding resolution to local visual cues available in the environment.

### Low proportion of object-responsive cells in OT

Newly activated place cells in OT could correspond to object responsive (OR) cells, which have been recorded in the hippocampus of freely moving rats (*Deshmukh and Knierim, 2013*). These cells tend to discharge systematically near several objects present in the environment. To test this hypothesis, we specifically looked for OR cells in our recordings. For this analysis, we took advantage of the fact that our animals were passing near the same objects in both back and forth trials. Indeed, OR cells should systematically discharge near several objects (if they do not code for objects identity) or the same object (if they in addition code for objects identity) in both back and forth trials. We defined object zones for each individual object (IOZ). Place cells were classified as OR cells if they were bidirectional (firing in both back and forth trials) and had at least one place field in a IOZ corresponding to the same object for both back and forth trials or several place fields in several IOZs corresponding to the same objects in both back and forth trials. In the track without objects no OR cell was detected. In the track with objects, OR cells represented only 2.07% of all place cells. We conclude that the vast majority of newly activated place cells in the presence of objects does not correspond to OR cells.

### Effects of 2D wall patterns on hippocampal spatial coding resolution

We next wondered whether the effect of objects on hippocampal spatial coding resolution could be recapitulated by having more 2D local visual cues in different positions along the track. We thus assessed hippocampal spatial coding in another environment devoid of the original 3D objects but enriched with different wall patterns along the track (Pattern No Objects track or PØT; **Figure 5A**). The percentage of active cells was not affected by the presence of different patterns along the track

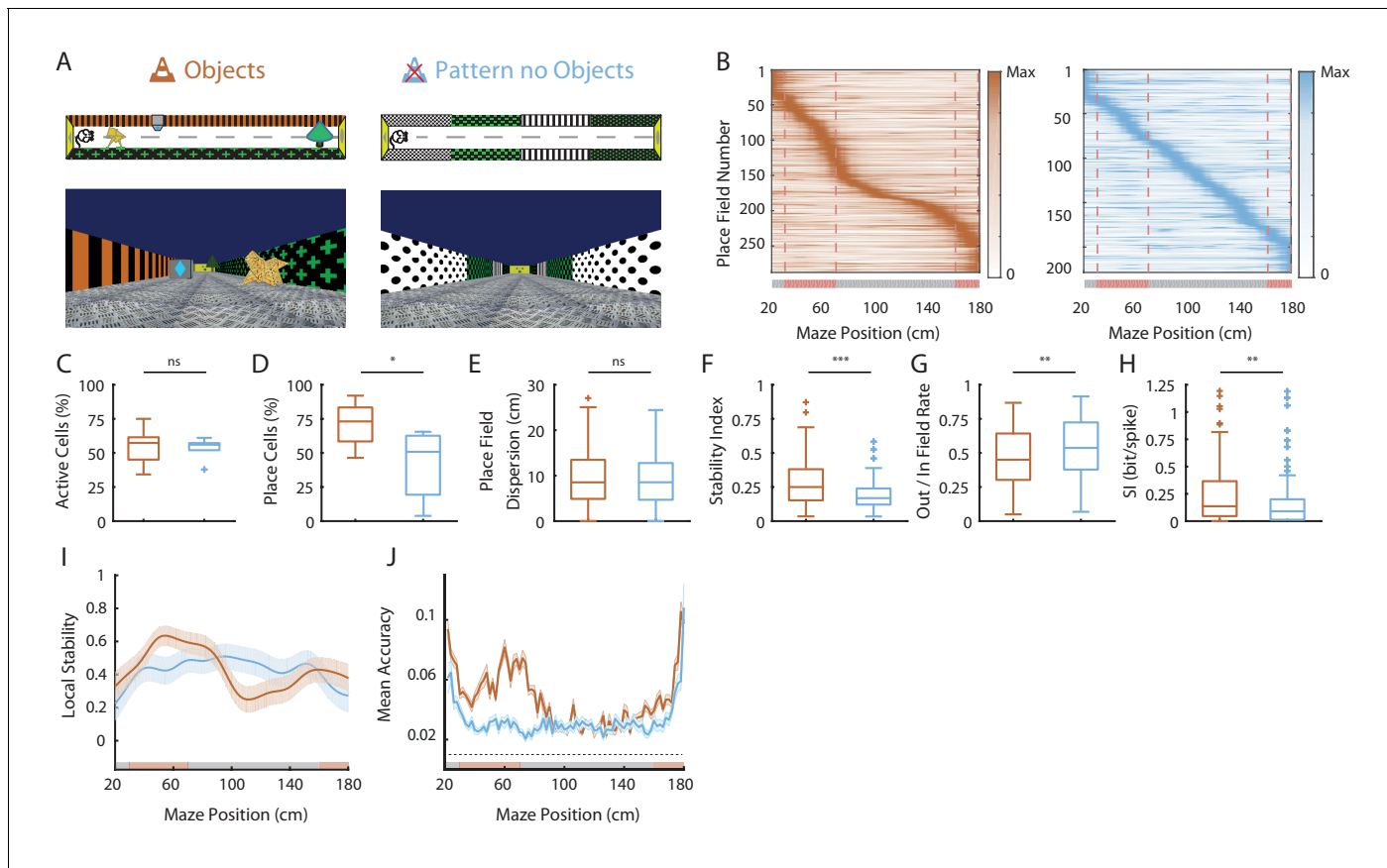


**Figure 5.** Effects of 2D wall patterns on hippocampal spatial coding resolution. (A) Schema (top) and picture (bottom) representing the original maze with objects (orange, left) and a maze with patterns on the walls but no objects (PØT; light blue, right). (B) Color-coded mean firing rate maps for all place fields recorded in the original maze with objects (orange, left) and on the PØT maze (light blue, right). The color codes for the intensity of the firing rate normalized by the peak rate. The place fields are ordered according to the position of their peak rate in each track (the reward zones are excluded). The tracks were divided into Objects Zones (OZ, in red on the x-axis) around the objects and No Object Zones ( $\bar{O}Z$ , in grey on the x-axis) deprived of objects. Red dotted lines depicts the boundaries of the OZ. (C–H) Box plots representing in the original (orange) and pattern no object (light blue) mazes the percentage of active cells (C), the percentage of place cells (D), the place field dispersion (E), the stability index (F), the out/in field rate (G) and the spatial information (SI; H). (I) Mean local stability index (solid orange or light blue lines)  $\pm$  SEM (orange or light blue shaded bands) at each position's bin in the original (orange) and pattern no object (light blue) mazes. (J) Mean BD accuracy (solid lines)  $\pm$  SEM (shaded bands) at each spatial bin in the original maze with objects (orange) or in the pattern no object maze (light blue).

DOI: <https://doi.org/10.7554/eLife.44487.017>

The following source data is available for figure 5:

**Source data 1.** Source data for **Figure 5**.

DOI: <https://doi.org/10.7554/eLife.44487.018>

(OT,  $54.64 \pm 4.79\%$ ,  $n = 8$  sessions in three mice; PØT,  $53.63 \pm 3.45\%$ ,  $n = 6$  sessions in two mice;  $p=1$ , one-way Anova test with post-hoc Bonferroni correction; **Figure 5C**). The percentage of place cells among active cells tended to be greater than in OT (OT,  $18.71 \pm 4.33\%$ ,  $n = 7$  sessions in three mice; PØT,  $42.16 \pm 10.58\%$ ,  $n = 5$  sessions in two mice;  $p=0.093$ , one-way Anova test with post-hoc Bonferroni correction). Also, the percentage of place cells in PØT was significantly lower than in OT (OT,  $71.11 \pm 5.54\%$ ,  $n = 8$  sessions in three mice;  $p=0.024$ , one-way Anova test with post-hoc Bonferroni correction; **Figure 5B–D**). Interestingly, place fields were uniformly distributed along the track enriched with patterns ( $n = 16$  spatial bins of 10 cm;  $p=0.23$ , test for non-uniformity; **Figure 5B**). This suggests that local 2D visual cues are sufficient to set place fields' position. Place field width was significantly decreased in PØT compared to OT (OT,  $51.46 \pm 3.34$  cm,  $n = 15$  place fields; PØT,  $41.51 \pm 1.17$  cm,  $n = 138$  place fields;  $Z = 2.62$ ,  $p=0.026$ , Kruskall-Wallis one-way test with post-hoc

Bonferroni correction). Accordingly, place field dispersion was significantly reduced compared to  $\emptyset$ T to a level comparable to OT ( $\emptyset$ T,  $5.95 \pm 0.45$  cm,  $n = 48$  place cells;  $\text{P}\emptyset\text{T}$ ,  $4.57 \pm 0.21$  cm,  $n = 157$  place cells;  $Z = 2.88$ ,  $p=0.011$ , Kruskall-Wallis one-way test with post-hoc Bonferroni correction; **Figure 5E**). Inter-trial firing stability, while significantly higher in  $\text{P}\emptyset\text{T}$  compared to  $\emptyset$ T ( $\emptyset$ T,  $0.12 \pm 0.01$ ,  $n = 48$  place cells;  $\text{P}\emptyset\text{T}$ ,  $0.19 \pm 0.01$ ,  $n = 157$  place cells;  $Z = 3.72$ ,  $p=0.0005$ , Kruskall-Wallis one-way test with post-hoc Bonferroni correction), was significantly lower than in OT (OT,  $0.28 \pm 0.01$ ,  $n = 193$  place cells;  $Z = 5.02$ ,  $p<10^{-4}$ , Kruskall-Wallis one-way test with post-hoc Bonferroni correction; **Figure 5F**). We conclude that local 2D visual cues can improve place fields stability to a certain extend without, however, reaching the level of stability observed in the presence of 3D virtual objects.

We next assessed spatial selectivity and information content in  $\text{P}\emptyset\text{T}$ . The ratio of place cells' out-of-field versus in-field firing was lower in  $\text{P}\emptyset\text{T}$  compared to  $\emptyset$ T ( $\emptyset$ T,  $0.65 \pm 0.02$ ,  $n = 48$  place cells;  $\text{P}\emptyset\text{T}$ ,  $0.53 \pm 0.02$  cm,  $n = 157$  place cells;  $Z = 3.38$ ,  $p=0.002$ , Kruskall-Wallis one-way test with post-hoc Bonferroni correction) but still significantly higher than in OT (OT,  $0.46 \pm 0.01$ ,  $n = 193$  place cells;  $Z = 3.02$ ,  $p=0.007$ , Kruskall-Wallis one-way test with post-hoc Bonferroni correction; **Figure 5G**). Accordingly, spatial information content was higher in  $\text{P}\emptyset\text{T}$  compared to  $\emptyset$ T ( $\emptyset$ T,  $0.056 \pm 0.01$ ,  $n = 48$  place cells;  $\text{P}\emptyset\text{T}$ ,  $0.16 \pm 0.02$ ,  $n = 157$  place cells;  $Z = 4.09$ ,  $p=0.0001$ , Kruskall-Wallis one-way test with post-hoc Bonferroni correction) but still significantly lower than in OT (OT,  $0.25 \pm 0.02$ ,  $n = 193$  place cells;  $Z = 2.73$ ,  $p=0.018$ , Kruskall-Wallis one-way test with post-hoc Bonferroni correction; **Figure 5H**).

Altogether these results indicate that local 2D visual cues can enhance the proportion of place cells among active cells and place cells' coding accuracy but to a lower extend compared to 3D virtual objects.

Finally, local stability in OZ was significantly higher in OT compared to  $\text{P}\emptyset\text{T}$  (OT-OZ:  $0.52 \pm 0.02$ ;  $\text{P}\emptyset\text{T}$ -OZ:  $0.39 \pm 0.016$ ,  $n = 30$  spatial bins of 2 cm for both;  $Z = 4.85$ ,  $p<10^{-5}$  two-tailed WRS test; **Figure 5I**). Accordingly, the same effect could be observed for the decoding accuracy (OT-OZ:  $0.07 \pm 0.02$ ;  $\text{P}\emptyset\text{T}$ -OZ:  $0.03 \pm 0.01$ ,  $n = 30$  spatial bins of 2 cm for both;  $Z = -5.83$ ,  $p<10^{-8}$  two-tailed WRS test; **Figure 5J**) in agreement with a strong influence of 3D objects on spatial coding resolution.

## Spatial coding resolution in a visually enriched environment

We next wondered whether the hippocampal mapping resolution was maximal in the presence of objects or whether it could be increased by further visually enriching the environment. We thus analyzed hippocampal place cells' coding in another environment containing the original 3D objects but enriched in visual cues such as different wall patterns in different positions along the track and high 3D columns outside the track (EOT,  $n =$  three mice; **Figure 6A**). The percentage of active cells was not increased by visually enriching the environment (OT,  $n = 5$  sessions in two mice; EOT,  $n = 5$  sessions in three mice;  $Z = -0.1$ ,  $p=1$ , two-tailed WRS test; **Figure 6C**) nor was the percentage of place cells (OT,  $n = 5$  sessions in two mice; EOT,  $n = 5$  sessions in three mice;  $t_8 = -1.38$ ,  $p=0.20$ , two-tailed unpaired t-test; **Figure 6B-D**). However, place fields were uniformly distributed along the track in the visually rich environment ( $n = 16$  spatial bins of 10 cm;  $p=0.23$ , test for non-uniformity), thus not clustered around objects as in the visually poor environment (**Figure 6B**). This suggests that local visual cues are important to set place fields' position (Renaudineau et al., 2007). However, all other attributes of place fields were not significantly different between the two environments (OT,  $n = 103$  place cells; EOT,  $n = 132$  place cells; out/in field firing ratio:  $Z = 0.57$ ,  $p=0.57$ ; Spatial info:  $Z = 0.42$ ,  $p=0.67$ ; Dispersion:  $Z = -1.88$ ,  $p=0.06$ ; Stability:  $Z = -0.06$ ,  $p=0.95$ ; two-tailed WRS test for all; **Figure 6E-H**). When looking at local stability of firing rates, we still observed a significant effect of objects in the visually enriched environment in OZ versus  $\emptyset$ Z (OZ,  $n = 60$  spatial bins of 2 cm;  $\emptyset$ Z:  $n = 100$  spatial bins of 2 cm;  $Z = -2.46$ ,  $p=0.014$ , two-tailed WRS test; **Figure 6I**). Interestingly, positions near objects were also decoded with a better accuracy using a Bayesian decoder than positions further away in the visually enriched environment (OZ:  $0.07 \pm 0.004$ ,  $n = 30$  spatial bins of 2 cm;  $\emptyset$ Z:  $0.057 \pm 0.003$ ,  $n = 50$  spatial bins of 2 cm;  $Z = -4.49$ ,  $p=0.004$ , two-tailed WRS test; **Figure 6J**).

Altogether these results suggest that in the presence of local visual cues, hippocampal spatial coding is not further improved by visually enriching the environment. However, place fields locations are influenced by additional visual cues along the track. Interestingly, despite a homogeneous

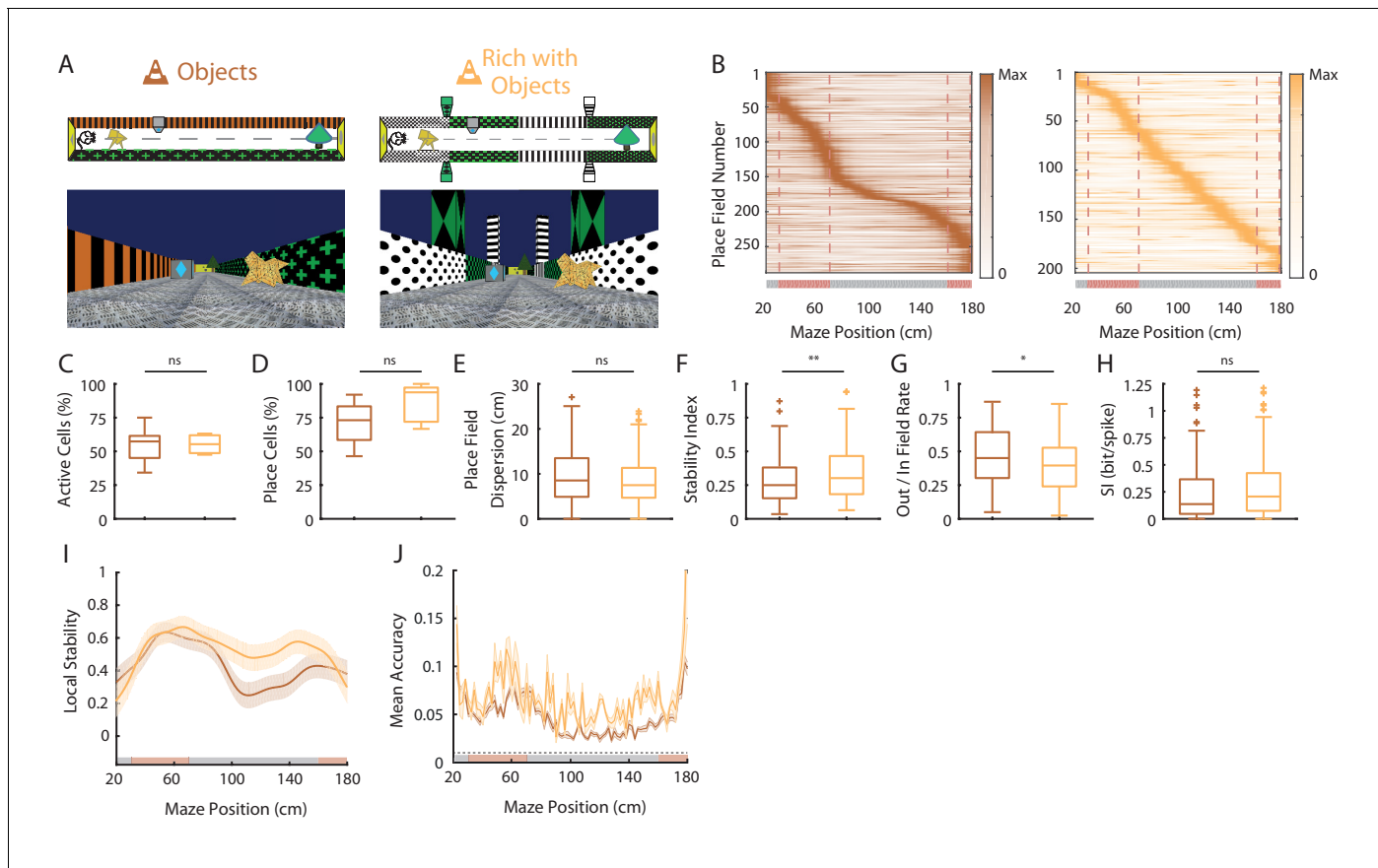


**Figure 6.** Spatial coding resolution in a visually enriched environment . (A) Schema (top) and picture (bottom) representing the original maze with objects (left) and a visually enriched maze with objects (right). (B) Color-coded mean firing rate maps for all place fields recorded in the original maze with objects (orange, left) and on the visually rich maze with objects (yellow, right). The color codes for the intensity of the firing rate normalized by the peak rate. The place fields are ordered according to the position of their peak rate in each track (the reward zones are excluded). The tracks were divided into Objects Zones (OZ, in red on the x-axis) around the objects and No Object Zones ( $\bar{O}Z$ , in grey on the x-axis) deprived of objects. Red dotted lines depicts the boundaries of the OZ. (C–H) Box plots representing in the original (orange) and pattern no object (light blue) mazes the percentage of active cells (C), the percentage of place cells (D), the place field dispersion (E), the stability index (F), the out/in field rate (G) and the spatial information (SI; H). (I) Mean local stability index (solid orange or yellow lines) $\pm$ SEM (orange or yellow shaded bands) at each position's bin in the original (orange) and visually rich (yellow) mazes. (J) Mean BD accuracy (solid lines) $\pm$ SEM (shaded bands) at each spatial bin in the original maze with objects (orange) or in the visually rich maze with objects (yellow).

DOI: <https://doi.org/10.7554/eLife.44487.019>

The following source data is available for figure 6:

**Source data 1.** Source data for **Figure 6**.

DOI: <https://doi.org/10.7554/eLife.44487.020>

distribution of place field locations, 3D objects could still locally influence hippocampal population decoding accuracy.

### Effects of local cues on hippocampal temporal coding resolution

The results so far suggest that local visual cues can increase spatial coding resolution when considering the spatial firing rate code. Place cells, however, do not only increase their firing rate inside the place field but also tend to fire at progressively earlier phases of the theta oscillation as an animal moves through the place field (O’Keefe and Recce, 1993). This phenomenon, called theta phase precession, is thought to further increase spatial coding resolution because different locations within the place field that are difficult to distinguish based on firing rate alone can be accurately separated

when phase is taken into account. In the temporal domain, increased spatial resolution would thus correspond to increased slope of the phase versus position relationship for identical field sizes.

We first looked for differences in the theta oscillation recorded in the Local Field Potential (LFP) between the two conditions. The mean frequency of the field theta oscillation was not significantly different when mice were running in the track with or without objects ( $\emptyset T$ :  $6.79 \pm 0.12$  Hz,  $n = 9$  sessions in three mice; OT:  $6.59 \pm 0.33$  Hz,  $n = 8$  sessions in two mice;  $Z = 1.26$ ,  $p=0.20$ , two-tailed WRS test) but was lower than that reported for mice navigating in real linear tracks (**Middleton and McHugh, 2016**). The power of theta oscillation (theta index see Materials and methods section) was also not significantly different ( $\emptyset T$ :  $3.31 \pm 0.23$ ,  $n = 9$  sessions in three mice; OT:  $3.38 \pm 0.16$ ,  $n = 8$  sessions in three mice;  $t_{15} = 0.26$ ,  $p=0.79$ , two-tailed unpaired t-test). Theta frequency was not modulated by running speed of the animal in  $\emptyset T$  ( $r = 0.02 \pm 0.02$ ,  $n = 9$  sessions in three mice; **Figure 7—figure supplement 1A,C**) as previously observed in virtual linear tracks when only distal cues are present (**Ravassard et al., 2013**). Theta frequency-speed modulation was, however, significant in OT ( $r = 0.08 \pm 0.03$ ,  $n = 8$  sessions in three mice;  $t_{15} = -1.44$ ,  $p=0.17$ , two-tailed unpaired t-test; **Figure 7—figure supplement 1A,C**). Theta amplitude was similarly modulated by running speed in both conditions ( $\emptyset T$ :  $r = 0.07 \pm 0.03$ ,  $n = 9$  sessions in three mice; OT:  $r = 0.03 \pm 0.02$ ,  $n = 8$  sessions in three mice;  $t_{15} = 0.08$ ,  $p=0.43$ , two-tailed unpaired t-test; **Figure 7—figure supplement 1B,D**). The proportion of active putative pyramidal cells with significant theta modulation was not different between conditions ( $\emptyset T$ : 92.24%,  $n = 361$  active cells; OT: 91.97%,  $n = 299$  active cells;  $\chi^2 = 0.01$ ,  $df = 1$ ,  $p=0.89$ , Chi-Square test). The coupling of spikes to theta oscillation was also not significantly different between conditions in terms of preferred phase ( $\emptyset T$ :  $203.91^\circ \pm 2.6$ ,  $n = 361$  active cells; OT:  $191.17^\circ \pm 2.87$ ,  $n = 299$  active cells;  $p=0.07$ , circular Kruskal-Wallis; **Figure 7—figure supplement 2A,B**) and strength (mean resultant vector length  $\emptyset T$ :  $0.18 \pm 0.006$ ,  $n = 361$  active cells; OT:  $0.19 \pm 0.009$ ,  $n = 155$  active cells;  $Z = -1.63$ ,  $p=0.1$ , two-tailed WRS test; **Figure 7—figure supplement 2A,C**).

We then analyzed place cells' theta phase precession. To compensate for decreased spatial stability in the  $\emptyset T$  condition, we took into account only trials with good correlation with the average place fields (Spatially Stable Trials or SST) for place cells recorded in the empty track (**Schlesiger et al., 2015**), but included all trials for place cells recorded in the track with objects. The stability index of SST fields in  $\emptyset T$  was slightly but significantly higher than the stability index of all fields in OT ( $\emptyset T$ ,  $n = 48$  SST fields; OT,  $n = 310$  fields;  $Z = 3.32$ ,  $p<10^{-3}$ , two-tailed WRS test). The percentage of fields with significant ( $p<0.05$ ) and negative correlation between phase and position (i.e. precessing fields) was high in the track with objects (40.22%), comparable to that observed in real linear tracks in mice but low in the empty track (7.46%;  $\chi^2 = 26.57$ ,  $df = 1$ ,  $p<10^{-6}$  compared to OT, Chi-Square test). Accordingly, the correlation between phase and position was significantly different from zero for place cells recorded in the track with objects ( $r = -0.14 \pm 0.018$ ,  $n = 177$  fields;  $p<10^{-14}$ , one sample sign-test; **Figure 7A and B**) but not for those recorded in the track without objects ( $r = 0.15 \pm 0.024$ ,  $n = 15$  fields;  $p=0.30$ , one sample sign-test; **Figure 7A and B**). Moreover, phase precession slopes (calculated on normalized place field sizes) were negative and significantly different from 0 for cells recorded in the track with objects ( $-2.00 \pm 0.17$  rad/U,  $n = 177$  fields;  $p<10^{-14}$ , one sample sign-test; **Figure 7C**) but not in the track without objects ( $1.82 \pm 0.44$  rad/U,  $n = 15$  fields;  $p=0.3$ , one sample sign-test; **Figure 7C**). Similar results were observed when a waveform-based method (which takes into account the asymmetry of theta waves, **Belluscio et al., 2012**) was used to estimate theta phase (**Figure 7—figure supplement 3**).

In the track without objects, the decrease in phase-position correlation could result from the higher inter-trial spatial dispersion, which could lead to spikes at different theta phases for identical positions. To assess this possibility, we performed phase-precession analysis on single-trial-detected fields and averaged the slopes of individual passes (**Schmidt et al., 2009**). The correlation was still negative and significantly different from 0 in OT ( $r = -0.13 \pm 0.025$ ,  $n = 208$  single-trial fields;  $t_{207} = -5.75$ ,  $p<10^{-8}$ , one sample sign-test) but not in  $\emptyset T$  ( $r = 0.042 \pm 0.04$ ,  $n = 41$  single-trial fields;  $t_{40} = 0.92$ ,  $p=0.35$ , one sample t-test). Similarly, the slope of the regression line was negative and significantly different from 0 in OT ( $-1.27 \pm 0.75$  rad/U,  $n = 208$  single-trial fields;  $p<10^{-3}$ , sign-test) but not in  $\emptyset T$  ( $0.74 \pm 0.96$ ,  $n = 41$  single-trial fields;  $p=0.93$ , sign-test).

Because a low percentage of active cells were place cells in the track without objects, we ran an additional analysis that is independent of place field detection. It exploits the fact that phase precessing cells emit theta paced spikes at a frequency slightly faster than the concurrent LFP theta

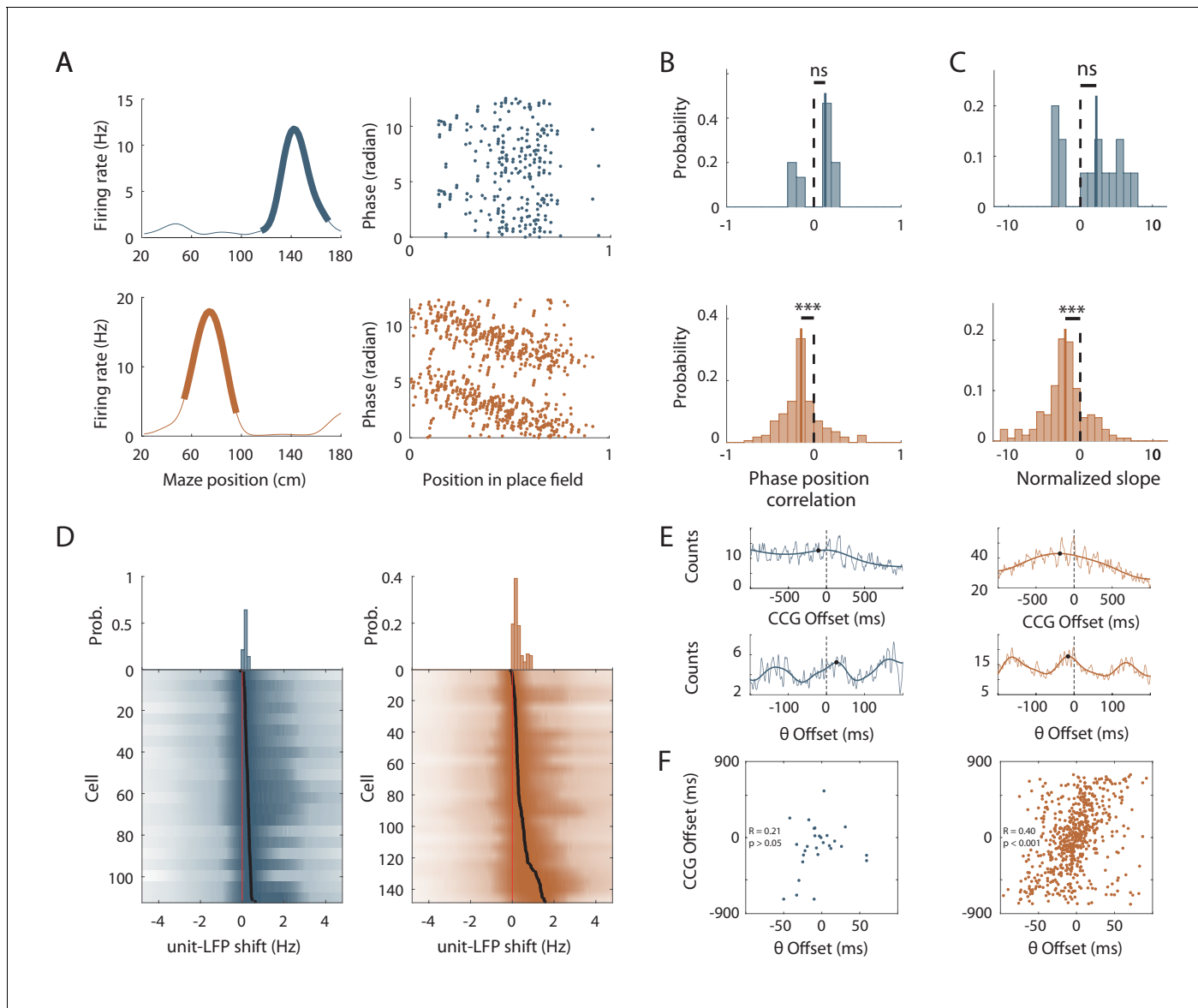


**Figure 7.** Effects of local cues on hippocampal temporal coding resolution . (A) Left: Mean firing rate maps of representative CA1 place cells with place fields highlighted by a bold line (left) recorded in the maze without objects (top, only spatially stable trials see Materials and methods section) and with objects (bottom). Right: spikes phase (radian) versus position in the corresponding place fields. (B–C) Distribution of significant phase position correlation (B) and slopes (C) in the condition without objects (top; correlation) and with objects (bottom). The median of the distribution is indicated by a bold line and 0 by a dotted line. (D) Color-coded cross-correlogram between the power spectra of neuronal spikes and LFP for each theta-modulated cell recorded on the maze without (bottom left, blue) and with (bottom right, orange) objects. Black dots indicate the maximum of each cross-correlation. Each cross-correlation is normalized by its maximum. Top: Distribution of the maximum cross-correlations used to quantify the frequency shift for all the cells. (E) Examples of cross-correlograms computed for two pairs of place cells with overlapping place fields at the behavioral (top) or theta time scale (bottom, see Materials and methods) in order to quantify Cross-Correlogram (CCG) and theta Offsets respectively in no object (blue; left) or object (orange; right) conditions. (F) Relationship between 'CCG' and 'theta' offsets in the cross-correlograms of all the spikes in overlapping place fields of neuron pairs recorded in no object (top; blue) and object condition (bottom; orange).

DOI: <https://doi.org/10.7554/eLife.44487.021>

The following source data and figure supplements are available for figure 7:

**Source data 1.** Source data for **Figure 7**.

DOI: <https://doi.org/10.7554/eLife.44487.025>

**Figure supplement 1.** Speed modulation of LFP theta frequency and amplitude in OT and  $\dot{\theta}$ T.

DOI: <https://doi.org/10.7554/eLife.44487.022>

Figure 7 continued on next page

Figure 7 continued

**Figure supplement 2.** Theta modulation of spikes in OT and  $\bar{O}T$ .

DOI: <https://doi.org/10.7554/eLife.44487.023>

**Figure supplement 3.** Effect of objects on theta phase precession estimated with a waveform-based approach Distribution of significant phase position correlation (left) and slopes (right) in the condition without objects (top, blue) and with (bottom, orange) when theta phase was detected using a waveform-based approach which takes into account theta waves asymmetry.

DOI: <https://doi.org/10.7554/eLife.44487.024>

oscillation (O'Keefe and Recce, 1993). We performed cross-correlation between the power spectra of neuronal spikes and LFP for all active cells with significant theta modulation of spiking activity ( $\bar{O}T$ : 112/342 cells = 32.74%; OT: 148/271 cells = 54.6%;  $\chi^2 = 29.59$ , df = 1,  $p < 10^{-7}$ , Chi-square test) and compared the frequency shift ( $>0$ ) between spiking and LFP theta oscillations between the two conditions (Geisler et al., 2007) (Figure 7D). The shift was significantly higher in the OT ( $0.45 \pm 0.03$  Hz, n = 148 active cells; Figure 7D) versus  $\bar{O}T$  ( $0.26 \pm 0.01$  Hz, n = 112 active cells;  $Z = -2.74$ ,  $p = 0.006$ , two-tailed WRS test; Figure 7D). Altogether, these results suggest that local visual cues are important for proper theta phase precession in the hippocampus.

To further investigate the effect of local visual cues on temporal coding, we next focused on theta-timescale spike coordination. Previous studies have reported, for place cells with overlapping place fields, a positive correlation between the physical distance separating their place fields' centers and the time (or phase) lag of their spikes within individual theta cycles (Skaggs et al., 1996; Dragoi and Buzsáki, 2006). Our analysis revealed a strong correlation between theta phase and physical distance in the presence of virtual 3D objects (OT:  $R = 0.39$ , n = 629 pairs in three mice;  $p < 10^{-24}$ , Pearson correlation; Figure 7E,F) but not otherwise ( $\bar{O}T$ :  $R = 0.21$ , n = 28 pairs in three mice;  $p = 0.26$ , Pearson correlation; Figure 7E,F). These results show that local visual cues are important for temporal coding in the hippocampus beyond theta phase precession.

## Discussion

Our study aimed at determining whether hippocampal spatial coding resolution can rapidly adapt to local features of the environment. We found that spatial coding resolution was increased in the presence of local visual cues through an increase in the proportion of spatially selective place cells among active cells but also enhanced place fields' spatial selectivity and stability. These effects were most prominent in the vicinity of local cues and dynamic upon their manipulations. Local sensory cues also proved to be important for temporal place cell coding such as theta phase precession and theta timescale spike coordination.

Spatial resolution can be improved by pooling information across neurons (Wilson and McNaughton, 1993). We found that local visual cues could dramatically increase the number of place cells among active cells (by a threefold factor). The mechanisms of place cell activation are not fully understood. Using sensory-based models of place cells activation (Hartley et al., 2000; Strösslin et al., 2005; Barry et al., 2006; Sheynikhovich et al., 2009) one can predict that an increase in the quantity/quality of sensory cues in an environment will enhance the number of place cells coding that environment (Geva-Sagiv et al., 2015). However, previous studies using local enrichment with multimodal sensory cues or real objects reported only weak or no effects on dorsal hippocampal cell activity. One study recording in rats navigating between cue-rich and cue-poor parts of the same track reported no effect on the proportion of place cells or on the density of place fields. Furthermore, population vector analysis did not reveal a better disambiguation of nearby locations in the cue-rich part of the track compared to the cue-poor suggesting similar spatial coding resolution (Battaglia et al., 2004). Other studies found no overall increase of place cells proportion in 2D environment containing real objects nor a specific bias for place cells to fire near the objects (Renaudineau et al., 2007; Deshmukh and Knierim, 2013). One possibility to explain the lack of recruitment of additional cells in these studies could be a high recruitment rate of the dorsal hippocampus even in the 'cue poor' condition due to the presence of uncontrolled local cues (Ravassard et al., 2013).

We found that place field density was specifically increased near objects. However, studies so far have revealed an homogeneous allocation of place fields in space (Muller et al., 1987; Rich et al.,

2014) in a given environment. Locally activated place cells could correspond to object-responsive (OR) cells, which tend to discharge near several objects or landmarks in a given environment (Deshmukh and Knierim, 2011). However, the proportion of these cells is generally low in the dorsal hippocampus (between 6 and 8%) which is in line with the fact that places near real objects are not overrepresented at the population level. We note, however, that this proportion may be underestimated and vary depending on the recording location along both the proximo-distal axis and radial axis (Geiller et al., 2017). For example, the distal part of CA1, closer to the subiculum, is more heavily innervated by the lateral entorhinal cortex where OR cells were first discovered (Deshmukh and Knierim, 2011) and which is believed to feed information about the ‘what’ visual stream to the hippocampus (Knierim et al., 2014). Extracellular recordings specifically targeting this area in the intermediate hippocampus reported an increased proportion of place cells with smaller place fields in the presence of objects (Burke et al., 2011). Interestingly, in this study, the decreased place field size was compensated for by increased place fields’ number such that the probability of place cell activation for any point in space was similarly low between the objects and non-objects conditions. However, because objects were distributed all along the maze in this study the local effect of objects was not evaluated. In the present work, the strong increase in the number of place fields in OZ resulted in a significant increase in the proportion of place cells active at these locations despite a local reduction in place field size (OZ:  $6.56 \pm 0.32\% / 10 \text{ cm}$ ,  $n = 12$  spatial bins of 10 cm, six in each direction; ØZ:  $4.50 \pm 0.29\% / 10 \text{ cm}$ ,  $n = 20$  spatial bins of 10 cm, 10 in each direction;  $t_{30} = -4.54$ ,  $p < 10^{-4}$ , two-tailed unpaired t-test). This result shows that while there might be a general mechanism to maintain a constant and low proportion of place cells activated at each position notably between dorsal and ventral parts of the hippocampus (Skaggs and McNaughton, 1992; Maurer et al., 2006) or between objects and non-objects conditions (when objects are distributed all along the track, Burke et al., 2011), spatial coding resolution can nevertheless be increased locally around virtual 3D objects. Whether virtual objects in our study are perceived by mice as real objects is unclear. They notably lack the multisensory component inherent to real objects (Connor and Knierim, 2017). Nevertheless, they triggered a large (50%) increase in place cell’s proportion which is not compatible with the modest proportion of OR cells reported in our and previous studies.

Instead, our results are more compatible with the hippocampal mapping system using local visual cues to improve its spatial coding resolution. Consistent with this hypothesis, spatial coding was not only quantitatively but also qualitatively increased with a higher spatial selectivity, spatial information content and stability of place fields. Previous studies have reported overrepresentations near rewarded locations (O’Keefe and Conway, 1978; Hollup et al., 2001; Dupret et al., 2010; Danielson et al., 2016; Gauthier and Tank, 2018; Sato et al., 2018) or specific sensory cues (Wiener et al., 1989; Hetherington and Shapiro, 1997; Sato et al., 2018). Importantly, we could also observe overrepresentations of the ends of the maze in ØT, where rewards are delivered and which are associated with prominent visual cues. Nevertheless, End-track fields had a low spatial information content and stability when compared to fields recorded in OT (but similar to On-track fields recorded in the same maze). This argues against increased spatial coding resolution at these locations and further suggests a possible dissociation between overrepresentation and increased spatial coding resolution. Finally, improved coding resolution near objects could be instantaneously tuned upon object manipulation while overrepresentations of specific sensory stimuli or rewarded locations usually takes several days to develop (Le Merre et al., 2018; Sato et al., 2018).

A previous study in rats specifically compared place cell coding in real and virtual reality environments with distal visual cues only (Ravassard et al., 2013). They reported a lower number of spatially modulated cells and lower spatial selectivity in the virtual environment and concluded that distal visual cues alone are not sufficient to fully engage the hippocampal mapping system. Our results complement this study by showing that local visual cues, on the other hand, can increase the proportion of spatially modulated cells (i.e. place cells) among active cells and spatial selectivity. Several factors could explain the specific effect of local visual cues on spatial coding observed in the present study. First, objects could constitute a stable reference point in space to refine estimation of the current subject’s position possibly through anchoring of the path integrator system (McNaughton et al., 2006; Poucet et al., 2015). Close to the objects, this effect could be further reinforced through motion parallax effect. Second, objects as local visual cues have a higher sensory resolution compared to distal visual cues. This can lead to increased spatial coding resolution

according to sensory based models of place cell activation ([Hartley et al., 2000](#); [Strösslin et al., 2005](#); [Barry et al., 2006](#)). In line with this, animals tend to increase their sensory sampling rate in order to get a better sensory resolution near important locations ([Geva-Sagiv et al., 2015](#)). Third, objects, as salient cues in the environment, could modify the attentional state of the animal and favor spatial awareness. Such rise in attention has been shown to increase spatial selectivity in mice ([Kentros et al., 2004](#)). However, we note that animals were not required to pay close attention to objects locations to perform the task, as task performance was not different between the  $\emptyset$ T and OT conditions. Alternatively, objects could represent a source of additional noise in the system thus requiring a higher number of spatially modulated cells and increased spatial selectivity for efficient position coding. However, position decoding was very poor in the maze without objects, which argues against this possibility.

The effects of local cues on spatial coding accuracy were even more pronounced in the temporal domain. Indeed, in the absence of local cues theta phase precession was strongly reduced as observed in rat running in place in a wheel ([Hirase et al., 1999](#)) despite the presence of place fields and patterns on the walls providing optic flow. When local cues were included, however, hippocampal place cells precessed at a rate comparable to that observed in real environments ([Middleton and McHugh, 2016](#)). An increased slope of theta phase precession in the presence of real objects was reported before ([Burke et al., 2011](#)) without a significant change in the correlation between phase and position. Because place fields were smaller in the presence of objects, this increase could result from a scaling of theta phase precession rate with place field size ([Huxter et al., 2003](#)). In our study, we measured theta phase precession on normalized field sizes and also using single trials. We observed a significant and positive correlation between phase and position in the presence of 3D objects, while this correlation was not different from 0 in the absence of local visual cues. This is consistent with improved temporal spatial information coding in the presence of local visual cues.

To ascertain that this effect did not result from changes in place fields' quality, additional analysis, independent of place fields' detection, were performed ([Geisler et al., 2007](#)). These analyses also showed that in the presence of local cues individual cells' firing tended to oscillate faster than theta oscillation recorded in the LFP (a sign of theta phase precession) while this was much less the case in the absence of local cues. Importantly, the frequency and power of the theta oscillation recorded in the LFP and the coupling of putative pyramidal cells' firing to this oscillation were also not significantly different between conditions and cannot explain observed differences. The only difference was an attenuation of theta frequency speed modulation in the absence of local cues while theta amplitude vs speed modulation was equivalent in both conditions. A similar absence of theta frequency vs speed modulation (with intact theta amplitude vs speed modulation) was observed in rats navigating virtual reality environments in the absence of local visual cues ([Ravassard et al., 2013](#)). However, in this study, theta phase precession was unaffected. Thus, the link between an absence of theta frequency vs speed modulation and reduced theta phase precession is not straightforward. Future studies are needed to decipher the mechanisms of the effect of local cues on theta phase precession. Theta phase precession is thought to be involved in the generation of theta sequences, where the time lags between spikes of place cells with overlapping place fields are proportional to the distance separating those fields. This so-called theta sequence compression is thought to be important for spatial memory. Here, we found that theta timescale coordination could be observed in the presence of 3D objects only. This suggests that local sensory cues are important for temporal coding beyond theta phase precession.

Altogether, our results show that enriching an environment with local visual cues allows coding at higher spatial resolution with a high number of spatially modulated cells, smaller firing fields, increased spatial selectivity and stability and good theta phase precession/theta timescale spike coordination. The use of virtual reality raises a growing interest in the field of neuroscience to study spatial cognition in rodents but also in non-human and human primates ([Epstein et al., 2017](#)). Our results suggest that enriching these environments with local visual cues could help comparing spatial coding in real and virtual environments.

We observed that local visual cues induce a rescaling of spatial coding which is both global and local. What would be the benefit of this rescaling? In the wild, rodents can travel kilometers away from their home to food locations through empty fields ([Taylor, 1978](#)). Mapping all parts of explored environment at high resolution would require a very large number of neurons and

computational power (**Geva-Sagiv et al., 2015**). Accordingly, place fields tend to be larger in bigger environments (**Fenton et al., 2008**) and the statistics of new place cells recruitment as an environment becomes bigger are non-uniform (**Rich et al., 2014**). Thus, there might be a computational benefit to be able to map at high resolution important places like home base or food locations and to map at lower resolution long transition routes between those locations (**Geva-Sagiv et al., 2015**). Such resolution could depend on the number of local sensory information as presented here. Future work should decipher whether increased spatial coding resolution is associated with better navigational accuracy and spatial memory.

## Materials and methods

### Animals

Data were acquired from 11 male mice C57BL/6J (Janvier/Charles River) between 8 and 12 weeks during the recording phase (weight: 21–23.6 g). The mice were housed 2 or three per cages before the first surgery and then individually with 12 inverted light/dark cycles. Trainings and recordings occurred during the dark phase.

### Ethics

All experiments were approved by the Institut National de la Santé et de la Recherche Médicale (INSERM) animal care and use committee and authorized by the Ministère de l'Education Nationale de l'Enseignement Supérieur et de la Recherche following evaluation by a local ethical committee (agreement number 02048.02), in accordance with the European community council directives (2010/63/UE).

### Surgical procedure to prepare head fixation

A first surgery was performed to implant a fixation bar later used for head-fixation. Animals were anesthetized with isoflurane (3%) before intraperitoneal injection of ketamine (100 mg/Kg) mixed with xylazine (10 mg/Kg) supplemented with a subcutaneous injection of buprenorphine (0.06 mg/Kg). Two jeweller's screws were inserted into the skull above the cerebellum to serve as reference and ground. A dental cement hat was then constructed leaving the skull above the hippocampi free to perform the craniotomies later on. The free skull was covered with a layer of agarose 2% (wt/vol) and sealed with silicon elastomer (Kwik-Cast, World Precision Instruments). A small titanium bar (0.65 g; 12 × 6 mm) was inserted in the hat above the cerebellum to serve as a fixation point for a larger head plate used for head fixation only during trainings and recordings.

### Virtual reality set up

A commercially available virtual reality system (Phenosys Jetball-TFT) was combined with a custom designed 3D printed concave plastic wheel (center diameter: 12.5 cm; side diameter: 7.5 cm; width: 14 cm, covered with silicon-based white coating) to allow 1D movement with a 1/1 coupling between movement of the mouse on the wheel and movement of its avatar in the virtual reality environment. This solution was preferred to the original spherical treadmill running in a X-only mode (which takes into account only rotations of the ball in the X axis to actualize the position of the avatar in the virtual reality environment) which also allows 1D movement but with a more variable coupling between movement of the mouse on the treadmill and its avatar in the virtual reality environment. The wheel was surrounded by six 19-inches TFT monitors, which altogether covered a 270 degrees angle. Monitors were elevated so that the mice's eyes level corresponded to the lower third of the screen height to account for the fact that rodents field of view is biased upward. The head fixation system (Luigs and Neumann) was located behind the animal to not interfere with the display of the virtual reality environment. The virtual reality environment was a virtual 200 cm long and 32 cm wide linear maze with different patterns on the side and end walls and virtual 3D objects (see virtual reality environments section). Movement of the wheel actualized the mouse's avatar position. The mouse could only perform forward or backward movements but could not turn back in the middle of the track (see training section).

## Virtual reality environments

### No objects track ( $\emptyset$ T)

Each side wall had a unique pattern (black and orange stripes on one wall; green crosses on black background on the other wall). End-walls had grey triangular or round shapes on a yellow background (**Figure 1A**).

### Objects track (OT)

This maze was identical to the  $\emptyset$ T maze concerning wall patterns and dimensions but three virtual objects were included on the sides between the animal trajectory and the walls (**Figure 1A**). The objects were a yellow origami crane (dimensions: 9 × 9 × 7 cm; position: 37 cm from end wall), a blue and grey cube (dimensions: 5 × 5 × 5 cm; position: 64 cm from end wall) and a tree (15 × 15 × 22 cm; position: 175 cm from end-wall). The animal could neither orient toward the objects nor get any sensory feedback from them by any other mean but vision.

### Pattern no objects track (P $\emptyset$ T)

This maze had the same dimensions as the previous mazes, but the side walls had distinct symmetrical patterns in different locations along the maze (50 cm long; black dots on white background, black and green squares, black and white stripes and green crosses on black background).

### Enriched objects track (EOT)

This maze was identical to the Pattern No Objects Track (P $\emptyset$ T) and included the same virtual reality objects (identical in dimensions and locations) to those of the Objects Track (OT) maze. Outside the maze walls, two large 3D columns were positioned on each side (dimensions 8 × 8 × 47 cm; positions 58 and 143 cm from end wall) to provide additional visual cues.

## Training

Mice were first habituated to the experimentalist through daily handling sessions of 20 min or more that continued throughout the experiment. After a 3 days post-surgery recovery period, mice were water-deprived (1 ml/day, including the quantity of water taken during the training). After 2–3 days of water deprivation, they were progressively trained to run in the virtual reality set up. First, mice were familiarized with running head-fixed on the wheel for water rewards in a black track (screens always black). During these sessions, animals received as a reward sweetened water (5% sucrose) for each 50 centimeters run on the wheel. When animals were comfortable with the setup, they were trained to run in one of three linear virtual tracks (familiar track) assigned randomly. When animals reached the end of the track, a liquid reward delivery tube extended in front of the animal and animal had to lick to get the reward (a 4  $\mu$ L drop of water of 5% sucrose). Animals were then teleported in the same position but facing the opposite direction of the maze and had to run up to the end of the maze in the opposite direction to get another reward. Animals were initially trained during 15 min sessions. Session time was progressively increased to reach 60 min. *Ad libidum* water access was restored if the weight of the animal decreased beneath 80% of the pre-surgery weight at any stage during training.

## Recording procedure

When animals reached a stable behavioral performance (at least one reward/minute during 60 min), we performed acute recordings using silicon probes (4/8 shanks; A-32/A-64 Buzsáki Probe, Neuro-nexus; see **Figure 1—figure supplement 1**). On the day before the first recording session, animals were anesthetized (induction: isoflurane 3%; maintenance: Xylazine/Ketamine 10/100 mg/Kg supplemented with Buprenorphine 0.1 mg/Kg) and a craniotomy was drilled above one hippocampus (centered on a location –2 mm posterior and  $\pm$ 2.1 mm lateral from bregma). The craniotomy was covered with agarose (2% in physiological saline) then sealed with silicon elastomer (Kwik-Cast, World Precision Instruments). This craniotomy was used to record acutely during 2–3 consecutive days (with the probe lowered in a new location every time). Then a second craniotomy was performed over the other hippocampus following the same procedure and recordings were performed during 2–3 additional days. Before each recording session, the backside of the probe's shanks was covered with a thin layer of a cell labeling red-fluorescent dye (Dil, Life technologies) so that its

location (tips of the shanks) could be assessed post-hoc histologically. The silicon probe was then lowered into the brain while the animal was allowed to walk freely on the wheel with the screens displaying a black background. The good positioning of the probe with recording sites in the CA1 pyramidal cell layer was verified by the presence of multiple units showing complex spike bursts on several recordings sites and the recording of sharp-wave ripples during quiet behavior. After positioning of the silicon probe the virtual reality environment was displayed on the screen. On the day of the last recording in each hippocampus, the backside of the probe's shanks was covered with a thin layer of a cell labeling red-fluorescent dye (Dil, Life technologies) so that its location (tips of the shanks) could be assessed histologically post-hoc. All mice ( $n = 11$ ) experienced a familiar environment (either ØT, OT, PØT or EOT) for around 20 back and forth trials. For mice trained in ØT or OT ( $n = 3$  and 3, respectively), this first exploration was followed, after 3 min of free running with the screens displaying a black background, by exploration of a new environment, identical to the previous one except for the presence of the three 3D objects (objects were added for mice trained in ØT and removed for mice trained in OT) for another 20 consecutive back and forth trials. For some of these mice ( $n = 2$  for ØT,  $n = 2$  for OT,  $n = 2$  for PØT and  $n = 2$  for EOT) sessions in the familiar track and novel track were divided into two sub-sessions interleaved by 3 min of free running with the screens black. The two sub-sessions in the familiar environment and the new environment were pulled together for analysis. Note that animals stayed head-fixed on the wheel surrounded by screens during the entire recording session.

### Data acquisition and pre-processing

The position of the animal in the virtual maze was digitalized by the virtual reality controlling computer (Phenosys) and then sent to a digital-analog card (0–4.5V, National Instrument Board NI USB-6008) connected to the external board (I/O Board, Open Ephys) of a 256 channels acquisition board (Open Ephys). Neurophysiological signals were acquired continuously on a 256-channels recording system (Open Ephys, Intan Technologies, RHD2132 amplifier board with RHD2000 USB interface board) at 25,000 Hz. Spike sorting was performed semi-automatically using KlustaKwik (Rossant et al., 2016; <https://github.com/klusta-team/klustakwik>). Clusters were then manually refined using cluster quality assessment, auto- and cross-correlograms, clusters waveforms and similarity matrix (Klustaviewa, Rossant et al., 2016).

### Data analysis

Data analysis was performed in the MATLAB software environment and the source code is available from GitHub (Marti et al., 2019; copy archived at [https://github.com/elife sciences-publications/codes\\_bourboulou\\_marti\\_2019](https://github.com/elife sciences-publications/codes_bourboulou_marti_2019)).

### Reward and object zones definition

The reward zones, located between the maze extremities and 10% of the track length (0–20 cm and 180–200 cm), were not considered in the analysis. The object zone was composed of two zones, one from 30 to 70 cm including both the origami crane and the cube and the other from 160 to 180 cm including the tree.

### Firing rate map

The maze was divided into 100 spatial bins measuring 2 cm. For each trial, the number of spikes and the occupancy time of the animal in each spatial bin were calculated to obtain the spikes number vector and the occupancy time vector, respectively. These vectors were smoothed using a Gaussian filter with a half-width set to 10 spatial bins. Spikes occurring during epochs when velocity was lower than 2 cm/s were removed from all analysis. The smoothed spikes number vector was divided by the smoothed occupancy time vector to obtain the firing rate vector for each trial. The firing rate vectors were pooled for a specific condition (e.g. Familiar Objects Track) and direction of the animal (e.g. back) to generate a firing rate map. These pooled vectors were also averaged to provide the mean firing rate vector, corresponding to the mean firing rate for each spatial bin.

## Pyramidal cell classification

Cells with a mean firing rate lower than 20 Hz and either a burst index (Royer et al., 2012) greater than 0 or the spike duration greater than 0.4 ms were classified as putative pyramidal neurons. They were classified as interneurons otherwise. To compute the proportion of active putative pyramidal cells, only sessions with at least 15 recorded neurons were included.

## Active cells classification

A cell was considered as active when the mean firing rate was greater than 0.5 Hz, the peak firing rate was greater than 1.5 Hz and the cell fired at least one spike in 50% of the trials. These three criteria had to be verified in either the forth or back direction.

## Place fields detection

To detect a mean place field, a bootstrap procedure was performed. For each trial, a new spikes train was generated using a Poisson process with  $\lambda$  equal to the mean firing rate of the trial and a 1 ms time interval. A ‘randomized’ firing rate map was then generated and the mean firing rate vector was determined and compared with the mean firing rate vector from the initial rate map. This operation was repeated 1000 times to determine a p-value vector (p-value for each 2 cm spatial bin). Place fields candidates were defined as a set of more than three continuous spatial bins associated with p-values lower than 0.01. Two place fields were merged when the distance between their closest edges was at most equal to five spatial bins (10 cm). Place fields’ edges were extended by at most five spatial bins (for each edge) when the p-value was below 0.30 for these bins. A field with a size greater than 45 spatial bins (90 cm) was not considered as a place field. To validate a mean place field, the cell had to verify a stability criterion. Spatial correlations were calculated between the firing rate vector of each trial and the mean firing rate vector. The spatial bins corresponding to other detected place fields were not considered in the spatial correlations. The place field was validated if the spatial correlations were greater than 0.60 for at least 40% of trials. Unless specified, when several mean place fields were detected, only the place field with the highest peak was conserved. An active cell with at least one place field in one direction was considered as a place cell. To compute the proportion of place cells, only sessions with at least nine active cells were included.

The same procedure was applied to detect place fields per lap without the stability criterion, which cannot be calculated on single trials. A place field per lap was conserved if it overlapped at least one spatial bin with the closest mean place field.

## Stability index

The stability index of a cell was computed as the mean of the spatial correlations between all pairs of firing rate vectors. This way, the cell stability index takes into account the activity patterns from all the trials and provides a reliable quantification of the inter-trial reproducibility of the cells activity. Note that this stability index is different from usual stability indexes based on correlations of mean firing rates between even and odd trials or two halves of the same recording session thus values obtained cannot be directly compared.

## Spatial Information

The spatial information (SI) was calculated according to the following formula (Skaggs et al., 1996):

$$SI = \sum_{i=1}^N \left[ \frac{FR_i}{FR} \times \frac{OT_i}{OT_T} \times \log_2 \left( \frac{FR_i}{FR} \right) \right]$$

where N is the number of spatial bins (N = 100),  $FR_i$  is the mean firing rate determined in the i-th spatial bin,  $FR$  is the mean firing rate,  $OT_i$  is the mean occupancy time determined in the i-th spatial bin,  $OT_T$  is the total occupancy time based on the mean occupancy time vector.

As another measure of spatial information, we computed the Mutual Information using the following formula:

$$MI = \sum_{i=1}^N \sum_{j=1}^4 p_{i,j} \log_2 \left( \frac{p_{i,j}}{p_i \cdot p_j} \right)$$

where N is the total number of spatial bins,  $p_i$  is the occupancy probability of the animal in the i-th spatial bin,  $p_j$  is the probability to obtain a firing rate amongst one of four non overlapping quartiles of firing rates and  $p_{i,j}$  is the joint probability of the animal to be in the i-th spatial bin with a firing rate in the j-th quartile. The Mutual Information was then normalized with a surrogate-based distribution to correct possible bias due to basal firing rate (*Souza et al., 2018*).

### Out/in-field firing ratio

The out/in-field firing ratio was computed as the ratio between the mean firing rate outside the mean place field (excluding secondary place fields) and the mean firing rate inside the mean place field.

### Place field dispersion

A place field dispersion measure has been computed to quantify how much each place field per lap was dispersed around the mean place field. The place field dispersion (PFD) was calculated according to the following formula:

$$PFD = \frac{L}{N} \left[ \frac{1}{M} \sum_{i=1}^M (C - C_i)^2 \right]^{\frac{1}{2}}$$

where C is the center of the mean place field,  $C_i$  is the center of the field in the i-th lap and M is the number of laps with a single-trial detected field, L is the total length of the maze and N is the number of spatial bins. The center of a place field was defined as the spatial bin with the highest firing rate.

### Place field width

Place field width was computed as the distance between the place field edges and only determined for entire place fields. A place field was considered as complete when its firing rate increased above 30% of the difference between highest and lowest place field activity and then dropped below this threshold.

### On-track and end-track fields

A mean place field was considered as End-Track field if the peak of the field was located at the beginning of the reward zone (i.e. at the 11-th or the 90-th spatial bin). All other fields were classified as On-Track fields.

### Distribution of place fields' position

To statistically assess whether the place fields were non-uniformly distributed in the maze, we tested the null hypothesis that all fields were uniformly distributed. Based on this hypothesis, the total number of place fields was redistributed with an equal probability to be in each 10 cm spatial bin. The standard deviation of this uniform distribution was then compared to the initial distribution. This operation was repeated 1000 times (bootstrap procedure) to obtain a p-value, corresponding to the probability of the place fields to be uniformly distributed. When this p-value was lower than 0.05, the null hypothesis was rejected and the distribution was considered as non-uniform. To ensure that single values of place fields' percentage in a given bin did not make the distribution non-uniform, values greater than the 93-th percentile and lower than the 6-th percentile have been excluded from the initial distribution.

### Local stability

A local stability index was developed to assess how consistent a firing rate was over the laps for a given spatial bin. To this end, two mean firing rate vectors were calculated, in the neighborhood of each spatial bin (2-spatial bins half-window) for even and odd trials. Local stability index was defined as the spatial correlation between these two vectors for a given spatial bin.

## Position decoding

To address how informative the firing rates of the CA1 pyramidal cells ensemble were about the position of the animal in the different virtual environments, we used Bayesian decoding and Firing Rate Vectors (FRV) methods. For each time window, the distribution of the animal position probability across the whole maze was calculated using the firing activity of all active cells (place cells and non place cells). The mode of this distribution (maximum of probability) was chosen as the decoded position for a given time window. We used a classical ‘memoryless’ Bayesian decoder (Brown et al., 1998; Zhang et al., 1998). The decoding of the spikes data was restricted to periods when the animal was running (speed >2 cm/s) or with good Theta/Delta ratio and cross-validated using the ‘leave one out’ approach. We computed the animal’s probability to be in each spatial bin  $x$  (2 cm) knowing that  $N$  cells fired  $n$  spikes in a time window according to the following formula:

$$P(x|n) = C(\tau, n)P(x) \left( \prod_{i=1}^N f_i(x)^{n_i} \right) \exp \left( -\tau \sum_{i=1}^N f_i(x) \right)$$

with  $P(x)$  a uniform spatial prior,  $f_i(x)$  the average firing rate of the neuron  $i$  over  $x$  (i.e. the tuning curve over the position),  $n_i$  the number of spikes emitted by the neuron  $i$  in the current time window and  $\tau$  the length of the time window (150 ms; non-overlapping) and  $C(\tau, n)$  a normalization factor intended to set the posterior probability for one time window to 1. This formula assumes that the spikes trains obey to a Poisson process and that cells activity is independent. Position decoding was also performed using the FRV method (Middleton and McHugh, 2016). For each 100 ms time bin, the Pearson correlations were calculated between firing rates across all cells and the mean firing rates from all cells for a given spatial bin. A decoding error was defined as the absolute value of the difference between decoded and real position. Accuracy was defined as the probability at the real position in a particular time bin. To ensure that the position decoding was not influenced by the number of cells, a drop cell approach was performed (van der Meer et al., 2010). Briefly, for  $M$  recorded active cells, the position was decoded using  $k$  different subsets of cells with increasing sizes  $5*k$  with  $k$  ranging from 1 to the last multiple of 5 <  $M$ . For the  $k$ -th subset, the decoding was repeated 50 times using  $5*k$  randomly selected cells and the median value of probabilities for a given time and spatial bin was chosen as the final probability. The presented results were computed for a subset composed of 20 cells ( $k = 4$ ).

## Map similarity over trials

To analyze the dynamic of the changes of spatial representation between familiar and novel conditions, map similarities were performed for 10 back and forth trials before and after the experimental manipulation. For each active putative pyramidal cell, map similarities consisted of the Pearson correlation between the firing rate map of each back and forth trial and a template firing rate map. This template firing rate map was calculated as the average of the firing rate map from all the laps in the condition with objects (most stable condition). The maps corresponding to back (forth) trials were correlated to the mean back (forth) trial map in the object condition and the correlations values were averaged to obtain a single value for this back and forth trial. When map similarity was determined for a lap in the object condition, the template firing rate map was computed without it.

## Object-responsive cells detection

OR cells tend to discharge systematically at the location of several objects (if they do not code for object identity) present in the environment or at least one object (if they in addition code for object identity). For this analysis, we took advantage of the fact that our animals were passing near the same objects in both back and forth trials. We defined individual objects zones (IOZ), one for each object. For a given object, IOZ corresponded to all spatial bins occupied by the object. Here are the IOZ defined for each object in both directions: origami crane: 30–46 cm, cube: 60–70 cm and tree 164–180 cm. Place cells were classified as OR cells if they were bidirectional (firing in both back and forth trials) and had at least one place field in a IOZ corresponding to the same object for both back and forth trials or several place fields in several IOZs corresponding to the same objects in both back and forth trials.

## Phase precession analysis

Phase precession was calculated on all spikes (above speed threshold) for the track with objects but restrained to Spatially Stable Trials (SST) in the no object condition to equalize stability between both conditions. SST consisted of at least three trials where the in-field correlation with the mean place field exceeded 0.6. To assess theta phase precession, the Local Field Potential (LFP) of the channel with the highest number of pyramidal cells (*Skaggs et al., 1996*) was filtered (4th order Chebyshev filter type II) in the theta band (4–12 Hz). The instantaneous theta phase for each time bin (1 ms) was determined by two different methods: either using the Hilbert transform of the filtered LFP or a waveform-based approach (*Belluscio et al., 2012*). In the later method, cycles extrema were detected in the wide-band signal (1–40 Hz) in each half cycles defined by a zero-crossings of a narrow-band filter (4–10 Hz). LFP theta band phase was then estimated by a linear interpolation between peaks, through and each half cycle in order to preserve theta asymmetry. Both methods produced similar results. Thus, the theta phases used in this paper were obtained using Hilbert transform (unless noted). Only theta phase locked cells were considered in the following analysis (non-uniform phase distribution,  $p < 0.05$ , Rayleigh test). Circular linear analysis was used to determine the correlation strength and slope value of the relation between spikes phases and normalized positions (0–1) through the mean place field (*Kempton et al., 2012*). Briefly, the phase precession slope was computed with a linear regression model between circular (spike phases) and linear (animal's position) data. The slope of the regression was used to scale the animal's position and to transform it into a circular variable. A circular-circular correlation could thus be computed on the data to assess the strength of the relationship between spike phases and animal's position. A significance value was determined by re-computing the correlation values for 1000 permutations of the spikes position.

Analysis of phase precession on single-trial detected fields was also performed (*Schmidt et al., 2009*). Phase precession slope and correlation values were computed similarly to the previously described method. The single lap slope and correlation values were averaged only for sessions with at least three significantly precessing trials where the cell emitted a minimum of four spikes inside the mean place field.

## Unit-LFP shift and spike phase spectrum

To quantify phase precession independently of the position of the animal and the place field detection, Unit-LFP shift was used. For all active putative pyramidal cells, a discrete multitaper spectrum in the theta band (4–12 Hz) of the cell's spikes was performed (mtpointspectrum, Chronux 2.11; <http://chronux.org/>) as well as the continuous multitaper spectrum of the simultaneously recorded LFP (mtnspectrunc, Chronux 2.11). A theta modulation index (*Mizuseki et al., 2009*) was defined for each cell spike spectrum as the mean power around the peak theta frequency  $\pm 0.5$  Hz divided by the mean power below 5 Hz or above 9 Hz. A cell was considered as theta modulated if this index was greater than 1.4. The cross correlogram was then calculated for theta modulated cells to determine the lag in the theta band between the LFP and the cells' spectrum (*Geisler et al., 2007*). A positive lag indicates that the cell is firing faster than the concurrent LFP.

## Speed modulation of theta frequency and amplitude

The instantaneous theta frequency was computed from the instantaneous theta phase extracted from the Hilbert transform of the filtered LFP in the theta band. For each time  $t_i$ , the instantaneous theta frequency ( $F_\theta(t_i)$ ) was determined based on the unwrapped phase:

$$F_\theta(t_i) = \frac{\text{Phase}(t_{i+1}) - \text{Phase}(t_i)}{2\pi * F_s}$$

where  $F_s$  is the sampling frequency.

Instantaneous theta amplitude was defined as the module of the LFP Hilbert transform and normalized by the mean LFP theta amplitude. The Pearson correlation coefficient was then calculated between the speed of the animal and theta frequency/amplitude.

A theta peak detection method was also used to calculate the instantaneous theta frequency. Theta peaks were detected with zero crossing of the instantaneous LFP phase and frequency was

deduced from the time between two successive theta peaks. This value was affected to all the time stamp of the corresponding cycle.

### Theta timescale correlation

To calculate the theta timescale lag between the spikes of two overlapping place fields, two cross-correlograms (CCGs) were computed (*Dragoi and Buzsáki, 2006; Robbe and Buzsáki, 2009; Skaggs et al., 1996*; CCGHeart; <http://fmatoobox.sourceforge.net/>). First a ‘Real-time scale’ CCG was computed with a 1 s time window and 3 ms time bin. The CCG time lag was defined as the peak of the filtered CCG between [0–2] Hz. ‘Theta time-scale’ CCG was computed with a 200 ms time window and 1 ms time bin. The theta time lag was defined as the peak of the filtered CCG between [0–20] Hz. Only pairs of cells with a CCG mean bin count of 1 count/ms were included in this analysis. The relation between the CCG time lag and theta time lag was assessed using Pearson correlation.

### Preferred theta phase

Preferred theta phase and Mean Resultant Vector Length of each cell were defined thanks to circ\_mean and circ\_r circular statistics MATLAB toolbox functions (*Berens, 2009*; <https://github.com/circstat/circstat-matlab>). Global phase 180° was defined as the maximal pyramidal cells activity (*Skaggs et al., 1996*).

### Statistics

All statistical analyses were conducted using MATLAB codes (MathWorks). For each distribution, a Lilliefors goodness-of-fit test was used to verify if the data were normally distributed and a Levene test was used to assess for equal variance. If normality or equal variance were not verified, we used the Wilcoxon rank sum test otherwise the Student t-test was used to compare two distributions. In case of multiple comparisons, the Kruskal-Wallis test with Bonferroni post-hoc test was used. Spatial correlations were computed using Pearson’s correlation coefficient. Chi-square test was used to compare percentages of phase precessing cells. For circular distributions comparison, we first tested if they came from a Von-Mises distributions (Watson Test) with a common concentration (circ\_ktest), if the distribution respected these constrains circular ANOVA: Watson-Williams multi-sample test for equal means (circ\_wwtest) was applied.

### Acknowledgements

The authors thank Caroline Filippi for help with histology; Mathieu Pasquet, Ludovic Petit, Susanne Reichinnek and Robert Martinez for technical assistance; David Dupret, Pierre-Pascal Lenck-Santini, Vincent Hok, Francesca Sargolini, Michaël Zugaro and members of the Epsztein lab for useful discussions; Bryan Souza and Adriano Tort lab for comments on a preprint version of this article; the animal facility, administrative and imaging platforms of INMED for support. This study was supported by INSERM, a rising star grant from of the A\*MIDEX project (n° ANR-11-IDEX-0001-02) funded by the «Investissements d’Avenir» French Government program (to JE), by the European Research Council under the European Community’s Seventh Framework Program (ERC-2013-StG-338141\_Intraspace to JE and ERC-2013-CoG-615699\_NeuroKinematics to DR) and by the ‘Agence National de la Recherche’ (ANRJCJC to JK).

---

### Additional information

#### Funding

Funder	Grant reference number	Author
Seventh Framework Programme	ERC-2013-CoG 615699- Neurokinematics	David Robbe
Agence Nationale de la Recherche	ANR-17-CE37-0005- GRIDSPACES	Julie Koenig

---

Seventh Framework Programme	ERC-2013-StG 338141 - IntraSpace	Jerome Epsztein
A*MIDEX under Investissements d'Avenir framework	ANR-11-IDEX-0001-02	Jerome Epsztein
Région PACA		Jerome Epsztein
Institut National de la Santé et de la Recherche Médicale		Jerome Epsztein

The funders had no role in study design, data collection and interpretation, or the decision to submit the work for publication.

#### Author contributions

Romain Bourboulou, Conceptualization, Software, Formal analysis, Investigation, Visualization, Writing—review and editing; Geoffrey Marti, Conceptualization, Data curation, Software, Formal analysis, Visualization, Writing—review and editing; François-Xavier Michon, Software, Writing—review and editing; Elissa El Feghaly, Investigation, Writing—review and editing; Morgane Nouguier, Conceptualization, Investigation; David Robbe, Resources, Writing—review and editing; Julie Koenig, Conceptualization, Resources, Software, Formal analysis, Supervision, Investigation, Writing—review and editing; Jerome Epsztein, Conceptualization, Resources, Supervision, Funding acquisition, Visualization, Writing—original draft, Project administration, Writing—review and editing

#### Author ORCIDs

Romain Bourboulou  <http://orcid.org/0000-0002-9133-8386>

David Robbe  <http://orcid.org/0000-0002-9450-0553>

Julie Koenig  <http://orcid.org/0000-0003-0516-6627>

Jerome Epsztein  <http://orcid.org/0000-0002-5344-3986>

#### Ethics

Animal experimentation: All experiments were approved by the Institut National de la Santé et de la Recherche Médicale (INSERM) animal care and use committee and authorized by the Ministère de l'Education Nationale de l'Enseignement Supérieur et de la Recherche (agreement number 02048.02), in accordance with the European community council directives (2010/63/UE).

#### Decision letter and Author response

Decision letter <https://doi.org/10.7554/eLife.44487.030>

Author response <https://doi.org/10.7554/eLife.44487.031>

---

## Additional files

#### Supplementary files

- Supplementary file 1. Details of the recorded units and animal behavior per recording session in different mazes. TA: Track Active. Rw.: Number of rewards.

DOI: <https://doi.org/10.7554/eLife.44487.026>

- Supplementary file 2. Details of place cells' firing properties per recording session in different mazes.

DOI: <https://doi.org/10.7554/eLife.44487.027>

- Transparent reporting form

DOI: <https://doi.org/10.7554/eLife.44487.028>

#### Data availability

All data generated or analyzed during this study are included in the manuscript and supporting files. Source data are provided for Figures 1–7.

## References

- Aronov D, Tank DW. 2014. Engagement of neural circuits underlying 2D spatial navigation in a rodent virtual reality system. *Neuron* **84**:442–456. DOI: <https://doi.org/10.1016/j.neuron.2014.08.042>, PMID: 25374363
- Barry C, Lever C, Hayman R, Hartley T, Burton S, O'Keefe J, Jeffery K, Burgess N. 2006. The boundary vector cell model of place cell firing and spatial memory. *Reviews in the Neurosciences* **17**:71–97. DOI: <https://doi.org/10.1515/REVNEURO.2006.17.1-2.71>, PMID: 16703944
- Battaglia FP, Sutherland GR, McNaughton BL. 2004. Local sensory cues and place cell directionality: additional evidence of prospective coding in the hippocampus. *Journal of Neuroscience* **24**:4541–4550. DOI: <https://doi.org/10.1523/JNEUROSCI.4896-03.2004>, PMID: 15140925
- Belluscio MA, Mizuseki K, Schmidt R, Kempter R, Buzsáki G. 2012. Cross-frequency phase-phase coupling between  $\theta$  and  $\gamma$  oscillations in the hippocampus. *Journal of Neuroscience* **32**:423–435. DOI: <https://doi.org/10.1523/JNEUROSCI.4122-11.2012>, PMID: 22238079
- Berens P. 2009. CircStat : A MATLAB Toolbox for circular statistics. *Journal of Statistical Software* **31**:257–266. DOI: <https://doi.org/10.18637/jss.v031.i10>
- Brown EN, Frank LM, Tang D, Quirk MC, Wilson MA. 1998. A statistical paradigm for neural spike train decoding applied to position prediction from ensemble firing patterns of rat hippocampal place cells. *The Journal of Neuroscience* **18**:7411–7425. DOI: <https://doi.org/10.1523/JNEUROSCI.18-18-07411.1998>, PMID: 9736661
- Burke SN, Maurer AP, Nematollahi S, Uprety AR, Wallace JL, Barnes CA. 2011. The influence of objects on place field expression and size in distal hippocampal CA1. *Hippocampus* **21**:783–801. DOI: <https://doi.org/10.1002/hipo.20929>, PMID: 21365714
- Chen G, King JA, Burgess N, O'Keefe J, a KJ, John O. 2013. How vision and movement combine in the hippocampal place code. *PNAS* **110**:378–383. DOI: <https://doi.org/10.1073/pnas.1215834110>, PMID: 23256159
- Cohen JD, Bolstad M, Lee AK. 2017. Experience-dependent shaping of hippocampal CA1 intracellular activity in novel and familiar environments. *eLife* **6**:e23040. DOI: <https://doi.org/10.7554/eLife.23040>, PMID: 28742496
- Connor CE, Knierim JJ. 2017. Integration of objects and space in perception and memory. *Nature Neuroscience* **20**:1493–1503. DOI: <https://doi.org/10.1038/nn.4657>, PMID: 29073645
- Danielson NB, Zaremba JD, Kaifosh P, Bowler J, Ladow M, Losonczy A. 2016. Sublayer-Specific coding dynamics during spatial navigation and learning in hippocampal area CA1. *Neuron* **91**:652–665. DOI: <https://doi.org/10.1016/j.neuron.2016.06.020>, PMID: 27397517
- Deshmukh SS, Knierim JJ. 2011. Representation of non-spatial and spatial information in the lateral entorhinal cortex. *Frontiers in Behavioral Neuroscience* **5**:69. DOI: <https://doi.org/10.3389/fnbeh.2011.00069>, PMID: 22065409
- Deshmukh SS, Knierim JJ. 2013. Influence of local objects on hippocampal representations: Landmark vectors and memory. *Hippocampus* **23**:253–267. DOI: <https://doi.org/10.1002/hipo.22101>, PMID: 23447419
- Dragoi G, Buzsáki G. 2006. Temporal encoding of place sequences by hippocampal cell assemblies. *Neuron* **50**:145–157. DOI: <https://doi.org/10.1016/j.neuron.2006.02.023>, PMID: 16600862
- Dupret D, O'Neill J, Pleydell-Bouverie B, Csicsvari J. 2010. The reorganization and reactivation of hippocampal maps predict spatial memory performance. *Nature Neuroscience* **13**:995–1002. DOI: <https://doi.org/10.1038/nn.2599>, PMID: 20639874
- Epstein RA, Patai EZ, Julian JB, Spiers HJ. 2017. The cognitive map in humans: spatial navigation and beyond. *Nature Neuroscience* **20**:1504–1513. DOI: <https://doi.org/10.1038/nn.4656>, PMID: 29073650
- Epsztein J, Brecht M, Lee AK. 2011. Intracellular determinants of hippocampal CA1 place and silent cell activity in a novel environment. *Neuron* **70**:109–120. DOI: <https://doi.org/10.1016/j.neuron.2011.03.006>, PMID: 21482360
- Fenton AA, Kao HY, Neymotin SA, Olypher A, Vayntrub Y, Lytton WW, Ludvig N. 2008. Unmasking the CA1 ensemble place code by exposures to small and large environments: more place cells and multiple, irregularly arranged, and expanded place fields in the larger space. *Journal of Neuroscience* **28**:11250–11262. DOI: <https://doi.org/10.1523/JNEUROSCI.2862-08.2008>, PMID: 18971467
- Gauthier JL, Tank DW. 2018. A dedicated population for reward coding in the hippocampus. *Neuron* **99**:179–193. DOI: <https://doi.org/10.1016/j.neuron.2018.06.008>, PMID: 30008297
- Geiller T, Fattah M, Choi JS, Royer S. 2017. Place cells are more strongly tied to landmarks in deep than in superficial CA1. *Nature Communications* **8**:14531. DOI: <https://doi.org/10.1038/ncomms14531>, PMID: 28218283
- Geisler C, Robbe D, Zugardo M, Sirota A, Buzsáki G. 2007. Hippocampal place cell assemblies are speed-controlled oscillators. *PNAS* **104**:8149–8154. DOI: <https://doi.org/10.1073/pnas.0610121104>, PMID: 17470808
- Geva-Sagiv M, Las L, Yovel Y, Ulanovsky N. 2015. Spatial cognition in bats and rats: from sensory acquisition to multiscale maps and navigation. *Nature Reviews Neuroscience* **16**:94–108. DOI: <https://doi.org/10.1038/nrn3888>, PMID: 25601780
- Hartley T, Burgess N, Lever C, Cacucci F, O'Keefe J, O'Keefe J. 2000. Modeling place fields in terms of the cortical inputs to the hippocampus. *Hippocampus* **10**:369–379. DOI: [https://doi.org/10.1002/1098-1063\(2000\)10:4<369::AID-HIPO3>3.0.CO;2-0](https://doi.org/10.1002/1098-1063(2000)10:4<369::AID-HIPO3>3.0.CO;2-0), PMID: 10985276
- Harvey CD, Collman F, Dombeck DA, Tank DW. 2009. Intracellular dynamics of hippocampal place cells during virtual navigation. *Nature* **461**:941–946. DOI: <https://doi.org/10.1038/nature08499>, PMID: 19829374

- Hetherington PA**, Shapiro ML. 1997. Hippocampal place fields are altered by the removal of single visual cues in a distance-dependent manner. *Behavioral Neuroscience* **111**:20–34. DOI: <https://doi.org/10.1037/0735-7044.111.1.20>, PMID: 9109621
- Hirase H**, Czurkó A, Csicsvari J, Buzsáki G. 1999. Firing rate and theta-phase coding by hippocampal pyramidal neurons during 'space clamping'. *European Journal of Neuroscience* **11**:4373–4380. DOI: <https://doi.org/10.1046/j.1460-9568.1999.00853.x>, PMID: 10594664
- Hollup SA**, Molden S, Donnett JG, Moser MB, Moser EI. 2001. Accumulation of hippocampal place fields at the goal location in an annular watermaze task. *The Journal of Neuroscience* **21**:1635–1644. DOI: <https://doi.org/10.1523/JNEUROSCI.21-05-01635.2001>, PMID: 11222654
- Hölscher C**, Schnee A, Dahmen H, Setia L, Mallot HA. 2005. Rats are able to navigate in virtual environments. *Journal of Experimental Biology* **208**:561–569. DOI: <https://doi.org/10.1242/jeb.01371>, PMID: 15671344
- Huxter J**, Burgess N, O'Keefe J, O'Keefe J. 2003. Independent rate and temporal coding in hippocampal pyramidal cells. *Nature* **425**:828–832. DOI: <https://doi.org/10.1038/nature02058>, PMID: 14574410
- Kemper R**, Leibold C, Buzsáki G, Diba K, Schmidt R. 2012. Quantifying circular-linear associations: hippocampal phase precession. *Journal of Neuroscience Methods* **207**:113–124. DOI: <https://doi.org/10.1016/j.jneumeth.2012.03.007>, PMID: 22487609
- Kentros CG**, Agnihotri NT, Streater S, Hawkins RD, Kandel ER. 2004. Increased attention to spatial context increases both place field stability and spatial memory. *Neuron* **42**:283–295. DOI: [https://doi.org/10.1016/S0896-6273\(04\)00192-8](https://doi.org/10.1016/S0896-6273(04)00192-8), PMID: 15091343
- Knierim JJ**, Neunuebel JP, Deshmukh SS. 2014. Functional correlates of the lateral and medial entorhinal cortex: objects, path integration and local-global reference frames. *Philosophical Transactions of the Royal Society B: Biological Sciences* **369**:20130369. DOI: <https://doi.org/10.1098/rstb.2013.0369>
- Knierim JJ**, Hamilton DA. 2011. Framing spatial cognition: neural representations of proximal and distal frames of reference and their roles in navigation. *Physiological Reviews* **91**:1245–1279. DOI: <https://doi.org/10.1152/physrev.00021.2010>, PMID: 22013211
- Knierim JJ**, Rao G. 2003. Distal landmarks and hippocampal place cells: effects of relative translation versus rotation. *Hippocampus* **13**:604–617. DOI: <https://doi.org/10.1002/hipo.10092>, PMID: 12921350
- Le Merre P**, Esmaeili V, Charrière E, Galan K, Salin PA, Petersen CCH, Crochet S. 2018. Reward-Based learning drives rapid sensory signals in medial prefrontal cortex and dorsal hippocampus necessary for Goal-Directed behavior. *Neuron* **97**:83–91. DOI: <https://doi.org/10.1016/j.neuron.2017.11.031>, PMID: 29249287
- Lee JW**, Kim WR, Sun W, Jung MW. 2012. Disruption of dentate gyrus blocks effect of visual input on spatial firing of CA1 neurons. *Journal of Neuroscience* **32**:12999–13003. DOI: <https://doi.org/10.1523/JNEUROSCI.2608-12.2012>, PMID: 22993417
- Marti G**, Bourboulou R, Epsztein J. 2019. Codesbourbouloumarti2019. [https://github.com/EpszteinLab/codes\\_bourboulou\\_marti\\_2019](https://github.com/EpszteinLab/codes_bourboulou_marti_2019)
- Maurer AP**, Cowen SL, Burke SN, Barnes CA, McNaughton BL. 2006. Organization of hippocampal cell assemblies based on theta phase precession. *Hippocampus* **16**:785–794. DOI: <https://doi.org/10.1002/hipo.20202>, PMID: 16921501
- McNaughton BL**, Battaglia FP, Jensen O, Moser EI, Moser MB. 2006. Path integration and the neural basis of the 'cognitive map'. *Nature Reviews Neuroscience* **7**:663–678. DOI: <https://doi.org/10.1038/nrn1932>, PMID: 16858394
- Middleton SJ**, McHugh TJ. 2016. Silencing CA3 disrupts temporal coding in the CA1 ensemble. *Nature Neuroscience* **19**:945–951. DOI: <https://doi.org/10.1038/nn.4311>, PMID: 27239937
- Mizuseki K**, Sirota A, Pastalkova E, Buzsáki G. 2009. Theta oscillations provide temporal windows for local circuit computation in the entorhinal-hippocampal loop. *Neuron* **64**:267–280. DOI: <https://doi.org/10.1016/j.neuron.2009.08.037>, PMID: 19874793
- Muller RU**, Kubie JL, Ranck JB. 1987. Spatial firing patterns of hippocampal complex-spike cells in a fixed environment. *The Journal of Neuroscience* **7**:1935–1950. DOI: <https://doi.org/10.1523/JNEUROSCI.07-07-01935.1987>, PMID: 3612225
- O'Keefe J**, Burgess N. 1996. Geometric determinants of the place fields of hippocampal neurons. *Nature* **381**:425–428. DOI: <https://doi.org/10.1038/381425a0>, PMID: 8632799
- O'Keefe J**, Conway DH. 1978. Hippocampal place units in the freely moving rat: why they fire where they fire. *Experimental Brain Research* **31**:573–590. DOI: <https://doi.org/10.1007/BF00239813>, PMID: 658182
- O'Keefe J**, Recce ML. 1993. Phase relationship between hippocampal place units and the EEG theta rhythm. *Hippocampus* **3**:317–330. DOI: <https://doi.org/10.1002/hipo.450030307>, PMID: 8353611
- O'Keefe J**, Nadel L. 1978. *The Hippocampus as a Cognitive Map*. Oxford Press.
- Poucet B**, Chaillan F, Truchet B, Save E, Sargolini F, Hok V. 2015. Is there a pilot in the brain? Contribution of the self-positioning system to spatial navigation. *Frontiers in Behavioral Neuroscience* **9**:292. DOI: <https://doi.org/10.3389/fnbeh.2015.00292>, PMID: 26578920
- Ravassard P**, Kees A, Willers B, Ho D, Aharoni DA, Cushman J, Aghajanian ZM, Mehta MR. 2013. Multisensory control of hippocampal spatiotemporal selectivity. *Science* **340**:1342–1346. DOI: <https://doi.org/10.1126/science.1232655>, PMID: 23641063
- Renaudineau S**, Poucet B, Save E. 2007. Flexible use of proximal objects and distal cues by hippocampal place cells. *Hippocampus* **17**:381–395. DOI: <https://doi.org/10.1002/hipo.20277>, PMID: 17372978
- Rich PD**, Liaw HP, Lee AK. 2014. Place cells. Large environments reveal the statistical structure governing hippocampal representations. *Science* **345**:814–817. DOI: <https://doi.org/10.1126/science.1255635>, PMID: 25124440

- Robbe D**, Buzsáki G. 2009. Alteration of theta timescale dynamics of hippocampal place cells by a cannabinoid is associated with memory impairment. *Journal of Neuroscience* **29**:12597–12605. DOI: <https://doi.org/10.1523/JNEUROSCI.2407-09.2009>, PMID: 19812334
- Rossant C**, Kadir SN, Goodman DFM, Schulman J, Hunter MLD, Saleem AB, Grosmark A, Belluscio M, Denfield GH, Ecker AS, Tolias AS, Solomon S, Buzsaki G, Carandini M, Harris KD. 2016. Spike sorting for large, dense electrode arrays. *Nature Neuroscience* **19**:634–641. DOI: <https://doi.org/10.1038/nn.4268>, PMID: 26974951
- Royer S**, Zemelman BV, Losonczy A, Kim J, Chance F, Magee JC, Buzsaki G. 2012. Control of timing, rate and bursts of hippocampal place cells by dendritic and somatic inhibition. *Nature Neuroscience* **15**:769–775. DOI: <https://doi.org/10.1038/nn.3077>, PMID: 22446878
- Sato M**, Mizuta K, Islam T, Kawano M, Takekawa T, Gomez-Dominguez D, Kim K, Yamakawa H, Ohkura M, Fukai T, Nakai J, Hayashi Y. 2018. Dynamic embedding of salience coding in hippocampal spatial maps. *bioRxiv*. DOI: <https://doi.org/10.1101/266767>
- Schlesiger MI**, Cannova CC, Boubil BL, Hales JB, Mankin EA, Brandon MP, Leutgeb JK, Leibold C, Leutgeb S. 2015. The medial entorhinal cortex is necessary for temporal organization of hippocampal neuronal activity. *Nature Neuroscience* **18**:1123–1132. DOI: <https://doi.org/10.1038/nn.4056>, PMID: 26120964
- Schmidt R**, Diba K, Leibold C, Schmitz D, Buzsaki G, Kempter R. 2009. Single-trial phase precession in the hippocampus. *Journal of Neuroscience* **29**:13232–13241. DOI: <https://doi.org/10.1523/JNEUROSCI.2270-09.2009>, PMID: 19846711
- Sheynikhovich D**, Chavarriaga R, Strösslin T, Arleo A, Gerstner W. 2009. Is there a geometric module for spatial orientation? Insights from a rodent navigation model. *Psychological Review* **116**:540–566. DOI: <https://doi.org/10.1037/a0016170>, PMID: 19618986
- Skaggs WE**, McNaughton BL, Gothard KM. 1993. An information-theoretic approach to deciphering the hippocampal code. In: Hanson S. J., Cowan J. D., Giles C. L. (Eds). *Advances in Neural Information Processing Systems*. 5. Morgan-Kaufmann. p. 1030–1037.
- Skaggs WE**, McNaughton BL, Wilson MA, Barnes CA. 1996. Theta phase precession in hippocampal neuronal populations and the compression of temporal sequences. *Hippocampus* **6**:149–172. DOI: [https://doi.org/10.1002/\(SICI\)1098-1063\(1996\)6:2<149::AID-HIPO6>3.0.CO;2-K](https://doi.org/10.1002/(SICI)1098-1063(1996)6:2<149::AID-HIPO6>3.0.CO;2-K), PMID: 8797016
- Skaggs WE**, McNaughton BL. 1992. Computational approaches to hippocampal function. *Current Opinion in Neurobiology* **2**:209–211. DOI: [https://doi.org/10.1016/0959-4388\(92\)90014-C](https://doi.org/10.1016/0959-4388(92)90014-C), PMID: 1638156
- Souza BC**, Pavão R, Belchior H, Tort ABL. 2018. On Information Metrics for Spatial Coding. *Neuroscience* **375**: 62–73. DOI: <https://doi.org/10.1016/j.neuroscience.2018.01.066>, PMID: 29432886
- Spiers HJ**, Hayman RM, Jovalekic A, Marozzi E, Jeffery KJ. 2015. Place field repetition and purely local remapping in a multicompartment environment. *Cerebral Cortex* **25**:10–25. DOI: <https://doi.org/10.1093/cercor/bht198>, PMID: 23945240
- Strösslin T**, Sheynikhovich D, Chavarriaga R, Gerstner W. 2005. Robust self-localisation and navigation based on hippocampal place cells. *Neural Networks* **18**:1125–1140. DOI: <https://doi.org/10.1016/j.neunet.2005.08.012>, PMID: 16263241
- Taylor KD**. 1978. Range of movement and activity of common rats (*Rattus norvegicus*) on agricultural land. *The Journal of Applied Ecology* **15**:663–677. DOI: <https://doi.org/10.2307/2402767>
- Terrazas A**, Krause M, Lipa P, Gothard KM, Barnes CA, McNaughton BL. 2005. Self-motion and the hippocampal spatial metric. *Journal of Neuroscience* **25**:8085–8096. DOI: <https://doi.org/10.1523/JNEUROSCI.0693-05.2005>, PMID: 16135766
- Thurley K**, Ayaz A. 2017. Virtual reality systems for rodents. *Current Zoology* **63**:109–119. DOI: <https://doi.org/10.1093/cz/zow070>, PMID: 29491968
- Tolman EC**. 1948. Cognitive maps in rats and men. *Psychological Review* **55**:189–208. DOI: <https://doi.org/10.1037/h0061626>, PMID: 18870876
- van der Meer MA**, Johnson A, Schmitzer-Torbert NC, Redish AD. 2010. Triple dissociation of information processing in dorsal striatum, ventral striatum, and hippocampus on a learned spatial decision task. *Neuron* **67**: 25–32. DOI: <https://doi.org/10.1016/j.neuron.2010.06.023>, PMID: 20624589
- Wiener SI**, Paul CA, Eichenbaum H. 1989. Spatial and behavioral correlates of hippocampal neuronal activity. *The Journal of Neuroscience* **9**:2737–2763. DOI: <https://doi.org/10.1523/JNEUROSCI.09-08-02737.1989>
- Wilson MA**, McNaughton BL. 1993. Dynamics of the hippocampal ensemble code for space. *Science* **261**:1055–1058. DOI: <https://doi.org/10.1126/science.8351520>, PMID: 8351520
- Youngstrom IA**, Strowbridge BW, . 2012. Visual landmarks facilitate rodent spatial navigation in virtual reality environments. *Learning & Memory* **19**:84–90. DOI: <https://doi.org/10.1101/lm.023523.111>, PMID: 22345484
- Zhang K**, Ginzburg I, McNaughton BL, Sejnowski TJ. 1998. Interpreting neuronal population activity by reconstruction: unified framework with application to hippocampal place cells. *Journal of Neurophysiology* **79**: 1017–1044. DOI: <https://doi.org/10.1152/jn.1998.79.2.1017>, PMID: 9463459



---

## Figures and figure supplements

Dynamic control of hippocampal spatial coding resolution by local visual cues

**Romain Bourboulou et al**

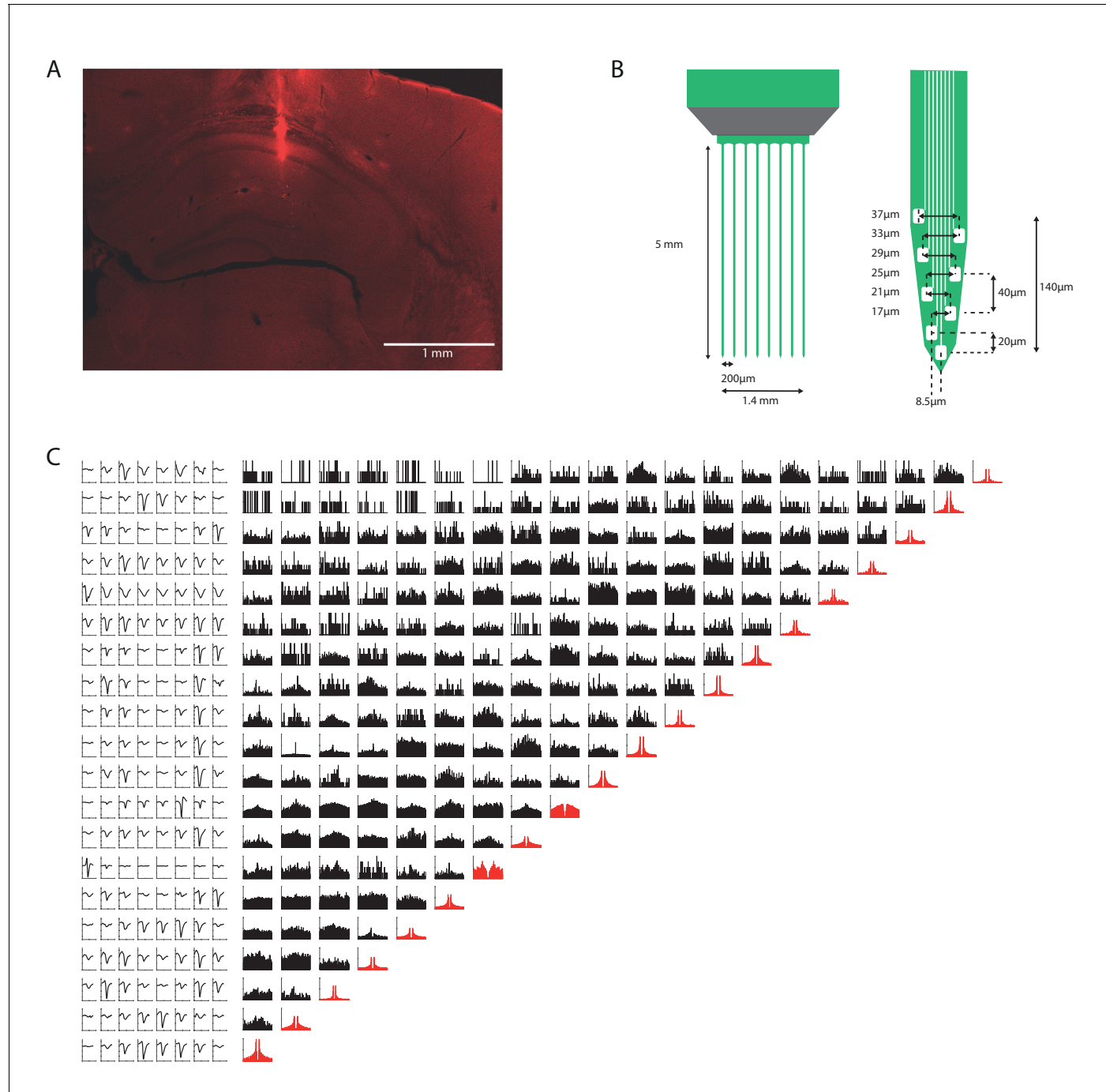


**Figure 1—figure supplement 1.** Histology and spike sorting. (A) Representative histology slide showing a silicon probe track ending in CA1 pyramidal layer. Scale bar: 1 mm. (B) Probe details: Shank and recording channels spacing (C) (Right) Auto-correlograms (red) and cross-correlograms (black) of 20 CA1 units recorded simultaneously. (Left) Average units waveforms (for visualization each row is normalized by the unit maximum average waveform).

DOI: <https://doi.org/10.7554/eLife.44487.003>

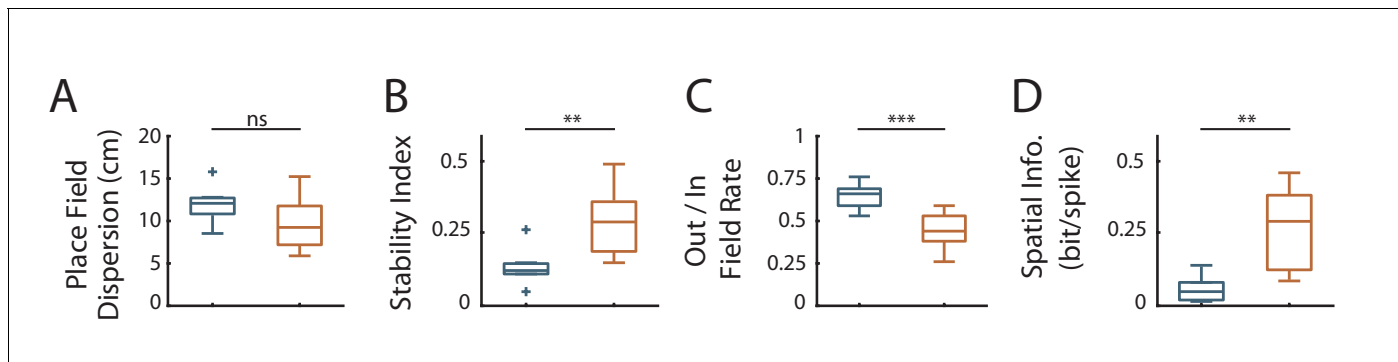


**Figure 1—figure supplement 2.** Effects of local visual cues on spatial coding resolution across different recording sessions. (A–D) Box plots of the place field dispersion (A; ØT:  $12.1 \pm 0.65$  cm, n = 8 recording sessions; OT:  $9.69 \pm 1.13$  cm, n = 8 recording sessions; t<sub>14</sub> = 1.86, p=0.08, two-tailed unpaired t-test), the stability index (B; ØT:  $0.14 \pm 0.02$ , n = 8 recording sessions; OT:  $0.29 \pm 0.04$ , n = 8 recording sessions; t<sub>14</sub> = -3.39, p=0.0044, two-tailed unpaired t-test), the out/in field firing rate (C; ØT:  $0.65 \pm 0.03$ , n = 8 recording sessions; OT:  $0.45 \pm 0.04$ , n = 8 recording sessions; t<sub>14</sub> = 4.40, p=0.0006, two-tailed unpaired t-test) and the spatial information (D; ØT:  $0.06 \pm 0.02$ , n = 8 recording sessions; OT:  $0.27 \pm 0.05$ , n = 8 recording sessions; Z = -2.88, p=0.0038, two-tailed unpaired t-test) without (blue) or with (orange) objects between different recording sessions.

DOI: <https://doi.org/10.7554/eLife.44487.004>

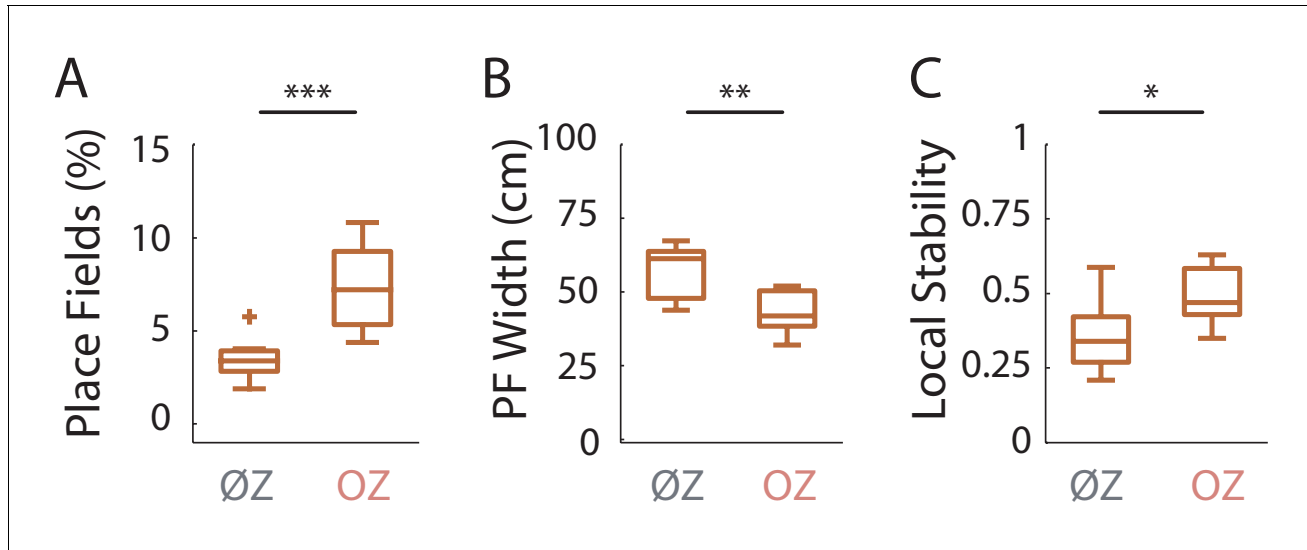


**Figure 2—figure supplement 1.** Virtual 3D objects improve spatial coding resolution locally across different recording sessions. (A–C) Box plots of the mean percentage of place fields per spatial bin (A; ØZ:  $3.49 \pm 0.40\% / 10 \text{ cm}$ , n = 8 recording sessions; OZ:  $7.36 \pm 0.82\% / 10 \text{ cm}$ , n = 8 recording sessions; t<sub>14</sub> = -4.24, p=0.0008, two-tailed unpaired t-test), the place field width (B; ØZ:  $57.1 \pm 3.19 \text{ cm}$ , n = 8 recording sessions; OZ:  $43.2 \pm 2.49 \text{ cm}$ , n = 8 recording sessions; t<sub>14</sub> = 3.46, p=0.0038, two-tailed unpaired t-test) and the local stability index (C; ØZ:  $0.36 \pm 0.04$ , n = 8 recording sessions; OZ:  $0.50 \pm 0.03$ , n = 8 recording sessions; t<sub>14</sub> = -2.53, p=0.02, two-tailed unpaired t-test) in ØZ and OZ in the maze with objects between different recording sessions.

DOI: <https://doi.org/10.7554/eLife.44487.007>

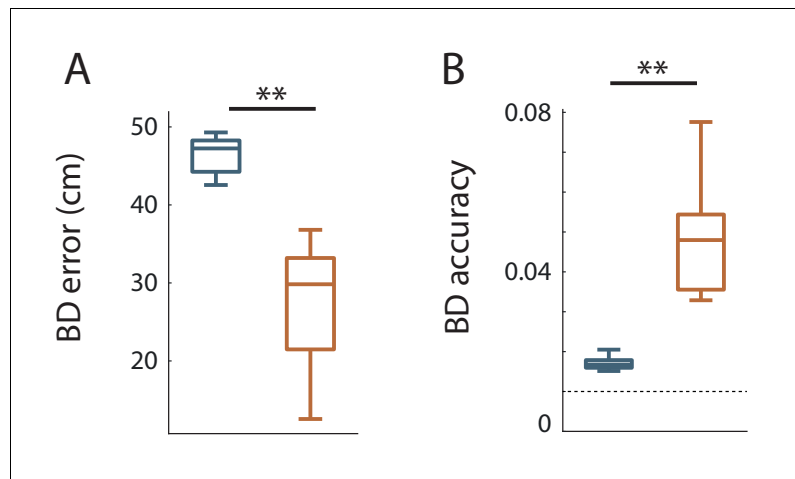


**Figure 3—figure supplement 1.** Virtual 3D objects improve hippocampal population coding accuracy across different recording sessions Box plots of the Bayesian decoding error. (A; BD error;  $\bar{O}T: 46.3 \pm 1.20$  cm, n = 5 recording sessions; OT:  $27.6 \pm 3.26$  cm, n = 7 recording sessions; Z = 2.76, p=0.0058) and Bayesian decoding accuracy (B; BD accuracy;  $\bar{O}T: 0.017 \pm 9 \times 10^{-4}$ , n = 5 recording sessions; OT:  $0.048 \pm 0.005$ , n = 7 recording sessions; Z = 2.76, p=0.0058) in the maze without (blue) and with (orange) objects.

DOI: <https://doi.org/10.7554/eLife.44487.010>

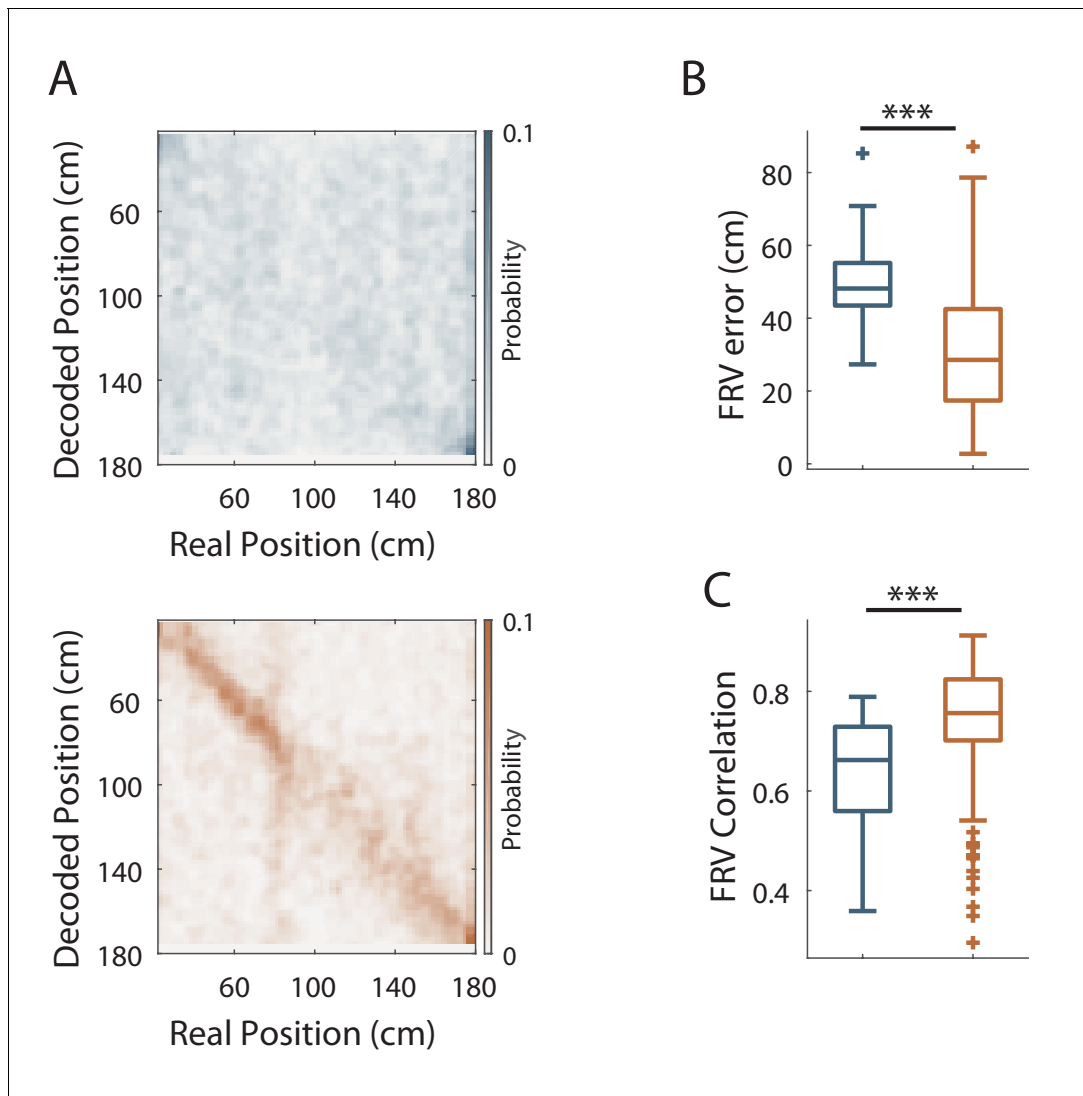


**Figure 3—figure supplement 2.** Firing Rate vector decoding in familiar conditions. (A) Confusion matrix between the real (x-axis) and the decoded position (y-axis) for all recording sessions performed on the track without objects (top, blue) or with objects (bottom, orange). (B) Box plots depicting the Firing Rate Vector decoding error (FRV error) in the maze with (orange) and without (blue) objects. (C) Box plots depicting the Firing Rate Vector decoding accuracy (FRV correlation) in the maze with and without objects.

DOI: <https://doi.org/10.7554/eLife.44487.011>

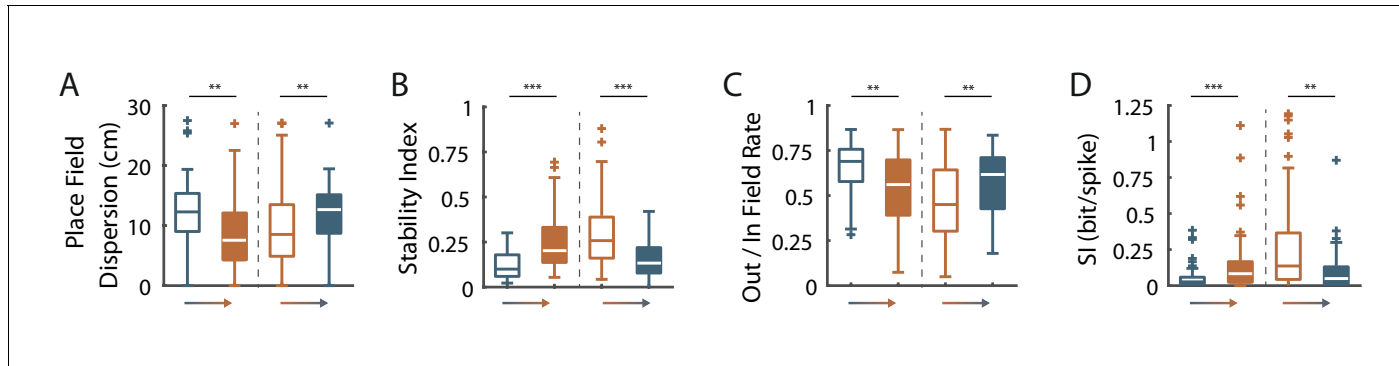


**Figure 4—figure supplement 1.** Spatial coding resolution adaptation upon objects manipulations is already visible during the first session in the new condition Box plots comparing familiar (empty boxes, all recording sessions) and new (filled boxes, first recording session) conditions upon objects manipulation. Two pairs of box plots are illustrated; Left: comparison between the familiar condition without objects (blue,  $\emptyset T_{\text{fam}}$ ) and the new condition with objects (orange,  $OT_{\text{new}}$ ). Right: comparison between the familiar maze with objects (orange,  $OT_{\text{fam}}$ ) and the new maze without objects (blue,  $\emptyset T_{\text{new}}$ ). A gradient color arrow shows the direction of the transition. Plots show the place field spatial dispersion (A;  $\emptyset T_{\text{fam}}$  vs  $OT_{\text{new}}$ ;  $Z = 2.85$ ,  $p=0.0043$ , two-tailed WRS test;  $OT_{\text{fam}}$  vs  $\emptyset T_{\text{new}}$ ;  $Z = -2.62$ ,  $p=0.008$ , two-tailed WRS test), the stability index (B;  $\emptyset T_{\text{fam}}$  vs  $OT_{\text{new}}$ ;  $Z = -4.91$ ,  $p<10^{-6}$ , two-tailed WRS test;  $OT_{\text{fam}}$  vs  $\emptyset T_{\text{new}}$ ;  $Z = 4.41$ ,  $p<10^{-4}$ , two-tailed WRS test), the out/in field firing (C;  $\emptyset T_{\text{fam}}$  vs  $OT_{\text{new}}$ ;  $Z = 3.34$ ,  $p=0.001$ , two-tailed WRS test;  $OT_{\text{fam}}$  vs  $\emptyset T_{\text{new}}$ ;  $Z = -2.71$ ,  $p=0.006$ , two-tailed WRS test) and the spatial information (SI; D;  $\emptyset T_{\text{fam}}$  vs  $OT_{\text{new}}$ ;  $Z = -3.94$ ,  $p<10^{-4}$ , two-tailed WRS test;  $OT_{\text{fam}}$  vs  $\emptyset T_{\text{new}}$ ;  $Z = 2.74$ ,  $p=0.006$ , two-tailed WRS test).

DOI: <https://doi.org/10.7554/eLife.44487.014>

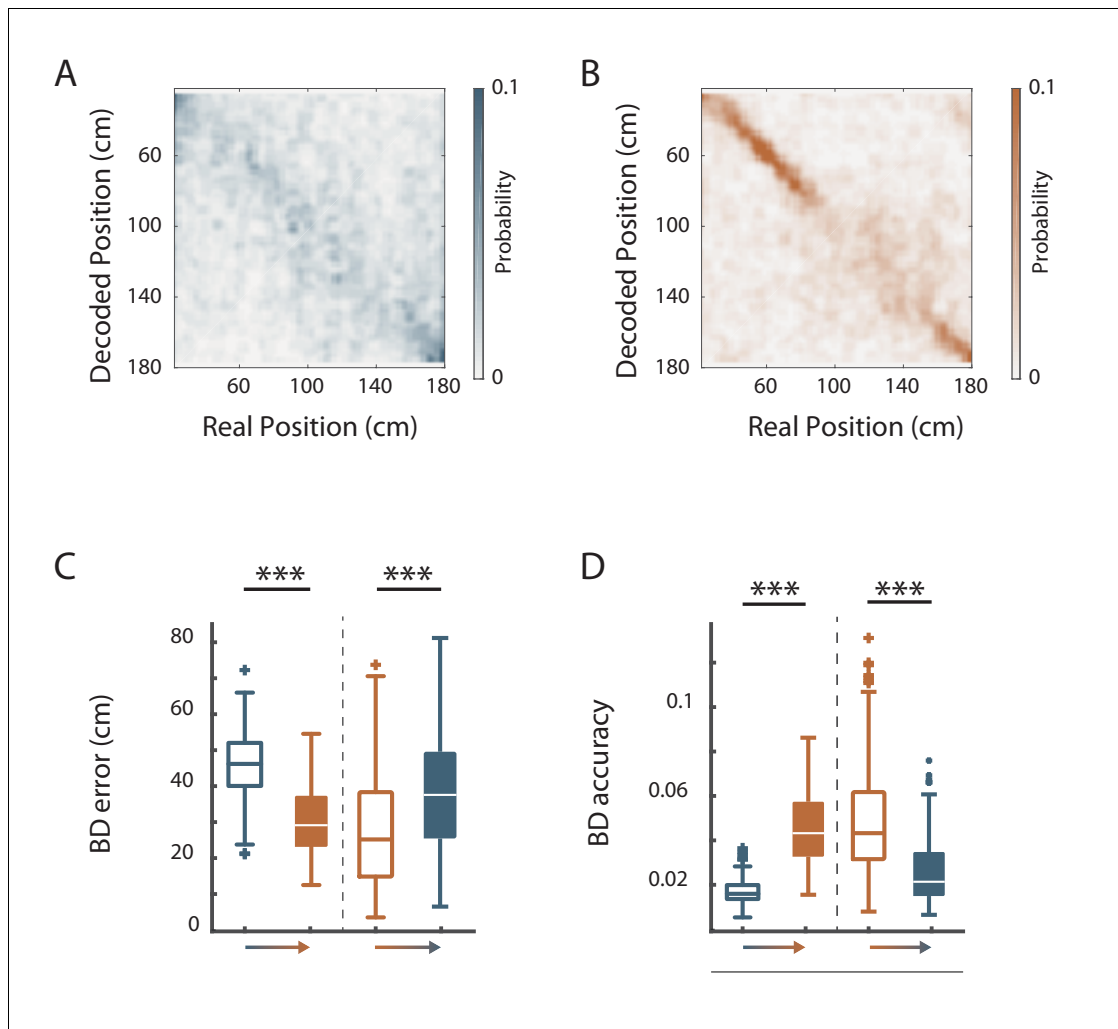


**Figure 4—figure supplement 2.** Virtual 3D objects modulation of hippocampal population coding accuracy upon objects manipulation. (A–B) Confusion matrix between the real (x-axis) and the decoded position (y-axis) for all new recording sessions performed on the track without objects (A, blue) or with objects (B, orange). (C–D) Box plots comparing Bayesian decoding in familiar (empty boxes) and new (filled boxes) conditions upon objects manipulation. Two pairs of box plots are illustrated; Left: comparison between the familiar condition without objects (blue,  $\emptyset T_{fam}$ ) and the new condition with objects (orange,  $OT_{new}$ ). Right: comparison between the familiar maze with objects (orange,  $OT_{fam}$ ) and the new maze without objects (blue,  $\emptyset T_{new}$ ). A gradient color arrow shows the direction of the transition. Plots show the Bayesian decoding error (C;  $\emptyset T_{fam}: 46.3 \pm 0.70$  cm,  $n = 180$  trials vs  $OT_{new}: 30.7 \pm 1.09$  cm,  $n = 86$  trials;  $t_{264} = 12.4$ ,  $p < 10^{-27}$ ; two-tailed unpaired t-test;  $OT_{fam}: 27.1 \pm 0.94$  cm,  $n = 249$  trials vs  $\emptyset T_{new}: 37.6 \pm 1.18$  cm,  $n = 175$  trials;  $Z = -6.58$ ,  $p < 10^{-35}$ , two-tailed WRS test) and the Bayesian decoding accuracy (D;  $\emptyset T_{fam}: 0.017 \pm 3.8 \times 10^{-4}$ ,  $n = 180$  trials vs  $OT_{new}: 0.046 \pm 1.8 \times 10^{-3}$ ,  $n = 86$  trials;  $Z = -12.6$ ,  $p < 10^{-35}$ , two-tailed WRS test;  $OT_{fam}: 0.05 \pm 1.5 \times 10^{-3}$ ,  $n = 249$  trials vs  $\emptyset T_{new}: 0.026 \pm 1.1 \times 10^{-3}$ ,  $n = 175$  trials;  $Z = 10.6$ ,  $p < 10^{-25}$ , two-tailed WRS test).

DOI: <https://doi.org/10.7554/eLife.44487.015>

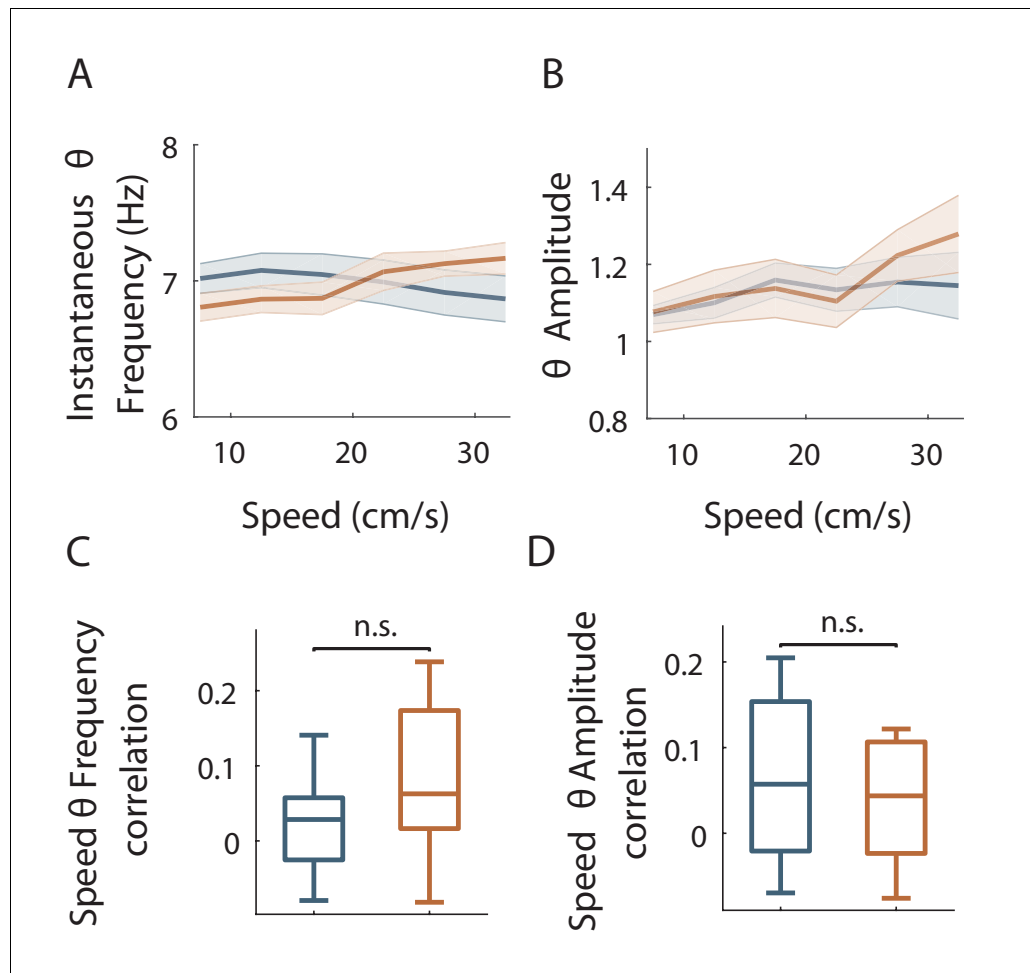


**Figure 7—figure supplement 1.** Speed modulation of LFP theta frequency and amplitude in OT and ØT. (A–B) Mean theta frequency (A) or amplitude (B) across all recording sessions as a function of animal speed (bin: 5 cm/s). (C–D) Box plots of the correlation between theta frequency (C) or amplitude (D) vs speed for individual sessions.

DOI: <https://doi.org/10.7554/eLife.44487.022>

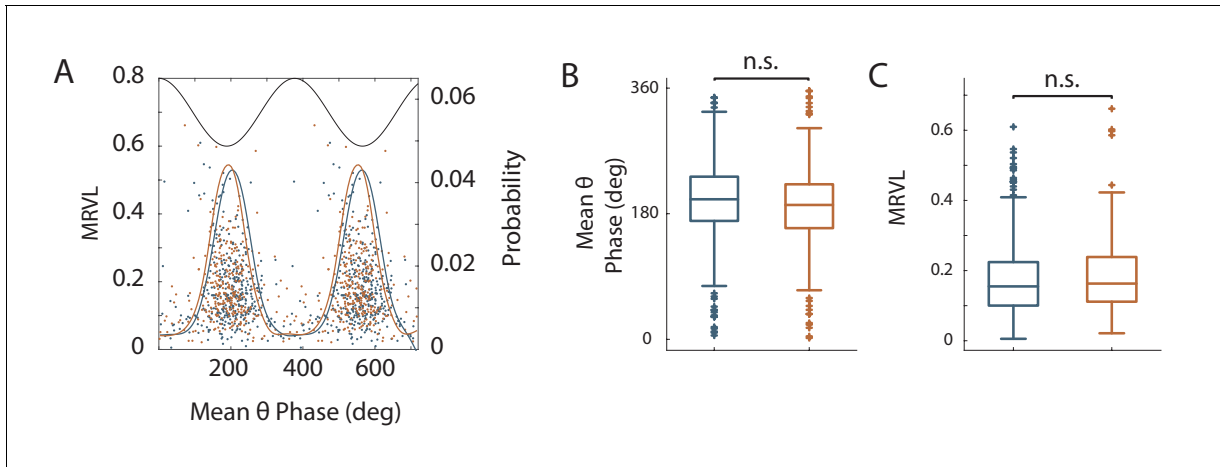


**Figure 7—figure supplement 2.** Theta modulation of spikes in OT and  $\emptyset$ T. (A) Mean theta phase plotted against strength of phase locking (Mean Resultant Vector Length: MRLV) for all theta modulated cells ( $p < 0.05$ , Rayleigh Test) in OT (orange) and  $\emptyset$ T (blue). Solid lines: probability distribution of the preferred theta phase for the two conditions. Black line: illustrative theta cycle (B) Box plots of the mean theta phase for OT(orange) and  $\emptyset$ T (blue) conditions (C) Box plots of the Mean Resultant Vector Length in OT(orange) and  $\emptyset$ T (blue) conditions.

DOI: <https://doi.org/10.7554/eLife.44487.023>

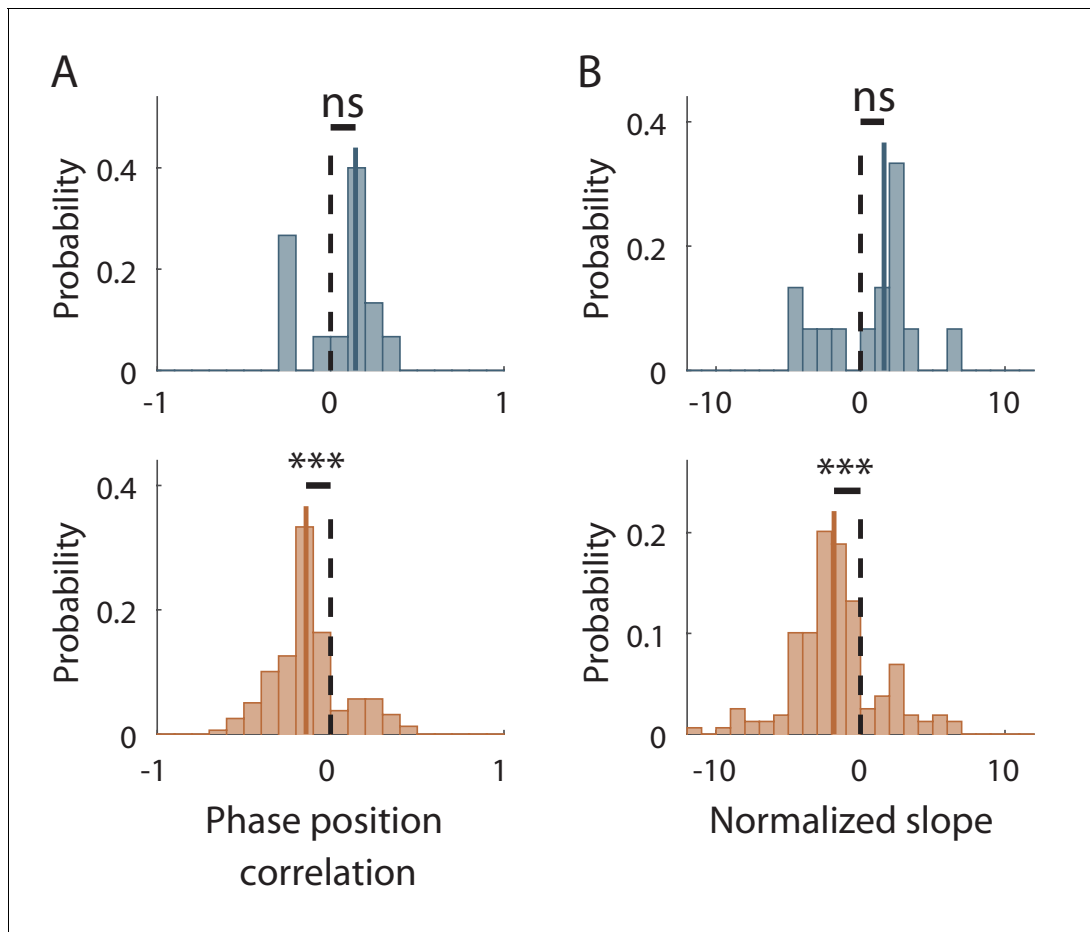


**Figure 7—figure supplement 3.** Effect of objects on theta phase precession estimated with a waveform-based approach Distribution of significant phase position correlation (left) and slopes (right) in the condition without objects (top, blue) and with (bottom, orange) when theta phase was detected using a waveform-based approach which takes into account theta waves asymmetry. The median of the distribution is indicated by a bold line and 0 by a dotted line. (A) The correlation between phase and position was significantly different from zero for place cells recorded in the track with objects ( $r = -0.14 \pm 0.016$ ,  $n = 159$  fields;  $p < 10^{-13}$ , one sample sign-test) but not for those recorded in the track without objects ( $r = 0.14 \pm 0.05$ ,  $n = 15$  fields;  $p = 0.30$ , one sample sign-test). (B) Phase precession slopes (calculated on normalized place field sizes) were negative and significantly different from 0 for cells recorded in the track with objects ( $-1.83 \pm 0.24$  rad/U,  $n = 159$  fields;  $p < 10^{-13}$ , one sample sign-test) but not in the track without objects ( $1.63 \pm 0.84$  rad/U,  $n = 15$  fields;  $p = 0.3$ , one sample sign-test).

DOI: <https://doi.org/10.7554/eLife.44487.024>



**Part III**  
**DISCUSSION**



# 6

## DISCUSSION

---

In this thesis work, we studied the effects of local visual cues on dorsal hippocampal spatial coding and particularly on its accuracy to represent space. In order to do so, we recorded the extracellular activity of dorsal CA1 place cells in mice shuttling back and forth in a virtual linear track. Virtual reality allowed us to finely control the sensory cues provided to the animal. We used several types of visual information such as 3D visual objects or 2D patterns on the walls to evaluate their relative impact on spatial coding resolution.

We observed that virtual objects improved the resolution of spatial coding globally and in their vicinity. The results obtained at the individual cells level were confirmed by a population decoding approach. These changes in rate coding quality were also observed for temporal coding. Local visual objects improved theta phase precession. An online modification of the objects availability during the recording session showed a quasi-instantaneous modification in spatial coding resolution following the manipulation. Finally, patterns on the walls led to an enhancement of spatial coding resolution, but in a lesser extent than for the object condition.

### 6.1 COMPARISON WITH PREVIOUS STUDIES USING PHYSICAL OBJECTS

Several models of place cells formation postulate that they can be activated thanks to external sensory cues [Hartley et al. 2000; Strosslin et al. 2005; Barry et al. 2006; Sheynikhovich et al. 2009; Laptev and Burgess 2019]. A rich environment, populated with various sensory stimuli, could thus lead to a higher place cells' recruitment and finer spatial coding than in an empty one. Battaglia et al. [2004] addressed this question with an experimental paradigm similar to ours. In this study, the authors recorded the activity of place cells in rats foraging in linear tracks with different enrichments in visuo-spatial cues. They used a cue-rich, a cue-poor and a track divided in a rich and poor area (combined cue-rich/cue-poor) (see § 4.2.3). Contrarily to our results, they did not observe any change in the proportion of detected place cells between the cue-rich and cue-poor tracks. This absence of changes in RW compared to VR could be due to a higher basal activation of the hippocampal spatial resources by uncontrolled local cues in their experiment (*e.g.*: olfactory cues). Coherently to their initial hypothesis, the authors observed a smaller scale of the spatial representation at the population level in presence of intra maze cues in the cue-

rich condition compared to a cue-poor condition. Curiously, no such change was observed in the combined condition between the cue-rich and the cue-poor regions of the same linear track. The visuo-spatial cues provided in the rich part of their track were small and potentially less salient. Thus, this could explain an absence of local effect of the enrichment by an overshadowing of this cues by other local ones.

Similarly, Burke et al. [2011] investigated the contribution of objects on place cells coding of rats circumnavigating in a circular linear track with several intra-maze objects (see § 4.2.3). In this experiment, they observed an augmentation of the number of place fields, but also a reduction of their size. This led to a homogenous probability for a given location in the maze to be represented by a place field. Burke et al. [2011] observed a stronger recruitment of hippocampal place cells but did not investigate local changes in place cells resolution as in our case. This could be explained by the fact that the objects were too close and numerous in Burke et al. [2011] to allow such quantification. These factors potentially led to a merger of the local effect on spatial coding of a single object with its neighbor. Also, as in Battaglia et al. [2004], potential uncontrolled local cues could have maintained a similar level of sensory drive along the maze. That is also why, in our case, VR was a useful tool to reach a better control of the visual information and an elimination of uncontrolled local cues.

Furthermore, Burke et al. [2011] performed their recordings in the distal part of the intermediate hippocampus. A lack of local modulation of spatial resolution could be explained by the fact that they mostly focused on the size of the place fields. Given that space is represented at a larger scale in the distal part of intermediate CA1, it could hide a modest or small variation of place fields' size. Also, a larger contribution of non-spatial information, due to stronger inputs from the LEC could influence the spatial code in this part of the hippocampus. In our study, we did not focus our analyses on a specific anatomical part of dorsal CA1. The randomization of the acute implantation sites added to the width of our multi-shanks silicon probes were not suited for such analysis. However, it allowed us to study the dorsal hippocampus as a whole.

## 6.2 COULD THE LOCAL CHANGE IN RESOLUTION BE DUE TO OBJECT-RESPONSIVE CELLS?

Previous studies already highlighted that proximal objects controlled place cells orientation, but did not evidence any clustering of place cells around proximal objects [Cressant et al. 1997, 1999; Lenck-Santini et al. 2005; Renaudineau et al. 2007; Lefort et al. 2019]. However, some other studies reported a population of spatially modulated cells in dorsal hippocampus, object-responsive cells, active at the location or near several objects [Gothard et al. 1996b; Deshmukh and

Knierim 2013; Geiller et al. 2017a]. Consequently, we wondered if, in our experiment, the accumulation of place fields in the vicinity of the objects could be caused by the firing of object-responsive cells. The identification of this type of cells implies the presence of one or multiple firing fields at the location or with a fixed distance to at least two objects. Otherwise, their activity can not be distinguished from "classical" place cells. In our case, we used the fact that mice were performing forward and backward journeys to identify them (see discussion and methods of the Results section § ii ). We were able to identify a very low proportion of putative object-responsive cells. The drastic increase of the number of place fields and over-representation in our study are not compatible with the proportion of object-responsive cells reported in Deshmukh and Knierim [2013] and Geiller et al. [2017a]. Furthermore, in one of the condition with object (rich with object), we observed no over-representation of the object-zones but local quantitative improvement of spatial coding instead. Consequently, we can not attribute our results to the activation of object-responsive cells only.

### 6.3 COMPARISON WITH PREVIOUS REPORTS OF HETEROGENOUS CODING IN PLACE CELLS

Wiener et al. [1989] and Hetherington and Shapiro [1997] reported that place cells were more frequently coding for location close to borders or to orienting cue cards on the walls. In Wiener et al. [1989], the authors used a random Monte Carlo analysis, in order to uncover a more important representation of a location than expected by chance: over-representation. This random distribution of the ensemble of place fields they detected allowed to estimate a chance level of the incidence of place fields for each location in the arena. By comparing the distribution of the place fields they detected with these surrogate data, the authors observed that in their task, place fields were more likely to be near the walls than in the center of the arena. Nevertheless, this over-representation could potentially be due to particularities of their behavioral paradigm. First, by looking at the distribution of the place fields in a goal directed task, they found an over-representation located close to goal positions. Second, they also observed a trend for animals to spend more time close to the borders. Thus we cannot totally rule out a behavioral bias leading to this over-representation. With a similar approach, Hetherington and Shapiro [1997] described an over-representation in the vicinity of the walls that carried a salient cue card in a random foraging task. These studies only focused on a quantitative aspect of place cells coding. However in a later study, Olypher et al. [2003] investigated a qualitative aspect of place cells coding and showed an augmentation of local spatial information in the vicinity of cue card on the wall of the recording arena.

Our results complement these previous studies about heterogenous coding of space in the hippocampus by analyzing quantitative and qualitative aspects of place cells coding at the same time. Also, we confirmed the results observed using individual cells data pooled across all recording sessions with analyses performed for populations of simultaneously recorded neurons. Interestingly, in experiments of Hetherington and Shapiro [1997] the authors recorded 3 and 45 cells respectively in CA1 and CA3 subfields of the hippocampus. Thus the firing change of place cells observed is very likely to take place in CA3. Because space coding differs in CA3 and CA1 [Leutgeb and Leutgeb 2007; Mizuseki et al. 2012; Lu et al. 2015], it would be of great interest to compare Hetherington and Shapiro [1997] results with recordings from CA3 in our experimental conditions. During my thesis, I acquired such data. However, *post-hoc* histological inspections of the electrode traces revealed an inconsistent proper marking (with dye) of the electrode's shanks so that it was sometimes impossible to know whether the shanks were in CA3 or DG. Also, the number of sessions and animals recorded in CA3-DG is not sufficient for the moment to answer this question.

In our study, in the poor track without object, we observed an over-representation of the beginning and end of the track. These over-representations were unlikely to be directly related to the delivery or the location of the reward as we did not considered 20 cm of the maze at each ends in our analyses. It could however be caused by a higher availability of visual cues due to the proximity with the walls at the ends of the corridor. Indeed, similar over-representation have already been observed at the location of a door [Spiers et al. 2015] or under an arch [Sato et al. 2018]. Albeit their high proportion, the overall quality of this end-track fields was lower than for on-track fields. This suggests that different types of over-representation could exist and subserve different functions (salient landmark, geometrical landmark, goal). This hypothesis is supported by the variety of dynamics observed for the formation and disappearance of goal over-representation (see 4.3.1). Nevertheless, over-representation and local variation of place field resolution got until now very little attention. As I will detail later (§ 6.7), the impact of these local variations of place cells number and their spatial coding resolution on areas downstream of the hippocampus and finally on animal behavior is not trivial and will need further investigations.

#### 6.4 TOWARD A BETTER UNDERSTANDING OF PLACE CELLS CODING IN VIRTUAL REALITY

After the demonstration by Holscher et al. [2005] that rodents could navigate in a virtual reality environment, neuronal recordings using such apparatus became increasingly popular. The success of this tech-

nique mostly resides in the fact the it allows a tight control of sensory information provided to the animal in 1D [Harvey et al. 2009; Chen et al. 2013; Domnisoru et al. 2013; Ravassard et al. 2013; Campbell et al. 2018; Casali et al. 2019] or 2D environments [Aronov and Tank 2014; Aghajan et al. 2015; Chen et al. 2018; Haas et al. 2018; Chen et al. 2019]. Also, it provides realistic environmental stimuli and contexts for techniques needing head fixation of the animal like *in-vivo* patch clamp or imaging [Harvey et al. 2009; Dombeck et al. 2010; Schmidt-Hieber and Häusser 2013; Villette et al. 2015](see Appendix iv).

Some of the first extracellular recordings of hippocampus in VR led to diverging hypothesis about place cells coding in these apparatus. Rats recorded by Aronov and Tank [2014] exhibited place, grid, head-direction and border cells coding similar in VR and in real environments. Conversely, Aghajan et al. [2015] described a lack of spatial selectivity for hippocampal place cells in their recording condition. These divergences could be explained first by critical differences in the method used to fix the animal's body in VR. In both apparatus rats were body harnessed, but only the fixation system in Aronov and Tank [2014] allowed physical rotation of the animal leading to a corresponding rotation in VR (see § 4.2.3). Thus, in Aghajan et al. [2015], the absence of vestibular inputs could have perturbed the orientation of the hippocampal maps and caused a lack of spatial selectivity. A second potential cause of discrepancies between these two studies relies within the constellation of visual cues used in VR. Indeed, the VR environment in Aronov and Tank [2014] contained multiple local visual cues, hanging from the roof and on the walls of the environment, while the VR environment of Aghajan et al. [2015] only contained distal visual cues. Thus, one possibility is that that local proximal cues might have contributed to the stable hippocampal spatial coding.

This thesis work supports the later explanation for an increase in the cellular recruitment and the spatial selectivity in VR. In our case, the use of patterns on the walls were not enough to reach the level of spatial coding improvements initiated by the introduction of local visual objects in VR. These results are compatible with observation of Radvansky and Dombeck [2018]. In this study, the authors trained mice to shuttle back and forth in an "olfactory space" (see § 4.2.3.2). Head-fixed mice were first trained in a virtual linear track in presence of two monotonically increasing odor gradients for the upward and downward directions<sup>1</sup>. After a correct learning of the task, mice were able to perform it in the dark, relying exclusively on the two odors gradients. Interestingly, Radvansky and Dombeck [2018] reported that making the odor gradients uninformative (flat odor concentration

<sup>1</sup> Visual information were first provided to guide the animal's learning of the task, but not once the animal successfully learned to perform the task and to accurately anticipate the rewards in the dark only using the odor gradients.

along the track) led to a drastic drop in the proportion of cells recruited during the task. These results highlight the fact that providing relevant local sensory cues promotes the activation of the hippocampal mapping system in VR. However we cannot exclude an important role of vestibular inputs for the stability of place fields in 2D VR environments. Further experiments in a 2D VR environment enriched in local cues are needed to clarify this point.

Aghajan et al. [2015] further observed that despite the strong instability of hippocampal spatial firing in their 2D virtual environment, hippocampal cells could be activated during short "motifs" of  $\sim 2$  seconds, exhibiting a similar structure between RW and VR (duration, firing rate, phase precession). Their location was diffuse in VR, partially explaining the spatial instability of cells firing. Curiously, the introduction of a triangular array of floating columns indicating the location of rewards inside the arena led to an improvement of place cells coding. In this new task, the animals had to unidirectionally navigate towards one of the pillars to obtain a reward before navigating to the next. In this condition, place cells firing was stabilized at the location and between reward locations. In this case, the improvement in spatial selectivity could either be caused by an anchoring of place fields by the floating column or a modification of the navigation strategy (beaconing, stereotypy,...). Indeed, these factors have been shown to deeply affect hippocampal activity [Markus et al. 1995; Poucet and Hok 2017] [but see Trullier et al. 1999].

Altogether these data encourage the use of more proximal visual cues in VR where most of the other sensory modalities available to the animal are made irrelevant for navigation. The higher availability in local virtual cues could facilitate the comparison of VR data with the one acquired in RW and promote the development of translational research between different species. It would also be interesting to investigate if non-visual discrete cues (odor, sound,...) could have a similar effect on place cells activity.

## 6.5 INFLUENCE OF VISUAL INFORMATION ON PHASE PRECESSION

In the absence of object, the temporal coding of place in our experiment cells was strongly affected and appeared similar to data acquired in rats running in a wheel [Hirase et al. 1999]. To take into account the higher instability of place cells firing we quantified this phenomenon at different scales. First, we focused on session-averaged data while restricting our analysis to spatially stable trials with the mean place field (see Methods ii). Then, we calculated phase precession on a lap-by-lap basis as in Schmidt et al. [2009]. All of these approaches failed to uncover a robust phase precession. In a second step, we adopted methods agnostic to the animal's position [Geisler et al. 2007; Mizuseki

et al. 2009]. These analyses rely on the fact that a phase precessing cell should oscillate faster than the concurrent theta wave. These methods confirmed a very affected phase coding in our poor condition without objects. Surprisingly, in this condition, the visual flow information provided to the animal did not appear to be sufficient to drive a strong enough theta frequency modulation by speed as observed in Ravassard et al. [2013]. Intriguingly, in Ravassard et al. [2013], theta phase precession was preserved. This could be explained by a richer visual environment between the condition they used and our poor condition. Notably, projection of a pattern on the floor, coherent with the rat movement in VR, could have provided additional speed information to the animal [Raudies and Hasselmo 2012; Raudies et al. 2012]. Also, the body fixation of the rat allowed it to move the head. In our case, the head fixation of the mice is likely to affect more deeply the vestibular system of the animal. One other explanation for the weak phase precession in our condition could be species differences with mice relying more on local cues for temporal spatial coding compared to rats [Hok et al. 2016]. Consequently, a loss of vestibular speed signal and a modest visual flow could have a more pronounced effect. The reintroduction of richer visual information provided a suitable substrate for place cells temporal coding in the other conditions of our experiment.

Beyond its spatial correlate, phase precession has been related to a variety of non spatial phenomena like jumping [Lenck-Santini et al. 2008], fixation in a nose poke [Takahashi et al. 2014] running in a wheel [Hirase et al. 1999; Pastalkova et al. 2008] and in relation to odor or sound presentation [Aronov et al. 2017; Terada et al. 2017]. Recently, Robinson et al. [2017] showed that phase precession could also be observed in hippocampal neurons while a rat sampled an object. In our case, the observed increase in phase precession can not be attributed to "object sampling" as phase precessing fields were not only located at the object location but everywhere in the environment. Also, the rich condition without object also led to an improvement in phase coding.

Visual information were not thought to be involved in the generation of phase precession. Indeed, in some of the behavioral correlates of this temporal coding, only static visual information were provided to the animal (wheel running, fixation,...). Our study showed that the type of visual cues provided to the animal can participate in the generation of phase precession. Nevertheless, the mechanism of this effect was not investigated in our experiment. We can however suppose that in our condition, with reduced vestibular inputs, a reliable speed signal can mostly be extracted from visual flow and the presence of virtual objects. In this context, the use of VR could be a useful tool to better understand the mechanism underlying the influence of external cues

on the generation of phase precession [Harvey et al. 2009; Aghajan et al. 2015; Haas et al. 2018].

## 6.6 ARE 3D VIRTUAL OBJECTS REALLY THAT IMPORTANT?

In VR, visually enriched environments have been reported to facilitate the learning of a behavioral task [Youngstrom and Strowbridge 2012]. In our team, we noticed that the animals were sometimes adopting naturalistic behaviors while passing in front of an object. Some mice tried to avoid the objects, by orienting their body position away from it, even if it was impossible to interact with them. Similar interaction with non-physical objects have been observed in augmented reality [Grosso et al. 2017]. In this task, 2D images of an object were projected on the floor of an arena. This projection was modified in real time according to the position and point of view of the animal to give it the impression of a 3D object (see § 5.3.3). Even if this "3D object" was not physical and only experienced through vision, it triggered spontaneous avoidance and novel object recognition behavior [Grosso et al. 2017]. In our experiment, the strong and consistent remapping following the introduction of the objects highly suggests that the animals noticed and perceived them.

It is known that rodents can perceive and distinguish 3D objects, even if they are presented only as 2D images or solely perceptible through vision [Burke et al. 2012; Ahn and Lee 2017; Connor and Knierim 2017; Ahn et al. 2019]. In our data, the improvement of spatial coding was more pronounced in the presence of objects than enriched wall patterns. In addition we did not observe any systematic influence of the wall patterns transitions or distal columns on place cells coding as reported in MEC by Kinkhabwala et al. [2018] and Casali et al. [2019]. This suggests that objects have a singular influence on place cells coding in VR. However, the particular parameters leading to such a strong effect on hippocampal spatial coding is still unresolved. One candidate explanation is that the saliency of objects is used by the animals, either due to the size, color, stability, parallax effect or dimension of the object. All these parameters have been shown to be crucial factors for the use of an object during real world navigation [Biegler and Morris 1996; Jeffery 1998; Zugaro et al. 2001; Caduff and Timpf 2008; Scaplen et al. 2014] (see § 5.3).

In recent experiments, we chose to test if the third dimension of an object could be important to influence the hippocampal coding. 3D objects could recruit perirhinal and lateral entorhinal cortex to a greater extent and support the spatial hippocampal representation with non-spatial information. Consequently, we used 2D compressions of the same 3D objects and positioned them with a parallel orientation in comparison to the track's walls. We preserved a distance to the wall identical to the one used in previous experiments. This experimental

design should allow us to investigate more specifically whether these 2D compressed objects play a similar role than 3D objects. Conversely to 2D objects, the shape of visual 3D objects change to a greater extent as an animal moves next to them and could provide a more accurate estimation of position for this reason. Hitherto, two animals have been recorded in this condition during my thesis. Other recordings will be needed to complement this preliminary data. Also, it would be interesting to examine if visual objects could trigger other primary sensory areas, suggesting that 3D visual objects could be recognized as "multimodal". This would be possible due to a cross-modal transfer of visual information to another modality (*e.g.*: touch) as in cross-modal object recognition [Winters and Reid 2010; Gaynor et al. 2018].

## 6.7 IS MORE REALLY BETTER AND BROADER WORSE?

A widespread thinking about place cells is that, the narrower they are, the better they will represent space. However, numerous works suggest that this postulate is not always true [Pouget et al. 2000; Quiroga and Panzeri 2009]. First we have already highlighted that a unique look at individual tuning of cells is not enough (see § 4.5). Indeed, the width of receptive fields can average out at the population level to lead to an accurate signal from a reader perspective. Additionally, previous studies also showed that a broadening of receptive fields could be advantageous to represent multidimensional or more robust information in some conditions [Pouget et al. 1999; Zhang and Sejnowski 1999; Shamir and Sompolinsky 2006; Kobak et al. 2019]. Also, an important point is notably to determine if larger place fields are stable in space from one trial to the next (as could be the case in the ventral hippocampus) or whether they result from a spatial instability of narrower place fields between trials. In our case we believe that the later explanation is more likely because the size of place fields detected on single trials was identical.

In the seminal study of Georgopoulos et al. [1986], the authors showed that a population of broadly tuned neurons of a monkey's motor cortex could carry a very precise prediction of the arm position. Similarly, in Keinath et al. [2014], decoding the activity of neurons in the ventral hippocampus of rats foraging in an arena led a precise position signal. Place cells in the ventral hippocampus are broadly tuned for space [Young et al. 1994; Kjelstrup et al. 2008; Royer et al. 2010], but the error of the decoder used in this study was comparable to dorsal hippocampus with narrower place fields. In our case, we characterized the place cells tuning by multiple factors (size, stability, signal to noise ratio,...). Population analyses were performed in order to consider a potential improvement of the position coding at the network level in a population of broadly tuned neurons (see § 4.5). With this approach, we confirmed the results we previously observed at the

individual cells level. All our analyses converged to a positive effect of visual cues and notably virtual objects on place cells coding quality. Furthermore, they confirmed the global and local improvements of space coding in the vicinity of the objects.

Heterogeneously distributed and tuned population can be more informative and resilient to noise [Wilke and Eurich 2002; Mlynarski and Hermundstad 2018]. Over-representing a particular location can be metabolically costly, however it could allow to make a behaviorally relevant location more robust and to avoid a costly error during behavior [Mlynarski and Hermundstad 2018]. In real world, a goal location is very important, storing it using very few or unreliable neuronal resources can later be costly if it does not allow to find it later. Similarly, highly informative locations, rich in salient sensory cues, could represent an asset for further use during navigation. Thus, an adaptation of the internal representation of space to the external availability and reliability of cues could strongly optimize behavior while minimizing the metabolical cost of storing this representation [Knill and Pouget 2004; Pfuhl et al. 2011; Jeffery et al. 2016].

In our task, the behavioral load was very low. Consequently, it suggests a latent selection and adaptation of the neuronal representation of space to the external world. It would however be of the upmost importance to link this phenomenon with a behavioral output. Can an animal use this increase in spatial resolution to find more accurately a reward? In this case, a better resolution of the hippocampal map could also be driven by non sensory rich but behaviorally important locations like a reward or nest. In parallel, this local adaptation to external cues could be more advantageous in big environments, where storing a cognitive representation could be much costly.

A previous study reported a better self-consistency of the hippocampal spatial code (better position decoding probability) in a task following an increase in the number of rewards [Wikenheiser and Redish 2011]. However the link between this neuronal coding precision and behavior is non trivial. A recent work highlighted that, in the visual cortex, population decoding of a very large population of neurons ( $\sim 20,000$  neurons) had discrimination thresholds of  $0.3^\circ$  in an orientation decoding task [Stringer et al. 2019a]. This performance was  $\sim 100$  times smaller than values reported in behaving mice. This implies that sensory information are lost during their processing or in biological bottlenecks while they are transferred to downstream areas [Attneave 1954; Barlow 1964]. How sensory information is selected from primary sensory to integrative areas of the brain will need more investigation for a better understanding of the neuronal basis of efficient and flexible behavior.

## 6.8 DIRECTIONALITY OF PLACE CELLS IN VIRTUAL REALITY

In a linear track, place cells can fire in only one direction or both, their firing is directional [McNaughton et al. 1983; Markus et al. 1995; Gothard et al. 1996a]. If a place cells is bidirectional (*e.g.*: fires in the inward and backward direction) in the linear track, a cell can either code for a distance from the starting point or for an allocentric position in the maze. In the previously mentioned study, Battaglia et al. [2004] investigated the influence of proximal sensory cues on this directional firing of place cells. They observed that the introduction of proximal sensory cues increased the proportion of bidirectional cells. In addition, local visuo-spatial cues increased the proportion of cells doing position coding compared to the cue-poor condition. In our task, we observed comparable effects of 3D virtual objects on the directional firing of place cells.

Coherently with previous reports of place cells recordings in virtual linear mazes in Ravassard et al. [2013], most of the bidirectional place cells were doing distance coding. However, the enrichment in visual information led to an increase in position coding of bidirectional cells. This result shows that directional firing of place cells in VR can be improved by visual information, in an head fixed animal. Also, it suggests that directional firing of place cells do not entirely depend on the head direction system relying on vestibular inputs. In our case, the increase in position coding could reflect the fact that the animal constructs a view-invariant allocentric representation of space in the presence of objects. These results are particularly interesting because our experimental apparatus used a wheel to detect the animal movements. It imposed us to "teleport" the animal in the other direction at the end of the maze to allow it to perform back and forth runs (see Method section of ii). Thus, the increase in position coding could imply that the animal understand that it made a 180° rotation at the same location. However, this correlate should be confirmed at the behavioral level. In order to answer this, we could design a task where the animal is trained to find a reward in only one direction. At the end of the maze, the animal could be teleported in the starting position without rotation. Then, during a test phase, we could change the teleportation at the end of the maze by a rotation and observe if the animal deduce the position of the reward in the backward direction. Simultaneous recordings of place cells activity could indicate us if the population of place cells perform more position coding if the reward is found using an allocentric reference frame. An other approach would consist in using the same experimental paradigm but to alternatively teleport the animal in the other direction or to perform a slow rotation of the environment at the track's ends (to improve the likeliness that the animal notices that the direction is changing). The comparison of place cells coding in these

two conditions could inform us if the teleportation is interpreted in a similar way than a passive rotation by the animal.

The results of this section have been partially presented in the form of posters in Bourboulou et al. [2017] and Nordlund et al. [2019]

### 6.9 EFFECT OF ATTENTION ON PLACE CELL CODING

We presented previously that attention during a navigation task could modulate the stability and the quality of place cells coding [Kentros et al. 2004; Muzzio et al. 2009a] (see § 4.3.2). At the sight of our results, we wondered if a similar process of directed attention to the object could be involved in the increased spatial resolution we observed. The head-fixation of our animals and the fact that they are constrained on a "line of exploration" (they can not move along the Y axis) could be a difficult situation to quantify directed attention towards the objects. A previous study by Vinck et al. [2015] showed that the pupil's diameter could be used as a proxy to quantify the level of arousal of a head-fixed animal. Thus, we chose to use the head fixation of the animal to our advantage and to develop a video system allowing us to track the animal behavior during the task. This approach will allow an easier tracking of the eyes and whiskers of the animal than in complex head-mounted systems used in freely moving rodents [Wallace et al. 2013; Meyer et al. 2018]. During the last year of my thesis, I developed a camera system allowing the tracking of the face of the animal during behavior without obstructing the animal's field of view. This system allows the capture of the animal profile at a frequency up to 60Hz with a minimalist interface developed in C++ (Basler C++ library and openCV). The video capture is synchronized with the acquisition of electrophysiological data thanks to a pulse generator (60Hz). Each pulse of this oscillator sends a signal to the electrophysiological acquisition system and trigger the acquisition of a frame. In parallel, I developed a pupil tracking algorithm usable with a user friendly Graphical User Interface (GUI) in Matlab. This system is currently under final testing and will allow a finer quantification of the animal arousal and behavior.

We will not constrain our analysis to the pupil but we will also quantify more complex eyes movements as well as movements of the whisker pad and tongue linked to whisking or licking [Vinck et al. 2015; Mathis et al. 2018; Nath et al. 2019; Stringer et al. 2019b]. Thus, we will soon have better indications of the mice behavior in the vicinity of objects. Do 3D objects trigger a higher arousal state leading to a better signal to noise ratio as in visual cortex? [Vinck et al. 2015] And does the animal try to investigate the virtual objects through whisking? These questions could unfortunately not be answered during the time of my thesis, but will soon be addressed in the team.

## 6.10 PUT LANDMARKS BACK IN THE COGNITIVE MAP

Most of the environment in which we evolve are bounded. Since the seminal discovery that the geometry of an environment could in itself be used during navigation [Cheng 1986; Cheng and Newcombe 2005], several evidence of an effect of geometry on spatially modulated neurons have been identified. Recordings from place cells have shown that, when an environment was extended or reduced in one direction, place fields exhibited a coherent stretch [O'Keefe and Burgess 1996; Diba and Buzsaki 2008]. Similar experiments performing a rescaling of an environment observed a comparable augmentation of place field size in the hippocampus (see § 4.2.4) [Muller and Kubie 1987; Diba and Buzsaki 2008; Fenton et al. 2008; Rich et al. 2014]. From this point of view, the scale of the hippocampal space coding seemed to be defined by borders of the arena. The later discovery of border or boundary vector cells emphasized the importance of limits of the environment in defining an internal map of space [Hartley et al. 2000; Barry et al. 2006; Solstad et al. 2008; Lever et al. 2009]. In parallel, the geometrical pattern of grid cells have been shown to be highly influenced by the borders of an arena [Krupic et al. 2014; Hardcastle et al. 2015; Stensola et al. 2015; Krupic et al. 2016, 2018; Hägglund et al. 2019]. Interestingly, a later study by Gupta et al. [2012] observed that theta sequences of place cells were representing the environment in a segmented way. The different chunks of space represented by the theta sequences were defined by geometrical components (maze intersections and turns) of the maze. Taken together, these works showed that borders seems to define the scale, and to segment and structure the way in which the properties of an environment are encoded. Similar segmentation of space in different sub-compartment by corners have been reported by Alexander and Nitz [2017] in retrosplenial cortex. It is worth noting that this segmentation of space by borders could extend from space to a segmentation of experience for episodic memory [McKenzie and Buzsáki 2016; Brunec et al. 2018; Buzsáki and Tingley 2018].

Inside this frame defined by borders, the internal representation of space is commonly thought to be homogenous [Muller et al. 1987; Yoon et al. 2013; Rich et al. 2014; Chaudhuri et al. 2019; Stella et al. 2019]. Goals in the environment have been observed to deform this cognitive map [Hollup et al. 2001; Dupret et al. 2010; Gauthier and Tank 2018; Sato et al. 2018; Boccaro et al. 2019; Butler and Hardcastle 2019; Lee et al. 2019]. Nevertheless, featural cues (non-geometrical cues) are often only conferred a role in setting the reference frame and orienting the internal map of space [Muller and Kubie 1987; Crescent et al. 1997, 1999; Renaudineau et al. 2007; Lefort et al. 2019]. Nowadays, multiple local influences of landmarks [Hetherington and Shapiro 1997; Olypher et al. 2003; Pérez-Escobar et al. 2016; Hägglund et al. 2019] or other local variations of space coding [Reifenstein et al.

[2012; Dunn et al. 2017; Ismakov et al. 2017; Gerlei et al. 2019] cast some doubts on the hypothesis of an homogenous spatial code. It is true that the geometry of an environment is more likely to be unchanged in time than the featural components of an environment. Nevertheless, this view is likely to be amplified in bounded, poor and small scale environments. It would be a key point for future research to consider the contribution of landmarks in the structure of the internal representation of space. For example, we could investigate if features of an environment cluster or chunk theta sequences or replay in either small or large scale environments. In large scale environment, borders are less prominent or absent [Lew 2011]. Nevertheless, in this context, the need to segment and organize the knowledge about the environment is even more important than in small ones. Consequently, it would be very interesting to investigate how landmarks structure the representation of space for small and large scale complex environments.

The influence of objects is likely not confined to dorsal hippocampus. In our experiment, we focused our interest on dorsal hippocampus in order to compare our results with the existing literature in this area [Battaglia et al. 2004; Ravassard et al. 2013; Aronov and Tank 2014]. An interesting direction to explore would be to perform recordings taking into account the longitudinal axis of the hippocampus. Along this axis, space is represented with an increasing scale [Young et al. 1994; Kjelstrup et al. 2008] and could be an efficient way to perform nested coding of space [Mathis et al. 2012; Contreras et al. 2018; Harland et al. 2018]. In our paradigm, bigger place fields in the ventral part of the hippocampus could behave similarly than in the dorsal hippocampus. They could also be more homogeneously distributed as these hippocampal cells integrate more non-spatial information. Additionally, recent evidence highlighted that medial entorhinal cells, including grid cells, could be sensitive to contextual or visual cues [Pérez-Escobar et al. 2016; Kinkhabwala et al. 2018; Casali et al. 2019; Høydal et al. 2019]. Thus, it would be very interesting in future experiments to record MEC neurons in our experimental set up. Medial septum inactivation, in order to affect grid cells firing patterns, would also be interesting to perform in order to study the contribution of grid cells inputs to the place cells firing patterns observed in our study [Koenig et al. 2011; Fattahi et al. 2018].

### 6.11 CONCLUSION

To summarize, our study showed a strong influence of local visual cues on the generation and resolution of the internal representation of space subtended by the hippocampus. Further experiments, in other brain areas involved in space processing or in more complex environments will allow us to better understand how the "cognitive map"

can change in relation to external cues. These local changes in spatial resolution could subserve a more efficient storage of information in the hippocampus. But also, they could be linked to an allocation of hippocampal resources for valuable locations (landmark, goal,...) in order to provide a more robust representation for an efficient behavior.



Part IV  
APPENDIX



1      **Title**

2      **Intracellular determinants of CA1 pyramidal  
3      cells activation or silencing during  
4      locomotion**

5      **Authors**

6      François-Xavier Michon<sup>1</sup>, Geoffrey Marti<sup>1</sup>, Caroline Filippi<sup>1</sup>, Romain Bourboulou<sup>1</sup>, Julie  
7      Koenig<sup>1</sup> and Jérôme Epsztein<sup>1\*</sup>

9      **Authors Affiliation:**

10     (1) National Institute for Health and Medical Research (INSERM UMR 1249), Aix-  
11     Marseille University, Institute of Neuroscience of the Mediterranean Sea (INMED)

13     **\* Corresponding Author:**

14     Jérôme Epsztein

15     jerome.epsztein@inserm.fr

16     Phone : ±33 0 4 91 82 81 47

17     INMED/INSERM U1249

18     Parc Scientifique de Luminy

19     163 route de Luminy

20     13273 Marseille Cedex 09

21

22    **Abstract**

23    Spontaneous locomotion strongly influences the state of the hippocampal network and is  
24    critically important for spatial information coding. However, the intracellular determinants  
25    of CA1 pyramidal cells activation during locomotion are poorly understood. Here we  
26    recorded the membrane potential of CA1 pyramidal cells (PCs) while non-overtrained mice  
27    spontaneously alternated between periods of movement and immobility during a virtual  
28    spatial navigation task. We found opposite membrane polarization between bursting and  
29    regular firing CA1 PCs during movement. Regular firing CA1 PCs were more depolarized and  
30    fired at higher frequency during movement compared to immobility while bursting CA1 PCs,  
31    located deep in the CA1 pyramidal cell layer and preferentially inhibited during sharp wave  
32    ripples, were hyperpolarized during movement in a speed dependent manner. This speed-  
33    dependent suppression of a subpopulation of CA1 PCs could enhance signal to noise ratio for  
34    efficient spatial coding during locomotion.

35    **Keywords**

36    Hippocampus; place cells; CA1 pyramidal cells; locomotion; patch-clamp; in vivo

37    **Introduction**

38    Spontaneous locomotion strongly modulates sensory perception and learning. In the  
39    neocortex, active exploration notably through locomotion can modify the response of  
40    neurons to sensory stimuli, and associated task performance (Crochet and Petersen, 2006;  
41    Niell and Stryker, 2010; Polack et al., 2013; McGinley et al., 2015; Vinck et al., 2015;  
42    Albergaria et al., 2018). Locomotion also profoundly modify hippocampal network dynamics  
43    and coding (Vanderwolf, 1969). During movement, the hippocampal local field potential  
44    (LFP) is dominated by theta (7-12 Hz) oscillations and activated hippocampal cells show place  
45    specific activity (O’Keefe and Dostrovsky, 1971; McNaughton et al., 1983; Wilson and  
46    McNaughton, 1993; Moser et al., 2017). This state is often referred to as the “online” state  
47    of the hippocampus when coding of spatial, temporal or contextual information occurs.  
48    During immobility, the hippocampal LFP is interrupted by large negative transients, called  
49    sharp waves during which fast oscillations or ripples (O’Keefe and Nadel, 1978; Buzsáki et al.,  
50    1992) organize the firing of hippocampal cells into sequences representing past or future  
51    locations (Buzsaki, 1989; Foster and Wilson, 2006; Gupta et al., 2010; Pfeiffer and Foster,  
52    2013; Buzsáki, 2015).

53              The cellular mechanisms of hippocampal pyramidal cells’ activation during  
54    locomotion are poorly understood. Active exploration is often associated with membrane  
55    potential depolarization of pyramidal cells in the somatosensory and visual cortex (Crochet  
56    and Petersen, 2006; Bennett et al., 2013; Arroyo et al., 2018), which could constitute a  
57    permissive state for sparse sensory coding. In the hippocampus, pyramidal cells active during  
58    locomotion (the place cells) show a systematic bump of depolarization in specific places  
59    leading to place-specific firing (the place field) but remains relatively hyperpolarized outside  
60    the place field (Harvey et al., 2009; Epsztein et al., 2011; Bittner et al., 2015; Cohen et al.,

61 2017; Grienberger et al., 2017) while silent cells have a uniform baseline  $V_m$  far away from  
62 threshold in every part of the environment (Epsztein et al., 2011; Bittner et al., 2015).  
63 However, the baseline  $V_m$  values of place and silent cells during locomotion largely overlap,  
64 ruling out a simple depolarized permissive state as the main difference explaining their  
65 activation. Alternatively, it could result from differences in their intrinsic membrane  
66 properties. Place cells in a new environment have a high intrinsic frequency of action  
67 potential firing (burst firing cells) even before the start of exploration while silent cells fire  
68 more regularly (regular firing cells) (Epsztein et al., 2011). Furthermore, depolarizing a silent  
69 cell by a constant current injection during locomotion is sufficient to induce place cell coding  
70 (Lee et al., 2012). Burst and regular firing cells could also correspond to two different cell  
71 types (Kandel and Spencer, 1961; Graves et al., 2012) that are differently engaged during  
72 locomotion. Finally, hippocampal cells silent during locomotion could be selectively  
73 suppressed through dedicated inhibitory sub circuits (Lapray et al., 2012; Arriaga and Han,  
74 2017).

75 To decipher between these scenarios, we combined whole-cell patch-clamp  
76 recordings of hippocampal CA1 pyramidal cells with extracellular field recordings using a  
77 multi-site linear silicon probe while head-fixed mice alternated spontaneously between  
78 periods of locomotion and immobility during a spatial navigation task in a familiar virtual  
79 reality environment. Intracellular recordings allowed us to probe CA1 pyramidal cells'  
80 intrinsic properties through direct current injections and the effect of locomotion on their  $V_m$   
81 dynamics. We describe an opposite membrane potential polarization of bursting and regular  
82 firing CA1 pyramidal cells during locomotion.

83

84 **Results**

85 **Whole-cell membrane potential recordings during spatial navigation in virtual reality**

86 Whole-cell current-clamp recordings were obtained from CA1 pyramidal cells in the dorsal  
87 hippocampus of head-restrained mice running on a circular treadmill (Fig. S1A) as they  
88 explored a linear virtual maze (Fig. S1B) enriched with different patterns and virtual 3D  
89 objects for water rewards (Fig. S1C). Because mice were not over trained ( $1.15 \pm 0.26$   
90 reward/min;  $n = 17$  recording sessions) they spontaneously alternated periods of immobility  
91 and movement during exploration (ratio time in immobility vs time in movement =  $0.48 \pm$   
92 0.04;  $n = 17$  recording sessions). This spontaneous behavior allowed us to analyze CA1  
93 pyramidal cells' membrane potential ( $V_m$ ) and firing during immobility and movement  
94 periods. In a subset of recordings LFP activity was recorded simultaneously to assess  $V_m$   
95 behavior during ripples spontaneously occurring during immobility periods.

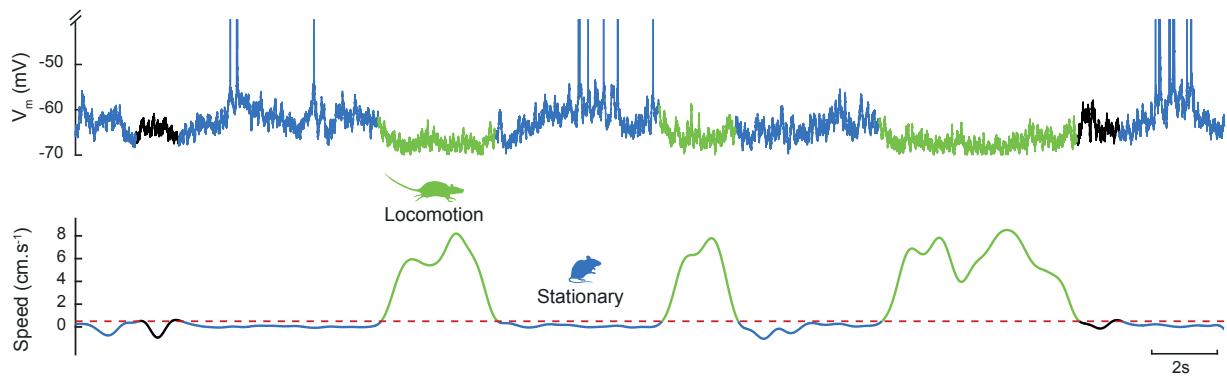
96

97 **Heterogeneous membrane potential dynamics of CA1 PCs during movement**

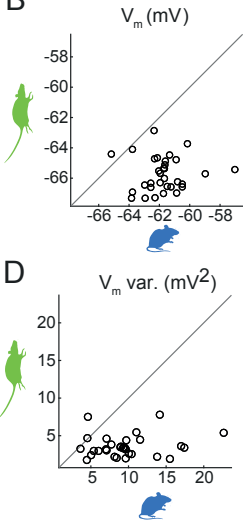
98 We analyzed data from 17 whole-cell recordings of CA1 pyramidal cells in 14 mice. To assess  
99 CA1 pyramidal cell  $V_m$  modulation during transitions from immobility to movement we  
100 calculated a modulation index (see methods). The vast majority of CA1 pyramidal cells ( $n =$   
101 16 out of 17; 94%) were significantly modulated during switches in behavioral states. Among  
102 those cells, a majority ( $n = 10$  out of 16; 62.5%) was negatively modulated meaning that their  
103 membrane potential was significantly more hyperpolarized during movement compared to  
104 immobility (HypM cells). A trace from a representative HypM CA1 pyramidal cell is illustrated  
105 in Fig. 1A. The membrane potential was consistently more hyperpolarized (Fig. 1A, B) and  
106 firing rate lower (Fig. 1A, C) during periods of movement. We note that this  $V_m$  behavior is

A

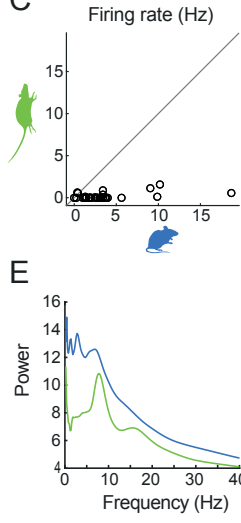
Michon et al. Fig.1



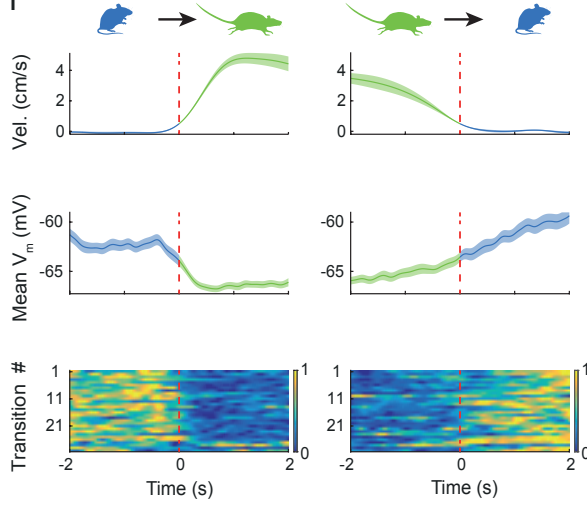
B



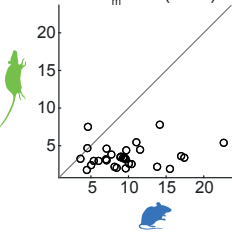
C



F



D



E

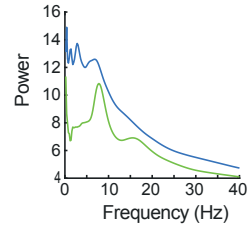


**Fig.1 Hyperpolarized cell during movement:**

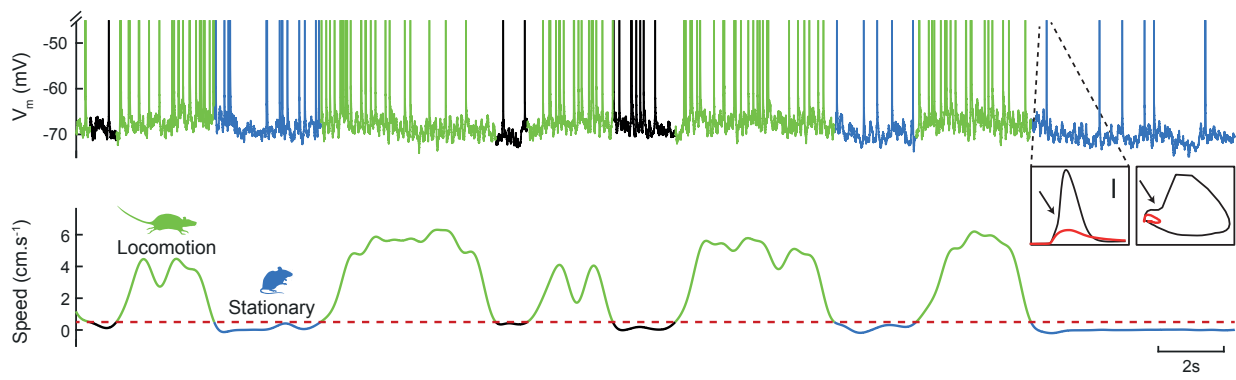
**A.** Trace of the  $V_m$  and speed of an animal during movement (green), during immobility (blue) or during an unaffected state (black) in a CA1 pyramidal cell recording. In the  $V_m$  trace, action potentials have been truncated to highlight subthreshold  $V_m$  changes during movement. **B.** Scatterplot of subthreshold  $V_m$  during movement versus immobility periods, each point correspond to mean value of one period. **C.** Scatterplot of mean firing frequency during movement versus immobility periods. **D.** Scatterplot of mean subthreshold  $V_m$  variance during movement versus immobility periods. **E.** Intracellular power spectrum during movement (green) and immobility (blue) periods. **F.** top to bottom : mean velocity, mean subthreshold  $V_m$  and normalized subthreshold  $V_m$  of each transition during initiation of movement (left) and for the stop of movement (right)

107 opposite to what is observed in layer 2/3 cortical pyramidal cells during movement (Polack  
108 et al., 2013). On the other hand,  $V_m$  variance was consistently lower (Fig. 1A, D) during  
109 movement, which is consistent with cortical pyramidal cells. This decrease was more  
110 pronounced for low frequency oscillations (Fig. 1E). To get an idea of the kinetics of these  
111 changes we focused on the times of transitions between immobility and movement periods  
112 and vice versa. The kinetics of  $V_m$  changes (Fig. 1F, middle) mimicked the kinetics of  
113 behavioral changes (Fig. 1F, top), which were faster for immobility to movement transitions.  
114 The effect was consistent from transition to transition in both directions (Fig. 1F, bottom).  
115 The other type of modulated cells ( $n = 6$  out of 16; 37.5%) was positively modulated meaning  
116 that their membrane potential was significantly more depolarized during movement (DepM  
117 cells). A trace from a representative DepM cell is represented in Fig. 2A. For this cell, the  
118 membrane potential was consistently more depolarized during movement versus immobility  
119 periods (Fig. 2A, B) and the firing rate was higher (Fig. 2A, C). Note that in this cell most  
120 action potentials were driven by underlying spikelets (Epsztein et al., 2010; Fig. 2A, inset).  
121 When focusing on the transition periods (Fig. 2F) we also observed a fast depolarization  
122 (hyperpolarization) upon transition to movement (immobility) but with a small time-lag  
123 compared to HypM cells. The transition by transition visualization (Fig. 2F, bottom) also  
124 revealed the consistency of the modulation.

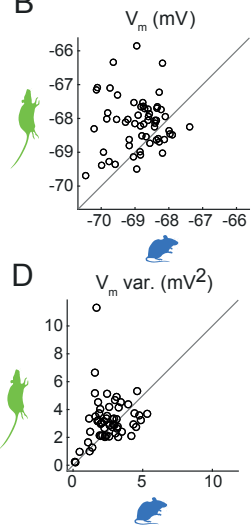
125 On average, HypM CA1 pyramidal cells displayed a  $\sim 2$  mV hyperpolarization during  
126 movement (Mov:  $-60.5 \pm 3.02$  mV; Imm:  $-58.4 \pm 3.13$  mV;  $n = 10$  cells,  $P < 10^{-3}$ , paired  $t$ -test;  
127 Fig. 3A), reduced variability (Mov:  $4.26 \pm 1.01$  mV $^2$ ; Imm:  $6.44 \pm 1.20$  mV $^2$ ;  $n = 10$  cells,  $P =$   
128 0.015, paired  $t$ -test; Fig. 3C) and reduced firing rate (Mov:  $3.06 \pm 1.80$  Hz; Imm:  $6.37 \pm 1.88$   
129 mV;  $n = 8$  cells,  $P = 6 \times 10^{-3}$ , paired  $t$ -test; Fig. 3B). The same conclusions were reached when  
130 analyzing all the transitions for HypM cells independently (Fig. S2;  $V_m$  expressed as Z-score).

A

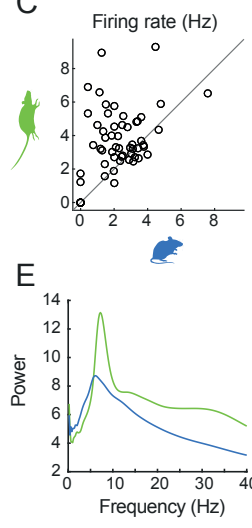
Michon et al. Fig.2



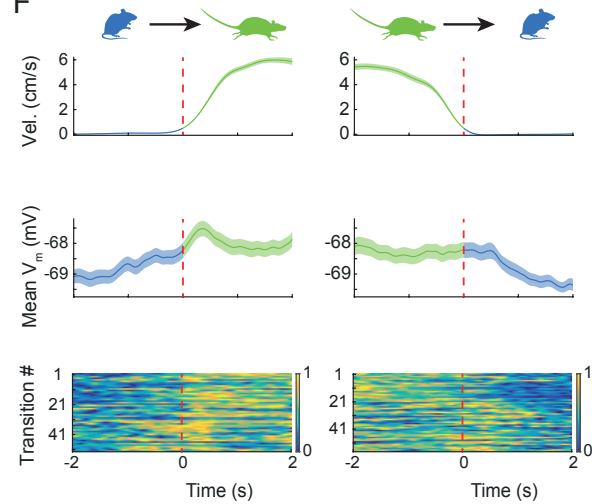
B



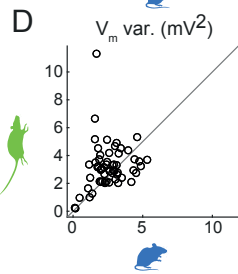
C



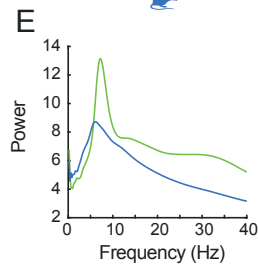
F



D



E

**Fig.2 Depolarized cell during movement:**

**A.** Trace of the  $V_m$  and speed of an animal during movement (green), during immobility (blue) or during an unaffected state (black) in a CA1 pyramidal cell recording. In the  $V_m$  trace, action potentials have been truncated to highlight subthreshold  $V_m$  changes during movement. Magnification: one action potential (black) and a superposed spikelet (red) and associated phase plot, bar = 20mV. In this recording, most of action potentials were generated thanks to spikelts. **B.** Scatterplot of subthreshold  $V_m$  during movement versus immobility periods, each point correspond to mean value of one period. **C.** Scatterplot of mean firing frequency during movement versus immobility periods. **D.** Scatterplot of mean subthreshold  $V_m$  variance during movement versus immobility periods. **E.** Intracellular power spectrum during movement (green) and immobility (blue) periods. **F.** top to bottom : mean velocity, mean subthreshold  $V_m$  and normalized subthreshold  $V_m$  of each transition during initiation of movement (left) and for the stop of movement (right)

131 For immobility to movement transitions (Fig. S2A-C, top), the  $V_m$  was hyperpolarized (Mov: -  
132  $0.5 \pm 0.06$ ; Imm:  $0.17 \pm 0.06$ ; n = 127 transitions,  $P < 10^{-13}$ , paired t-test), firing rate was  
133 decreased (Mov:  $2.04 \pm 0.53$  Hz; Imm:  $3.35 \pm 0.48$  Hz; n = 127 transitions with firing,  $P < 10^{-6}$ ,  
134 signed rank test) and variance was decreased (Mov:  $2.24 \pm 0.21$  mV $^2$ ; Imm:  $3.87 \pm 0.26$  mV $^2$ ;  
135 n = 127 transitions,  $P < 10^{-8}$ , signed rank test).

136 In DepM CA1 pyramidal cells, the depolarization during movement was smaller ~0.6  
137 mV (Mov:  $-62.4 \pm 3.57$  mV; Imm:  $-63.0 \pm 3.61$  mV; n = 6 cells,  $P = 0.006$ , paired t-test; Fig. 3A)  
138 and the  $V_m$  variance was not significantly different (Mov:  $3.35 \pm 0.81$  mV $^2$ ; Imm:  $2.52 \pm 0.71$   
139 mV $^2$ ; n = 6 cells,  $P = 0.17$ , paired t-test; Fig. 3C). Accordingly, the firing rate was not  
140 significantly modulated for these cells (Mov:  $2.73 \pm 1.49$  Hz; Imm:  $2.04 \pm 1.3$  mV $^2$ ; n = 4 cells,  
141  $P = 0.13$ , paired t-test; Fig. 3B). When analyzing all transitions from immobility to movement  
142 (Fig. S2A-C, bottom), qualitatively similar results were observed: a small depolarization  
143 (Mov:  $0.12 \pm 0.04$ ; Imm:  $-0.26 \pm 0.04$  mV; n = 180 transitions,  $P < 10^{-12}$ , paired t-test)  
144 without significant change in the variance (Mov:  $2.01 \pm 0.13$  mV $^2$ ; Imm:  $2.04 \pm 0.12$  mV $^2$ ; n =  
145 180 transitions,  $P < 10^{-12}$ , signed rank test) yielding a small but significant increase in firing  
146 rate (Mov:  $1.98 \pm 0.28$  Hz; Imm:  $1.38 \pm 0.18$  Hz; n = 180 transitions,  $P = 10^{-4}$ , signed rank  
147 test).

148 We note that HypM cells were on average more depolarized than DepM cells during  
149 immobility (HypM:  $-58.4 \pm 3.13$  mV, n = 10 cells; DepM:  $-63.0 \pm 3.61$  mV, n = 6 cells;  $P =$   
150 0.37, unpaired t-test). To determine if this difference could account for the opposite  
151 modulation between HypM and DepM cells by locomotion we excluded all HypM cells more  
152 depolarized than -55 mV during immobility. This strongly reduced the difference in baseline  
153  $V_m$  between HypM and DepM cells (HypM:  $-64.6 \pm 2.76$  mV, n = 6 cells; DepM:  $-63 \pm 3.61$  mV,

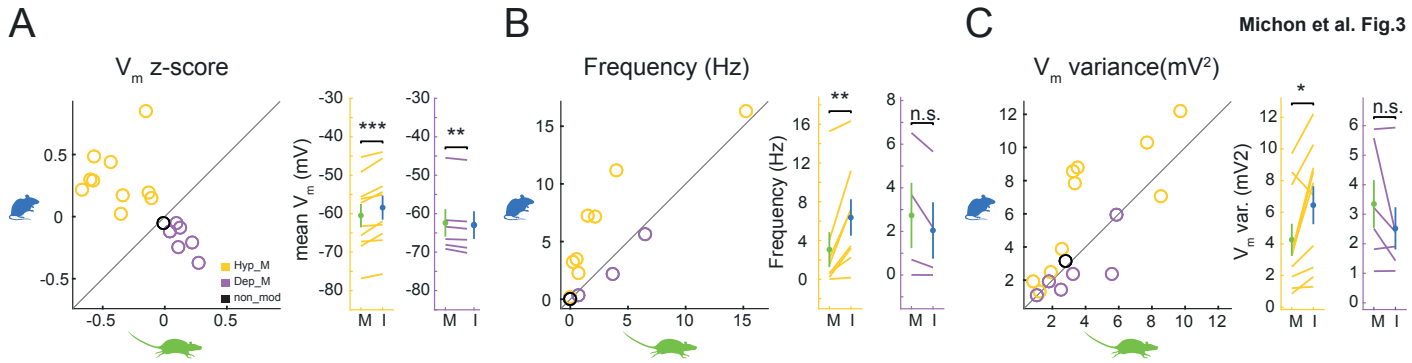


**Fig.3 Opposite modulation of subth.Vm during movement**

**A.** Left: Mean subthreshold  $V_m$  during movement versus immobility of hyperpolarized cells (Hyp M group, in yellow), depolarized cells (Dep M group in purple) and non modulated cells (black) during movement. Right: Mean subthreshold  $V_m$  during movement versus immobility of Hyp M cells ( $\Delta = -2.07 \pm 0.42$  mV,  $n=10$ ,  $p=7.88 \cdot 10^{-4}$ , paired t-test) and Dep M cells ( $\Delta = 0.58 \pm 0.13$  mV,  $n=6$ ,  $p=0.006$ , paired t-test). **B.** Left: Same as A for the firing frequency; cells that are totally silent during movement and during immobility were removed. Right : Mean firing frequency during movement versus immobility of Hyp M cells ( $\Delta = -3.32 \pm 0.87$  Hz,  $n=8$ ,  $p=0.006$ , paired t-test) and Dep M cells ( $\Delta = 0.68 \pm 0.33$  Hz,  $n=4$ ,  $p=0.128$ , paired t-test). **C.** Left : Same as A and B for the subthreshold  $V_m$  variance. Right: Mean subthreshold  $V_m$  variance during movement versus immobility of Hyp M cells ( $\Delta = -2.18 \pm 0.72$  mV $^2$ ,  $n=10$ ,  $p=0.015$ , paired t-test) and Dep M cells ( $\Delta = 0.82 \pm 0.52$  mV $^2$ ,  $n=6$ ,  $p=0.171$ , paired t-test).

154 n = 6 cells;  $P = 0.73$ , unpaired  $t$ -test). However, HypM cells were still on average  
155 hyperpolarized by  $\sim 1.7$  mV during movement (Mov:  $-66.3 \pm 2.76$  mV; Imm:  $-64.6 \pm 2.76$  mV;  
156 n = 6 cells,  $P = 0.038$ , paired  $t$ -test). Thus, although we cannot exclude a contribution of  
157 baseline  $V_m$  differences between HypM and DepM cells in the effect we observed, the effect  
158 can still be observed when this difference is strongly reduced. The difference between HypM  
159 and DepM cells was also not related to changes in animal performance in terms of number  
160 of reward per minute (HypM:  $1.08 \pm 0.44$ , n = 10 recording sessions; DepM:  $1.2 \pm 0.23$ , n = 6  
161 recording sessions;  $P = 0.18$ , rank sum test; Fig. S3) or ratio of time spent in movement and  
162 immobility (HypM:  $0.44 \pm 0.06$ , n = 10 recording sessions; DepM:  $0.55 \pm 0.04$ , n = 6 recording  
163 sessions;  $P = 0.25$ , rank sum test; Fig. S2).

164

165 **Heterogeneous speed dependent modulation of membrane potential dynamics in CA1 PCs**  
166 Previous extracellular recordings report a speed dependent modulation of CA1 pyramidal  
167 cells firing rate during locomotion (McNaughton et al., 1983; Czurkó et al., 1999). We  
168 wondered whether similar speed dependent modulation could be observed at the  
169 subthreshold level. For each HypM and DepM cells we calculated the correlation between  
170 the Z-scored  $V_m$  and speed binned at  $0.05$  cm.s $^{-1}$ . A majority of HypM (n = 8 out of 10)  
171 showed significant and negative correlations between speed and  $V_m$ . Two example cells are  
172 shown in Fig. 4A (top) for recordings performed in a slow (maximal running speed  $\sim 6$  cm.s $^{-1}$ )  
173 and a fast (maximal running speed  $\sim 15$  cm.s $^{-1}$ ) animal. In both cases the faster the animal  
174 ran the more the cell got hyperpolarized. As a population, HypM cells were significantly and  
175 negatively modulated by speed ( $r: -0.46 \pm 0.09$ ; n = 10,  $P < 0.001$ , one sample  $t$ -test; Fig. 4B).  
176 Only half of DepM cells showed significant and positive correlation between speed and  $V_m$ .

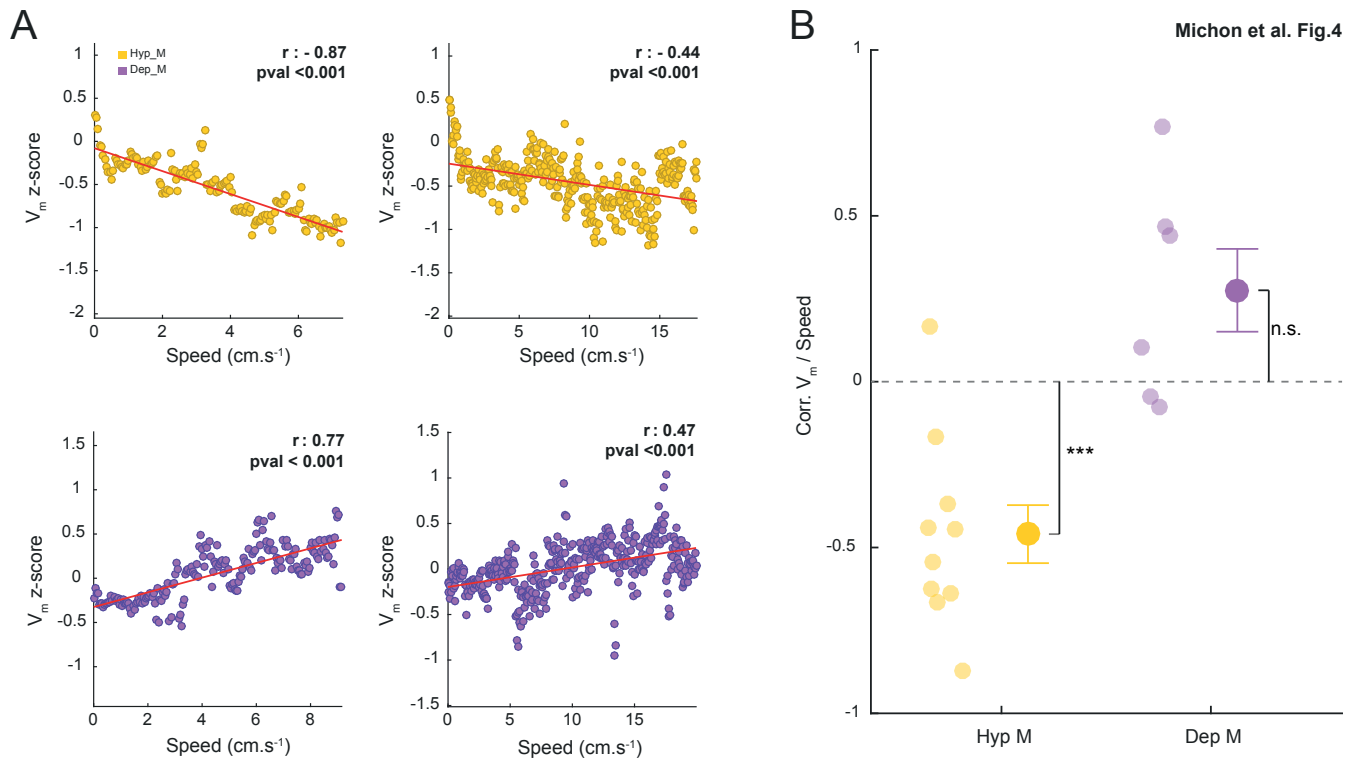


**Fig.4 Speed correlation of Hyp M cells and Dep M cells**

**A.** Example of correlation between speed and subthreshold  $V_m$  z-score in 2 Hyp M cells (up) and 2 Dep M cells (down). Each point corresponds to the mean value of subthreshold  $V_m$  z-scored value in speed bins (size of bins:  $0.05\text{cm.s}^{-1}$ ). **B.** Mean correlation of speed with subthreshold  $V_m$  z-scored for Hyp M ( $r = -0.46 \pm 0.09$ ,  $n=10$ ,  $p=7.54 \cdot 10^{-4}$ , t-test) cells and Dep M cells ( $r = 0.27 \pm 0.14$ ,  $n=6$ ,  $p=0.1$ , t-test).

177 Two example cells are shown in Fig. 4 A (bottom) for recordings performed in a slow  
178 (maximal running speed  $\sim 8 \text{ cm.s}^{-1}$ ) and a fast (maximal running speed  $\sim 15 \text{ cm.s}^{-1}$ ) animal. As  
179 a population, DepM cells showed no significant correlation between  $V_m$  and speed ( $r: 0.27 \pm$   
180  $0.14; n = 6, P = 0.1$ , one sample  $t$ -test).

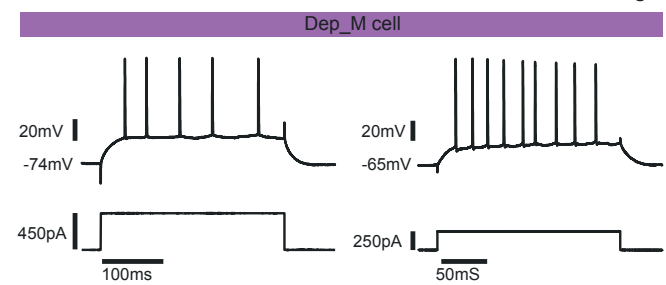
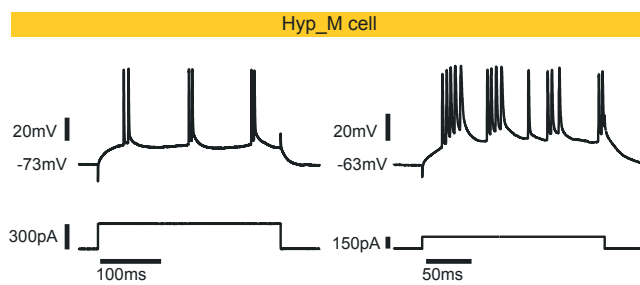
181

182 **Opposite membrane potential modulation of bursting and regular firing CA1 PCs during**  
183 **movement**

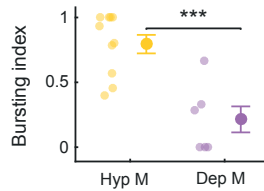
184 Our initial analysis revealed that CA1 pyramidal cells can be divided into two subgroups  
185 based on their membrane potential and firing rate modulations during locomotion. A first  
186 group (HypM cells) showed a large and speed dependent hyperpolarization together with  
187 reduced variance and firing rate during locomotion while a second group showed more  
188 moderate depolarization without significant change in variance and a smaller increase in  
189 firing rate. Previous *in vivo* whole-cell recordings in freely moving rats exploring a new  
190 environment have revealed differences in CA1 pyramidal cell activation during locomotion  
191 between bursting and regular firing cells (Epsztein et al., 2011). We next thought to  
192 determine if different intrinsic properties could also exist between HypM and DepM CA1  
193 pyramidal cells in head-fixed mice exploring a familiar environment. We thus analyzed the  
194 response of HypM and DepM cells to depolarizing pulses of current injected *via* the patch  
195 pipette before exploration of the virtual environment. As in anesthetized rats, distinct  
196 bursting and regular firing behaviors could be observed among CA1 pyramidal cells recorded  
197 in awake mice (Fig. 5A). Unexpectedly, HypM cells exhibited far more bursting than DepM  
198 cells (fraction of APs in burst or bursting index, HypM:  $0.79 \pm 0.08, n = 10$ ; DepM:  $0.21 \pm$   
199  $0.11, n = 6, P < 10^{-3}$ , unpaired  $t$ -test; Fig. 5B). Over all recorded cells there was a significant

A

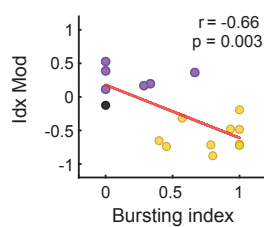
Michon et al. Fig.5



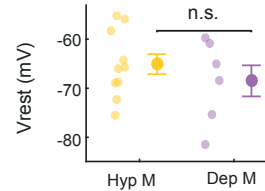
B



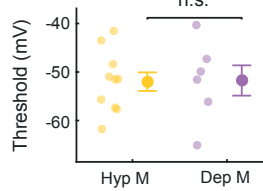
C



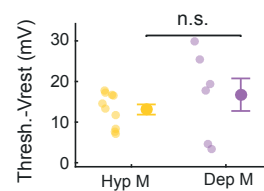
D



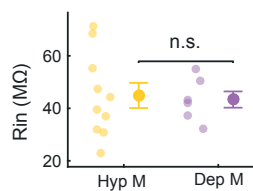
E



F



G



H

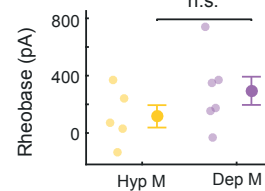


**Fig.5 Intrinsic properties of Hyp M cells vs Dep M cells**

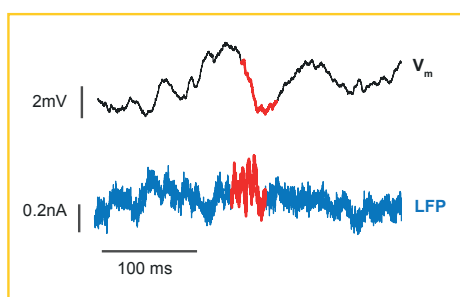
**A.** Firing pattern of two Hyp M and two Dep M cells in response to depolarizing current injection. **B.** Bursting index of Hyp M versus Dep M cells (mean<sub>Hyp M</sub> =  $0.79 \pm 0.08$ , n=10, mean<sub>Dep M</sub> =  $0.21 \pm 0.11$ , n=6,  $p = 4.95 \cdot 10^{-4}$ , t-test). **C.** Correlation of the bursting index with index ( $r=-0.66$ ,  $p=0.003$ ). **D.** V<sub>rest</sub> of Hyp M versus Dep M cells (mean<sub>Hyp M</sub> =  $-65.09 \pm 2.15$  mV, n=10, mean<sub>Dep M</sub> =  $-68.49 \pm 3.47$  mV, n=6,  $p=0.39$ , t-test). **E.** Threshold of Hyp\_M versus Dep M cells (mean<sub>Hyp M</sub> =  $-51.99 \pm 2.02$  mV, n=10, mean<sub>Dep M</sub> =  $-51.74 \pm 3.42$  mV, n=6,  $p=0.95$ , t-test). **F.** Thresh.-Vm rest of Hyp\_M versus Dep M cells (mean<sub>Hyp M</sub> =  $13.10 \pm 1.32$  mV, n=10, mean<sub>Dep</sub> =  $16.74 \pm 4.39$  mV, n=6,  $p=0.36$ , t-test). **G.** Input resistance of Hyp\_M versus Dep M cells (mean<sub>Hyp M</sub> =  $44.9 \pm 5.06$  MΩ, n=10, mean<sub>Dep M</sub> =  $43.3 \pm 3.39$  MΩ, n=6,  $p=0.83$ , t-test). **H.** Rheobase of Hyp M versus Dep M cells (mean<sub>Hyp M</sub> =  $116.19 \pm 87.37$  pA, n=5, mean<sub>Dep M</sub> =  $294.33 \pm 107.81$  pA, n=6,  $p=0.24$ , t-test).

200 correlation between bursting and modulation indexes ( $r = -0.66$ ;  $P = 0.003$ ; Fig. 5C). Other  
201 pre-exploration intrinsic parameters were not significantly different between HypM and  
202 DepM cells. This was the case for pre-exploration baseline membrane potential (HypM:  $-65.1$   
203  $\pm 2.15$ ,  $n = 10$ ; DepM:  $-68.5 \pm 3.47$ ;  $n = 6$ ,  $P = 0.39$ , unpaired  $t$ -test; Fig. 5D), the firing  
204 threshold (HypM:  $-52.0 \pm 2.02$ ,  $n = 10$ ; DepM:  $-51.8 \pm 3.42$ ,  $n = 6$ ;  $P = 0.36$ , unpaired  $t$ -test;  
205 Fig. 5E), the difference between firing threshold and baseline  $V_m$  (HypM:  $13.1 \pm 1.32$ ,  $n = 10$ ;  
206 DepM:  $16.75 \pm 4.39$ ,  $n = 6$ ;  $P = 0.36$ , ranksum  $t$ -test; Fig. 5F), the input resistance (HypM:  
207  $44.9 \pm 5.06$ ,  $n = 10$ ; DepM:  $43.3 \pm 3.39$ ,  $n = 6$ ;  $P = 0.83$ , unpaired  $t$ -test; Fig. 5G) and the  
208 rheobase ( HypM:  $116 \pm 87$ ,  $n = 10$ ; DepM:  $294 \pm 107$ ,  $n = 6$ ;  $P = 0.24$ , unpaired  $t$ -test; Fig.  
209 5H).

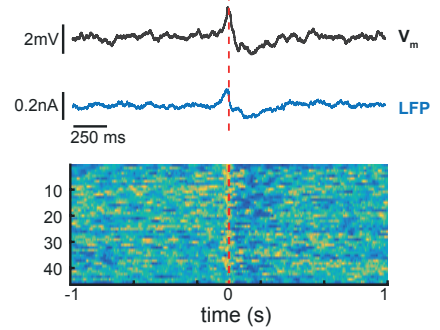
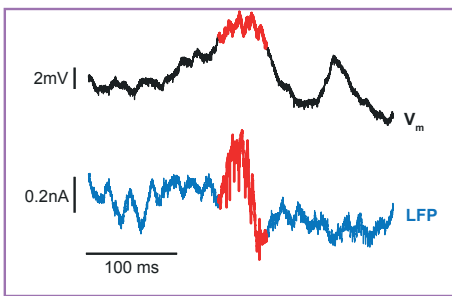
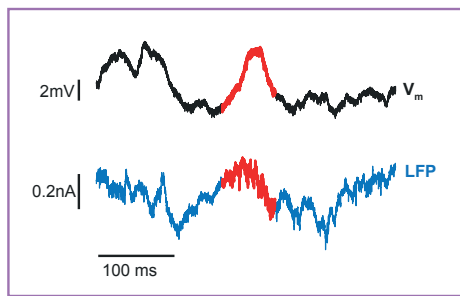
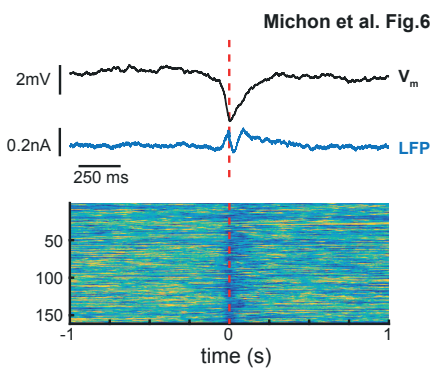
210

211 **Heterogeneous membrane potential modulation of CA1 PCs during sharp-wave ripples**  
212 Sharp waves ripple (SWRs) are transient events recorded in the local field potential of CA1  
213 during periods of immobility, slow wave sleep and anesthesia (Girardeau and Zugaro, 2011;  
214 English et al., 2014; Buzsáki, 2015; Roumis and Frank, 2015; Valero et al., 2015; Colgin, 2016;  
215 Hulse et al., 2016; Gan et al., 2017). They result from the dendritic excitation of CA1  
216 pyramidal cells dendrites by the synchronous discharge of upstream CA3 pyramidal neurons.  
217 Recently, different anatomically defined CA1 pyramidal cells were shown to be differently  
218 modulated during SWRs (Valero et al., 2015) with CA1 pyramidal cells located deep in the  
219 pyramidal cell layer (close to stratum oriens) preferentially hyperpolarized and cells located  
220 more superficially in the pyramidal cell layer (closer to stratum radiatum) preferentially  
221 depolarized. To see if similar differential modulation could be observed between HypM and  
222 DepM CA1 pyramidal cells, we analyzed intracellular  $V_m$  modulations during ripples recorded

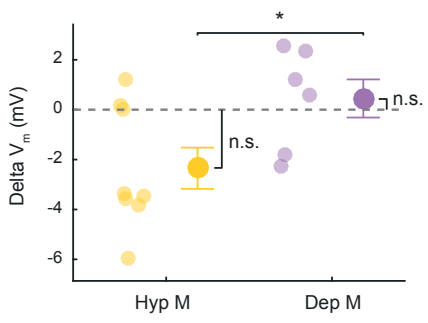
A



B



C



D

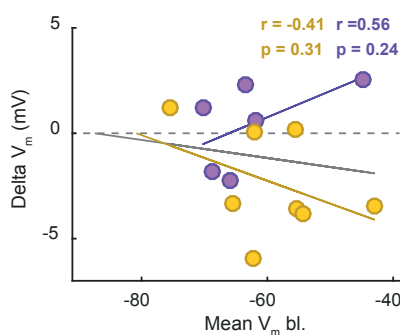


**Fig.6 -  $V_m$  modulation of Hyp M cells and Dep M cells during ripples**

**A.** Examples of subthreshold  $V_m$  modulation (black trace) during a ripple (red trace) detected in LFP (blue trace). Up: subthreshold  $V_m$  is hyperpolarized during ripple. Down: subthreshold  $V_m$  is depolarized during ripple. **B.** Mean subthreshold  $V_m$ , associated mean LFP and subthreshold  $V_m$  normalized aligned on ripple occurrence. Up: example of cell hyperpolarized during ripple. Down: Example of a cell depolarized during ripple. **C.** Mean delta subthreshold  $V_m$  modulation during ripple for Hyp M cells (mean<sub>Hyp M</sub> =  $-2.35 \pm 0.88$  mV, n=8, p=0.45, ranksum) versus Dep M cells (mean<sub>Dep M</sub> =  $0.45 \pm 0.84$  mV, n=6, p= 0.61, t-test), (Hyp M vs Dep M, p=0.046, t-test). **D.** correlation between subthreshold  $V_m$  baseline (before ripple) and Mean delta Subth. $V_m$

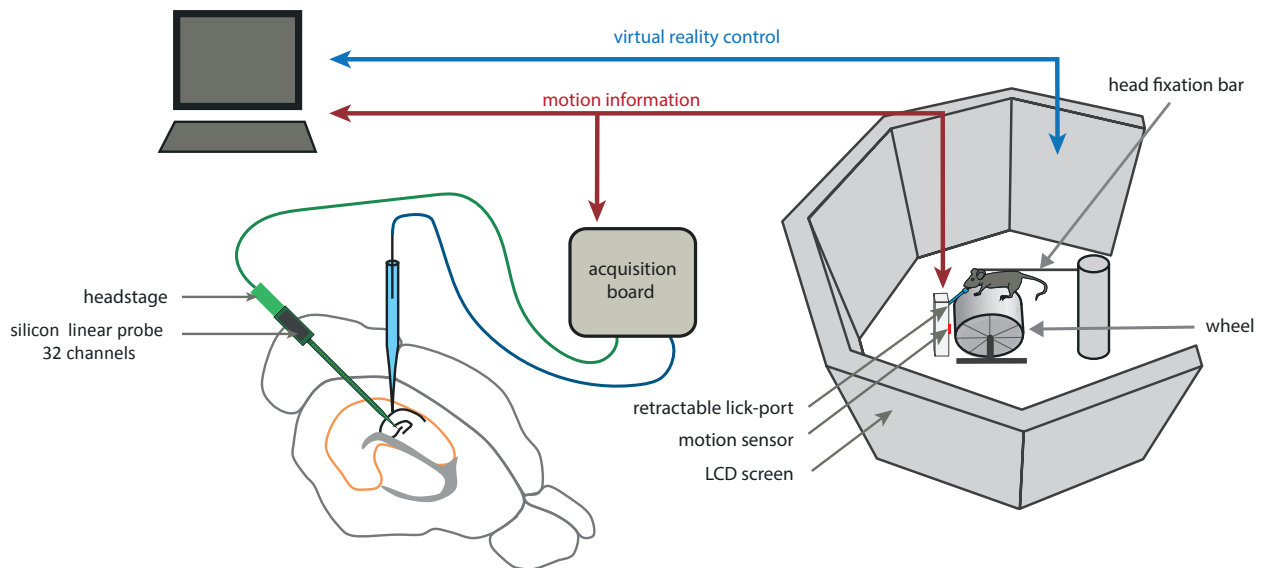
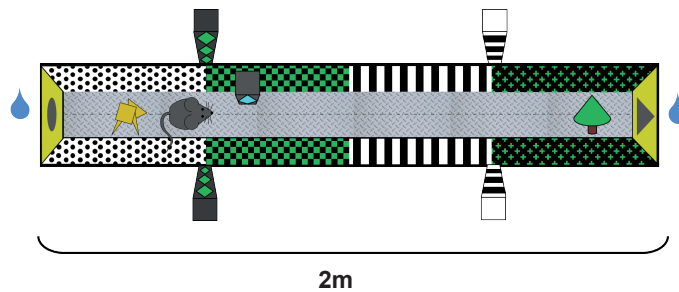
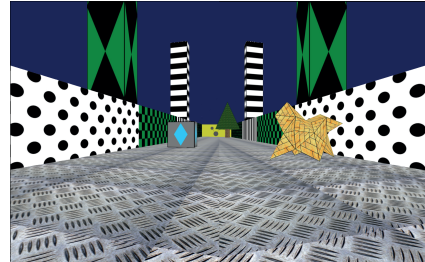
223 in the LFP using a linear silicon probe. A majority of HypM cells ( $n = 5/8$ ; 62.5%) were  
224 preferentially hyperpolarized during ripples with other HypM cells not significantly  
225 modulated while DepM cells showed a mixed behavior. Overall, HypM and Dep M cells were  
226 differently modulated during ripples (HypM:  $-2.35 \pm 0.88$ ,  $n = 8$ ; DepM:  $0.45 \pm 0.84$  mV,  $n = 6$ ;  
227  $P = 0.046$ , unpaired *t*-test; Fig. 6A-C). This difference could not be explained by differences in  
228 pre-ripple baseline  $V_m$  (HypM:  $-59.1 \pm 3.36$  mV,  $n = 8$ ; DepM:  $-62.5 \pm 3.78$  mV,  $n = 6$ ;  $P = 0.52$ ,  
229 unpaired *t*-test; Fig. 6D). To see if the preferential hyperpolarization of HypM cells could be  
230 correlated to the position of their cell body in the CA1 pyramidal cell layer we used post-hoc  
231 revelation of biocytin filled neurons. A staining against calbindin was used to mark more  
232 superficially located CA1 pyramidal cells and determine the border between stratum  
233 pyramidale and stratum radiatum (Valero et al., 2015). The cell bodies of the 6 HypM CA1  
234 pyramidal cells successfully labeled were all 20  $\mu\text{m}$  deeper than the border (mean:  $39.2 \pm$   
235  $6.26$   $\mu\text{m}$ ,  $n = 6$ ; range:  $23.7 - 68.2$   $\mu\text{m}$ ) indicating that they were preferentially located deep  
236 within the CA1 pyramidal cell layer (Valero et al., 2015).

237

238

**A**

Michon et al. Fig.sup.1

**B****C**

#### Article - Figure sup. 1 - Virtual reality setup

**A.** Schema of the virtual reality set up. The mouse is head-fixed and located on a wheel surrounded by LCD screens where a virtual environment is displayed.

**B.** Schema of the top of view of the linear track.

**C.** first person view of the linear track used

239 **Discussion**

240 Locomotion is a strong modulator of hippocampal network dynamics (Vanderwolf, 1969) and  
241 is important for the sparse coding of spatial information by hippocampal place cells  
242 (Rowland et al., 2011). To get a better understanding of the cellular mechanisms of  
243 hippocampal cells activation (or silence) during locomotion, we recorded the membrane  
244 potential of CA1 pyramidal cells as head-fixed mice spontaneously alternated between  
245 periods of movement and immobility during a spatial navigation task in a virtual reality  
246 environment. The  $V_m$  of most CA1 pyramidal was modulated during transitions from  
247 immobility to movement and vice versa. The majority ( $\sim 2/3$ ) of CA1 pyramidal cells were  
248 hyperpolarized during movement while the remaining cells were depolarized.  
249 Hyperpolarization of CA1 pyramidal cells during movement was of high magnitude ( $\sim 2$  mV)  
250 and associated with reduced  $V_m$  variance and lower firing rates. However, depolarization of  
251 CA1 pyramidal cells during movement was more moderate ( $\sim 0.6$  mV), not associated with  
252 reduced  $V_m$  variance and only slightly higher baseline firing rates. The proportion of  
253 hyperpolarized cells during movement ( $2/3$ ) in our recordings fits well with the proportion of  
254 silent cells in a given environment estimated by extracellular as well as intracellular  
255 recordings (Thompson and Best, 1989; Wilson and McNaughton, 1993; Epsztein et al., 2011).  
256 Thus, a straightforward interpretation of our results is that locomotion-dependent  
257 hyperpolarization of a majority of CA1 pyramidal cells in a given environment allows them to  
258 stay silent in that environment. In line with this, a recent report highlighted the important  
259 role of baseline  $V_m$  in controlling place cells activation in a given environment (Lee et al.,  
260 2012). In this report a slight depolarization (by a few millivolts) of the baseline  $V_m$  of silent  
261 pyramidal cells was sufficient to induce a spatially modulated bump of depolarization in  
262 these cells and convert them to place cell coding. This suggests that intrinsic properties, and

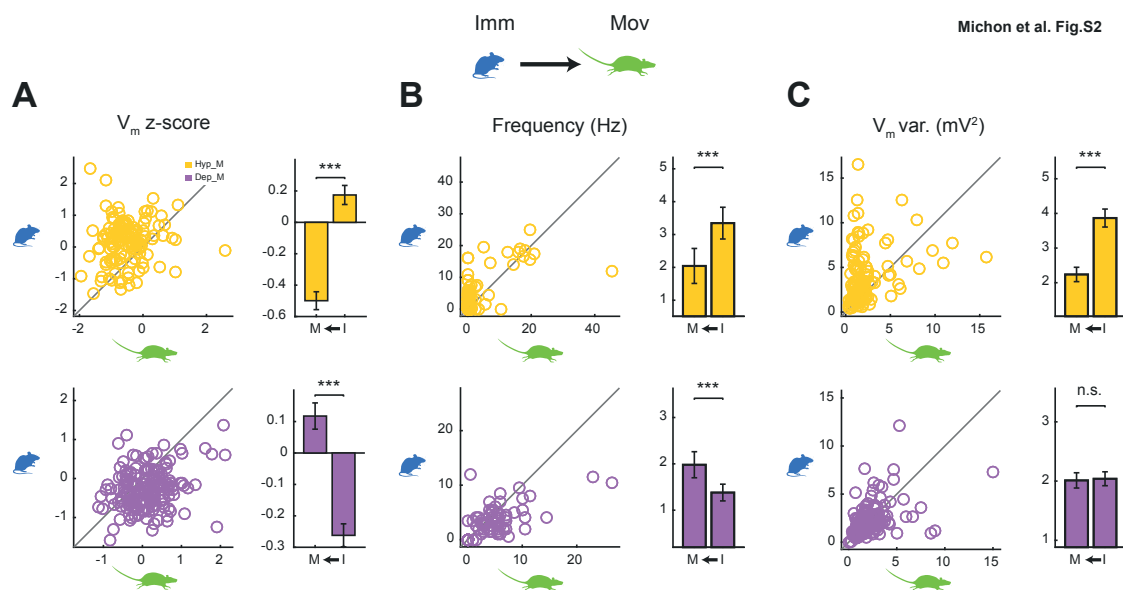


**Figure S2 -  $V_m$  modulation of Hyp M cells and Dep M cells during initiation or stop of locomotion**

**A.** Scatterplots and barplots of Subthreshold  $V_m$  z-scored before initiation of movement (immobility) and after the transition (movement) for all transitions of Hyp M cells (up) ( $P = 4.82 \cdot 10^{-14}$ , paired t-test) and Dep M cells (down) cells ( $P = 4.95 \cdot 10^{-13}$ , paired t-test) **B.** Scatterplots and barplots of Frequency before initiation of movement (immobility) and after the transition (movement) for all transitions of Hyp M cells (up) ( $P = 7.79 \cdot 10^{-7}$ , signed rank test) and Dep M cells (down) ( $P = 5.68 \cdot 10^{-5}$ , signed rank test) **C.** Scatterplots and barplots of Subthreshold  $V_m$  variance before initiation of movement (immobility) and after the transition (movement) for all transitions of Hyp M cells (up) ( $P = 2.96 \cdot 10^{-9}$ , signed rank test) and Dep M cells (down) ( $P = 0.359$ , signed rank test)

notably voltage-gated conductance activated below the firing threshold such as  $I_{NaP}$  (Hsu et al., 2018) can rapidly convert a silent cell into a place cell. In this framework, most CA1 pyramidal receive spatially modulated inputs but intrinsic conductances, probably in conjunction with specific synaptic inhibition, can gate those inputs in the majority of CA1 pyramidal cells such that only a minority of them (the place cells) can respond to these inputs with spatially modulated firing. In this context, the locomotion-dependent hyperpolarization of the baseline  $V_m$  of a majority of CA1 pyramidal cells that we describe could constitute an efficient way to prevent incidental depolarization (and associated place coding) of silent pyramidal cells, thus preserving the sparse coding scheme of the hippocampus. On the other hand, the depolarization of a minority of CA1 pyramidal cells could represent a permissive state for position coding. Alternatively cells hyperpolarized during movement could represent a recently described population of cells that specifically code position during immobility (Kay et al., 2016). We think however that this possibility is unlikely given that immobility place cells represented a small minority of all CA1 pyramidal cells while HypM cells represented the majority of recorded cells in our study. Unfortunately the behavior of the mice and short duration of the recordings prevented the analysis of the spatial modulation of HypM cells' firing. Finally, HypM cells could correspond to transitions from an internal state dominated by large irregular activities (LIA) when CA1 pyramidal cells'  $V_m$  is on average more depolarized to theta state when CA1 pyramidal cells'  $V_m$  is on average more hyperpolarized (Hulse et al., 2017). However, in this report the authors found no clear changes in  $V_m$  or its variability across transitions to theta state and theta periods tended to occur away from identified periods of LIA making this explanation also unlikely. The difference with our results where clear modulation in  $V_m$  and its variability (at least for HypM cells) were observed around transitions to movement (an most probably to a theta state)

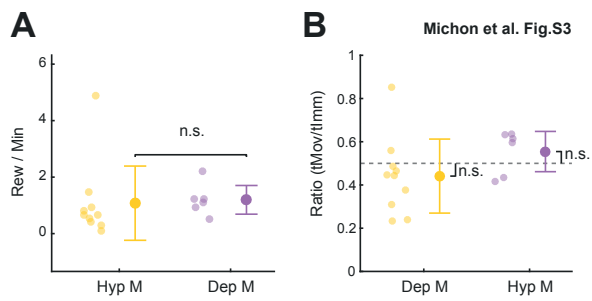


**Figure S3 – Behavior control**

**A.** Mean number of reward per minute for Hyp M cells versus Dep M cells ( $P = 0.18$ , Wilcoxon ranksum test).

**B.** Ratio of the time spent in movement on time spent in immobility for Hyp M cells ( $P = 0.33$ , one sample t-test) versus Dep M cells ( $P = 0.25$ , one sample t-test ).

287 could lie in the fact that our animals were actively engaged in a spatial navigation task unlike  
288 animals in the previous report (see for instance the difference in running speed values).

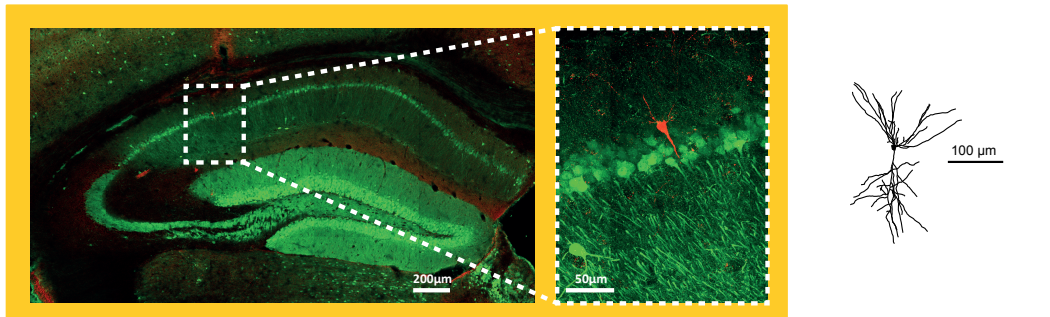
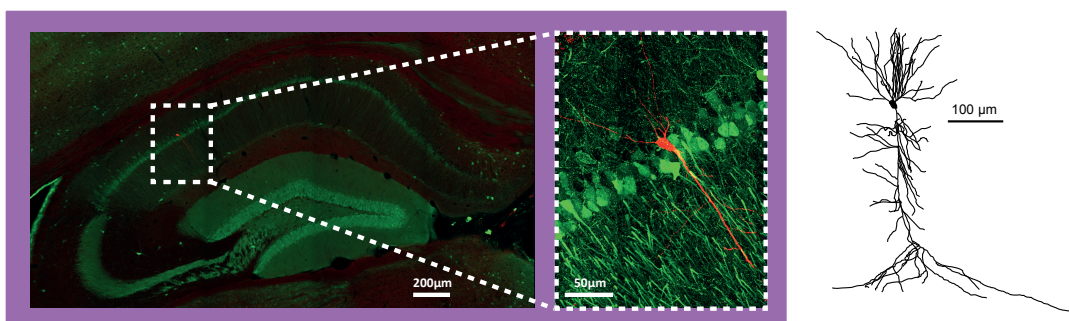
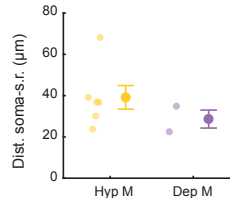
289

290 **Cellular mechanisms of locomotion-dependent bimodal modulation of CA1 pyramidal cells**

291  $V_m$

292 The bimodal modulation of CA1 pyramidal cells  $V_m$  during locomotion could result from  
293 locomotion dependent modulation of the excitatory/inhibitory synaptic balance. This  
294 balance is however difficult to predict from the existing literature. The overall activity of CA1  
295 pyramidal cells in the hippocampus is reduced during movement compared to periods of  
296 quiet wakefulness or during sleep (Kay and Frank, 2017). However, the firing rate of cells  
297 active during locomotion is positively modulated by speed (McNaughton et al., 1983; Czurkó  
298 et al., 1999). The source of this modulation could be extra-hippocampal. The activity of  
299 glutamatergic cells in the medial septum is positively modulated by speed (Fuhrmann et al.,  
300 2015). These cells mostly contact interneurons so they could influence pyramidal cells'  $V_m$   
301 through feedforward disinhibition. Recent experimental work using juxtacellular recordings  
302 followed by post-hoc identification in freely moving rat have observed that PV basket cells  
303 but not Ivy cells fire more during movement compared to immobility (Lapray et al., 2012).  
304 More recent work using two photon imaging reported that most PV-positive and SOM-  
305 positive interneurons' activity is positively modulated by speed (Arriaga and Han, 2017). This  
306 is consistent with the speed-dependent hyperpolarization of the majority of recorded CA1  
307 pyramidal cells. However, a small population of interneurons showed an opposite behavior  
308 (i.e. their activity was negatively correlated with speed) and could account for the speed  
309 dependent depolarization of a minority of recorded CA1 pyramidal neurons in our study.

310

**A****B****C**

**Figure S4 - Histological revelation of recorded cells**

**A.** Left : Location and magnification of the revelation of a Hyp M recorded neuron filled with biocytin (red) and labeling of calbindin positive neurons (green). Right : reconstruction of the same neuron and location on radial axes of CA1 based on calbindin labeling **B.** same as A. but for a Dep M neuron **C.** Distance between soma and beginning of stratum radiatum for Hyp M and Dep M cells

311   **Opposite modulation of bursting and regular firing cells during locomotion and functional**  
312   **implications for hippocampal spatial coding**

313   Intracellular recordings *in vitro* (Graves et al., 2012) and *in vivo* (Kandel and Spencer, 1961;  
314   Epsztein et al., 2011) have revealed that CA1 pyramidal cells can respond to intracellularly  
315   injected steps of current with two different firing behaviors: firing groups of action  
316   potentials with short interspike intervals, also referred to as burst firing cells or action  
317   potentials with larger inter-spike intervals also referred to as regular firing cells. *In vitro*, the  
318   distribution of burst firing and regular firing CA1 pyramidal cells have been shown to vary  
319   along the proximo-distal axis (Jarsky et al., 2008) and to correspond to two different classes  
320   of neurons (Graves et al., 2012). Importantly, bursting and regular firing neurons appears to  
321   be functionally different (Epsztein et al., 2011; Cembrowski et al., 2018). In freely moving  
322   rats, burst firing cells are more readily recruited for spatial coding than regular firing cells  
323   when animals explore a new environment (Epsztein et al., 2011). However, the intracellular  
324   determinants of place cells coding vary between familiar and new environment with a likely  
325   switch from intrinsic to synaptic determinants (Cohen et al., 2017). We observed a  
326   preferential locomotion dependent hyperpolarization of bursting CA1 pyramidal cells during  
327   locomotion when mice explored a familiar environment while regular firing cells were  
328   depolarized. Interestingly, the bursting index, which reflects the propensity of spikes to be  
329   fired as bursts in a given cell, correlated with the strength and sign of the modulation. If  
330   bursting cells are preferentially recruited to be active and code for position as rats moves  
331   around in a new environment, locomotion-dependent hyperpolarization could counter  
332   select them to code in a familiar environment. Future work should examine the spatial  
333   coding of burst and regular firing cells in a familiar environment as well as the locomotion-  
334   dependent modulation of their  $V_m$  in a new environment.

335        Extracellular recordings have also revealed a differential distribution of bursting and  
336        regular firing cells along the deep-superficial axis in CA1, with deep cells located close to  
337        *stratum oriens* preferentially firing in bursts and superficial cells located close to *stratum*  
338        *radiatum* preferentially firing regularly (Mizuseki et al., 2011). While the link between  
339        intrinsic (as determined by intracellular step current injections) and functional (as  
340        determined by extracellular recordings of spontaneous firing) bursting properties are  
341        currently unknown, it is tempting to speculate that some correspondence exists between  
342        these cell classes. Recently, deep CA1 pyramidal cells were shown to be preferentially  
343        inhibited during sharp wave ripples (Valero et al., 2015), a behavior that was also observed  
344        for HypM bursting cells in the present study whose soma were not located superficially  
345        within the CA1 pyramidal cell layer. Interestingly, a recent report have shown that deep and  
346        superficial cells are differently engaged in spatial coding depending on the type of  
347        information available to the animal (Fattah et al., 2018). Deep cells are recruited to code  
348        positions close to external landmark cues (Geiller et al., 2017) when coding can rely on  
349        allothetic information while superficial cells are recruited to code positions away from  
350        landmarks when coding must rely on idiothetic information (Fattah et al., 2018). The  
351        opposite membrane potential modulation during locomotion between burst firing and  
352        regular firing cells could also provide a mean to differently recruit deep and superficial cells  
353        for spatial coding depending on external cues available for self-location.

354

355 **Material and methods**

356 **Animals**

357 All the experiments have been approved by the Institut National de la Santé et de la  
358 Recherche Médicale (INSERM), animal care and use committee and authorized by the  
359 Ministère de l'Education Nationale de l'Enseignement Supérieur et de la Recherche  
360 (agreement n° 02048.02), in agreement with the directives of the European Community  
361 Council (2010/63 / EU). Data were acquired on 13 C57BL6 mice and 1 CD-1 mouse aged from  
362 five to eight weeks weighting between 18 g and 28 g at the first surgery. The mice were  
363 housed 2 or 3 per cages before the first surgery and then individually with 12h inverted  
364 light/dark cycles. Trainings and recordings occurred during the dark phase. Water and food  
365 have been provided *ad libitum* upstream of the surgeries. After recovery from the first  
366 surgery, the mice were restricted to 1 ml/day of water and their weight and health were  
367 monitored daily during the following experiments.

368

369 **Surgery**

370 A first surgery is performed to implant a fixation bar used later for the fixation of the head.  
371 The animals were anesthetized with induction of 3% isoflurane followed by an  
372 intraperitoneal injection of Ketamine (100 mg/kg) mixed with Xylazine (10 mg/kg)  
373 supplemented with subcutaneous Buprenorphine injection (0.06 mg/kg). Jeweler's screws  
374 were inserted into the skull above the cerebellum and above the olfactory bulbs to anchor  
375 dental cement. A dental cement cap was then constructed leaving two areas of the skull free  
376 to subsequently perform the craniotomies necessary for registration (in reference to  
377 Bregma: Antero-Posteriority (AP): -2mm, Medio-Laterality (ML): -2.2) for the first target

378 necessary for intracellular recording and AP: -3mm and ML: -3.1 for the second target  
379 necessary for LFP recordings). In 4/14 mice, a LFP electrode (coated tungsten wire) was  
380 placed with an angle of 45° on z axis of an orthogonal reference frame and 45° on x axis until  
381 reaching the CA1 pyramidal layer determined by the presence of sharp wave-ripples. The  
382 electrode was then fixed with dental cement. The cement-free skull was coated with a 2%  
383 agarose layer and sealed with silicon elastomer (Kwik-Cast, World Precision Instruments). A  
384 small titanium bar (0.65 g, 12 x 6 mm) was subsequently inserted into the dental cement cap  
385 above the cerebellum. This bar is continuously present on the animals head and will serve as  
386 a point of attachment to a larger metal plate used only during training and recordings for  
387 fixing the head of the animals on the virtual reality device.

388

#### 389 **Virtual reality set up**

390 A commercially available virtual reality system (Phenosys Jetball-TFT) was combined with a  
391 custom designed 3D printed concave plastic wheel (center diameter: 12.5 cm; side diameter:  
392 7.5 cm; width: 14 cm, covered with silicon-based white coating) to allow 1D movement with  
393 a 1/1 coupling between the movements of the mouse on the wheel and the movements of  
394 its avatar in the virtual reality environment. The plastic wheel was preferred to the original  
395 ball which had a more variable coupling due to its lateral rotations. The movement  
396 information is transmitted to the computer which subsequently updates the position of the  
397 avatar in the virtual environment. The wheel was surrounded by six 19-inch TFT monitors  
398 covering a 270-degree angle (Fig.S1A). The monitors were put up so that the level of mouse's  
399 eyes corresponded to the lower third of the height of the screen. This elevation was made to  
400 take into account that the field of view of rodents is generally oriented upwards. A head  
401 fixation system (Luigs and Neumann) was located behind the animal to avoid interfering with

402 the display of the virtual reality environment. The movement of the wheel updated the  
403 position of the mouse. The mouse could only move forward or backward but could not go  
404 back to the middle of the track (see training section).

405

406 **Virtual Environments**

407 The environment used for trainings (10/14 mice, 13/17 cells) and during recording sessions  
408 (14/14 mice, 17/17 cells) was a 200-cm long and 32-cm wide virtual corridor composed of  
409 four successive symmetrical and distinct patterns (respectively black dots on a white  
410 background, black and green squares, black and white strips, green crosses on a black  
411 background) with two target images at the ends (gray circles on a yellow background and  
412 triangles on a yellow background; Fig.S1B,C). Three objects were present in the  
413 environment: a yellow origami crane (dimensions: 9 x 9 x 7 cm: position: 37 cm from the  
414 beginning of the corridor), a gray cube with a blue diamond pattern (dimensions: 5 x 5 x 5  
415 cm, position: 64 cm from the beginning of the corridor) and a tree (dimensions: 15 x 15 x 22  
416 cm, position: 175 cm from the beginning of the corridor), as well as symmetrical columns  
417 present outside the corridor (dimensions: 8 x 8 x 47 cm, positions from the beginning of the  
418 corridor: 58 and 143 cm, patterns: black rhombus on green background, black and white  
419 horizontal stripes). For five recordings, after exploration of this previous maze, mice were  
420 teleported in the same version of that maze except for objects in the environment which  
421 were removed from it. Four mice were trained in a virtual maze which was empty except a  
422 black and grey rhombus floor pattern and with a green circle place at 200 cm on the ground  
423 indicating the reward zone.

424    **Habituation and trainings**

425    The mice were first habituated to the experimenter by at least two daily manipulation  
426    sessions of at least 20 minutes which continued throughout the experiment. After a period  
427    of post-operative recovery of at least 3 days, mice were restricted to water (1 ml/day,  
428    including the amount of water taken during training) and their weight was controlled daily.  
429    Access to *ad libitum* water was restored if the weight of the animals decreased by less than  
430    80% of the pre-operative weight at any stage of training. Then, after 2 or 3 days of water  
431    deprivation, they were gradually trained to run in the virtual reality device. In first place,  
432    mice became familiar with the device by being head fixed on the wheel in a black virtual  
433    environment where it is possible to recover sweet water rewards (5%) of 8 µl every 50 cm.  
434    Following at least one training in the black environment, the animals were trained to run in  
435    the virtual environment described in the previous section. When an animal reaches the end  
436    of the labyrinth, a sweet water reward of 5% of 8 µl is given *via* an arm that unfolds and a  
437    pump controlled by a tactile licking sensor. Once the reward is taken by the animal, the arm  
438    returns to its original position and the avatar is teleported in the opposite direction until the  
439    next reward at the end of the corridor. Animals were initially trained during 10 minutes daily  
440    sessions in the environment with periods of breaks in a black environment without any task.  
441    During training, the time in the black environment was gradually increased to 60 minutes in  
442    order to better mimic the recording conditions.

443

444    **Recording procedures**

445    When animals reached stable behavioral performances in the training maze (at least 6  
446    training sessions and at least 1 session with 1.2 reward/minute performance), we performed  
447    intracellular recordings of hippocampal pyramidal cells as well as a recording of hippocampal

448 field using either a wire placed during initial surgery or a linear silicon probe (A-32 Buzsaki  
449 Probe, Neuronexus) with 32 recordings channels spaced with 25 or 50  $\mu\text{m}$  placed during  
450 recording day. For 2/17 recorded cells, LFP recordings were too noisy to be analyzed. The  
451 day before the recording, animals were anesthetized (induction: isoflurane 3%, maintenance  
452 with sleep mix: medetomidine (225 mg/kg), midazolam (6 mg/kg), and fentanyl (7.5 mg/kg),  
453 awaken with awake mix: atipamezole (1 mg/kg), flumazenil (600 mg/kg), and naloxone (180  
454 mg/kg)) and craniotomies were performed. Craniotomies were covered with agarose (~ 3%  
455 in saline) and then sealed with silicon elastomer (Kwik-Cast, World Precision Instruments).  
456 On the day of recording, the back of the silicon probe was covered with a thin layer of a red  
457 fluorescent dye (Dil, Life Technologies) so that the recording location was evaluated post-  
458 hoc histologically. The silicon probe was then descended in the brain with an angle of 45° on  
459 the z axis of an orthogonal reference frame and 45° on the x axis while the animal could  
460 move freely on the wheel with the screens displaying a black environment. The correct  
461 positioning of the probe in the pyramidal cell layer CA1 was verified by the presence of  
462 sharp-wave ripples during the stop of the animal on several channels. From the depth of  
463 CA1, the probe was then lowered with an additional 600-1100  $\mu\text{m}$  depth in order to reach  
464 other structures such as the dentate gyrus and CA3. After positioning the silicon probe, the  
465 intracellular recordings were performed.

466 Patch pipettes were made and visually checked the same morning of recording sessions. The  
467 average resistance of the pipettes was between 5 and 8 M $\Omega$  and was filled with an  
468 intracellular solution containing (in mM) K-gluconate: 135, HEPES: 10, Na<sub>2</sub>-phosphocreatine:  
469 10, KCl: 4, MgATP: 4, and Na<sub>3</sub>GTP: 0.3 (pH adjusted to 7.2), plus biocytin (0.05%) to allow the  
470 revelation of the recorded cells. The very first pipette of a recording session was filled with  
471 an extracellular medium (Ringer) and descended above the hippocampus to estimate the

472 depth of the CA1 layer (based on observation in the signal "sharp-wave ripples" during  
473 immobility). Once the CA1 depth was estimated, other pipettes were lowered into a voltage  
474 clamp configuration with a pulse of 10 mV at 20 Hz and a high pressure (> 400 mmpA) to  
475 reach around -100  $\mu$ m ahead the estimated depth of CA1. The pressure of the pipettes was  
476 then decreased to ~30 mmPA to allow clamping of the cells. If a recording pipette was  
477 clogged during the descent, it was replaced. Once the G $\Omega$  seal was obtained, a cell was  
478 opened by a negative pressure deflection to go into full cell configuration and the recording  
479 was set in a current clamp configuration. A discharge pattern was executed (current steps  
480 starting from -400 pA with an increment of 50 pA) upstream of each record in the virtual  
481 environment. Once the discharge pattern was performed, the virtual environment described  
482 previously was displayed and animals went back and forth. For 9/17 recordings,  
483 hyperpolarizing steps of current were injected (-100 pA) every 40 s during exploration. In  
484 case of failure of G $\Omega$ -seal or loss of the cell, the pipette was changed and the procedure was  
485 repeated.

486

#### 487 **Data acquisition**

488 The position of the animal in the virtual environment was digitized by the computer  
489 controlling the virtual reality (Phenosys) and sent to a digital - analogue card (0-4.5V, NI USB-  
490 6008 National Instrument Map) connected to a specialized acquisition card for intracellular  
491 recordings (molecular device, Digidata 1550A) and also connected to an external analog card  
492 (I / O card, Open Ephys) of a 256-channel acquisition card (Open Ephys) specialized in multi-  
493 channel probe recording.

494 The Open Ephys system and linear silicon probe recordings were not available during the  
495 first recordings present in this study so initial recordings (4/14 mice, 6/17 recorded cells)  
496 were carried out on continuous signals acquired on the molecular device card, Digidata  
497 1550A with a frequency of acquisition of 20 kHz. For other recordings (10/14 mice, 11/17  
498 recorded cells), electrophysiological signals were acquired on Open Ephys card at an  
499 acquisition frequency of 25 kHz (Open Ephys, Intan Technologies, RHD2132 amplifier with a  
500 RHD2000 USB card).

501

502 **Histological revelation, labelling and reconstruction:**

503 Biocytin revelation: After patch recording sessions, all animals were perfused with 4% PFA  
504 and brains were collected to put in a 4% PFA solution during 24h - 48h (depending on state  
505 of perfusion), then transferred in a 1X PBS solution before being sliced with 50-100 µm  
506 thickness. All animals received protocol of biocytin revelation. Biocytin was revealed by an  
507 incubation of streptavidin coupled with an Alexa 594 fluorophore (10/14 animals) or coupled  
508 with cyanin 3 (4/10 animals) at 1/1000 concentration in mix of 1X PBS, 0.3% triton and 2%  
509 Normal Goat Serum (NGS) (in order to permeabilize membranes and reduces nonspecific  
510 liaisons) under agitation at 4°C protected from light during 48h-72h. Slices were then  
511 washed during 10 minutes 3 times under agitation protected from light at 4°C with 1X PBS.  
512 Localization of labelled cells was determined with an Olympus SZX 16 stereomicroscope.  
513 Slice within the soma of labeled cell, as well as 2 slices before and 2 slices after, were  
514 identified and received calbindin positive labeling protocol (12/14 animals, 14/17 cells).

515 Calbindin labelling: Interest slices were incubated with a mix of 1X PBS, 0.3% triton and 7%  
516 NGS, during 2h at 4°C protected from light. Then, slices were incubated and agitated during

517 24h at 4°C protected from light with a primary rabbit antibody anti-calbin at 1/1000 in a mix  
518 of 1X PBS, 0.3% triton, 2% NGS added with streptavidin coupled with a fluorophore at  
519 1/1000 (Alexa 594 or cyanine 3) in order to maintain labeling of biocytin. After 3 washes of  
520 10 min in a mix of 1X PBS and triton 0.3%, slices were then incubated and agitated during  
521 24h at 4°C protected from light with a secondary donkey antibody anti-rabbit coupled with  
522 Alexa 488 fluorophore at 1/1000 in mix of 1X PBS, 0.3% triton, 2% NGS added with  
523 streptavidin coupled with a fluorophore at 1/1000 (Alexa 594 or cyanine 3). Finally, slices  
524 were washed during 10min 3 times in a mix of 1X PBS and 0.3% triton with agitation at 4°C  
525 protected from light and then 2 more washes with only 1X PBS in the same condition. Slices  
526 were then mounted between blades and coverslips using Vectashield (containing DAPI) and  
527 then sealed with uncolored nail polish.

528 **Microscope & reconstruction:** 6 brains were acquired using Leica SP5X streptal microscope in  
529 order to reconstruct labelled cells. Acquisition was made with a resolution of 2048 x 2048  
530 using a x40 lens and done with stacks 0.46 µm of thickness. 2 fully labelled neurons were  
531 reconstructed thanks to Neurolucida® software (Fig. S4). These two neurons were also  
532 acquired with a x10 lens for a wide view and x40 for an isolated view of the neuron using a  
533 Zeiss LSM 800 microscope.

534

535 **Data Analysis**

536 Analyzes were performed by custom developed programs written in MATLAB (MathWorks).  
537 17 cells were recorded with duration from 1 to 23 min in the maze (mean: 8 min 25 s ± 1 min  
538 34 s). Animals performed at least one lap in the environment (mean: 6.82 ± 1.3).

539    Intrinsic properties: Intrinsic properties features comes from pattern discharge executed  
540    before exploration of the environment. The resting membrane potential of the cells was  
541    determined as the average of the first 15 milliseconds of the recording. Series and the input  
542    resistances were calculated by fitting a linear curve on all the hyperpolarizing and  
543    depolarizing current steps excluding steps with action potentials. The discharge threshold  
544    has been recovered on the first action potential emitted by the cell in response to a  
545    minimum current. It was defined as the value of the membrane potential where the  
546    derivative of the signal exceeded  $10 \text{ mV.s}^{-1}$ . The spike amplitude was calculated as the  
547    difference between peak of this first action potential and the threshold. The Rheobase was  
548    calculated by fitting a linear regression curve on the firing frequency depending on steps of  
549    current. The value taken was the theoretical minimal injection of current needed to evoke  
550    one spike. Rheobase values were then validated manually if aberrant values were found by  
551    the fit (11/17 values kept). The bursting index was calculated on the first current step with  
552    at least 5 action potentials (AP) and by calculating the ratio of the number of action potential  
553    discharging in bursts (PA with an inter-potential interval less than 10 ms) over the total  
554    number of action potential present during the pulse.

555

556    Subthreshold  $V_m$ : Subthreshold  $V_m$  has been determined using the following steps. First, a  
557    window of stable  $V_m$  were selected on recorded cells. Artifacts (aberrant loss of signal) were  
558    manually selected and removed by linearizing the  $V_m$  between edges (9/17 recordings).  
559    Influence of series resistance on  $V_m$  was automatically corrected following the Ohm law  $U =$   
560     $R_s.I$ , based on series resistance values taken from intrinsic properties. Action potentials from  
561     $V_m$  were detected automatically using a high pass filter (100 Hz) and an adjustable threshold

562 equal to 4 times the  $V_m$  standard deviation (s.d.). Good detection of spikes was then checked  
563 manually. Edges of spikes were defined as 2 ms before and 8 ms after action potential peak.  
564 Complex spikes from  $V_m$  were detected using different filters and thresholds. A vector was  
565 computed in order to detect slow component of a complex spike. This vector corresponds to  
566 a band pass filtered  $V_m$  (0.5-20 Hz), which positive values were squared. The final vector was  
567 z-scored. Putative indexes of complex spike were detected using 2 thresholds. A first  
568 threshold was equal to 10 (value of z-score) and then extended using a lower threshold  
569 equal to 5 when the difference between both threshold indexes did not exceed 30 ms. Short  
570 detected events inferior to 30 ms were then removed. Next, edges of putative events were  
571 asymmetrically extended by 25 ms before and 4 ms after putative complex spikes. Finally, all  
572 putative complex spikes edges were checked and manually corrected if needed. Spikes and  
573 complex spikes were removed by linearizing the  $V_m$  between edges of events. Small  $V_m$  drift  
574 was compensated using a low pass filter (0.1 Hz) in order to realign  $V_m$ . Hyperpolarizing steps  
575 of current were automatically detected on the current trace and removed from the  $V_m$  trace  
576 by linearizing. Current trace was first filtered at 1 Hz, then indexes were found by using a  
577 threshold equal to 5 times the standard deviation of the current trace. Only periods < 200  
578 ms were included. Indexes separated by less than 40 ms were merged. Finally indexes were  
579 extended with 10 ms before and 40 ms after edges of detected periods.

580

581 Locomotion/immobility periods: To detect locomotion and immobility periods, the velocity  
582 vector was calculated on the signal position in the environment (6/17 recordings) or, when  
583 available, directly on the signal of the motion sensor downsampled at 100 Hz and then  
584 smoothed (11/17 recordings). The speed corresponds to the derivative of the smoothed

585 position vector then smoothed again with a half-width Gaussian of 0.5 s. Because the reward  
586 system freezes the virtual environment in the reward zone but did not physically stop the  
587 wheel on which the animal is walking, rewards zone were excluded from the analysis when  
588 the wheel movement signal was not available. Putative periods of locomotion and  
589 immobility were detected by applying a speed threshold of 0.5 cm.s<sup>-1</sup>. Then, periods  
590 separated by less than 0.5 s have been merged. Finally, only periods greater than or equal to  
591 2 s have been preserved, others were unlabeled. Transitions periods were defined as periods  
592 centered on the index for which the animal went from immobility to locomotion or vice  
593 versa. Transitions had a total duration of 4 s (2 s immobility and 2 s locomotion).

594

595 Subthreshold V<sub>m</sub> features during Locomotion/Immobility: Mean subthreshold V<sub>m</sub>,  
596 subthreshold V<sub>m</sub> variance and mean spontaneous firing rate were calculated for each  
597 locomotion/immobility period. To be able to compare the V<sub>m</sub> of different neurons, the Z-  
598 score was computed on the subthreshold V<sub>m</sub>. Intracellular spectrogram was computed by  
599 using a time-frequency decomposition with complex Morlet wavelets with central  
600 frequencies from 0 to 40 Hz in 0.2 Hz steps on a downsampled signal (250 Hz). Power values  
601 in a given frequency range were normalized by the squared root of the frequency. Then  
602 mean power values were calculated during immobility and locomotion periods. For  
603 scatterplots in Fig.1 and Fig.2, only successive periods of immobility and movement were  
604 considered in order to be able to plot values face to face in scatter plots. For the  
605 supplementary figure 3, scatter plots during transitions periods come from values between -  
606 2 s and -1 s versus values between +1 s and +2 s (0 s being the center of the transition).

607

608    Modulation index computation: Cells were classified as Depolarized (Dep M) or  
609    hyperpolarized (Hyp M) during locomotion depending on a subthreshold  $V_m$  modulation  
610    index. This index was calculated by counting for each period of locomotion occurring before  
611    or after a given period of immobility the percentage of  $V_m$  values higher than the median of  
612    the  $V_m$  during the immobility period. 750 ms before and after each locomotion/immobility  
613    was removed to compute this index. The percentage has been rescaled to get an index from  
614    -1 to 1 used to classify DepM and HypM cells.

615

616    Speed correlation: Z-score Subthreshold  $V_m$  trace was filtered with a lowpass filter at 5Hz,  
617    then downsampled at 100Hz and smoothed with a half-width Gaussian of 1 sec. Next, for  
618    each neuron a correlation coefficient was computed by calculating the correlation  
619    coefficient between averaged Z-score Subth.  $V_m$  values and Speed vector binned in 0.05  
620    cm.s-1 bins containing at least 4 values. For each neuron a mean coefficient correlation was  
621    also calculated based on the mean of correlation coefficient during each moving periods.

622

623    Ripples detection: Ripples were detected on the CA1 LFP signal when available (15/17  
624    recordings) during immobility. To detect ripples, LFP signal was filtered between 100Hz  
625    and 300Hz, then squared and smoothed with an half Gaussian of 10 ms and finally z-scored.  
626    Putative indexes of ripples were detected using 2 thresholds. A first threshold was equal to 5  
627    times the s.d. of the signal and then extended using a lower threshold equal to 2 times the  
628    signal s.d. when the difference between both threshold indexes did not exceed 18 ms. Then  
629    putative ripples periods were merged if they were separated by an amount of time inferior  
630    to 30 ms. Next, periods of ripples were extended by 5 ms in each direction and then, a time

631 restriction was applied in order to conserve only putative periods of at least 25 ms. Finally,  
632 putative periods of ripples were then checked manually and time of occurrence of ripple was  
633 taken as the index of maximum of signal in the ripple period.

634

635 Ripples modulation features computation: Subthreshold  $V_m$  modulation by ripples was  
636 computed by using a shuffling method repeated 1000 times. At each iteration, a randomized  
637 vector was calculated by shuffling the subthreshold  $V_m$  values within a time window from 2  
638 times the length of the ripple before its start to the end of the ripple. Then the number of  
639 times where subthreshold  $V_m$  was superior or inferior of randomized vector was counted. If  
640 the subthreshold  $V_m$  is superior or inferior to 95% of the 1000 randomized vectors for 10%  
641 of the ripple period duration, then the modulation of the  $V_m$  by the ripple was considered as  
642 significant. Baseline used to calculate  $\Delta V_m$  modulation during ripple was calculated as  
643 the mean of Subthreshold  $V_m$  within a time window from 2 times the length of ripple to its  
644 start.  $\Delta V_m$  was computed as the maximum or minimum significant subthreshold  $V_m$   
645 value minus the Baseline. If two significant  $V_m$  modulations were present in one ripple  
646 period, the first one occurring was taken to calculate the  $\Delta V_m$ .

647

648 Statistical analysis: All statistical analyses were conducted using Matlab codes (MathWorks).  
649 For each distribution, a Lilliefors goodness-of-fit test was used to verify if the data were  
650 normally distributed and a Levene test was used to assess for equal variance. If normality or  
651 equal variance were not verified, we used the Wilcoxon rank sum test otherwise the Student  
652 t-test was used. For paired test, normality was verified by Lilliefors goodness-of-fit test. If

653 normality was not verified, we used the Wilcoxon signed rank test otherwise the Student  
654 paired t-test. In figure or text, all results were given with means  $\pm$  the s.e.m..

655      **References**

- 656      Albergaria C, Silva NT, Pritchett DL, Carey MR (2018) Locomotor activity modulates associative  
657      learning in mouse cerebellum. *Nat Neurosci* 21:725-735.
- 658
- 659      Arriaga M, Han EB (2017) Dedicated Hippocampal Inhibitory Networks for Locomotion and  
660      Immobility. *J Neurosci* 37:9222–9238.
- 661
- 662      Arroyo S, Bennett C, Hestrin S (2018) Correlation of Synaptic Inputs in the Visual Cortex of Awake,  
663      Behaving Mice. *Neuron* 99:1289–1301.
- 664
- 665      Bennett C, Arroyo S, Hestrin S (2013) Subthreshold mechanisms underlying state-dependent  
666      modulation of visual responses. *Neuron* 80:350–357.
- 667
- 668      Bittner KC, Grienberger C, Vaidya SP, Milstein AD, Macklin JJ, Suh J, Tonegawa S, Magee JC (2015)  
669      Conjunctive input processing drives feature selectivity in hippocampal CA1 neurons. *Nat Neurosci*  
670      18:1133–1142.
- 671
- 672      Buzsaki G (1989) Two-stage model of memory trace formation: a role for “noisy” brain states.  
673      *Neuroscience*. 31:551-570.
- 674
- 675      Buzsáki G (2015) Hippocampal sharp wave-ripple: A cognitive biomarker for episodic memory and  
676      planning. *Hippocampus* 25:1073–1188.
- 677
- 678      Buzsáki G, Horváth Z, Urioste R, Hetke J, Wise K (1992) High-frequency network oscillation in the  
679      hippocampus. *Science* 256:1025-1027.
- 680
- 681      Cembrowski MS, Phillips MG, DiLisio SF, Shields BC, Winnubst J, Chandrashekhar J, Bas E, Spruston N  
682      (2018) Dissociable Structural and Functional Hippocampal Outputs *via* Distinct Subiculum Cell  
683      Classes. *Cell* 173:1280–1292.
- 684
- 685      Cohen JD, Bolstad M, Lee AK (2017) Experience-dependent shaping of hippocampal CA1 intracellular  
686      activity in novel and familiar environments. *Elife* 6:1–27.
- 687
- 688      Colgin LL (2016) Rhythms of the hippocampal network. *Nat Rev Neurosci* 17:239–249.
- 689
- 690      Crochet S, Petersen CCH (2006) Correlating whisker behavior with membrane potential in barrel  
691      cortex of awake mice. *Nat Neurosci*. 9:608-610.
- 692
- 693      Czurkó A, Hirase H, Csicsvari J, Buzsáki G (1999) Sustained activation of hippocampal pyramidal cells  
694      by ‘space clamping’ in a running wheel. *Eur J Neurosci* 11:344–352.
- 695
- 696      English DF, Peyrache A, Stark E, Roux L, Vallentin D, Long MA, Buzsáki G (2014) Excitation and  
697      Inhibition Compete to Control Spiking during Hippocampal Ripples: Intracellular Study in Behaving  
698      Mice. *J Neurosci* 34:16509–16517.
- 699
- 700      Epsztein J, Brecht M, Lee AK (2011) Intracellular Determinants of Hippocampal CA1 Place and Silent  
701      Cell Activity in a Novel Environment. *Neuron* 70:109–120.
- 702
- 703      Epsztein J, Lee AK, Chorov E, Brecht M (2010) Impact of spikelets on hippocampal CA1 pyramidal cell  
704      activity during spatial exploration. *Science* 327:474–477.

- 705  
706 Fattah M, Sharif F, Geiller T, Royer S (2018) Differential Representation of Landmark and Self-Motion  
707 Information along the CA1 Radial Axis: Self-Motion Generated Place Fields Shift toward Landmarks  
708 during Septal Inactivation. *J Neurosci* 38:6766–6778.
- 709  
710 Foster DJ, Wilson MA (2006) Reverse replay of behavioural sequences in hippocampal place cells  
711 during the awake state. *Nature* 440:680–683.
- 712  
713 Fuhrmann F, Justus D, Sosulina L, Kaneko H, Beutel T, Friedrichs D, Schoch S, Schwarz MK, Fuhrmann  
714 M, Remy S (2015) Locomotion, Theta Oscillations, and the Speed-Correlated Firing of Hippocampal  
715 Neurons Are Controlled by a Medial Septal Glutamatergic Circuit. *Neuron* 86:1253–1264.
- 716  
717 Gan J, Weng S ming, Pernía-Andrade AJ, Csicsvari J, Jonas P (2017) Phase-Locked Inhibition, but Not  
718 Excitation, Underlies Hippocampal Ripple Oscillations in Awake Mice In Vivo. *Neuron* 93:308–314.
- 719  
720 Geiller T, Fattah M, Choi JS, Royer S (2017) Place cells are more strongly tied to landmarks in deep  
721 than in superficial CA1. *Nat Commun* 8:14531.
- 722  
723 Girardeau G, Zugaro M (2011) Hippocampal ripples and memory consolidation. *Curr Opin Neurobiol*  
724 21:452–459.
- 725  
726 Graves AR, Moore SJ, Bloss EB, Mensh BD, Kath WL, Spruston N (2012) Hippocampal Pyramidal  
727 Neurons Comprise Two Distinct Cell Types that Are Countermodulated by Metabotropic Receptors.  
728 *Neuron* 76:776–789.
- 729  
730 Grienberger C, Milstein AD, Bittner KC, Romani S, Magee JC (2017) Inhibitory suppression of  
731 heterogeneously tuned excitation enhances spatial coding in CA1 place cells. *Nat Neurosci* 20:417–  
732 426.
- 733  
734 Gupta AS, van der Meer MAA, Touretzky DS, Redish AD (2010) Hippocampal Replay Is Not a Simple  
735 Function of Experience. *Neuron* 65:695–705.
- 736  
737 Harvey CD, Collman F, Dombeck DA, Tank DW (2009) Intracellular dynamics of hippocampal place  
738 cells during virtual navigation. *Nature* 461:941–946.
- 739  
740 Hsu CL, Zhao X, Milstein AD, Spruston N (2018) Persistent Sodium Current Mediates the Steep  
741 Voltage Dependence of Spatial Coding in Hippocampal Pyramidal Neurons. *Neuron* 99:147–162.
- 742  
743 Hulse BK, Lubenov E V., Siapas AG (2017) Brain State Dependence of Hippocampal Subthreshold  
744 Activity in Awake Mice. *Cell Rep* 18:136–147.
- 745  
746 Hulse BK, Moreaux LC, Lubenov E V., Siapas AG (2016) Membrane Potential Dynamics of CA1  
747 Pyramidal Neurons during Hippocampal Ripples in Awake Mice. *Neuron* 89:800–813.
- 748  
749 Jarsky T, Mady R, Kennedy B, Spruston N (2008) Distribution of bursting neurons in the CA1 region  
750 and the subiculum of the rat hippocampus. *J Comp Neurol* 506:535–547.
- 751  
752 Kandel ER, Spencer WA (1961) Electrophysiology of hippocampal neurons: II. After-potentials and  
753 repetitive firing. *J Neurophysiol* 24:243–259.
- 754  
755 Kay K, Frank LM (2018) Three brain states in the hippocampus and beyond. *Hippocampus*. In press.
- 756

- 757 Kay K, Sosa M, Chung JE, Karlsson MP, Larkin MC, Frank LM (2016) A hippocampal network for spatial  
758 coding during immobility and sleep. *Nature* 531:185–190.
- 759
- 760 Lapray D, Lasztoczi B, Lagler M, Viney TJ, Katona L, Valenti O, Hartwich K, Borhegyi Z, Somogyi P,  
761 Klausberger T (2012) Behavior-dependent specialization of identified hippocampal interneurons. *Nat  
762 Neurosci* 15:1265–1271.
- 763
- 764 Lee D, Lin BJ, Lee AK (2012) Hippocampal place fields emerge upon single-cell manipulation of  
765 excitability during behavior. *Science* 337:849–853.
- 766
- 767 McGinley MJ, David S V., McCormick DA (2015) Cortical Membrane Potential Signature of Optimal  
768 States for Sensory Signal Detection. *Neuron* 87:179–192.
- 769
- 770 McNaughton BL, Barnes CA, O’Keefe J (1983) The contributions of position, direction, and velocity to  
771 single unit activity in the hippocampus of freely-moving rats. *Exp Brain Res.* 52:41–49.
- 772
- 773 Mizuseki K, Diba K, Pastalkova E, Buzsáki G (2011) Hippocampal CA1 pyramidal cells form functionally  
774 distinct sublayers. *Nat Neurosci* 14:1174–1183.
- 775
- 776 Moser EI, Moser M-B, McNaughton BL (2017) Spatial representation in the hippocampal formation: a  
777 history. *Nat Neurosci* 20:1448–1464.
- 778
- 779 Niell CM, Stryker MP (2010) Modulation of Visual Responses by Behavioral State in Mouse Visual  
780 Cortex. *Neuron* 65:472–479.
- 781
- 782 O’Keefe J, Dostrovsky J (1971) The hippocampus as a spatial map. Preliminary evidence from unit  
783 activity in the freely-moving rat. *Brain Res* 34:171–175.
- 784
- 785 O’Keefe J, Nadel L (1978) The hippocampus as a cognitive map. London: Oxford University Press.
- 786
- 787 Pfeiffer BE, Foster DJ (2013) Hippocampal place-cell sequences depict future paths to remembered  
788 goals. *Nature* 497:74–79.
- 789
- 790 Polack PO, Friedman J, Golshani P (2013) Cellular mechanisms of brain state-dependent gain  
791 modulation in visual cortex. *Nat Neurosci* 16:1331–1339.
- 792
- 793 Roumis DK, Frank LM (2015) Hippocampal sharp-wave ripples in waking and sleeping states. *Curr  
794 Opin Neurobiol* 35:6–12.
- 795
- 796 Rowland DC, Yanovich Y, Kentros CG (2011) A stable hippocampal representation of a space requires  
797 its direct experience. *Proc Natl Acad Sci* 108:14654–14658.
- 798
- 799 Thompson LT, Best PJ (1989) Place Cells and Silent Cells in the Hippocampus Rats of. *J Neurosci*  
800 9:2382–2390.
- 801
- 802 Valero M, Cid E, Averkin RG, Aguilar J, Sanchez-Aguilera A, Viney TJ, Gomez-Dominguez D, Bellistri E,  
803 De La Prida LM (2015) Determinants of different deep and superficial CA1 pyramidal cell dynamics  
804 during sharp-wave ripples. *Nat Neurosci* 18:1281–1290.
- 805
- 806 Vanderwolf CH (1969) Hippocampal electrical activity and voluntary movement in the rat.  
807 *Electroencephalogr Clin Neurophysiol.* 26:407–418.
- 808

- 809 Vinck M, Batista-Brito R, Knoblich U, Cardin JA (2015) Arousal and Locomotion Make Distinct  
810 Contributions to Cortical Activity Patterns and Visual Encoding. *Neuron* 86:740–754.  
811  
812 Wilson M, McNaughton B (1993) Dynamics of the hippocampal ensemble code for space. *Science*  
813 (80- ) 261:1055–1058.  
814

## COLOPHON

This document generated using a slight modification of the template `classicthesis` developed by André Miede and Ivo Pletikosić<sup>2</sup>. The style was inspired by Robert Bringhurst's seminal book on typography "*The Elements of Typographic Style*" and Aaron Turon PhD Thesis.

The really nice rats you found in the illustration of this thesis work were adapted from Etienne Ackermann github repository <sup>3</sup>.

*Final Version as of October 27, 2019 (classicthesis v4.6).*

---

<sup>2</sup> <https://ctan.org/pkg/classicthesis>

<sup>3</sup> <https://github.com/eackermann/ratpack>



Part V  
BIBLIOGRAPHY



## BIBLIOGRAPHY

---

- Acsády, László, Anita Kamondi, Attila Sík, Tamás Freund, and György Buzsáki (1998). "GABAergic cells are the major postsynaptic targets of mossy fibers in the rat hippocampus." In: *Journal of Neuroscience* 18.9, pp. 3386–3403 (cit. on p. 15).
- Agarwal, Gautam, Ian H. Stevenson, Antal Bereényi, Kenji Mizuseki, György Buzsáki, and Friedrich T. Sommer (2014). "Spatially distributed local fields in the hippocampus encode rat position." In: *Science* 344.6184, pp. 626–630 (cit. on p. 67).
- Aggleton, J P, P R Hunt, and J N Rawlins (Feb. 1986). "The effects of hippocampal lesions upon spatial and non-spatial tests of working memory." In: *Behavioural brain research* 19.2, pp. 133–46 (cit. on p. 69).
- Aghajan, Zahra M., Lavanya Acharya, Jason J. Moore, Jesse D. Cushman, Cliff Vuong, and Mayank R. Mehta (Jan. 2015). "Impaired spatial selectivity and intact phase precession in two-dimensional virtual reality." In: *Nature neuroscience* 18.1, pp. 121–8 (cit. on pp. 44, 45, 56, 137, 138, 140).
- Agster, Kara L., Inês Tomás Pereira, Michael P Saddoris, and Rebecca D. Burwell (2016). "Subcortical connections of the perirhinal, postrhinal, and entorhinal cortices of the rat. II. efferents." In: *Hippocampus* 26.9, pp. 1213–30 (cit. on pp. 20–22).
- Ahn, Jae Rong, Hyun Woo Lee, and Inah Lee (2019). "Rhythmic Pruning of Perceptual Noise for Object Representation in the Hippocampus and Perirhinal Cortex in Rats." In: *Cell Reports* 26.9, 2362–2376.e4 (cit. on pp. 80, 140).
- Ahn, Jae Rong and Inah Lee (2017). "Neural Correlates of Both Perception and Memory for Objects in the Rodent Perirhinal Cortex." In: *Cerebral Cortex* 27.7, pp. 3856–3868 (cit. on pp. 77, 80, 140).
- Aikath, Devdeep, Aldis P. Weible, David C. Rowland, and Clifford G. Kentros (2014). "Role of self-generated odor cues in contextual representation." In: *Hippocampus* 24.8, pp. 1039–1051 (cit. on pp. 48–50).
- Alexander, Andrew S., Lucas C. Carstensen, James R. Hinman, Florian Raudies, G. William Chapman, and Michael E. Hasselmo (2019). "Egocentric boundary vector tuning of the retrosplenial cortex." In: *bioRxiv*, pp. 1–56 (cit. on p. 81).
- Alexander, Andrew S. and Douglas A. Nitz (2017). "Spatially Periodic Activation Patterns of Retrosplenial Cortex Encode Route Sub-spaces and Distance Traveled." In: *Current Biology* 27.11, 1551–1560.e4 (cit. on pp. 54, 145).
- Allen, Kevin, J. Nick P. Rawlins, David M. Bannerman, and Jozsef Csicsvari (Oct. 2012). "Hippocampal place cells can encode multiple trial-dependent features through rate remapping." In: *The Journal of neuroscience* 32.42, pp. 14752–66 (cit. on p. 39).
- Alme, Charlotte B., Chenglin Miao, Karel Jezek, Alessandro Treves, Edvard I. Moser, and May-Britt Moser (2014). "Place cells in the hippocampus: Eleven maps for eleven rooms." In: *Pnas* 111.52 (cit. on pp. 40, 41).
- Almog, Noam, Gilad Tocker, Tora Bonnevie, Edvard Moser, May-britt Moser, and Dori Derdikman (2019). "During hippocampal inactivation , grid cells maintain their synchrony , even when the grid pattern is lost." In: *bioRxiv*, pp. 1–21 (cit. on p. 31).
- Amaral, D; and P. Lavenex (2006). "Ch 3. Hippocampal Neuroanatomy." In: *The Hippocampus Book*. Oxford University Press (cit. on p. 13).
- Amaral, David G. (1978). "A golgi study of cell types in the hilar region of the hippocampus in the rat." In: *Journal of Comparative Neurology* 182.5, pp. 851–914 (cit. on p. 15).
- Amaral, David G., Cynthia Dolorfo, and Pablo Alvarez-Royo (1991). "Organization of CA1 projections to the subiculum: A PHA-L analysis in the rat." In: *Hippocampus* 1.4, pp. 415–435 (cit. on p. 19).

- Amaral, David G., Helen E. Scharfman, and Pierre Lavenex (2007). "The dentate gyrus: fundamental neuroanatomical organization (dentate gyrus for dummies)." In: *Progress in Brain Research*. Vol. 163, pp. 3–22 (cit. on p. 13).
- Andersen, P., T. V.P. Bliss, and K. K. Skrede (1971). "Lamellar organization of hippocampal excitatory pathways." In: *Experimental Brain Research* 13.2, pp. 222–238 (cit. on p. 13).
- Andersen, Per, Richard Morris, David Amaral, Tim Bliss, and John O'Keefe (Dec. 2006). *The Hippocampus Book*. Ed. by Per Andersen, Richard Morris, David Amaral, Tim Bliss, and John O'Keefe. Oxford University Press (cit. on pp. 16, 17).
- Aoki, Yuki, Hideyoshi Igata, Yuji Ikegaya, and Takuya Sasaki (Apr. 2019). "The Integration of Goal-Directed Signals onto Spatial Maps of Hippocampal Place Cells." In: *Cell Reports* 27.5, 1516–1527.e5 (cit. on p. 56).
- Aranzi, Giulio Cesare (1587). *De humano foetu liber*. Text in Latin with Greek references. Venetiis: Apud Iacobum Brechtanum (cit. on p. 12).
- Aronov, Dmitriy, Rhino Nevers, and David W. Tank (2017). "Mapping of a non-spatial dimension by the hippocampal-entorhinal circuit." In: *Nature* 543:7647, pp. 719–722 (cit. on pp. 28, 32, 139).
- Aronov, Dmitriy and David W. Tank (Oct. 2014). "Engagement of neural circuits underlying 2D spatial navigation in a rodent virtual reality system." In: *Neuron* 84.2, pp. 442–56 (cit. on pp. 45, 137, 146).
- Attneave, Fred (1954). "Some Informational Aspects of Visual Perception." In: *Psychological Review* 61.3 (cit. on pp. 35, 142).
- Banino, Andrea, Caswell Barry, Benigno Uria, Charles Blundell, Timothy Lillicrap, Piotr Mirowski, Alexander Pritzel, Martin J Chadwick, Thomas Degris, Joseph Modayil, Greg Wayne, Hubert Soyer, Fabio Viola, Brian Zhang, Ross Goroshin, Neil Rabinowitz, Razvan Pascanu, Charlie Beattie, Stig Petersen, Amir Sadik, Stephen Gaffney, Helen King, Koray Kavukcuoglu, Demis Hassabis, Raia Hadsell, and Dhrushan Kumaran (2018). "Vector-based navigation using grid-like representations in artificial agents." In: *Nature* 557:7705, pp. 429–433 (cit. on p. 32).
- Barlow, H. B. (1961). "Possible Principles Underlying the Transformations of Sensory Messages." In: *Sensory Communication*, pp. 216–234 (cit. on p. 35).
- Barlow, John S. (1964). "Inertial navigation as a basis for animal navigation." In: *Journal of Theoretical Biology* 6.1, pp. 76–117 (cit. on pp. 6, 142).
- Barry, Caswell, Robin Hayman, Neil Burgess, and Kathryn J Jeffery (2007). "Experience-dependent rescaling of entorhinal grids." In: *Nature neuroscience* 10.6, pp. 682–684 (cit. on pp. 30, 32).
- Barry, Caswell, Colin Lever, Robin Hayman, Tom Hartley, Stephen Burton, O'Keefe John, Kate Jeffery, Neil Burgess, John O'Keefe, Kate Jeffery, and Neil Burgess (Jan. 2006). "The boundary vector cell model of place cell firing and spatial memory." eng. In: *Reviews in the neurosciences* 17.1-2, pp. 71–97 (cit. on pp. 52, 53, 133, 145).
- Battaglia, Francesco P, Gary R Sutherland, and Bruce L McNaughton (May 2004). "Local sensory cues and place cell directionality: additional evidence of prospective coding in the hippocampus." In: *The Journal of neuroscience : the official journal of the Society for Neuroscience* 24.19, pp. 4541–50 (cit. on pp. 46, 47, 63, 87, 133, 134, 143, 146).
- Behrens, Timothy E J, Timothy H Muller, James C R Whittington, Shirley Mark, Alon B Baram, Kimberley L Stachenfeld, and Zeb Kurth-Nelson (2018). "What is a cognitive map? Organising knowledge for flexible behaviour." In: (cit. on p. 32).
- Bellmund, Jacob L.S., Peter Gärdenfors, Edvard I. Moser, and Christian F. Doeller (2018). "Navigating cognition: Spatial codes for human thinking." In: *Science (New York, N.Y.)* 362.6415 (cit. on p. 32).
- Benhamou, Simon (2010). "Orientation and Navigation." In: *Encyclopedia of Behavioral Neuroscience*. Vol. 2, pp. 497–503 (cit. on p. 1).
- Biegler, R. and Richard G. M. Morris (Feb. 1994). "Landmark stability is a prerequisite for spatial but not discrimination learning." In: *Nature* 361.6413, pp. 631–633 (cit. on pp. 74, 84).

- Biegler, R and R G M Morris (1996). "Landmark stability: Further studies pointing to a role in spatial learning." In: *Quarterly Journal of Experimental Psychology Section B-Comparative and Physiological Psychology* 49.4, pp. 307–345 (cit. on pp. 74, 75, 84, 140).
- Bir, Shyamal C., Sudheer Ambekar, Sunil Kukreja, and Anil Nanda (2015). "Julius Caesar Arantius (Giulio Cesare Aranzi, 1530–1589) and the hippocampus of the human brain: history behind the discovery." In: *Journal of Neurosurgery* 122.4, pp. 971–975 (cit. on p. 12).
- Boccara, Charlotte N., Francesca Sargolini, Veslemøy Hult Thoresen, Trygve Solstad, Menno P. Witter, Edvard I. Moser, and May Britt Moser (2010). "Grid cells in pre-and parasubiculum." In: *Nature Neuroscience* 13.8, pp. 987–994 (cit. on pp. 30, 52).
- Boccara, Charlotte N., Michele Nardin, Federico Stella, Joseph O'Neill, Jozsef Csicsvari, Joseph O'Neill, and Jozsef Csicsvari (2019). "The entorhinal cognitive map is attracted to goals." In: *Science* 1447.March, pp. 1443–1447 (cit. on pp. 32, 57, 145).
- Bostock, Elizabeth, Robert U. Muller, and John L. Kubie (Apr. 1991). "Experience-dependent modifications of hippocampal place cell firing." In: *Hippocampus* 1.2, pp. 193–205 (cit. on pp. 26, 27, 44, 64).
- Bourboulou, Romain, Geoffrey Marti, François-Xavier Michon, Elissa El Feghaly, Morgane Nouguier, David Robbe, Julie Koenig, and Jerome Epsztein (Mar. 2019). "Dynamic control of hippocampal spatial coding resolution by local visual cues." In: *eLife* 8, pp. 1–30 (cit. on pp. 33, 45, 50).
- Bourboulou, Romain, Geoffrey Marti, François-Xavier Michon, Morgane Nouguier, David Robbe, Julie Koenig, and Jérôme Epsztein (2017). "Influence of proximal 3D objects on hippocampal spatial representation in mice navigating virtual linear mazes." In: *Society for Neuroscience 2017* (cit. on p. 144).
- Brandon, Mark P., Julie Koenig, and Stefan Leutgeb (2014). "Parallel and convergent processing in grid cell, head-direction cell, boundary cell, and place cell networks." In: *Wiley Interdisciplinary Reviews: Cognitive Science* 5.2, pp. 207–219 (cit. on pp. 20, 24).
- Brodmann, K (1909). *Vergleichende Lokalisationslehre der Grosshirnrinde in ihren Prinzipien dargestellt auf Grund des Zellenbaues*. German. Leipzig: Johann Ambrosius Barth (cit. on p. 20).
- Brown, Emery N., Loren M. Frank, Dengda Tang, Michael C Quirk, and Matthew A Wilson (1998). "A statistical paradigm for neural spike train decoding applied to position prediction from ensemble firing patterns of rat hippocampal place cells." In: *Journal of Neuroscience* 18.18, pp. 7411–7425 (cit. on pp. 27, 34, 66, 67).
- Brunec, Iva K., Morris Moscovitch, and Morgan D. Barense (2018). "Boundaries Shape Cognitive Representations of Spaces and Events." In: *Trends in Cognitive Sciences* 22.7, pp. 637–650 (cit. on p. 145).
- Brunns, Conner R. and Brent C. Chamberlain (2019). "The influence of landmarks and urban form on cognitive maps using virtual reality." In: *Landscape and Urban Planning* 189.May 2018, pp. 296–306 (cit. on p. 73).
- Buckmaster, Paul S., H. Jürgen Wenzel, Dennis D. Kunkel, and Philip A. Schwartzkroin (1996). "Axon arbors and synaptic connections of hippocampal mossy cells in the rat *in vivo*." In: *Journal of Comparative Neurology* 366.2, pp. 270–292 (cit. on p. 15).
- Burak, Yoram (Apr. 2014). "Spatial coding and attractor dynamics of grid cells in the entorhinal cortex." In: *Current opinion in neurobiology* 25, pp. 169–75 (cit. on p. 31).
- Burak, Yoram and Ila R Fiete (2009). "Accurate Path Integration in Continuous Attractor Network Models of Grid Cells." In: *PLoS Computational Biology* 5.2 (cit. on pp. 31, 32).
- Burgess, Neil and John O'Keefe (1996). "Neuronal computations underlying the firing of place cells and their role in navigation." In: *Hippocampus* 6.6, pp. 749–762 (cit. on p. 55).
- Burgess, Neil, Hugo J. Spiers, and Eleni Paleologou (2004). "Orientational manoeuvres in the dark: Dissociating allocentric and egocentric influences on spatial memory." In: *Cognition* 94.2, pp. 149–166 (cit. on p. 74).

- Burke, S. N., A. P. Maurer, A. L. Hartzell, S. Nematollahi, A. Uprety, J. L. Wallace, and C. A. Barnes (Oct. 2012). "Representation of three-dimensional objects by the rat perirhinal cortex." In: *Hippocampus* 22.10, pp. 2032–44 (cit. on pp. 79, 140).
- Burke, Sara N. and Carol A. Barnes (2015). "The neural representation of 3-dimensional objects in rodent memory circuits." In: *Behavioural Brain Research* 285, pp. 60–66 (cit. on pp. 47, 69, 70, 77, 82, 84).
- Burke, Sara N., Andrew P. Maurer, Saman Nematollahi, Ajay R. Uprety, Jenelle L. Wallace, and Carol A. Barnes (July 2011). "The influence of objects on place field expression and size in distal hippocampal CA1." In: *Hippocampus* 21.7, pp. 783–801 (cit. on pp. 24, 47, 48, 54, 82, 83, 87, 134).
- Burwell, R.D. and K.L. Agster (2008). "Anatomy of the Hippocampus and the Declarative Memory System." In: *Learning and Memory: A Comprehensive Reference*. Elsevier, pp. 47–66 (cit. on p. 21).
- Burwell, Rebecca D. and David G. Amaral (1998). "Cortical afferents of the perirhinal, postrhinal, and entorhinal cortices of the rat." In: *Journal of Comparative Neurology* 398.2, pp. 179–205 (cit. on pp. 20, 79).
- Bush, Daniel, Caswell Barry, Daniel Manson, and Neil Burgess (Aug. 2015). "Using Grid Cells for Navigation." In: *Neuron* 87.3, pp. 507–520 (cit. on p. 32).
- Butler, William N and Kiah Hardcastle (2019). "Remembered reward locations restructure entorhinal spatial maps." In: 1452.March, pp. 1447–1452 (cit. on pp. 32, 57, 145).
- Buzsáki, György (Jan. 2002). "Theta Oscillations in the Hippocampus." In: *Neuron* 33.3, pp. 325–340 (cit. on p. 33).
- Buzsáki, György, Costas A Anastassiou, and Christof Koch (2012). "The origin of extracellular fields and currents—EEG, ECoG, LFP and spikes." In: *Nature reviews. Neuroscience* 13.6, pp. 407–20 (cit. on p. 33).
- Buzsáki, György, Jozsef Csicsvari, George Dragoi, Kenneth Harris, Darrell Henze, and Hajime Hirase (2002). "Homeostatic maintenance of neuronal excitability by burst discharges in vivo." In: *Cerebral cortex (New York, N.Y. : 1991)* 12.9, pp. 893–9 (cit. on p. 54).
- Buzsáki, György and Kenji Mizuseki (2014). "The log-dynamic brain: how skewed distributions affect network operations." In: *Nature Reviews Neuroscience* 15.4, pp. 264–78 (cit. on p. 41).
- Buzsáki, György and David Tingley (2018). "Space and Time: The Hippocampus as a Sequence Generator." In: *Trends in Cognitive Sciences* 22.10, pp. 853–869 (cit. on p. 145).
- Caduff, David and Sabine Timpf (Nov. 2008). "On the assessment of landmark salience for human navigation." In: *Cognitive Processing* 9.4, pp. 249–267 (cit. on pp. 73, 78, 140).
- Cai, Denise J., Daniel Aharoni, Tristan Shuman, Justin Shobe, Jeremy Biane, Weilin Song, Brandon Wei, Michael Veshkini, Mimi La-Vu, Jerry Lou, Sergio E. Flores, Isaac Kim, Yoshitake Sano, Miou Zhou, Karsten Baumgaertel, Ayal Lavi, Masakazu Kamata, Mark Tuszyński, Mark Mayford, Peyman Golshani, and Alcino J. Silva (June 2016). "A shared neural ensemble links distinct contextual memories encoded close in time." In: *Nature* 534.7605, pp. 115–118 (cit. on p. 40).
- Campbell, Malcolm G., Samuel A. Ocko, Caitlin S. Mallory, Isabel I.C. Low, Surya Ganguli, and Lisa M. Giocomo (2018). "Principles governing the integration of landmark and self-motion cues in entorhinal cortical codes for navigation." In: *Nature Neuroscience* 21.8, pp. 1096–1106 (cit. on p. 137).
- Canto, Cathrin B., Floris G. Wouterlood, and Menno P. Witter (2008). "What does the anatomical organization of the entorhinal cortex tell us?" In: *Neural Plasticity* 2008 (cit. on p. 21).
- Carr, Harvey A. (1917). "Maze studies with the white rat." In: *The journal of animal behavior*. Ed. by Madison Bentley, Edward L. Thorndike, Gilbert V. Hamilton, Margaret F. Washburn, Samuel J. Holmes, John B. Watson, Walter S. Hunter, William M. Wheeler, Harvey A. Carr, and Robert M. Yerkes. Vol. 7, pp. 259–275 (cit. on p. 3).

- Carr, Harvey and John B. Watson (Jan. 1908). "Orientation in the white rat." In: *Journal of Comparative Neurology and Psychology* 18.1, pp. 27–44 (cit. on pp. 3–5).
- Casali, Giulio, Sarah Shipley, Charlie Dowell, Robin Hayman, and Caswell Barry (Jan. 2019). "Entorhinal Neurons Exhibit Cue Locking in Rodent VR." In: *Frontiers in Cellular Neuroscience* 12.January, pp. 1–8 (cit. on pp. 137, 140, 146).
- Cei, Anne, Gabrielle Girardeau, Céline Drieu, Karim El Kanbi, and Michaël Zugaro (2014). "Reversed theta sequences of hippocampal cell assemblies during backward travel." In: *Nature neuroscience* 17.5, pp. 719–24 (cit. on p. 34).
- Chan, Edgar, Oliver Baumann, Mark A. Bellgrove, and Jason B. Mattingley (2012). "From objects to landmarks: The function of visual location information in spatial navigation." In: *Frontiers in Psychology* 3.AUG, pp. 1–11 (cit. on pp. 73, 76).
- Chapuis, Julie, Yaniv Cohen, Xiaobin He, Zhijian Zhang, Sen Jin, Fuqiang Xu, and Donald A. Wilson (2013). "Lateral entorhinal modulation of piriform cortical activity and fine odor discrimination." In: *Journal of Neuroscience* 33.33, pp. 13449–13459 (cit. on p. 21).
- Chaudhuri, Rishidev, Berk Gercek, Biraj Pandey, Adrien Peyrache, and Ila Fiete (Aug. 2019). "The intrinsic attractor manifold and population dynamics of a canonical cognitive circuit across waking and sleep." In: *Nature Neuroscience*, pp. 1–21 (cit. on pp. 30, 145).
- Chen, Guifen, John a King, Neil Burgess, and John O'Keefe (Jan. 2013). "How vision and movement combine in the hippocampal place code." In: *Proceedings of the National Academy of Sciences of the United States of America* 110.1, pp. 378–83 (cit. on pp. 45, 137).
- Chen, Guifen, John Andrew King, Yi Lu, Francesca Cacucci, and Neil Burgess (2018). "Spatial cell firing during virtual navigation of open arenas by head-restrained mice." In: *eLife* 7, pp. 1–25 (cit. on p. 137).
- Chen, Guifen, Yi Lu, John A King, Francesca Cacucci, and Neil Burgess (Feb. 2019). "Differential influences of environment and self-motion on place and grid cell firing patterns." eng. In: *Nature communication* 10.2019, pp. 11–13 (cit. on p. 137).
- Chen, Guifen, Daniel Manson, Francesca Cacucci, and Thomas Joseph Wills (2016). "Absence of Visual Input Results in the Disruption of Grid Cell Firing in the Mouse." In: *Current Biology* 26.17, pp. 2335–2342 (cit. on p. 32).
- Chen, Longtang L., Lie Huey Lin, Edward J. Green, Carol A. Barnes, and Bruce L. McNaughton (1994). "Head-direction cells in the rat posterior cortex - I. anatomical distribution and behavioral modulation." In: *Experimental Brain Research* 101.1, pp. 8–23 (cit. on p. 29).
- Chen, Longtang L., Lie-Huey Lin, Carol A. Barnes, and Bruce L. McNaughton (2004). "Head-direction cells in the rat posterior cortex." In: *Experimental Brain Research* 101.1, pp. 24–34 (cit. on p. 29).
- Cheng, Ken (July 1986). "A purely geometric module in the rat's spatial representation." In: *Cognition* 23.2, pp. 149–178 (cit. on pp. 51, 145).
- Cheng, Ken and Nora S Newcombe (2005). "Is there a geometric module for spatial orientation ? Squaring theory and evidence." In: 12.1, pp. 1–23 (cit. on p. 145).
- Chevaleyre, Vivien and Rebecca A. Piskorowski (2016). "Hippocampal Area CA2: An Overlooked but Promising Therapeutic Target." In: *Trends in molecular medicine* 22.8, pp. 645–655 (cit. on p. 18).
- Cho, Jeiwon and Patricia E. Sharp (2001). "Head direction, place, and movement correlates for cells in the rat retrosplenial cortex." In: *Behavioral Neuroscience* 115.1, pp. 3–25 (cit. on p. 29).
- Chorev, Edith, Jérôme Epsztein, Arthur R. Houweling, Albert K. Lee, and Michael Brecht (2009). "Electrophysiological recordings from behaving animals-going beyond spikes." In: *Current Opinion in Neurobiology* 19.5, pp. 513–519 (cit. on p. 40).
- Claiborne, Brenda J., David G. Amaral, and W. Maxwell Cowan (1986). "A light and electron microscopic analysis of the mossy fibers of the rat dentate gyrus." In: *Journal of Comparative Neurology* 246.4, pp. 435–458 (cit. on p. 14).
- Colgin, Laura Lee (2013). "Mechanisms and Functions of Theta Rhythms." In: *Annual Review of Neuroscience* 36.1, pp. 295–312 (cit. on pp. 33, 67).

- Collett, T S, B A Cartwright, and B A Smith (1986). "Landmark learning and visuo-spatial memories in gerbils." In: pp. 835–851 (cit. on pp. 46, 53, 71, 72).
- Collett, Thomas S., Paul Graham, Robert A. Harris, and Natalie Hempel-de-Ibarra (2006). "Navigational Memories in Ants and Bees: Memory Retrieval When Selecting and Following Routes." In: *Advances in the Study of Behavior* 36.06, pp. 123–172 (cit. on pp. 5, 71).
- Commins, Sean, John P. Aggleton, and Shane M. O'Mara (2002). "Physiological evidence for a possible projection from dorsal subiculum to hippocampal area CA1." In: *Experimental Brain Research* 146.2, pp. 155–160 (cit. on p. 19).
- Connor, Charles E. and James J. Knierim (Oct. 2017). "Integration of objects and space in perception and memory." eng. In: *Nature neuroscience* 20.11, pp. 1493–1503 (cit. on pp. 84, 140).
- Constantinescu, Alexandra O., J. X. O'Reilly, and Timothy E. J. Behrens (June 2016). "Organizing conceptual knowledge in humans with a gridlike code." In: *Science* 352.6292, pp. 1464–1468 (cit. on p. 32).
- Contreras, Marco, Tatiana Pelc, Martin Llofriu, Alfredo Weitzenfeld, and Jean-Marc Fellous (2018). "The ventral hippocampus is involved in multi-goal obstacle-rich spatial navigation." In: *Hippocampus* 28.12, pp. 853–866 (cit. on pp. 66, 146).
- Couey, Jonathan J, Aree Witoelar, Sheng-Jia Zhang, Kang Zheng, Jing Ye, Benjamin Dunn, Rafal Czajkowski, May-Britt Moser, Edvard I Moser, Yasser Roudi, and Menno P Witter (Mar. 2013). "Recurrent inhibitory circuitry as a mechanism for grid formation." In: *Nature neuroscience* 16.3, pp. 318–24 (cit. on p. 31).
- Cressant, Arnaud, Robert U. Muller, and Bruno Poucet (Apr. 1997). "Failure of centrally placed objects to control the firing fields of hippocampal place cells." In: *The Journal of neuroscience : the official journal of the Society for Neuroscience* 17.7, pp. 2531–42 (cit. on pp. 46, 51, 75, 134, 145).
- (1999). "Further study of the control of place cell firing by intra-apparatus objects." In: *Hippocampus* 9.4, pp. 423–31 (cit. on pp. 46, 75, 134, 145).
- Cui, Zhenzhong, Charles R. Gerfen, and W. Scott Young (2013). "Hypothalamic and other connections with dorsal CA2 area of the mouse hippocampus." In: *Journal of Comparative Neurology* 521.8, pp. 1844–1866 (cit. on p. 18).
- Cullen, Kathleen E. and Jeffrey S. Taube (2017). "Our sense of direction: Progress, controversies and challenges." In: *Nature Neuroscience* 20.11, pp. 1465–1473 (cit. on pp. 29, 30).
- Danielson, Nathan B., Jeffrey D. Zaremba, Patrick Kaifosh, John Bowler, Max Ladow, and Attila Losonczy (Aug. 2016). "Sublayer-Specific Coding Dynamics during Spatial Navigation and Learning in Hippocampal Area CA1." eng. In: *Neuron* 91.3, pp. 652–665 (cit. on pp. 55, 57, 62).
- Darwin, Charles (1873). "Origin of certain instincts." In: *Nature* 7.179, pp. 417–418 (cit. on pp. 5, 6).
- De Lavilleon, Gaetan, Marie Lacroix, Laure Rondi-Reig, and Karim Benchenane (2013). "Explicit memory creation during sleep: a causal role of place cell on navigation." In: *Nature Neuroscience* February, pp. 1–39 (cit. on p. 28).
- Deshmukh, Sachin S., Jeremy L. Johnson, and James J. Knierim (2012). "Perirhinal cortex represents nonspatial, but not spatial, information in rats foraging in the presence of objects: Comparison with lateral entorhinal cortex." In: *Hippocampus* 22.10, pp. 2045–2058 (cit. on pp. 79, 80).
- Deshmukh, Sachin S. and James J. Knierim (2011). "Representation of non-spatial and spatial information in the lateral entorhinal cortex." eng. In: *Frontiers in behavioral neuroscience* 5.October, p. 69 (cit. on pp. 47, 61, 80, 81, 83).
- (Apr. 2013). "Influence of local objects on hippocampal representations: Landmark vectors and memory." eng. In: *Hippocampus* 23.4, pp. 253–267 (cit. on pp. 46, 53, 81–83, 134, 135).
- Deshpande, Aditi, Matteo Bergami, Alexander Ghanem, Karl Klaus Conzelmann, Alexandra Lepier, Magdalena Götz, and Benedikt Berninger (2013). "Retrograde monosynaptic tracing reveals the temporal evolution of inputs onto new neurons in

- the adult dentate gyrus and olfactory bulb." In: *Proceedings of the National Academy of Sciences of the United States of America* 110.12 (cit. on p. 19).
- Dethier, Vincent Gaston and Eliot Stellar (1961). *Animal behavior*. Ed. by Prentice Hall. 1st editio, p. 152 (cit. on p. 1).
- Diba, K. and G. Buzsaki (2008). "Hippocampal Network Dynamics Constrain the Time Lag between Pyramidal Cells across Modified Environments." In: *Journal of Neuroscience* 28.50, pp. 13448–13456 (cit. on pp. 34, 145).
- Diehl, Geoffrey W., Olivia J. Hon, Stefan Leutgeb, and Jill K. Leutgeb (2017). "Grid and Nongrid Cells in Medial Entorhinal Cortex Represent Spatial Location and Environmental Features with Complementary Coding Schemes." In: *Neuron* 94.1, 83–92.e6 (cit. on pp. 61, 81).
- Doeller, Christian F., Caswell Barry, and Neil Burgess (Feb. 2010). "Evidence for grid cells in a human memory network." In: *Nature* 463.7281, pp. 657–61 (cit. on p. 30).
- Dolorfo, Cynthia L. and David G. Amaral (1998). "Entorhinal cortex of the rat: Topographic organization of the cells of origin of the perforant path projection to the dentate gyrus." In: *Journal of Comparative Neurology* 398.1, pp. 25–48 (cit. on p. 24).
- Dombeck, Daniel a, Christopher D Harvey, Lin Tian, Loren L Looger, and David W Tank (2010). "Functional imaging of hippocampal place cells at cellular resolution during virtual navigation." In: *Nature neuroscience* 13.11, pp. 1433–1440 (cit. on pp. 40, 50, 137).
- Domnisoru, Cristina, Amina a Kinkhabwala, and David W Tank (2013). "Membrane potential dynamics of grid cells." In: *Nature* 495.7440, pp. 199–204 (cit. on p. 137).
- Dorus, Roy M. and Wendell L. Gray (June 1932). "The rôle of kinesthesia in retention by rats." In: *Journal of Comparative Psychology* 13.3, pp. 447–451 (cit. on p. 4).
- Dragoi, George (2013). "Internal operations in the hippocampus: single cell and ensemble temporal coding." In: *Frontiers in Systems Neuroscience* 7.August, pp. 1–4 (cit. on p. 41).
- Drieu, Céline and Michaël Zugaro (2019). "Hippocampal Sequences During Exploration : Mechanisms and Functions." In: 13.June, pp. 1–22 (cit. on p. 34).
- Dudchenko, Paul A., Emma R. Wood, and Anna Smith (2019). "A new perspective on the head direction cell system and spatial behavior." In: *Neuroscience & Biobehavioral Reviews* (cit. on p. 28).
- Dudek, Serena M., Georgia M. Alexander, and Shannon Farris (2016). "Rediscovering area CA2: Unique properties and functions." In: *Nature Reviews Neuroscience* 17.2, pp. 89–102 (cit. on pp. 17, 18).
- Dunn, Benjamin, Daniel Wennberg, Ziwei Huang, and Yasser Roudi (2017). "Grid cells show field-to-field variability and this explains the aperiodic response of inhibitory interneurons." In: pp. 1–33 (cit. on p. 146).
- Dupret, David, Joseph O'Neill, Barty Pleydell-Bouverie, and Jozsef Csicsvari (Aug. 2010). "The reorganization and reactivation of hippocampal maps predict spatial memory performance." eng. In: *Nature neuroscience* 13.8, pp. 995–1002 (cit. on pp. 55, 57, 145).
- Duvelle, Éléonore, Roddy M. Grieves, Vincent Hok, Bruno Poucet, Angelo Arleo, Kate Jeffery, and Etienne Save (2019). "Insensitivity of place cells to the value of spatial goals in a two-choice flexible navigation task." In: *The Journal of Neuroscience* 39.13, pp. 1578–18 (cit. on p. 56).
- Ego-Stengel, Valérie and Matthew A. Wilson (Feb. 2007). "Spatial selectivity and theta phase precession in CA1 interneurons." In: *Hippocampus* 17.2, pp. 161–174 (cit. on p. 33).
- Eichenbaum, H, M Kuperstein, A Fagan, and J Nagode (Mar. 1987). "Cue-sampling and goal-approach correlates of hippocampal unit activity in rats performing an odor-discrimination task." In: *The Journal of neuroscience : the official journal of the Society for Neuroscience* 7.3, pp. 716–32 (cit. on p. 55).
- Eichenbaum, H, C Stewart, and R G Morris (1990). "Hippocampal representation in place learning." In: *The Journal of neuroscience : the official journal of the Society for Neuroscience* 10.11, pp. 3531–42 (cit. on p. 3).

- Eichenbaum, Howard (2017). "The role of the hippocampus in navigation is memory." In: *Journal of Neurophysiology* 117.4, pp. 1785–1796 (cit. on pp. 28, 55).
- (2018). "Barlow versus Hebb: When is it time to abandon the notion of feature detectors and adopt the cell assembly as the unit of cognition?" In: *Neuroscience Letters* 680, pp. 88–93 (cit. on pp. 25, 64).
- Ennaceur, Abdelkader and Kamel Meliani (1992). "A new one-trial test for neurobiological studies of memory in rats." In: *Behavioural Brain Research* 51.1, pp. 83–92 (cit. on p. 70).
- Epstein, Russell A. (2005). "The cortical basis of visual scene processing." In: *Visual Cognition* 12.6, pp. 954–978 (cit. on p. 81).
- (2008). "Parahippocampal and retrosplenial contributions to human spatial navigation." In: *Trends in Cognitive Sciences* 12.10, pp. 388–396 (cit. on p. 81).
- Epstein, Russell A., Eva Zita Patai, Joshua B. Julian, and Hugo J. Spiers (Oct. 2017). "The cognitive map in humans: spatial navigation and beyond." eng. In: *Nature neuroscience* 20.11, pp. 1504–1513 (cit. on p. 81).
- Epsztein, Jérôme, Michael Brecht, and Albert K. Lee (Apr. 2011). "Intracellular Determinants of Hippocampal CA1 Place and Silent Cell Activity in a Novel Environment." eng. In: *Neuron* 70.1, pp. 109–120 (cit. on pp. 40, 41).
- Etienne, A. S. (1987). "The Control of Short-Distance Homing in the Golden Hamster." In: *Cognitive Processes and Spatial Orientation in Animal and Man*. Dordrecht: Springer Netherlands, pp. 233–251 (cit. on pp. 6, 7).
- Etienne, Ariane S. and Kathryn J. Jeffery (2004). "Path integration in mammals." In: *Hippocampus* 14.2, pp. 180–192 (cit. on p. 6).
- Evans, Gary W., Catherine Smith, and Kathy Pezdek (1982). "Cognitive maps and urban form." In: *Journal of the American Planning Association* 48.2, pp. 232–244 (cit. on p. 73).
- Fattah, Mohammad, Farnaz Sharif, Tristan Geiller, and Sébastien Royer (2018). "Differential Representation of Landmark and Self-Motion Information along the CA1 Radial Axis: Self-Motion Generated Place Fields Shift toward Landmarks during Septal Inactivation." In: *The Journal of Neuroscience* 38.30, pp. 6766–6778 (cit. on pp. 46, 84, 146).
- Fenton, A. A., H.-Y. Kao, S. A. Neymotin, A. Olypher, Y. Vayntrub, W. W. Lytton, and N. Ludvig (Oct. 2008). "Unmasking the CA1 Ensemble Place Code by Exposures to Small and Large Environments: More Place Cells and Multiple, Irregularly Arranged, and Expanded Place Fields in the Larger Space." eng. In: *Journal of Neuroscience* 28.44, pp. 11250–11262 (cit. on pp. 53, 145).
- Fenton, André A, William W Lytton, Jeremy M Barry, Pierre-Pascal Lenck-Santini, Larissa E Zinyuk, Stepan Kubík, Jan Bures, Bruno Poucet, Robert U Muller, and Andrey V Olypher (Mar. 2010). "Attention-like modulation of hippocampus place cell discharge." In: *The Journal of neuroscience : the official journal of the Society for Neuroscience* 30.13, pp. 4613–25 (cit. on pp. 38, 39, 59).
- Fenton, Andre A and R U Muller (Mar. 1998). "Place cell discharge is extremely variable during individual passes of the rat through the firing field." In: *Proceedings of the National Academy of Sciences of the United States of America* 95.6, pp. 3182–7 (cit. on pp. 38, 53, 54, 59).
- Fernandez-Lamo, Ivan, Daniel Gomez-Dominguez, Alberto Sanchez-Aguilera, Azahara Oliva, Aixa Victoria Morales, Manuel Valero, Elena Cid, Antal Berenyi, and Liset Menendez de la Prida (2019). "Proximodistal Organization of the CA2 Hippocampal Area." In: *Cell Reports* 26.7, 1734–1746.e6 (cit. on p. 18).
- Fiete, I. R., Y. Burak, and T. Brookings (2008). "What Grid Cells Convey about Rat Location." In: *Journal of Neuroscience* 28.27, pp. 6858–6871 (cit. on p. 32).
- Finkelstein, Arseny, Dori Derdikman, Alon Rubin, Jakob N Foerster, Liora Las, and Nachum Ulanovsky (2015). "Three-dimensional head-direction coding in the bat brain." In: *Nature* 517.7533, pp. 159–164 (cit. on p. 28).
- Finkelstein, Arseny, Nachum Ulanovsky, Misha Tsodyks, and Johnatan Aljadeff (2018). "Optimal dynamic coding by mixed-dimensionality neurons in the head-direction system of bats." In: *Nature Communications* 9.1 (cit. on p. 66).

- Foster, T., C. Castro, and B. McNaughton (June 1989). "Spatial selectivity of rat hippocampal neurons: dependence on preparedness for movement." In: *Science* 244.4912, pp. 1580–1582 (cit. on pp. 33, 43).
- Franklin, Keith B J and George Paxinos (2013). *Paxinos and Franklin's The mouse brain in stereotaxic coordinates*. English (cit. on p. 14).
- Freund, T F and G Buzsaki (1996). "Interneurons of the Hippocampus." In: *Hippocampus* 470 (cit. on pp. 15, 19).
- Furtak, Sharon C., Shau-Ming Wei, Kara L. Agster, and Rebecca D. Burwell (2007). "Functional neuroanatomy of the parahippocampal region in the rat: The perirhinal and postrhinal cortices." In: *Hippocampus* 17.9, pp. 709–722 (cit. on pp. 12, 20, 79).
- Fyhn, Marianne, Torkel Hafting, Alessandro Treves, May-Britt Moser, and Edvard I Moser (2007). "Hippocampal remapping and grid realignment in entorhinal cortex." In: *Nature* 446.7132, pp. 190–4 (cit. on p. 31).
- Fyhn, Marianne, Torkel Hafting, Menno P Witter, Edvard I Moser, and May-Britt Moser (2008). "Grid Cells in Mice." In: *Hippocampus* 1238, pp. 1230–1238 (cit. on p. 30).
- Fyhn, Marianne, Sturla Molden, Stig Hollup, May-Britt Moser, and Edvard I Moser (Aug. 2002). "Hippocampal Neurons Responding to First-Time Dislocation of a Target Object." In: *Neuron* 35.3, pp. 555–566 (cit. on pp. 55, 57).
- Fyhn, Marianne, Sturla Molden, Menno P. Witter, Edvard I Moser, and May-Britt Moser (Aug. 2004). "Spatial representation in the entorhinal cortex." In: *Science (New York, N.Y.)* 305.5688, pp. 1258–64 (cit. on pp. 30, 81).
- Gagliardo, A. (2013). "Forty years of olfactory navigation in birds." In: *Journal of Experimental Biology* 216.12, pp. 2165–2171 (cit. on p. 50).
- Gallistel, CR (1990). *The organization of learning*. Vol. 14. 9. MIT Press (cit. on pp. 1, 6, 42).
- Gardner, Richard J., Li Lu, Tanja Wernle, May-Britt Moser, and Edvard I. Moser (Apr. 2019). "Correlation structure of grid cells is preserved during sleep." In: *Nature Neuroscience* 22.4, pp. 598–608 (cit. on p. 31).
- Gauthier, Jeffrey L. and David W. Tank (July 2018). "A Dedicated Population for Reward Coding in the Hippocampus." eng. In: *Neuron* 99.1, 179–193.e7 (cit. on pp. 55–57, 145).
- Gavrilov, V. V., S. I. Wiener, and A. Berthoz (1996). "Discharge correlates of hippocampal neurons in rats passively displaced on a mobile robot." In: *Society for Neuroscience Abstracts* 22, p. 910 (cit. on p. 43).
- Gaynor, Leslie S., Sarah A. Johnson, Jack Morgan Mizell, Keila T. Campos, Andrew P. Maurer, Russell M. Bauer, and Sara N. Burke (2018). "Impaired discrimination with intact crossmodal association in aged rats: A dissociation of perirhinal cortical-dependent behaviors." In: *Behavioral Neuroscience* 132.3, pp. 138–151 (cit. on pp. 70, 141).
- Geiller, Tristan, Mohammad Fattahi, June-Seek Seek Choi, and Sébastien Sébastien Royer (Feb. 2017a). "Place cells are more strongly tied to landmarks in deep than in superficial CA1." eng. In: *Nature Communications* 8, p. 14531 (cit. on pp. 24, 46, 53, 63, 83, 84, 87, 135).
- Geiller, Tristan, Sébastien Royer, and June-Seek Choi (2017b). "Segregated Cell Populations Enable Distinct Parallel Encoding within the Radial Axis of the CA1 Pyramidal Layer." In: 26.1, pp. 1–10 (cit. on pp. 18, 24, 62, 82).
- Geisler, Caroline, David Robbe, Michael Zugaro, Anton Sirota, Gyorgy Buzsaki, Michael Zugaro, Anton Sirota, and Gyorgy Buzsaki (May 2007). "Hippocampal place cell assemblies are speed-controlled oscillators." eng. In: *Proceedings of the National Academy of Sciences of the United States of America* 104.19, pp. 8149–8154 (cit. on pp. 34, 138).
- Georgopoulos, Apostolos P., Joseph T. Lurito, Michael Petrides, Andrew B Schwartz, and Joe T. Massey (1989). "Mental rotation of the neuronal population vector." In: *Science* 243.4888, pp. 234–236 (cit. on p. 65).

- Georgopoulos, Apostolos P, Andrew B Schwartz, and Ronald E Kettner (Sept. 1986). "Neuronal population coding of movement direction." In: *Science* 233.4771, pp. 1416–9 (cit. on pp. 65, 141).
- Gerlei, Klara, Jessica Passlack, Holly Stevens, Ioannis Papastathopoulos, and Matthew F Nolan (2019). "Grid cells implement a location-dependent directional code." In: (cit. on pp. 32, 146).
- Geva-Sagiv, Maya, Liora Las, Yossi Yovel, and Nachum Ulanovsky (Feb. 2015). "Spatial cognition in bats and rats: From sensory acquisition to multiscale maps and navigation." eng. In: *Nature Reviews Neuroscience* 16.2, pp. 94–108 (cit. on p. 5).
- Gil, Mariana, Mihai Ancau, Magdalene I. Schlesiger, Angela Neitz, Kevin Allen, Rodrigo J. De Marco, and Hannah Monyer (2018). "Impaired path integration in mice with disrupted grid cell firing." In: *Nature Neuroscience* 21.1, pp. 81–93 (cit. on pp. 6, 32).
- Giocomo, Lisa M., Tor Stensola, Tora Bonnevie, Tiffany Van Cauter, May Britt Moser, and Edvard I. Moser (2014). "Topography of head direction cells in medial entorhinal cortex." In: *Current Biology* 24.3, pp. 252–262 (cit. on p. 29).
- Girardeau, Gabrielle, Karim Benchenane, Sidney I Wiener, György Buzsáki, and Michaël B Zugaro (Oct. 2009). "Selective suppression of hippocampal ripples impairs spatial memory." In: *Nature neuroscience* 12.10, pp. 1222–3 (cit. on p. 28).
- Gire, David H., Vikrant Kapoor, Annie Arrighi-Allisan, Agnese Seminara, and Venkatesh N. Murthy (2016). "Mice develop efficient strategies for foraging and navigation using complex natural stimuli." In: *Current Biology* 26.10, pp. 1261–1273 (cit. on pp. 2, 50).
- Gonçalves, J. Tiago, Simon T. Schafer, and Fred H. Gage (2016). "Adult Neurogenesis in the Hippocampus: From Stem Cells to Behavior." In: *Cell* 167.4, pp. 897–914 (cit. on p. 14).
- Gonzalez-Sulser, Alfredo, Daniel Parthier, Antonio Candela, Christina McClure, Hugh Pastoll, Derek Garden, Gülsen Sürmeli, and Matthew F. Nolan (2014). "Gabaergic projections from the medial septum selectively inhibit interneurons in the medial entorhinal cortex." In: *Journal of Neuroscience* 34.50, pp. 16739–16743 (cit. on p. 21).
- Gothard, K M, W E Skaggs, and B L McNaughton (1996a). "Dynamics of mismatch correction in the hippocampal ensemble code for space: interaction between path integration and environmental cues." In: *The Journal of neuroscience : the official journal of the Society for Neuroscience* 16.24, pp. 8027–8040 (cit. on pp. 10, 143).
- Gothard, K. M., W. E. Skaggs, K. M. Moore, and Bruce L. McNaughton (Jan. 1996b). "Binding of hippocampal CA1 neural activity to multiple reference frames in a landmark-based navigation task." In: *The Journal of neuroscience : the official journal of the Society for Neuroscience* 16.2, pp. 823–35 (cit. on pp. 46, 53, 64, 72, 82, 83, 134).
- Green, J D and A A Arduini (Nov. 1954). "Hippocampal electrical activity in arousal." In: *Journal of neurophysiology* 17.6, pp. 533–57 (cit. on pp. 32, 33).
- Grieves, Roddy M., Éléonore Duvelle, and Paul A. Dudchenko (2018). "A boundary vector cell model of place field repetition." In: *Spatial Cognition and Computation* 18.3, pp. 217–256 (cit. on p. 53).
- Grieves, Roddy M., Emma R. Wood, and Paul A. Dudchenko (2016). "Place cells on a maze encode routes rather than destinations." In: *eLife* 5.JUNE2016, pp. 1–24 (cit. on p. 56).
- Grosmark, Andres D. and György Buzsáki (Mar. 2016). "Diversity in neural firing dynamics supports both rigid and learned hippocampal sequences." In: *Science (New York, N.Y.)* 351.6280, pp. 1440–3 (cit. on p. 41).
- Grosso, Nicholas A. Del, Justin J. Graboski, Weiwei Chen, Eduardo Blanco-Hernández, and Anton Sirota (2017). "Virtual Reality system for freely-moving rodents." In: *bioRxiv* (cit. on pp. 78, 140).
- Gu, Yi, Sam Lewallen, Amina A. Kinkhabwala, Cristina Dominisoru, Kijung Yoon, Jeffrey L. Gauthier, Ila R. Fiete, and David W. Tank (2018). "A Map-like Micro-Organization of Grid Cells in the Medial Entorhinal Cortex." In: *Cell* 175.3, 736–750.e30 (cit. on p. 31).

- Gupta, Anoopum S., Matthijs A.A. Van Der Meer, David S. Touretzky, and A. David Redish (2012). "Segmentation of spatial experience by hippocampal theta sequences." In: *Nature Neuroscience* 15.7, pp. 1032–1039 (cit. on pp. 54, 145).
- Haas, Olivia V., Josephine Henke, Christian Leibold, and Kay Thurley (2018). "Modality-specific Subpopulations of Place Fields Coexist in the Hippocampus." In: *Cerebral Cortex* May, pp. 1–12 (cit. on pp. 137, 140).
- Hafting, Torkel, Marianne Fyhn, Sturla Molden, May-Britt Moser, and Edvard I Moser (Aug. 2005). "Microstructure of a spatial map in the entorhinal cortex." In: *Nature* 436.7052, pp. 801–6 (cit. on pp. 10, 11, 30, 61, 81).
- Hägglund, Martin, Maria Mørreanet, May-britt Moser, and Edvard I Moser (2019). "Grid-Cell Distortion along Geometric Borders Report Grid-Cell Distortion along Geometric Borders." In: *Current Biology*, pp. 1–8 (cit. on pp. 32, 145).
- Hampson, R E, J D Simeral, and S a Deadwyler (1999). "Distribution of spatial and nonspatial information in dorsal hippocampus." In: *Nature* 402.6762, pp. 610–614 (cit. on p. 27).
- Hardcastle, Kiah, Surya Ganguli, and Lisa M. Giocomo (2015). "Environmental Boundaries as an Error Correction Mechanism for Grid Cells." In: *Neuron*, pp. 1–13 (cit. on pp. 7, 42, 145).
- Hargreaves, Eric L. (June 2005). "Major Dissociation Between Medial and Lateral Entorhinal Input to Dorsal Hippocampus." In: *Science* 308.5729, pp. 1792–1794 (cit. on pp. 60, 81).
- Harland, Bruce, Marcos Contreras, and Jean-Marc Fellous (July 2018). "A Role for the Longitudinal Axis of the Hippocampus in Multiscale Representations of Large and Complex Spatial Environments and Mnemonic Hierarchies." In: *The Hippocampus - Plasticity and Functions*. InTech, pp. 67–105 (cit. on p. 146).
- Harris, Kenneth D. (May 2005). "Neural signatures of cell assembly organization." In: *Nature reviews. Neuroscience* 6.5, pp. 399–407 (cit. on p. 39).
- Harris, Kenneth D., Jozsef Csicsvari, Hajime Hirase, G Dragoi, and György Buzsáki (2003). "Supplementary information - Organization of cell assemblies in the hippocampus." In: *Nature* 8.4, pp. 246–246 (cit. on pp. 39, 67).
- Harris, Robert A., Natalie Hempel de Ibarra, Paul Graham, and Thomas S. Collett (Nov. 2005). "Priming of visual route memories." In: *Nature* 438.7066, pp. 302–302 (cit. on p. 5).
- Hartley, T, N Burgess, C Lever, F Cacucci, and J O'Keefe (2000). "Modeling place fields in terms of the cortical inputs to the hippocampus." eng. In: *Hippocampus* 10.4, pp. 369–379 (cit. on pp. 52, 53, 133, 145).
- Hartline, H K (1938). "The response of single optic nerve fibers of the vertebrate eye to illumination of the retina." In: *American Journal of Physiology* 121, pp. 400–415 (cit. on p. 25).
- Harvey, Christopher D., Forrest Collman, Daniel A. Dombeck, and David W. Tank (Oct. 2009). "Intracellular dynamics of hippocampal place cells during virtual navigation." eng. In: *Nature* 461.7266, pp. 941–946 (cit. on pp. 40, 137, 140).
- Hayashi, Yuichiro (Apr. 2019). "NMDA receptor-dependent dynamics of hippocampal place cell ensembles." In: *Journal of Neuroscience*, pp. 0243–19 (cit. on p. 38).
- Hayman, R. M.A., J. G. Donnett, and K. J. Jeffery (2008). "The fuzzy-boundary arena-A method for constraining an animal's range in spatial experiments without using walls." In: *Journal of Neuroscience Methods* 167.2, pp. 184–190 (cit. on p. 51).
- Hebb, D O (July 1949). *The organization of behavior*. Tech. rep. (cit. on p. 64).
- Henriksen, Espen J., Laura L. Colgin, Carol A. Barnes, Menno P. Witter, May Britt Moser, and Edvard I. Moser (2010). "Spatial representation along the proximodistal axis of CA1." In: *Neuron* 68.1, pp. 127–137 (cit. on pp. 24, 27, 61, 87).
- Hetherington, Phil A. and Matthew L. Shapiro (Feb. 1997). "Hippocampal place fields are altered by the removal of single visual cues in a distance-dependent manner." eng. In: *Behavioral neuroscience* 111.1, pp. 20–34 (cit. on pp. 135, 136, 145).
- Hirase, H, A Czurkó, J Csicsvari, and György Buzsáki (Dec. 1999). "Firing rate and theta-phase coding by hippocampal pyramidal neurons during 'space clamping'." eng. In: *The European journal of neuroscience* 11.12, pp. 4373–80 (cit. on pp. 138, 139).

- Hjorth-Simonsen, A. and B Jeune (Feb. 1972). "Origin and termination of the hippocampal perforant path in the rat studied by silver impregnation." In: *The Journal of Comparative Neurology* 144.2, pp. 215–231 (cit. on p. 20).
- Hjorth-Simonsen, A. (1972). "Projection of the lateral part of the entorhinal area to the hippocampus and fascia dentata." In: *Journal of Comparative Neurology* 146.2, pp. 219–231 (cit. on p. 20).
- Hok, V., P.-P. Lenck-Santini, S. Roux, E. Save, R. U. Muller, and B. Poucet (Jan. 2007). "Goal-Related Activity in Hippocampal Place Cells." In: *Journal of Neuroscience* 27.3, pp. 472–482 (cit. on pp. 56, 58).
- Hok, V, E Save, and B Poucet (2005). "Coding for Spatial Goals in the Prelimbic-Infralimbic." In: *Proceedings of the National Academy of Sciences (PNAS)* 102.12, pp. 4602–4607 (cit. on p. 57).
- Hok, Vincent, Ehsan Chah, Etienne Save, and Bruno Poucet (2013). "Prefrontal cortex focally modulates hippocampal place cell firing patterns." In: *The Journal of Neuroscience* 33.8, pp. 3443–51 (cit. on pp. 56, 57).
- Hok, Vincent, Pierre-Yves Jacob, Pierrick Bordiga, Bruno Poucet, and Etienne Save (2018). "A spatial code in the dorsal lateral geniculate nucleus." In: *bioRxiv*, p. 473520 (cit. on pp. 28, 34).
- Hok, Vincent, Bruno Poucet, Éléonore Duvelle, Étienne Save, and Francesca Sargolini (2016). "Spatial cognition in mice and rats: similarities and differences in brain and behavior." In: *Wiley Interdisciplinary Reviews: Cognitive Science* 7.6, pp. 406–421 (cit. on p. 139).
- Hollup, S A, S Molden, J G Donnett, M B Moser, and E I Moser (Mar. 2001). "Accumulation of hippocampal place fields at the goal location in an annular watermaze task." eng. In: *The Journal of neuroscience : the official journal of the Society for Neuroscience* 21.5, pp. 1635–44 (cit. on pp. 55, 145).
- Holscher, C., A Schnee, H Dahmen, L Setia, and H A Mallot (Feb. 2005). "Rats are able to navigate in virtual environments." eng. In: *Journal of Experimental Biology* 208.3, pp. 561–569 (cit. on p. 136).
- Honda, Yoshiko, Hiroshi Sasaki, Yoshitomo Umitsu, and Norio Ishizuka (2012). "Zonal distribution of perforant path cells in layer III of the entorhinal area projecting to CA1 and subiculum in the rat." In: *Neuroscience Research* 74.3-4, pp. 200–209 (cit. on p. 19).
- Honzik, Charles H (1936). *The sensory Basis of maze learning in rats*. English. Baltimore (cit. on pp. 3, 5).
- Høydal, Øyvind Arne, Emilie Ranheim Skytøen, Sebastian Ola Andersson, May Britt Moser, and Edvard I. Moser (2019). "Object-vector coding in the medial entorhinal cortex." In: *Nature* 568.7752, pp. 400–404 (cit. on pp. 32, 81, 146).
- Hunter, Walter Samuel (1913). "The delayed reaction in animals and children." PhD thesis. University of Chicago (cit. on p. 7).
- Huxter, John R., Timothy J. Senior, Kevin Allen, and Jozsef Csicsvari (2008). "Theta phase-specific codes for two-dimensional position, trajectory and heading in the hippocampus." In: *Nature Neuroscience* 11.5, pp. 587–594 (cit. on p. 33).
- Huxter, John, Neil Burgess, and John O'Keefe (Oct. 2003). "Independent rate and temporal coding in hippocampal pyramidal cells." eng. In: *Nature* 425.6960, pp. 828–832 (cit. on p. 67).
- Igarashi, Kei M., Hiroshi T. Ito, Edvard I. Moser, and May Britt Moser (2014a). "Functional diversity along the transverse axis of hippocampal area CA1." In: *FEBS Letters* 588.15, pp. 2470–2476 (cit. on pp. 20, 24, 61, 62).
- Igarashi, Kei M., Li Lu, Laura L. Colgin, May Britt Moser, and Edward I. Moser (2014b). "Coordination of entorhinal-hippocampal ensemble activity during associative learning." In: *Nature* 510.7503, pp. 143–147 (cit. on p. 23).
- Insanally, Michele N, Ioana Carcea, Rachel E Field, Chris C Rodgers, Brian DePasquale, Kanaka Rajan, Michael R DeWeese, Badr F Albanna, and Robert C Froemke (Jan. 2019). "Spike-timing-dependent ensemble encoding by non-classically responsive cortical neurons." In: *eLife* 8, pp. 212–263 (cit. on p. 66).

- Ishihara, Yoshihisa and Takaichi Fukuda (2016). "Immunohistochemical investigation of the internal structure of the mouse subiculum." In: *Neuroscience* 337, pp. 242–266 (cit. on p. 19).
- Ishizuka, Norio, W. Maxwell Cowan, and David G. Amaral (1995). "A quantitative analysis of the dendritic organization of pyramidal cells in the rat hippocampus." In: *Journal of Comparative Neurology* 362.1, pp. 17–45 (cit. on pp. 16, 18, 62).
- Ismakov, Revekka, Omri Barak, Kate Jeffery, and Dori Derdikman (Aug. 2017). "Grid Cells Encode Local Positional Information." In: *Current biology : CB* 27.15, 2337–2343.e3 (cit. on pp. 32, 146).
- Jackson, Jadin and A. David Redish (2007). "Network dynamics of hippocampal cell-assemblies resemble multiple spatial maps within single tasks." In: *Hippocampus* 17.12, pp. 1209–29 (cit. on p. 39).
- Jacob, Pierre Yves, Giulio Casali, Laure Spieser, Hector Page, Dorothy Overington, and Kate Jeffery (2017). "An independent, landmark-dominated head-direction signal in dysgranular retrosplenial cortex." In: *Nature Neuroscience* 20.2, pp. 173–175 (cit. on p. 30).
- Jacob, Pierre-Yves, Fabrizio Capitano, Bruno Poucet, Etienne Save, and Francesca Sargolini (2019). "Path integration maintains spatial periodicity of grid cell firing in a 1D circular track." In: *Nature Communications* 10.2019, p. 840 (cit. on p. 32).
- Jacobs, Joshua, Christoph T. Weidemann, Jonathan F. Miller, Alec Solway, John F. Burke, Xue Xin Wei, Nanthia Suthana, Michael R. Sperling, Ashwini D. Sharan, Itzhak Fried, and Michael J. Kahana (2013). "Direct recordings of grid-like neuronal activity in human spatial navigation." In: *Nature Neuroscience* 16.9, pp. 1188–1190 (cit. on p. 30).
- Jacobs, Lucia F (2012). "From chemotaxis to the cognitive map: the function of olfaction." In: *Proceedings of the National Academy of Sciences of the United States of America* 109 Suppl, pp. 10693–700 (cit. on pp. 2, 48, 50).
- James, William (1890). *The principles of psychology, Vol I.* New York: Henry Holt and Co (cit. on pp. 59, 60).
- Jankowski, Maciej M., Johannes Passecker, Md Nurul Islam, Seralynne Vann, Jonathan T. Erichsen, John P. Aggleton, and Shane M. O'Mara (2015). "Evidence for spatially-responsive neurons in the rostral thalamus." In: *Frontiers in Behavioral Neuroscience* 9.October, pp. 1–18 (cit. on pp. 28, 52).
- Janzen, Gabriele and Miranda Van Turennout (2004). "Selective neural representation of objects relevant for navigation." In: *Nature Neuroscience* 7.6, pp. 673–677 (cit. on pp. 75, 76).
- Janzen, Gabriele and Cornelis G. Weststeijn (2007). "Neural representation of object location and route direction: An event-related fMRI study." In: *Brain Research* 1165.1, pp. 116–125 (cit. on p. 76).
- Jaramillo, Jorge and Richard Kemper (Apr. 2017). "Phase precession: a neural code underlying episodic memory?" In: *Current Opinion in Neurobiology* 43, pp. 130–138 (cit. on pp. 33, 34).
- Jayakumar, Ravikrishnan P, Manu S Madhav, Francesco Savelli, Hugh T Blair, Noah J Cowan, and James J Knierim (Feb. 2019). "Recalibration of path integration in hippocampal place cells." In: *Nature* 566.7745, pp. 533–537 (cit. on p. 42).
- Jeewajee, A, C Barry, O'Keefe John, and N Burgess (Jan. 2008). "Grid cells and theta as oscillatory interference: electrophysiological data from freely moving rats." In: *Hippocampus* 18.12, pp. 1175–85 (cit. on p. 33).
- Jeffery, Kate J., Hector J.I. Page, and Simon M. Stringer (2016). "Optimal cue combination and landmark-stability learning in the head direction system." In: *Journal of Physiology* 594.22, pp. 6527–6534 (cit. on pp. 30, 142).
- Jeffery, Kathryn J. (1998). "Learning of landmark stability and instability by hippocampal place cells." In: *Neuropharmacology* 37.4-5, pp. 677–687 (cit. on pp. 74, 84, 140).
- (2007). "Do discrimination tasks discourage multi-dimensional stimulus processing?. Evidence from a cross-modal object discrimination in rats." In: *Behavioural Brain Research* 183.2, pp. 213–221 (cit. on p. 70).

- Jeffery, Kathryn J., Rakesh L. Anand, and Michael I. Anderson (Feb. 2006). "A role for terrain slope in orienting hippocampal place fields." In: *Experimental Brain Research* 169.2, pp. 218–225 (cit. on p. 51).
- Jeffery, Kathryn J. and Michael I. Anderson (2003). "Dissociation of the geometric and contextual influences on place cells." In: *Hippocampus* 13.7, pp. 868–872 (cit. on p. 50).
- Jeffery, Kathryn J. and John M. O'Keefe (1999). "Learned interaction of visual and idiothetic cues in the control of place field orientation." In: *Experimental Brain Research* 127.2, pp. 151–161 (cit. on pp. 74, 84).
- Jensen, Ole and John E Lisman (2000). "Position Reconstruction From an Ensemble of Hippocampal Place Cells: Contribution of Theta Phase Coding." In: *Journal of Neurophysiology*, pp. 78– (cit. on p. 34).
- Jensen, Robert (2006). "Behaviorism, latent learning, and cognitive maps: Needed revisions in introductory psychology textbooks." In: *Behavior Analyst* 29.2, pp. 187–209 (cit. on p. 9).
- Jezek, Karel, Espen J. Henriksen, Alessandro Treves, Edvard I. Moser, and May-Britt Moser (2011). "Theta-paced flickering between place-cell maps in the hippocampus." In: *Nature* 478.7368, pp. 246–249 (cit. on p. 39).
- Johnson, Adam, André A Fenton, Cliff Kentros, and A. David Redish (Feb. 2009). "Looking for cognition in the structure within the noise." In: *Trends in cognitive sciences* 13.2, pp. 55–64 (cit. on pp. 38, 39).
- Jones, Gareth and Marc W. Holderied (2007). "Bat echolocation calls: Adaptation and convergent evolution." In: *Proceedings of the Royal Society B: Biological Sciences* 274.1612, pp. 905–912 (cit. on p. 5).
- Jones, Matthew W. and Thomas J. McHugh (2011). "Updating hippocampal representations: CA2 joins the circuit." In: *Trends in Neurosciences* 34.10, pp. 526–535 (cit. on p. 17).
- Jones, Matthew W. and Matthew A. Wilson (2005). "Phase precession of medial pre-frontal cortical activity relative to the hippocampal theta rhythm." In: *Hippocampus* 15.7, pp. 867–873 (cit. on p. 34).
- Jung, M W, S I Wiener, and B L McNaughton (1994). "Comparison of spatial firing characteristics of units in dorsal and ventral hippocampus of the rat." In: *The Journal of neuroscience : the official journal of the Society for Neuroscience* 14.12, pp. 7347–7356 (cit. on pp. 27, 34).
- Kanwisher, Nancy and R. Epstein (1998). "A cortical representation of the local visual environment." In: *Nature* 392.6676, pp. 598–601 (cit. on p. 81).
- Karlsson, Mattias P. and Loren M. Frank (2009). "Awake replay of remote experiences in the hippocampus." In: *Nature Neuroscience* 12.7, pp. 913–918 (cit. on p. 41).
- Kay, Kenneth, Jason E Chung, Marielena Sosa, Jonathan S Schor, Mattias P Karlsson, Margaret C Larkin, Daniel F Liu, and Loren M Frank (2019). "Regular cycling between representations of alternatives in the hippocampus." In: *bioRxiv* (cit. on p. 39).
- Keinath, Alexander T., Melissa E. Wang, Ellen G. Wann, Robin K. Yuan, Joshua T. Dudman, and Isabel A. Muzzio (2014). "Precise spatial coding is preserved along the longitudinal hippocampal axis." In: *Hippocampus* 24.12, pp. 1533–1548 (cit. on pp. 64, 66, 141).
- Keinath, Alexandra T., Russell A Epstein, and Vijay Balasubramanian (2018). "Environmental deformations dynamically shift the grid cell spatial metric." In: *eLife* 7, pp. 1–22 (cit. on pp. 7, 32).
- Kelemen, Eduard and André A. Fenton (June 2010). "Dynamic Grouping of Hippocampal Neural Activity During Cognitive Control of Two Spatial Frames." In: *PLoS Biology* 8.6. Ed. by Howard B. Eichenbaum, e1000403 (cit. on p. 39).
- Kentros, Clifford G., Naveen T. Agnihotri, Samantha Streater, Robert D. Hawkins, and Eric R. Kandel (Apr. 2004). "Increased attention to spatial context increases both place field stability and spatial memory." eng. In: *Neuron* 42.2, pp. 283–295 (cit. on pp. 58, 144).

- Kerr, Kristin M, Kara L Agster, Sharon C Furtak, and Rebecca D Burwell (2007). "Functional Neuroanatomy of the Parahippocampal Region: The Lateral and Medial Entorhinal Areas." In: *Hippocampus* (cit. on pp. 20–22).
- Kessels, Roy P C, Amy van Doormaal, and Gabriele Janzen (2011). "Landmark recognition in Alzheimer's dementia: Spared implicit memory for objects relevant for navigation." In: *PLoS ONE* 6.4, pp. 2–6 (cit. on p. 76).
- Khan, Adil Ghani, Manaswini Sarangi, and Upinder Singh Bhalla (2012). "Rats track odour trails accurately using a multi-layered strategy with near-optimal sampling." In: *Nature Communications* 3, pp. 703–710 (cit. on pp. 2, 50).
- Kim, S. M., S. Ganguli, and L. M. Frank (2012). "Spatial Information Outflow from the Hippocampal Circuit: Distributed Spatial Coding and Phase Precession in the Subiculum." In: *Journal of Neuroscience* 32.34, pp. 11539–11558 (cit. on p. 33).
- Kim, Sung Soo, Hervé Rouault, Shaul Druckmann, and Vivek Jayaraman (2017). "Ring attractor dynamics in the Drosophila central brain." In: *Science (New York, N.Y.)* 356.6340, pp. 849–853 (cit. on pp. 28, 30).
- Kinkhabwala, Amina, Yi Gu, Dmitriy Aronov, and David W Tank (2018). "Visual cue-related activity of cells in the medial entorhinal cortex during navigation in virtual reality." In: *bioRxiv*, p. 453787 (cit. on pp. 140, 146).
- Kinsky, Nathaniel R., David W. Sullivan, William Mau, Michael E. Hasselmo, and Howard B. Eichenbaum (2018). "Hippocampal Place Fields Maintain a Coherent and Flexible Map across Long Timescales." In: *Current biology : CB* 28.22, pp. 3578–3588 (cit. on p. 38).
- Kitamura, T., M. Pignatelli, J. Suh, K. Kohara, A. Yoshiki, K. Abe, and S. Tonegawa (Feb. 2014). "Island Cells Control Temporal Association Memory." In: *Science* 343.6173, pp. 896–901 (cit. on pp. 22, 23).
- Kjelstrup, Kirsten Brun, Trygve Solstad, Vegard Heimly Brun, Torkel Hafting, Stefan Leutgeb, Menno P Witter, E. I. Moser, and M.-B. Moser (July 2008). "Finite Scale of Spatial Representation in the Hippocampus." In: *Science* 321.5885, pp. 140–143 (cit. on pp. 24, 27, 63, 66, 87, 141, 146).
- Knierim, James J. and Derek A. Hamilton (Oct. 2011). "Framing spatial cognition: neural representations of proximal and distal frames of reference and their roles in navigation." eng. In: *Physiological reviews* 91.4, pp. 1245–79 (cit. on pp. 44, 46).
- Knierim, James J. and Geeta Rao (2003). "Distal landmarks and hippocampal place cells: effects of relative translation versus rotation." eng. In: *Hippocampus* 13.5, pp. 604–17 (cit. on p. 44).
- Knierim, James J, Joshua P Neunuebel, and Sachin S Deshmukh (Feb. 2014). "Functional correlates of the lateral and medial entorhinal cortex: objects, path integration and local-global reference frames." In: *Philosophical transactions of the Royal Society of London. Series B, Biological sciences* 369.1635, p. 20130369 (cit. on pp. 20, 47).
- Knierim, JJ, HS Kudrimoti, and BL McNaughton (1995). "Place cells, head direction cells, and the learning of landmark stability." In: *The Journal of Neuroscience* 15.3, pp. 1648–1659 (cit. on p. 75).
- Knight, Rebecca, Caitlin E. Piette, Hector Page, Daniel Walters, Elizabeth Marozzi, Marko Nardini, Simon Stringer, and Kathryn J. Jeffery (2014). "Weighted cue integration in the rodent head direction system." In: *Philosophical Transactions of the Royal Society B: Biological Sciences* 369.1635 (cit. on p. 30).
- Knill, David C. and Alexandre Pouget (2004). "The Bayesian brain: The role of uncertainty in neural coding and computation." In: *Trends in Neurosciences* 27.12, pp. 712–719 (cit. on p. 142).
- Kobak, Dmitry, Jose L Pardo-Vazquez, Mafalda Valente, Christian K Machens, and Alfonso Renart (Apr. 2019). "State-dependent geometry of population activity in rat auditory cortex." In: *eLife* 8, pp. 1–27 (cit. on p. 141).
- Kobayashi, T., A. H. Tran, H. Nishijo, T. Ono, and G. Matsumoto (2003). "Contribution of hippocampal place cell activity to learning and formation of goal-directed navigation in rats." In: *Neuroscience* 117.4, pp. 1025–1035 (cit. on pp. 55, 57).

- Koenig, Julie, Ashley N. Linder, Jill K. Leutgeb, and Stefan Leutgeb (2011). "The spatial periodicity of grid cells is not sustained during reduced theta oscillations." In: *Science* 332.6029, pp. 592–595 (cit. on p. 146).
- Kohara, Keigo, Michele Pignatelli, Alexander J. Rivest, Hae Yoon Jung, Takashi Kitamura, Junghyup Suh, Dominic Frank, Koichiro Kajikawa, Nathan Mise, Yuichi Obata, Ian R. Wickersham, and Susumu Tonegawa (2014). "Cell type-specific genetic and optogenetic tools reveal hippocampal CA2 circuits." In: *Nature Neuroscience* 17.2, pp. 269–279 (cit. on p. 18).
- Kornienko, Olga, Patrick Latuske, Mathis Bassler, Laura Kohler, and Kevin Allen (2018). "Non-rhythmic head-direction cells in the parahippocampal region are not constrained by attractor network dynamics." In: *eLife* 7, pp. 1–25 (cit. on p. 30).
- Kropff, Emilio, James E. Carmichael, May-Britt Moser, and Edvard I. Moser (2015). "Speed cells in the medial entorhinal cortex." In: *Nature* 523, pp. 419–424 (cit. on pp. 61, 81).
- Krupic, Julija, Marius Bauza, Stephen Burton, Caswell Barry, and John O'Keefe (2015). "Grid cell symmetry is shaped by environmental geometry." In: *Nature* 518.7538, pp. 232–235 (cit. on p. 32).
- Krupic, Julija, Marius Bauza, Stephen Burton, Colin Lever, and O'Keefe John (2014). "How environment geometry affects grid cell symmetry and what we can learn from it." In: *Philosophical transactions of the Royal Society of London. Series B, Biological sciences* 369, p. 20130188 (cit. on p. 145).
- Krupic, Julija, Marius Bauza, Stephen Burton, and John O'Keefe (2016). "Framing the grid: effect of boundaries on grid cells and navigation." In: *Journal of Physiology* 594.22, pp. 6489–6499 (cit. on p. 145).
- (2018). "Local transformations of the hippocampal cognitive map." In: *Science* 359.6380, pp. 1143–1146 (cit. on pp. 32, 145).
- Kubie, John L. and André A. Fenton (2012). "Linear Look-Ahead in Conjunctive Cells: An Entorhinal Mechanism for Vector-Based Navigation." In: *Frontiers in Neural Circuits* 6.April, pp. 1–15 (cit. on p. 32).
- Lánský, P., Andre A Fenton, and J. Vaillant (2001). "The overdispersion in activity of place cells." In: *Neurocomputing* 38-40, pp. 1393–1399 (cit. on p. 39).
- Lánský, Petr and Jean Vaillant (2000). "Stochastic model of the overdispersion in the place cell discharge." In: *Bio Systems* 58.1-3, pp. 27–32 (cit. on p. 39).
- Laptev, Dmitri and Neil Burgess (2019). "Neural dynamics indicate parallel integration of environmental and self-motion information by place and grid cells." In: *bioRxiv*, pp. 1–36 (cit. on p. 133).
- Latuske, Patrick, Olga Kornienko, Laura Kohler, and Kevin Allen (2018). "Hippocampal Remapping and Its Entorhinal Origin." In: *Frontiers in Behavioral Neuroscience* 11.January, pp. 1–13 (cit. on p. 26).
- Laughlin, Simon B and Terrence J Sejnowski (2003). "Communication in Neuronal Networks." In: 301.September, pp. 1870–1875 (cit. on p. 35).
- Laughlin, Simon B, Rob R De Ruyter Van Steveninck, and John C Anderson (1998). "The metabolic cost of neural information." In: 1.1 (cit. on p. 35).
- Lavenex, P. and F. Schenk (1995). "Influence of local environmental olfactory cues on place learning in rats." In: *Physiology and Behavior* 58.6, pp. 1059–1066 (cit. on p. 48).
- Le Duigou, Caroline, Jean Simonnet, Maria T. Teleńczuk, Desdemona Fricker, and Richard Miles (2014). "Recurrent synapses and circuits in the CA3 region of the hippocampus: An associative network." In: *Frontiers in Cellular Neuroscience* 7.JAN, pp. 1–13 (cit. on p. 16).
- Lee, Albert K., Ian D. Manns, Bert Sakmann, and Michael Brecht (Aug. 2006). "Whole-Cell Recordings in Freely Moving Rats." In: *Neuron* 51.4, pp. 399–407 (cit. on p. 40).
- Lee, Albert K., Jérôme Epsztein, and Michael Brecht (2009). "Head-anchored whole-cell recordings in freely moving rats." In: *Nature Protocols* 4.3, pp. 385–392 (cit. on p. 40).

- Lee, Albert K and Matthew A Wilson (Dec. 2002). "Memory of Sequential Experience in the Hippocampus during Slow Wave Sleep." In: *Neuron* 36.6, pp. 1183–1194 (cit. on p. 41).
- Lee, Heekyung, Cheng Wang, Sachin S. Deshmukh, and James J. Knierim (2015). "Neural Population Evidence of Functional Heterogeneity along the CA3 Transverse Axis: Pattern Completion versus Pattern Separation." In: *Neuron* 87.5, pp. 1093–1105 (cit. on p. 61).
- Lee, Jae Sung, John Briguglio, Sandro Romani, and Albert K Lee (Apr. 2019). "The statistical structure of the hippocampal code for space as a function of time, context, and value." In: *bioRxiv* (cit. on pp. 41, 55–57, 145).
- Lee, Jong Won, Woon Ryoung Kim, Woong Sun, and Min Whan Jung (Sept. 2012). "Disruption of dentate gyrus blocks effect of visual input on spatial firing of CA1 neurons." eng. In: *The Journal of neuroscience : the official journal of the Society for Neuroscience* 32.38, pp. 12999–3003 (cit. on p. 44).
- Lefort, Julie Marie, Jean Vincent, Lucille Tallot, Frédéric Jarlier, Chris Innocentius De Zeeuw, Laure Rondi-Reig, and Christelle Rochefort (2019). "Impaired cerebellar Purkinje cell potentiation generates unstable spatial map orientation and inaccurate navigation." In: *Nature Communications* 10.1, p. 2251 (cit. on pp. 134, 145).
- Lein, Edward S., Edward M. Callaway, Thomas D. Albright, and Fred H. Gage (2005). "Redefining the boundaries of the hippocampal CA2 subfield in the mouse using gene expression and 3-dimensional reconstruction." In: *Journal of Comparative Neurology* 485.1, pp. 1–10 (cit. on p. 17).
- Lenck-Santini, P. P., B. Rivard, R. U. Muller, and Bruno Poucet (2005). "Study of CA1 place cell activity and exploratory behavior following spatial and nonspatial changes in the environment." In: *Hippocampus* 15.3, pp. 356–369 (cit. on pp. 82, 134).
- Lenck-Santini, Pierre Pascal, André A. Fenton, and Robert U. Muller (2008). "Discharge properties of hippocampal neurons during performance of a jump avoidance task." In: *Journal of Neuroscience* 28.27, pp. 6773–6786 (cit. on p. 139).
- Lenck-Santini, Pierre Pascal, Etienne Save, and Bruno Poucet (2001). "Evidence for a relationship between place-cell spatial firing and spatial memory performance." In: *Hippocampus* 11.4, pp. 377–390 (cit. on p. 28).
- Lenck-Santini, Pierre-Pascal, Robert U Muller, Etienne Save, and Bruno Poucet (2002). "Relationships between place cell firing fields and navigational decisions by rats." In: *The Journal of neuroscience : the official journal of the Society for Neuroscience* 22.20, pp. 9035–47 (cit. on pp. 74, 84).
- Leonard, B and Bruce L McNaughton (1990). *Spatial representation in the rat: Conceptual, behavioral, and neurophysiological perspectives*. Hillsdale, NJ, US (cit. on pp. 9, 35).
- Leutgeb, Stefan and Jill K. Leutgeb (2007). "Pattern separation, pattern completion, and new neuronal codes within a continuous CA3 map." In: *Learning and Memory* 14.11, pp. 745–757 (cit. on p. 136).
- Leutgeb, Stefan, Jill K Leutgeb, Carol A Barnes, Edvard I Moser, Bruce L McNaughton, and May-Britt Moser (2005a). "Independent codes for spatial and episodic memory in neuronal ensembles." In: *Science* 309.July, pp. 619–623 (cit. on p. 61).
- Leutgeb, Stefan, Jill K Leutgeb, Carol a Barnes, Edvard I Moser, Bruce L McNaughton, and May-Britt Moser (July 2005b). "Independent codes for spatial and episodic memory in hippocampal neuronal ensembles." In: *Science (New York, N.Y.)* 309.5734, pp. 619–23 (cit. on p. 26).
- Lever, C, S Burton, A Jeewajee, J O'Keefe, and N Burgess (2009). "Boundary Vector Cells in the Subiculum of the Hippocampal Formation." In: *Journal of Neuroscience* 29.31, pp. 9771–9777 (cit. on pp. 52, 54, 145).
- Lew, Adina R (2011). "Looking Beyond the Boundaries : Time to Put Landmarks Back on the Cognitive Map ?" In: *Psychological Bulletin* 137.3, pp. 484–507 (cit. on p. 146).
- Li, X. -G, P. Somogyi, A. Ylinen, and G. Buzsáki (1994). "The hippocampal CA3 network: An in vivo intracellular labeling study." In: *Journal of Comparative Neurology* 339.2, pp. 181–208 (cit. on pp. 16, 17).

- Lipp, Hans-Peter, Alexei L Vyssotski, David P Wolfer, Sophie Renaudineau, Maria Savini, Gerhard Tröster, and Giacomo Dell'Osso (July 2004). "Pigeon Homing along Highways and Exits." In: *Current Biology* 14.14, pp. 1239–1249 (cit. on p. 5).
- Lisman, John E. and Ole Jensen (2013). "The Theta-Gamma Neural Code." In: *Neuron* 77.6, pp. 1002–1016 (cit. on p. 33).
- Liu, Annie, Andrew E Papale, James Hengenius, Khusbu Patel, Bard Ermentrout, and Nathaniel N Urban (2019). "Mouse navigation strategies for odor source localization." In: *bioRxiv* (cit. on pp. 2, 50).
- Lorente De Nò, R (1934). "Studies on the structure of the cerebral cortex. II. Continuation of the study of the ammonic system." In: *Journal für Psychologie und Neurologie* 46, pp. 113–177 (cit. on pp. 13, 16, 18, 62).
- Lu, Li, Kei M. Igarashi, Menno P. Witter, Edvard I. Moser, and May Britt Moser (2015). "Topography of Place Maps along the CA3-to-CA2 Axis of the Hippocampus." In: *Neuron* 87.5, pp. 1078–1092 (cit. on pp. 16, 18, 61, 62, 87, 136).
- Maboudi, Kourosh, Etienne Ackermann, Laurel Watkins de Jong, Brad E. Pfeiffer, David Foster, Kamran Diba, and Caleb Kemere (2018). "Uncovering temporal structure in hippocampal output patterns." In: *eLife* 7 (cit. on p. 67).
- Mahan, Margaret Y. and Apostolos P. Georgopoulos (2014). "Encyclopedia of computational neuroscience." In: *Encyclopedia of Computational Neuroscience* (cit. on p. 65).
- Malhotra, Sushant, Robert W.A. Cross, and Matthijs A.A. van der Meer (Jan. 2012). "Theta phase precession beyond the hippocampus." In: *Reviews in the Neurosciences* 23.1, pp. 39–65 (cit. on pp. 33, 34).
- Mallory, Caitlin S. and Lisa M. Giocomo (2018). "Heterogeneity in hippocampal place coding." In: *Current Opinion in Neurobiology* 49, pp. 158–167 (cit. on p. 62).
- Mamad, Omar, Lars Stumpf, Harold M. McNamara, Charu Ramakrishnan, Karl Deisseroth, Richard B. Reilly, and Marian Tsanov (Sept. 2017). "Place field assembly distribution encodes preferred locations." In: *PLOS Biology* 15.9. Ed. by Jozsef Csicsvari (cit. on pp. 55, 57).
- Manns, Joseph R and Howard Eichenbaum (2009). "A cognitive map for object memory in the hippocampus — Learning & Memory." In: 404, pp. 616–624 (cit. on pp. 82, 83).
- Markus, Etan J, Carol a Barnes, Bruce L McNaughton, Victoria L Gladden, and William E Skaggs (1994). "Spatial Information Content and Reliability." In: *Hippocampus* 4.4, pp. 410–421 (cit. on pp. 43, 44).
- Markus, Etan J, L McNaughton, Y L Qin, B Leonard, W E Skaggs, B L McNaughton, and C A Barnes (Nov. 1995). "Interactions between Location and Task Affect the Spatial and Directional Firing of Hippocampal Neurons." In: *The Journal of Neuroscience* 15.11, pp. 7079–94 (cit. on pp. 58, 64, 138, 143).
- Marozzi, E., L. L. Ginzberg, A. Alenda, and K. J. Jeffery (2015). "Purely Translational Realignment in Grid Cell Firing Patterns Following Nonmetric Context Change." In: *Cerebral Cortex* November, pp. 4619–4627 (cit. on p. 32).
- Marr, D (1971). "Simple memory: a theory for archicortex." In: *Philosophical transactions of the Royal Society of London. Series B, Biological sciences* 262.841, pp. 23–81 (cit. on pp. 16, 61).
- Marr, David (1982). *Vision*. The MIT Press (cit. on p. 10).
- Mathis, Alexander, Andreas V. M. Herz, and Martin Stemmler (2012). "Optimal Population Codes for Space: Grid Cells Outperform Place Cells." In: *Neural Computation* 24.9, pp. 2280–2317 (cit. on pp. 30, 32, 35, 146).
- Mathis, Alexander, Pranav Mamtanna, Kevin M. Cury, Taiga Abe, Venkatesh N. Murthy, Mackenzie Weygandt Mathis, and Matthias Bethge (2018). "DeepLabCut: markerless pose estimation of user-defined body parts with deep learning." In: *Nature Neuroscience* 21.9, pp. 1281–1289 (cit. on p. 144).
- Matsumoto, Nobuyoshi, Takuma Kitanishi, and Kenji Mizuseki (2019). "The subiculum: Unique hippocampal hub and more." In: *Neuroscience Research* 143, pp. 1–12 (cit. on p. 19).

- Maurer, Andrew P., Stephen L. Cowen, Sara N. Burke, Carol A. Barnes, and Bruce L. McNaughton (2006). "Organization of Hippocampal Cell Assemblies Based on Theta Phase Precession." In: *Hippocampus* (cit. on pp. 33, 67).
- Maurer, Andrew P., Shea R. VanRhoads, Gary R. Sutherland, Peter Lipa, and Bruce L. McNaughton (2005). "Self-motion and the origin of differential spatial scaling along the septo-temporal axis of the hippocampus." In: *Hippocampus* 15.7, pp. 841–852 (cit. on pp. 53, 63, 66).
- McKenzie, Sam and György Buzsáki (2016). "Hippocampal Mechanisms for the Segmentation of Space by Goals and Boundaries." In: *Micro-, Meso- and Macro-Dynamics of the Brain*. Ed. by György Buzsáki and Yves Christen. Cham: Springer International Publishing, pp. 1–21 (cit. on p. 145).
- McNaughton, B L, C A Barnes, J L Gerrard, K Gothard, M W Jung, J J Knierim, H Kudrimoti, Y Qin, W E Skaggs, M Suster, and K L Weaver (1996). "Deciphering the hippocampal polyglot: the hippocampus as a path integration system." In: *The Journal of experimental biology* 199.Pt 1, pp. 173–85 (cit. on pp. 9, 32, 42).
- McNaughton, B. L., C. A. Barnes, and J. O'Keefe (1983). "The contributions of position, direction, and velocity to single unit activity in the hippocampus of freely-moving rats." In: *Experimental Brain Research* 52.1, pp. 41–49 (cit. on pp. 27, 38, 143).
- McNaughton, B. L., L L Chen, and E. J. Markus (Apr. 1991). ""Dead Reckoning," Landmark Learning, and the Sense of Direction: A Neurophysiological and Computational Hypothesis." In: *Journal of Cognitive Neuroscience* 3.2, pp. 190–202 (cit. on p. 9).
- McNaughton, B.L. and R.G.M. Morris (Jan. 1987). "Hippocampal synaptic enhancement and information storage within a distributed memory system." In: *Trends in Neurosciences* 10.10, pp. 408–415 (cit. on p. 16).
- McNaughton, Bruce L, Francesco P Battaglia, Ole Jensen, Edvard I Moser, and May Britt Moser (Aug. 2006). "Path integration and the neural basis of the 'cognitive map'." eng. In: *Nature reviews. Neuroscience* 7.8, pp. 663–678 (cit. on pp. 31, 32, 42).
- Meer, M. A. A. van der and A. D. Redish (2011). "Theta Phase Precession in Rat Ventral Striatum Links Place and Reward Information." In: *Journal of Neuroscience* 31.8, pp. 2843–2854 (cit. on p. 34).
- Meer, Matthijs A.A. van der, Alyssa A. Carey, and Youki Tanaka (2017). "Optimizing for generalization in the decoding of internally generated activity in the hippocampus." In: *Hippocampus* 27.5, pp. 580–595 (cit. on p. 66).
- Mercer, Audrey, Hayley L. Trigg, and Alex M. Thomson (2007). "Characterization of neurons in the CA2 subfield of the adult rat hippocampus." In: *Journal of Neuroscience* 27.27, pp. 7329–7338 (cit. on p. 18).
- Meshulam, Leenoy, Jeffrey L. Gauthier, Carlos D. Brody, David W. Tank, and William Bialek (2017). "Collective Behavior of Place and Non-place Neurons in the Hippocampal Network." In: *Neuron* 96.5, 1178–1191.e4 (cit. on p. 67).
- Meyer, Arne F, Jasper Poort, John O'Keefe, Maneesh Sahani, and Jennifer F Linden (2018). "A miniature head-mounted camera system for freely moving mice." In: *bioRxiv*, pp. 1–37 (cit. on p. 144).
- Miao, Chenglin, Qichen Cao, May Britt Moser, and Edvard I. Moser (2017). "Parvalbumin and Somatostatin Interneurons Control Different Space-Coding Networks in the Medial Entorhinal Cortex." In: *Cell* 171.3, 507–521.e17 (cit. on p. 32).
- Middleton, Steven J. and Thomas J. McHugh (July 2016). "Silencing CA3 disrupts temporal coding in the CA1 ensemble." eng. In: *Nature neuroscience* 19.7, pp. 945–951 (cit. on p. 67).
- Miller, Jared and Laura Carlson (2011). "Selecting landmarks in novel environments." In: *Psychonomic Bulletin and Review* 18.1, pp. 184–191 (cit. on p. 73).
- Minini, Loredana and Kathryn J Jeffery (2006). "Do rats use shape to solve "shape discriminations"?" In: *Learning & memory (Cold Spring Harbor, N.Y.)* 13.3, pp. 287–97 (cit. on pp. 70, 77).
- Mittelstaedt, H. and M.-L. Mittelstaedt (1982). "Homing by Path Integration." In: *Avian Navigation*. Chap. Homing by, pp. 290–297 (cit. on p. 6).

- Mittelstaedt, M. L. and H. Mittelstaedt (1980). "Homing by path integration in a mammal." In: *Naturwissenschaften* 67.11, pp. 566–567 (cit. on pp. 6, 7).
- Mizumori, S J and J D Williams (1993). "Directionally selective mnemonic properties of neurons in the lateral dorsal nucleus of the thalamus of rats." In: *The Journal of neuroscience : the official journal of the Society for Neuroscience* 13.9, pp. 4015–28 (cit. on p. 29).
- Mizuseki, Kenji and György Buzsáki (2013). "Preconfigured, skewed distribution of firing rates in the hippocampus and entorhinal cortex." In: *Cell Reports* 4.5, pp. 1010–1021 (cit. on p. 41).
- Mizuseki, Kenji, Kamran Diba, Eva Pastalkova, and György Buzsáki (2011). "Hippocampal CA1 pyramidal cells form functionally distinct sublayers." In: *Nature Neuroscience* 14.9, pp. 1174–1183 (cit. on pp. 24, 62).
- Mizuseki, Kenji, Sébastien Royer, Kamran Diba, and György Buzsáki (2012). "Activity dynamics and behavioral correlates of CA3 and CA1 hippocampal pyramidal neurons." In: *Hippocampus* 22.8, pp. 1659–1680 (cit. on p. 136).
- Mizuseki, Kenji, Anton Sirota, Eva Pastalkova, György Buzsáki, György Buzsáki, Eva Pastalkova, Kenji Mizuseki, Anton Sirota, and György Buzsáki (Oct. 2009). "Theta oscillations provide temporal windows for local circuit computation in the entorhinal-hippocampal loop." eng. In: *Neuron* 64.2, pp. 267–280 (cit. on pp. 33, 138).
- Mlynarski, Wiktor F. and Ann M. Hermundstad (2018). "Adaptive coding for dynamic sensory inference." In: *eLife* 7, pp. 1–43 (cit. on pp. 35, 142).
- Monaco, Joseph D, Geeta Rao, Eric D Roth, and James J Knierim (2014). "Attentive scanning behavior drives one-trial potentiation of hippocampal place fields." In: *Nature neuroscience* 17.5, pp. 725–31 (cit. on p. 60).
- Morris, R. G. M., P. Garrud, J. N. P. Rawlins, and J. O'Keefe (June 1982). "Place navigation impaired in rats with hippocampal lesions." In: *Nature* 297.5868, pp. 681–683 (cit. on p. 55).
- Morris, Richard (May 1984). "Developments of a water-maze procedure for studying spatial learning in the rat Richard." In: *Journal of neuroscience methods* 11.1, pp. 47–60 (cit. on pp. 43, 55).
- Morris, Richard G.M. (May 1981). "Spatial localization does not require the presence of local cues." In: *Learning and Motivation* 12.2, pp. 239–260 (cit. on p. 43).
- Moser, Edvard I., Menno P. Witter, and May-Britt Moser (Aug. 2010). "Entorhinal Cortex." In: *Handbook of Brain Microcircuits*. Oxford University Press, pp. 175–190 (cit. on p. 22).
- Moser, Edvard I., Emilio Kropff, and May-Britt Moser (Jan. 2008). "Place cells, grid cells, and the brain's spatial representation system." In: *Annual review of neuroscience* 31, pp. 69–89 (cit. on p. 61).
- Muller, R U, E Bostock, J S Taube, and J L Kubie (Dec. 1994). "On the directional firing properties of hippocampal place cells." In: *The Journal of neuroscience : the official journal of the Society for Neuroscience* 14.12, pp. 7235–51 (cit. on pp. 26, 28).
- Muller, R U, J L Kubie, and J B Ranck (July 1987). "Spatial firing patterns of hippocampal complex-spike cells in a fixed environment." eng. In: *The Journal of neuroscience : the official journal of the Society for Neuroscience* 7.7, pp. 1935–50 (cit. on pp. 38, 145).
- Muller, Robert U and John L Kubie (July 1987). "The effects of changes in the environment on the spatial firing of hippocampal complex-spike cells." In: *The Journal of neuroscience : the official journal of the Society for Neuroscience* 7.7, pp. 1951–68 (cit. on pp. 26, 44, 51, 53, 64, 145).
- Murphy, Joseph John (1873). "Instinct: A Mechanical Analogy." In: *Nature* 7.182, p. 483 (cit. on pp. 5, 6).
- Murray, Elisabeth A., Steven P. Wise, and Kim S. Graham (2018). "Representational specializations of the hippocampus in phylogenetic perspective." In: *Neuroscience Letters* 680, pp. 4–12 (cit. on p. 11).
- Muzzio, Isabel A., Clifford Kentros, and Eric Kandel (2009a). "What is remembered? Role of attention on the encoding and retrieval of hippocampal representations." In: *Journal of Physiology* 587.12, pp. 2837–2854 (cit. on pp. 59, 144).

- Muzzio, Isabel A., Liat Levita, Jayant Kulkarni, Joseph Monaco, Clifford Kentros, Matthew Stead, Larry F. Abbott, and Eric R. Kandel (2009b). "Attention enhances the retrieval and stability of visuospatial and olfactory representations in the dorsal hippocampus." In: *PLoS Biology* 7.6 (cit. on p. 59).
- Naber, P. A., M. P. Witter, and F. H. Lopes Da Silva (1999). "Perirhinal cortex input to the hippocampus in the rat: Evidence for parallel pathways, both direct and indirect. A combined physiological and anatomical study." In: *European Journal of Neuroscience* 11.11, pp. 4119–4133 (cit. on p. 22).
- Naber, Pieterke A., Menno P. Witter, and Fernando H. Lopes Da Silva (2001). "Evidence for a direct projection from the postrhinal cortex to the subiculum in the rat." In: *Hippocampus* 11.2, pp. 105–117 (cit. on p. 61).
- Nath, Tanmay, Alexander Mathis, An Chi Chen, Amir Patel, Matthias Bethge, and Mackenzie Weygandt Mathis (2019). "Using DeepLabCut for 3D markerless pose estimation across species and behaviors." In: *Nature Protocols* 14.7, pp. 2152–2176 (cit. on p. 144).
- Nilssen, Eirik S., Thanh P. Doan, Shinya Ohara, and Menno P. Witter (2019). "A reappraisal of the lateral and medial entorhinal subdivisions mediating parallel cortical pathways." In: *Hippocampus* in press.June, pp. 1–17 (cit. on p. 22).
- Nordlund, Mathilde, Dianne Lalaina, Geoffrey Marti, Romain Bourboulou, François-Xavier Michon, Jérôme Epsztein, and Julie Koenig (2019). "Contribution of grid cells inputs to distance/position coding in CA1 place cells." In: *NeuroFrance*, P2.164 (cit. on p. 144).
- O'Keefe, J. and D. H. Conway (Apr. 1978). "Hippocampal place units in the freely moving rat: why they fire where they fire." eng. In: *Experimental brain research* 31.4, pp. 573–90 (cit. on pp. 26, 40, 63).
- O'Keefe, J and J Dostrovsky (1971). "Short Communications The hippocampus as a spatial map . Preliminary evidence from unit activity in the freely-moving rat." In: *Brain Research* 34, pp. 171–175 (cit. on pp. 10, 11, 25, 26, 28).
- O'Keefe, John (1976). "Place units in the Hippocampus of the Moving Rat." In: *Experimental Neurology* 51, pp. 78–109 (cit. on p. 83).
- (1979). "A review of the hippocampal place cells." In: *Progress in Neurobiology* 13.4, pp. 419–439 (cit. on pp. 27, 51).
- O'Keefe, John and Neil Burgess (May 1996). "Geometric determinants of the place fields of hippocampal neurons." In: *Nature* 381.6581, pp. 425–8 (cit. on pp. 51–53, 145).
- O'Keefe, John, Neil Burgess, James G. Donnett, Kathryn J. Jeffery, and Eleanor A. Maguire (1998). "Place cells, navigational accuracy, and the human hippocampus." In: *Philosophical Transactions of the Royal Society B: Biological Sciences* 353.1373, pp. 1333–1340 (cit. on p. 27).
- O'Keefe, John and Lynn Nadel (1978). *The hippocampus as a cognitive map* (cit. on pp. 1, 2, 4, 5, 9, 35, 74, 82, 83, 87).
- O'Keefe, John and Michael L Recce (July 1993). "Phase relationship between hippocampal place units and the EEG theta rhythm." eng. In: *Hippocampus* 3.3, pp. 317–330 (cit. on pp. 33, 34, 67).
- O'Mara, Shane M. (2005). "The subiculum : what it does , what it might do , and what neuroanatomy has yet to tell us." In: *Journal of Anatomy*, pp. 271–282 (cit. on p. 19).
- O'Mara, Shane M., Sean Commins, Michael Anderson, and John Gigg (2001). "The subiculum: A review of form, physiology and function." In: *Progress in Neurobiology* 64.2, pp. 129–155 (cit. on p. 19).
- Olypher, A V, P La, P Lånsky, Robert U Muller, and Andre A Fenton (2003). "Quantifying location-specific information in the discharge of rat hippocampal place cells." In: *Journal of Neuroscience Methods* 127, pp. 123–125 (cit. on pp. 135, 145).
- Olypher, Andrey V, P. Lánský, and Andre A Fenton (2002). "Properties of the extra-propositional signal in hippocampal place cell discharge derived from the overdispersion in location-specific firing." In: *Neuroscience* 111.3, pp. 553–566 (cit. on pp. 39, 59).

- Omer, David B., Shir R. Maimon, Liora Las, and Nachum Ulanovsky (2018). "Social place-cells in the bat hippocampus." In: *Science* 359.6372, pp. 218–224 (cit. on pp. 82, 84).
- Packard, Mark G. and James L. McGaugh (1996). "Inactivation of hippocampus or caudate nucleus with lidocaine differentially affects expression of place and response learning." In: *Neurobiology of Learning and Memory* 65.1, pp. 65–72 (cit. on p. 3).
- Papi, Floriano (2001). "Animal navigation at the end of the century: A retrospect and a look forward." In: *Italian Journal of Zoology* 68.3, pp. 171–180 (cit. on p. 50).
- Park, Eun Hye, Dino Dvorak, and Andre A Fenton (2011). "Ensemble place codes in hippocampus: CA1, CA3, and dentate gyrus place cells have multiple place fields in large environments." In: *PLoS ONE* 6.7, pp. 1–9 (cit. on p. 54).
- Parron, Carole and Etienne Save (Dec. 2004). "Evidence for entorhinal and parietal cortices involvement in path integration in the rat." In: *Experimental brain research* 159.3, pp. 349–59 (cit. on p. 32).
- Pastalkova, Eva, Vladimir Itskov, Asohan Amarasingham, and György Buzsáki (2008). "Internally Generated Cell Assembly Sequences in the Rat Hippocampus." In: *Science* 321.September, pp. 1322–1328 (cit. on pp. 28, 139).
- Pastoll, Hugh, Lukas Solanka, Mark C.W. van Rossum, and Matthew F. Nolan (2013). "Feedback Inhibition Enables Theta-Nested Gamma Oscillations and Grid Firing Fields." In: *Neuron* 77.1, pp. 141–154 (cit. on p. 31).
- Pearce, John M, Amanda D L Roberts, and Mark Good (1998). "Maps But Not Heading Vectors." In: *Nature* 62.1989, pp. 1997–1999 (cit. on p. 74).
- Pérez-Escobar, José Antonio, Olga Kornienko, Patrick Latuske, Laura Kohler, and Kevin Allen (2016). "Visual landmarks sharpen grid cell metric and confer context specificity to neurons of the medial entorhinal cortex." In: *eLife* 5.JULY, pp. 1–21 (cit. on pp. 32, 145, 146).
- Peyrache, Adrien, Marie M Lacroix, Peter C Petersen, and György Buzsáki (2015). "Internally organized mechanisms of the head direction sense." In: *Nature Neuroscience* October 2014 (cit. on p. 30).
- Peyrache, Adrien, Natalie Schieberstein, and Gyorgy Buzsáki (2017). "Transformation of the head-direction signal into a spatial code." In: *Nature Communications* 8.1 (cit. on p. 30).
- Pfuhl, G., H. Tjelmeland, and R. Biegler (2011). "Precision and Reliability in Animal Navigation." In: *Bulletin of Mathematical Biology* 73.5, pp. 951–977 (cit. on p. 142).
- Piaget, Jean (1952). *The origins of intelligence in children*. New York: W W Norton & Co (cit. on p. 9).
- (1955). "The Construction of Reality in the Child." In: (cit. on pp. 69, 84).
- Posani, Lorenzo, Simona Cocco, and Rémi Monasson (Aug. 2018). "Integration and multiplexing of positional and contextual information by the hippocampal network." In: *PLOS Computational Biology* 14.8. Ed. by Daniel Bush, e1006320 (cit. on p. 39).
- Poucet, B. and V. Hok (2017). "Remembering goal locations." In: *Current Opinion in Behavioral Sciences* 17.July, pp. 51–56 (cit. on pp. 55, 138).
- Poucet, B., V. Hok, F. Sargolini, and E. Save (2012). "Stability and variability of place cell activity during behavior: functional implications for dynamic coding of spatial information." In: *Journal of physiology, Paris* 106.3-4, pp. 62–71 (cit. on p. 38).
- Poucet, Bruno (1993). "Spatial cognitive maps in animals: new hypotheses on their structure and neural mechanisms." In: *Psychological Reviews* 100.2, pp. 163–182 (cit. on p. 9).
- Poucet, Bruno, Franck Chaillan, Bruno Truchet, Etienne Save, Francesca Sargolini, and Vincent Hok (2015). "Is there a pilot in the brain? Contribution of the self-positioning system to spatial navigation." eng. In: *Frontiers in behavioral neuroscience* 9.October, p. 292 (cit. on p. 38).
- Poucet, Bruno, Catherine Thinus-Blanc, and Robert U. Muller (1994). "Place cells in the ventral hippocampus of rats." In: *NeuroReport* 5.16, pp. 2045–2048 (cit. on pp. 63, 87).

- Pouget, Alexandre, Peter Dayan, and Richard Zemel (Nov. 2000). "Information processing with population codes." In: *Nature Reviews Neuroscience* 1.2, pp. 125–132 (cit. on p. 141).
- Pouget, Alexandre, Sophie Deneve, Jean Christophe Ducom, and Peter E. Latham (1999). "Narrow versus wide tuning curves: What's best for a population code?" In: *Neural Computation* 11.1, pp. 85–90 (cit. on p. 141).
- Quiroga, Rodrigo Quian and Stefano Panzeri (Mar. 2009). "Extracting information from neuronal populations: information theory and decoding approaches." In: *Nature reviews. Neuroscience* 10.3, pp. 173–85 (cit. on pp. 38, 64, 66, 141).
- Quirk, Gregory J., Robert U. Muller, and John L. Kubie (June 1990). "The firing of hippocampal place cells in the dark depends on the rat's recent experience." In: *The Journal of neuroscience : the official journal of the Society for Neuroscience* 10.6, pp. 2008–17 (cit. on p. 43).
- Radvansky, Brad A. and Daniel A. Dombeck (2018). "An olfactory virtual reality system for mice." In: *Nature Communications* 9.1, pp. 1–14 (cit. on pp. 28, 50, 137).
- Ramon y Cajal, Santiago Felipe (1909). *Histologie du système nerveux de l'homme & des vertébrés*. Translation of author's *Textura del sistema nervioso del hombre y de los vertebrados*, 1899–1904. Paris: Maloine (cit. on pp. 13, 15, 20, 25).
- (1917). *Recuerdos de mi Vida*. Vol. 2, p. 43 (cit. on p. 11).
- Ramsden, Helen L., Gülsen Sürmeli, Steven G. McDonagh, and Matthew F. Nolan (2015). "Laminar and Dorsorostral Molecular Organization of the Medial Entorhinal Cortex Revealed by Large-scale Anatomical Analysis of Gene Expression." In: *PLoS Computational Biology* 11.1, pp. 1–38 (cit. on p. 22).
- Ranck, James (1973). "Studies on single neurons in dorsal hippocampal formation and septum in unrestrained rats: Part I. Behavioral correlates and firing repertoires." In: *Experimental neurology* (cit. on pp. 11, 25, 26, 55, 67).
- Ranck, James B. (1984). "Head-direction cells in the deep cell layers of dorsal pre-subiculum in freely moving rats." In: *Soc Neurosci Abstr*, 10:176.12 (cit. on pp. 10, 28).
- (2005). "Foreword: History of the Discovery of Head Direction Cells." In: *Head Direction Cells and the Neural Mechanisms of Spatial Orientation*. Ed. by Sidney I. Wiener and Jeffrey S. Taube (cit. on p. 28).
- Raudies, Florian and Michael E. Hasselmo (2012). "Modeling boundary vector cell firing given optic flow as a cue." In: *PLoS Computational Biology* 8.6 (cit. on pp. 53, 139).
- Raudies, Florian, Ennio Mingolla, and Michael E. Hasselmo (2012). "Modeling the influence of optic flow on grid cell firing in the absence of other cues." In: *Journal of Computational Neuroscience* 33, pp. 475–493 (cit. on p. 139).
- Ravassard, Pascal, Ashley Kees, Bernard Willers, David Ho, Daniel A Aharoni, Jesse Cushman, Zahra M. Aghajan, and Mayank R. Mehta (June 2013). "Multisensory control of hippocampal spatiotemporal selectivity." eng. In: *Science (New York, N.Y.)* 340.6138, pp. 1342–1346 (cit. on pp. 44, 45, 137, 139, 143, 146).
- Ray, Saikat, Robert Naumann, Andrea Burgalossi, Qiusong Tang, Helene Schmidt, and Michael Brecht (Feb. 2014). "Grid-layout and theta-modulation of layer 2 pyramidal neurons in medial entorhinal cortex." In: *Science (New York, N.Y.)* 343.6173, pp. 891–6 (cit. on p. 22).
- Redish, A D, F P Battaglia, M K Chawla, A D Ekstrom, J L Gerrard, P Lipa, E S Rosenzweig, P F Worley, J F Guzowski, B L McNaughton, and C A Barnes (2001). "Independence of firing correlates of anatomically proximate hippocampal pyramidal cells." In: *The Journal of neuroscience : the official journal of the Society for Neuroscience* 21.5, RC134 (cit. on p. 27).
- Redish, A David (1997). "Beyond the cognitive map: Contributions to a computational neuroscience theory of rodent navigation." In: *School of Computer Science*, p. 328 (cit. on p. 3).
- (Mar. 2016). "Vicarious trial and error." In: *Nature reviews. Neuroscience* 17.3, pp. 147–59 (cit. on pp. 9, 35).

- Redish, A. D., Adam Elga, and David Touretzky (1996). "A coupled attractor model of the rodent head direction system." In: *Network: Computation in Neural Systems* 7, pp. 671–685 (cit. on p. 30).
- Reifenstein, E. T., R. Kempter, S. Schreiber, M. B. Stemmler, and a. V. M. Herz (2012). "Grid cells in rat entorhinal cortex encode physical space with independent firing fields and phase precession at the single-trial level." In: *Proceedings of the National Academy of Sciences* 109.16, pp. 6301–6306 (cit. on pp. 32, 34, 145).
- Renaudineau, Sophie, Bruno Poucet, and Etienne Save (2007). "Flexible use of proximal objects and distal cues by hippocampal place cells." In: *Hippocampus* 17.5, pp. 381–95 (cit. on pp. 46, 75, 134, 145).
- Ribak, Charles E. and Gary M. Peterson (1991). "Intragranular mossy fibers in rats and gerbils from synapses with the somata and proximal dendrites of basket cells in the dentate gyrus." In: *Hippocampus* 1.4, pp. 355–364 (cit. on p. 14).
- Rich, P. D., H.-P. Liaw, and A. K. Lee (Aug. 2014). "Large environments reveal the statistical structure governing hippocampal representations." In: *Science* 345.6198, pp. 814–817 (cit. on pp. 41, 54, 145).
- Rigotti, Mattia, Omri Barak, Melissa R. Warden, Xiao Jing Wang, Nathaniel D. Daw, Earl K. Miller, and Stefano Fusi (2013). "The importance of mixed selectivity in complex cognitive tasks." In: *Nature* 497.7451, pp. 585–590 (cit. on p. 66).
- Rivard, Bruno, Yu Li, Pierre-Pascal Lenck-Santini, Bruno Poucet, and Robert U. Muller (2004). "Representation of Objects in Space by Two Classes of Hippocampal Pyramidal Cells." In: *The Journal of General Physiology* 124.1, pp. 9–25 (cit. on p. 51).
- Robinson, Nick T.M., James B. Priestley, Jon W. Rueckemann, Aaron D. Garcia, Vittoria A. Smeglin, Francesca A. Marino, and Howard Eichenbaum (2017). "Medial Entorhinal Cortex Selectively Supports Temporal Coding by Hippocampal Neurons." In: *Neuron* 94.3, 677–688.e6 (cit. on p. 139).
- Rolls, E T, Robertson R G., and P Georges-François (1999). "Head direction cells in the primate hippocampal formation." In: *Hippocampus* 9, pp. 206–219 (cit. on p. 28).
- Rolls, Edmund T. (2007). "An attractor network in the hippocampus." In: *Learning & Memory* 14.11, pp. 714–731 (cit. on p. 16).
- Rolls, Edmund T. and Alessandro Treves (2011). "The neuronal encoding of information in the brain." In: *Progress in Neurobiology* 95.3, pp. 448–490 (cit. on p. 37).
- Rossier, Jérôme, Françoise Schenk, Yulii Kaminsky, and Jan Bures (2000). "The place preference task: A new tool for studying the relation between behavior and place cell activity in rats." In: *Behavioral Neuroscience* 114.2, pp. 273–284 (cit. on p. 58).
- Rothblat, Lawrence A. and Laura L. Hayes (1987). "Short-Term Object Recognition Memory in the Rat: Nonmatching With Trial-Unique Junk Stimuli." In: *Behavioral Neuroscience* 101.4, pp. 587–590 (cit. on p. 69).
- Rowland, David C and Clifford G. Kentros (Mar. 2008). "Plasticity, Attention, and the Stabilization of Hippocampal Representations." In: *Hippocampal Place Fields*. Oxford University Press, pp. 107–126 (cit. on p. 59).
- Royer, Sébastien, Anton Sirota, Jagdish Patel, and György Buzsáki (Feb. 2010). "Distinct representations and theta dynamics in dorsal and ventral hippocampus." In: *The Journal of neuroscience : the official journal of the Society for Neuroscience* 30.5, pp. 1777–87 (cit. on pp. 63, 64, 66, 141).
- Rubin, Alon, Nitzan Geva, Liron Sheintuch, and Yaniv Ziv (Dec. 2015). "Hippocampal ensemble dynamics timestamp events in long-term memory." In: *eLife* 4, pp. 1–16 (cit. on p. 38).
- Ruddle, Roy A., Stephen J. Payne, and Dylan M. Jones (1997). "Navigating Buildings in "Desk-Top" Virtual Environments: Experimental Investigations Using Extended Navigational Experience." In: *Journal of Experimental Psychology: Applied* 3.2, pp. 143–159 (cit. on p. 73).
- Saleem, Aman B., E. Mika Diamanti, Julien Fournier, Kenneth D. Harris, and Matteo Carandini (2018). "Coherent encoding of subjective spatial position in visual cortex and hippocampus." In: *Nature* 562.7725, pp. 124–127 (cit. on p. 28).

- Sarel, Ayelet, Arseny Finkelstein, Liora Las, and Nachum Ulanovsky (Jan. 2017). "Vectorial representation of spatial goals in the hippocampus of bats." In: *Science* 355.6321, pp. 176–180 (cit. on p. 56).
- Sargolini, Francesca, Marianne Fyhn, Torkel Hafting, Bruce L McNaughton, Menno P Witter, May-Britt Moser, and Edvard I Moser (May 2006). "Conjunctive representation of position, direction, and velocity in entorhinal cortex." In: *Science (New York, N.Y.)* 312.5774, pp. 758–62 (cit. on pp. 29–31, 61, 81).
- Sargolini, Francesca, Vincent Hok, Bruno Poucet, Etienne Save, Pierre Yves Jacob, and F. Capitano (2019). "Spatial goals locally modify the grid-like firing pattern of the grid cells." In: *NeuroFrance*, P2.104 (cit. on p. 57).
- Sato, Masaaki, Masako Kawano, Kotaro Mizuta, Tanvir Islam, Min Goo Lee, and Yasunori Hayashi (2017). "Hippocampus-Dependent Goal Localization by Head-Fixed Mice in Virtual Reality." In: *Eneuro* 4.3, ENEURO.0369–16.2017 (cit. on p. 55).
- Sato, Masaaki, Kotaro Mizuta, Tanvir Islam, Masako Kawano, Takashi Takekawa, Daniel Gomez-Dominguez, Karam Kim, Hiroshi Yamakawa, Masamichi Ohkura, Tomoki Fukai, Junichi Nakai, and Yasunori Hayashi (Jan. 2018). "Dynamic embedding of salience coding in hippocampal spatial maps." In: *bioRxiv*, p. 266767 (cit. on pp. 55, 56, 136, 145).
- Save, Etienne, Arnaud Cressant, C Thinus-Blanc, and B Poucet (1998). "Spatial firing of hippocampal place cells in blind rats." In: *The Journal of neuroscience : the official journal of the Society for Neuroscience* 18.5, pp. 1818–26 (cit. on p. 48).
- Save, Etienne and Mojdeh Moghaddam (1996). "Effects of lesions of the associative parietal cortex on the acquisition and use of spatial memory in egocentric and allocentric navigation tasks in the rat." In: *Behavioral Neuroscience* 110.1, pp. 74–85 (cit. on p. 3).
- Save, Etienne, Ludek Nerad, and Bruno Poucet (2000). "Contribution of multiple sensory information to place field stability in hippocampal place cells." In: *Hippocampus* 10.1, pp. 64–76 (cit. on pp. 48, 50).
- Savelli, Francesco and James J. Knierim (2019). "Origin and role of path integration in the cognitive representations of the hippocampus: computational insights into open questions." In: *The Journal of Experimental Biology* 222.Supp1, jeb188912 (cit. on pp. 6, 7, 10).
- Savelli, Francesco, D. Yoganarasimha, and James J. Knierim (2008). "Influence of boundary removal on the spatial representations of the medial entorhinal cortex." In: *Hippocampus* 18.12, pp. 1270–1282 (cit. on p. 52).
- Scaplen, Kristin M., Arune A. Gulati, Victoria L. Heimer-Mcginn, and Rebecca D. Burwell (2014). "Objects and landmarks: Hippocampal place cells respond differently to manipulations of visual cues depending on size, perspective, and experience." In: *Hippocampus* 24.11, pp. 1287–1299 (cit. on pp. 69, 77, 78, 140).
- Scaplen, Kristin M., Rohan N. Ramesh, Negin Nadvar, Omar J. Ahmed, and Rebecca D. Burwell (2017). "Inactivation of the Lateral Entorhinal Area Increases the Influence of Visual Cues on Hippocampal Place Cell Activity." In: *Frontiers in Systems Neuroscience* 11.May, pp. 1–13 (cit. on p. 78).
- Schaffer, Karl (1892). "Beitrag zur Histologie der Ammonshornformation." In: *Archiv für mikroskopische Anatomie* 39.1, pp. 611–632 (cit. on p. 16).
- Scharfman, Helen E. and Catherine E. Myers (2013). "Hilar mossy cells of the dentate gyrus: a historical perspective." In: *Frontiers in Neural Circuits* 6.January, pp. 1–17 (cit. on p. 15).
- Schinazi, Victor R. and Russell A. Epstein (2010). "Neural correlates of real-world route learning." In: *NeuroImage* 53.2, pp. 725–735 (cit. on p. 76).
- Schmidt-Hieber, Christoph and Michael Häusser (2013). "Cellular mechanisms of spatial navigation in the medial entorhinal cortex." In: *Nature Neuroscience* 16.3, pp. 325–331 (cit. on p. 137).
- Schmidt-Hieber, Christoph and Matthew F. Nolan (2017). "Synaptic integrative mechanisms for spatial cognition." In: *Nature Neuroscience* 20.11, pp. 1483–1492 (cit. on p. 41).

- Schmidt, R., K. Diba, C. Leibold, D. Schmitz, G. Buzsaki, and R. Kempter (Oct. 2009). "Single-Trial Phase Precession in the Hippocampus." eng. In: *Journal of Neuroscience* 29.42, pp. 13232–13241 (cit. on pp. 34, 138).
- Seelig, Johannes D. and Vivek Jayaraman (2015). "Neural dynamics for landmark orientation and angular path integration." In: *Nature* 521.7551, pp. 186–191 (cit. on pp. 28, 30).
- Shamir, Maoz and Haim Sompolinsky (2006). "Implications of neuronal diversity on population coding." In: *Neural Computation* 18.8, pp. 1951–1986 (cit. on p. 141).
- Shannon, C. E. (1948). "A Mathematical Theory of Communication." In: *The Bell System Technical Journal* Vol.27.1948, pp. 379–423 (cit. on pp. 37, 38).
- Sharp, P E and C Green (Apr. 1994). "Spatial correlates of firing patterns of single cells in the subiculum of the freely moving rat." In: *The Journal of neuroscience : the official journal of the Society for Neuroscience* 14.4, pp. 2339–56 (cit. on p. 61).
- Sharp, Patricia E. (1999). "Subicular place cells expand or contract their spatial firing pattern to fit the size of the environment in an open field but not in the presence of barriers: Comparison with hippocampal place cells." In: *Behavioral Neuroscience* 113.4, pp. 643–662 (cit. on p. 52).
- Sherrington, Charles S. (1906). *The integrative action of the nervous system*. Yale University Mrs. Hepsa Ely Silliman memorial lectures. New Haven, CT, US: Yale University Press, pp. xvi, 411–xvi, 411 (cit. on p. 25).
- Sheynikhovich, Denis, Ricardo Chavarriaga, Thomas Strosslin, Angelo Arleo, and Wulfram Gerstner (July 2009). "Is there a geometric module for spatial orientation? Insights from a rodent navigation model." eng. In: *Psychological review* 116.3, pp. 540–566 (cit. on p. 133).
- Sik, A, N. Tamamaki, and T F Freund (Dec. 1993). "Complete Axon Arborization of a Single CA3 Pyramidal Cell in the Rat Hippocampus, and its Relationship With Postsynaptic Parvalbumin-containing Interneurons." In: *European Journal of Neuroscience* 5.12, pp. 1719–1728 (cit. on p. 16).
- Simon, Benhamou (1996). "No evidence for cognitive mapping in rats." In: *Animal Behaviour* 52.September 1995, pp. 201–212 (cit. on p. 9).
- Simoncelli, Eero P (2003). "Vision and the statistics of the visual environment." In: pp. 144–149 (cit. on p. 35).
- Simoncelli, Eero P and Bruno A Olshausen (Mar. 2001). "Natural image statistics and neural representation." In: *Annual review of neuroscience* 24.1, pp. 1193–216 (cit. on p. 35).
- Skaggs, W E, J J Knierim, H S Kudrimoti, and B L McNaughton (1995). "A model of the neural basis of the rat's sense of direction." In: *Advances in neural information processing systems* 7.1984, pp. 173–80 (cit. on p. 30).
- Skaggs, William E, Bruce L McNaughton, Katalin M Gothard, and Etan J Markus (1993). "An Information-Theoretic Approach to Deciphering the Hippocampal Code." In: *Advances in neural information processing systems* 5.1990. Ed. by S J Hanson, J D Cowan, and C L Giles, pp. 1030–1037 (cit. on p. 37).
- Skaggs, William E, Bruce L McNaughton, Matthew A. Wilson, and Carol A. Barnes (Apr. 1996). "Theta phase precession in hippocampal neuronal populations and the compression of temporal sequences." eng. In: *Hippocampus* 6.2, pp. 149–172 (cit. on p. 37).
- Small, Willard S. (Jan. 1901). "Experimental Study of the Mental Processes of the Rat. II." In: *The American Journal of Psychology* 12.2, p. 206 (cit. on p. 3).
- Solstad, Trygve, Charlotte N Boccara, Emilio Kropff, May-Britt Moser, and Edvard I Moser (2008). "Representation of geometric borders in the entorhinal cortex." In: *Science* 322.December, pp. 1865–1868 (cit. on pp. 52, 61, 145).
- Soltesz, Ivan and Attila Losonczy (2018). "CA1 pyramidal cell diversity enabling parallel information processing in the hippocampus." In: *Nature Neuroscience* 21.4, pp. 484–493 (cit. on pp. 18, 24).
- Song, Eun Young, Yun Bok Kim, Young Ho Kim, and Min Whan Jung (2005). "Role of active movement in place-specific firing of hippocampal neurons." In: *Hippocampus* 15.1, pp. 8–17 (cit. on p. 43).

- Souza, Bryan C., Rodrigo Pavão, Hindiael Belchior, and Adriano B.L. L Tort (Apr. 2018). "On Information Metrics for Spatial Coding." eng. In: *Neuroscience* 375.Ii, pp. 62–73 (cit. on p. 38).
- Speakman, A. and J. O'Keefe (1990). "Hippocampal Complex Spike Cells do not Change Their Place Fields if the Goal is Moved Within a Cue Controlled Environment." In: *European Journal of Neuroscience* 2.6, pp. 544–555 (cit. on p. 57).
- Spiers, Hugo J., Robin M A Hayman, Aleksandar Jovalekic, Elizabeth Marozzi, and Kathryn J. Jeffery (Jan. 2015). "Place field repetition and purely local remapping in a multicompartment environment." eng. In: *Cerebral Cortex* 25.1, pp. 10–25 (cit. on p. 136).
- Stackman, Robert W. and Jeffrey S. Taube (Nov. 1998). "Firing Properties of Rat Lateral Mammillary Single Units: Head Direction, Head Pitch, and Angular Head Velocity." In: *The Journal of Neuroscience* 18.21, pp. 9020–9037 (cit. on p. 29).
- Stankiewicz, Brian J. and Amy A. Kalia (2007). "Acquisition of Structural Versus Object Landmark Knowledge." In: *Journal of Experimental Psychology: Human Perception and Performance* 33.2, pp. 378–390 (cit. on p. 73).
- Stella, Federico, Peter Baracskay, Joseph O Neill, and Jozsef Csicsvari (2019). "Hippocampal Reactivation of Random Trajectories Article Hippocampal Reactivation of Random Trajectories Resembling Brownian Diffusion." In: *Neuron*, pp. 1–12 (cit. on p. 145).
- Stensola, Hanne, Tor Stensola, Trygve Solstad, Kristian FrØland, May Britt Moser, and Edvard I. Moser (Dec. 2012). "The entorhinal grid map is discretized." In: *Nature* 492.7427, pp. 72–78 (cit. on pp. 30, 31).
- Stensola, Tor, Hanne Stensola, May-Britt Moser, and Edvard I. Moser (2015). "Shearing-induced asymmetry in entorhinal grid cells." In: *Nature* 518.7538, pp. 207–212 (cit. on pp. 32, 145).
- Stewart, Sarah, Ali Jeewajee, Thomas J. Wills, Neil Burgess, and Colin Lever (2014). "Boundary coding in the rat subiculum." In: *Philosophical Transactions of the Royal Society B: Biological Sciences* 369.1635 (cit. on p. 52).
- Strange, Bryan a, Menno P Witter, Ed S Lein, and Edvard I Moser (2014). "Functional organization of the hippocampal longitudinal axis." In: *Nature Publishing Group* 15.10, pp. 655–669 (cit. on pp. 21, 63, 64, 66).
- Strien, N M van, N L M Cappaert, and M P Witter (2009). "The anatomy of memory: an interactive overview of the parahippocampal–hippocampal network." In: *Nature Reviews Neuroscience* 10.4, pp. 272–282 (cit. on p. 24).
- Stringer, Carsen, Michalis Michaelos, and Marius Pachitariu (2019a). "High precision coding in mouse visual cortex." In: *bioRxiv*, p. 679324 (cit. on pp. 67, 142).
- Stringer, Carsen, Marius Pachitariu, Nicholas Steinmetz, Charu Bai Reddy, Matteo Carandini, and Kenneth D. Harris (2019b). "Spontaneous behaviors drive multidimensional, brainwide activity." In: *Science* 364.6437 (cit. on p. 144).
- Strosslin, Thomas, Denis Sheynikhovich, Ricardo Chavarriaga, and Wulfram Gerstner (Nov. 2005). "Robust self-localisation and navigation based on hippocampal place cells." eng. In: *Neural networks : the official journal of the International Neural Network Society* 18.9, pp. 1125–1140 (cit. on p. 133).
- Sun, Chen, Takashi Kitamura, Jun Yamamoto, Jared Martin, Michele Pignatelli, Lacey J. Kitch, Mark J. Schnitzer, and Susumu Tonegawa (2015). "Distinct speed dependence of entorhinal island and ocean cells, including respective grid cells." In: *Proceedings of the National Academy of Sciences*, p. 201511668 (cit. on p. 30).
- Sun, Yanjun, Amanda Q. Nguyen, Joseph P. Nguyen, Luc Le, Dieter Saur, Jiwon Choi, Edward M. Callaway, and Xiangmin Xu (2014). "Cell-type-specific circuit connectivity of hippocampal CA1 revealed through cre-dependent rabies tracing." In: *Cell Reports* 7.1, pp. 269–280 (cit. on p. 19).
- Swanson, LW and PE Sawchenko (1981). "Evidence for collateral projections by neurons in Ammon's horn, the dentate gyrus, and the subiculum: a multiple retrograde labeling study in the rat." In: *The Journal of* 1.5, pp. 548–559 (cit. on p. 16).

- Szirmai, Imre, György Buzsáki, and Anita Kamondi (2012). "120 years of hippocampal Schaffer collaterals." In: *Hippocampus* 22.7, pp. 1508–1516 (cit. on p. 16).
- Takahashi, Muneyoshi, Hiroshi Nishida, A. David Redish, and Johan Lauwereyns (2014). "Theta phase shift in spike timing and modulation of gamma oscillation: A dynamic code for spatial alternation during fixation in rat hippocampal area CA1." In: *Journal of Neurophysiology* 111.8, pp. 1601–1614 (cit. on p. 139).
- Tampuu, Ardi, Tabet Matisen, H. Freyja Ólafsdóttir, Caswell Barry, and Raul Vicente (Feb. 2019). "Efficient neural decoding of self-location with a deep recurrent network." In: *PLOS Computational Biology* 15.2. Ed. by Francesco P. Battaglia, e1006822 (cit. on p. 67).
- Tang, Qiusong, Andrea Burgalossi, Christian Laut Ebbesen, Saikat Ray, Robert Naumann, Helene Schmidt, Dominik Spicher, and Michael Brecht (2014). "Pyramidal and stellate cell specificity of grid and border representations in layer 2 of medial entorhinal cortex." In: *Neuron* 84.6, pp. 1191–1197 (cit. on p. 30).
- Taube, J S (1995). "Head direction cells recorded in the anterior thalamic nuclei of freely moving rats." In: *The Journal of neuroscience : the official journal of the Society for Neuroscience* 15, pp. 70–86 (cit. on p. 29).
- Taube, J S, R U Muller, and J B Ranck (Feb. 1990a). "Head-direction cells recorded from the postsubiculum in freely moving rats. I. Description and quantitative analysis." In: *The Journal of neuroscience : the official journal of the Society for Neuroscience* 10.2, pp. 420–35 (cit. on pp. 28, 29).
- (1990b). "Head-direction cells recorded from the postsubiculum in freely moving rats. II. Effects of environmental manipulations." In: *The Journal of neuroscience : the official journal of the Society for Neuroscience* 10.2, pp. 436–47 (cit. on p. 28).
- Taube, Jeffrey S (2007). "The head direction signal: origins and sensory-motor integration." In: *Annual review of neuroscience* 30, pp. 181–207 (cit. on pp. 29, 30).
- Terada, Satoshi, Yoshio Sakurai, Hiroyuki Nakahara, and Shigeyoshi Fujisawa (2017). "Temporal and Rate Coding for Discrete Event Sequences in the Hippocampus." In: *Neuron* 94.6, 1248–1262.e4 (cit. on p. 139).
- Terrazas, Alejandro, Michael Krause, Peter Lipa, Katalin M Gothard, Carol A Barnes, and Bruce L McNaughton (Aug. 2005). "Self-motion and the hippocampal spatial metric." eng. In: *The Journal of neuroscience : the official journal of the Society for Neuroscience* 25.35, pp. 8085–96 (cit. on pp. 42, 43).
- Thompson, L T and Phillip J Best (July 1989). "Place cells and silent cells in the hippocampus of freely-behaving rats." In: *The Journal of neuroscience : the official journal of the Society for Neuroscience* 9.7, pp. 2382–90 (cit. on p. 40).
- Thompson, L. T. and P. J. Best (1990). "Long-term stability of the place-field activity of single units recorded from the dorsal hippocampus of freely behaving rats." In: *Brain Research* 509.2, pp. 299–308 (cit. on p. 38).
- Tolman, Edward C (July 1948). "Cognitive Map in rats and men." eng. In: *Psychological review* 55.4, pp. 189–208 (cit. on pp. 1, 6–8, 11, 35, 87).
- Tomás Pereira, Inês, Kara L. Agster, and Rebecca D. Burwell (2016). "Subcortical connections of the perirhinal, postrhinal, and entorhinal cortices of the rat. I. afferents." In: *Hippocampus* 26.9, pp. 1189–1212 (cit. on pp. 20–22).
- Trettel, Sean G., John B. Trumper, Ernie Hwaun, Ila R. Fiete, and Laura Lee Colgin (Apr. 2019). "Grid cell co-activity patterns during sleep reflect spatial overlap of grid fields during active behaviors." In: *Nature Neuroscience* 22.4, pp. 609–617 (cit. on p. 31).
- Trouche, Stéphanie, Pavel V. Perestenko, Gido M. Van De Ven, Claire T. Bratley, Colin G. McNamara, Natalia Campo-Urriza, S. Lucas Black, Leon G. Reijmers, and David Dupret (2016). "Recoding a cocaine-place memory engram to a neutral engram in the hippocampus." In: *Nature Neuroscience* 19.4, pp. 564–567 (cit. on p. 28).
- Trullier, O., R. Shibata, A. B. Mulder, and S. I. Wiener (1999). "Hippocampal neuronal position selectivity remains fixed to room cues only in rats alternating between place navigation and beacon approach tasks." In: *European Journal of Neuroscience* 11.12, pp. 4381–4388 (cit. on pp. 56, 58, 138).

- Tsao, Albert, May-Britt Moser, and Edvard I. Moser (2013). "Traces of Experience in the Lateral Entorhinal Cortex." In: *Current Biology* 23.5, pp. 399–405 (cit. on pp. 81, 83).
- Tsao, Albert, Jørgen Sugar, Li Lu, Cheng Wang, James J. Knierim, May Britt Moser, and Edvard I. Moser (2018). "Integrating time from experience in the lateral entorhinal cortex." In: *Nature* 561.7721, pp. 57–62 (cit. on p. 61).
- Turi, Gergely Farkas, Wen Ke Li, Spyridon Chavlis, Ioanna Pandi, Justin O'Hare, James Benjamin Priestley, Andres Daniel Grosmark, Zhenrui Liao, Max Ladow, Jeff Fang Zhang, Boris Valery Zemelman, Panayiota Poirazi, and Attila Losonczy (2019). "Vasoactive Intestinal Polypeptide-Expressing Interneurons in the Hippocampus Support Goal-Oriented Spatial Learning." In: *Neuron* 101.6, 1150–1165.e8 (cit. on p. 57).
- Valero, Manuel and Liset Menendez de la Prida (2018). "The hippocampus in depth: a sublayer-specific perspective of entorhinal–hippocampal function." In: *Current Opinion in Neurobiology* 52, pp. 107–114 (cit. on pp. 18, 24).
- Van Cauter, Tiffany, Jeremy Camon, Alice Alvernhe, Coralie Elduayen, Francesca Sargolini, and Etienne Save (2013). "Distinct roles of medial and lateral entorhinal cortex in spatial cognition." In: *Cerebral Cortex* 23.2, pp. 451–459 (cit. on pp. 47, 61).
- Vanderwolf, C. H. (1992). "Hippocampal activity, olfaction, and sniffing: an olfactory input to the dentate gyrus." In: *Brain Research* 593.2, pp. 197–208 (cit. on p. 50).
- (2001). "The hippocampus as an olfacto-motor mechanism: Were the classical anatomists right after all?" In: *Behavioural Brain Research* 127.1-2, pp. 25–47 (cit. on p. 50).
- Vanderwolf, Cornelius H. (1969). "Hippocampal electrical activity and voluntary movement in the rat." In: *Electroencephalography and clinical neurophysiology* 26, pp. 407–418 (cit. on pp. 32, 33).
- Varga, Csaba, Soo Yeun Lee, and Ivan Soltesz (2010). "Target-selective GABAergic control of entorhinal cortex output." In: *Nature Neuroscience* 13.7, pp. 822–824 (cit. on p. 23).
- Ven, Gido M. van de, Stéphanie Trouche, Colin G. McNamara, Kevin Allen, and David Dupret (2016). "Hippocampal Offline Reactivation Consolidates Recently Formed Cell Assembly Patterns during Sharp Wave-Ripples." In: *Neuron* 92.5, pp. 968–974 (cit. on p. 41).
- Villette, Vincent, Arnaud Malvache, Thomas Tressard, Nathalie Dupuy, and Rosa Cossart (2015). "Internally Recurring Hippocampal Sequences as a Population Template of Spatiotemporal Information." In: *Neuron* 88.2, pp. 357–366 (cit. on pp. 40, 137).
- Vinck, Martin, Renata Batista-Brito, Ulf Knoblich, and Jessica A. Cardin (2015). "Arousal and Locomotion Make Distinct Contributions to Cortical Activity Patterns and Visual Encoding." In: *Neuron* 86.3, pp. 740–754 (cit. on p. 144).
- Wallace, Damian J., David S. Greenberg, Juergen Sawinski, Stefanie Rulla, Giuseppe Notaro, and Jason N.D. Kerr (2013). "Rats maintain an overhead binocular field at the expense of constant fusion." In: *Nature* 498.7452, pp. 65–69 (cit. on p. 144).
- Wallace, Douglas G., Bogdan Gorny, and Ian Q. Whishaw (2002). "Rats can track odors, other rats, and themselves: Implications for the study of spatial behavior." In: *Behavioural Brain Research* 131.1-2, pp. 185–192 (cit. on pp. 2, 50).
- Wang, Cheng, Xiaojing Chen, Heekyung Lee, Sachin S. Deshmukh, D. Yoganarasimha, Francesco Savelli, and James J. Knierim (Nov. 2018). "Egocentric coding of external items in the lateral entorhinal cortex." In: *Science* 362.6417, pp. 945–949 (cit. on p. 81).
- Watson, John B. (1907). "Kinaesthetic and organic sensations: Their role in the reactions of the white rat to the maze." In: *The Psychological Review: Monograph Supplements* 8.2, pp. i–101 (cit. on pp. 3, 4).
- Weible, A. P., D. C. Rowland, C. K. Monaghan, N. T. Wolfgang, and C. G. Kentros (2012). "Neural Correlates of Long-Term Object Memory in the Mouse Anterior Cingulate Cortex." In: *Journal of Neuroscience* 32.16, pp. 5598–5608 (cit. on pp. 81, 83).

- Wiener, Sidney I, C A Paul, and Howard Eichenbaum (Aug. 1989). "Spatial and behavioral correlates of hippocampal neuronal activity." In: *The Journal of Neuroscience* 9.8, 2737 LP –2763 (cit. on p. 135).
- Wikenheiser, Andrew M. and A. David Redish (2011). "Changes in reward contingency modulate the trial-to-trial variability of hippocampal place cells." In: *Journal of Neurophysiology* 106.2, pp. 589–598 (cit. on p. 142).
- Wilke, Stefan D. and Christian W. Eurich (2002). "Representational accuracy of stochastic neural populations." In: *Neural Computation* 14.1, pp. 155–189 (cit. on p. 142).
- Wilson, David I.G., Rosamund F. Langston, Magdalene I. Schlesiger, Monica Wagner, Sakurako Watanabe, and James A. Ainge (2013). "Lateral entorhinal cortex is critical for novel object-context recognition." In: *Hippocampus* 23.5, pp. 352–366 (cit. on p. 61).
- Wilson, M. and B. McNaughton (Aug. 1993). "Dynamics of the hippocampal ensemble code for space." eng. In: *Science* 261.5124, pp. 1055–1058 (cit. on pp. 27, 65).
- Winters, B. D. and J. M. Reid (2010). "A Distributed Cortical Representation Underlies Crossmodal Object Recognition in Rats." In: *Journal of Neuroscience* 30.18, pp. 6253–6261 (cit. on pp. 70, 141).
- Witter, M P, F G Wouterlood, P A Naber, and T Van Haeften (June 2000). "Anatomical organization of the parahippocampal-hippocampal network." In: *Annals of the New York Academy of Sciences* 911.1, pp. 1–24 (cit. on pp. 24, 61).
- Witter, Menno P. P. (2012). "Chapter 5 - Hippocampus." In: *The Mouse Nervous System*. Elsevier, pp. 112–139 (cit. on p. 13).
- Witter, Menno P. P. and David G. Amaral (2004). "Hippocampal formation." In: G.T. Paxinos (ed) *The Rat Nervous System*. Pp. 635–704 (cit. on pp. 13, 24, 61).
- Witter, Menno P., Thanh P. Doan, Bente Jacobsen, Eirik S. Nilssen, and Shinya Ohara (2017). "Architecture of the Entorhinal Cortex A Review of Entorhinal Anatomy in Rodents with Some Comparative Notes." In: *Frontiers in Systems Neuroscience* 11.June, pp. 1–12 (cit. on pp. 20, 22–24).
- Wittner, Lucia, Darrell A. Henze, László Záborszky, and György Buzsáki (2007). "Three-dimensional reconstruction of the axon arbor of a CA3 pyramidal cell recorded and filled in vivo." In: *Brain Structure and Function* 212.1, pp. 75–83 (cit. on p. 17).
- Worley, P F (1992). "Navigation by fragment fitting: a theory of hippocampal function." In: *Hippocampus* 2.2, pp. 165–187 (cit. on p. 39).
- Yartsev, Michael M, Menno P Witter, and Nachum Ulanovsky (2011). "Grid cells without theta oscillations in the entorhinal cortex of bats." In: *Nature* 479.7371, pp. 103–107 (cit. on p. 30).
- Ylinen, A, A Bragin, Z Nádasdy, G Jandó, I Szabó, A Sik, and G Buzsáki (1995). "Sharp wave-associated high-frequency oscillation (200 Hz) in the intact hippocampus: network and intracellular mechanisms." In: *The Journal of neuroscience : the official journal of the Society for Neuroscience* 15.1 Pt 1, pp. 30–46 (cit. on p. 62).
- Yoder, Ryan M., Benjamin J. Clark, and Jeffrey S. Taube (2011). "Origins of landmark encoding in the brain." In: *Trends in Neurosciences* 34.11, pp. 561–571 (cit. on pp. 30, 46).
- Yoder, Ryan M and Jeffrey S Taube (2009). "Head direction cell activity in mice: robust directional signal depends on intact otolith organs." In: *The Journal of neuroscience : the official journal of the Society for Neuroscience* 29.4, pp. 1061–76 (cit. on p. 28).
- Yoganarasimha, D., Geeta Rao, and James J. Knierim (2011). "Lateral entorhinal neurons are not spatially selective in cue-rich environments." In: *Hippocampus* 21.12, pp. 1363–1374 (cit. on pp. 61, 81).
- Yoon, Kijung, Michael a Buice, Caswell Barry, Robin Hayman, Neil Burgess, and Ilia R Fiete (Aug. 2013). "Specific evidence of low-dimensional continuous attractor dynamics in grid cells." In: *Nature Neuroscience* 16.8, pp. 1077–1084 (cit. on pp. 31, 145).
- Young, B J, G D Fox, and H Eichenbaum (1994). "Correlates of hippocampal complex-spike cell activity in rats performing a nonspatial radial maze task." In: *The*

- Journal of neuroscience : the official journal of the Society for Neuroscience* 14.November, pp. 6553–6563 (cit. on pp. 63, 66, 87, 141, 146).
- Youngstrom, Isaac A. and Ben W. Strowbridge (Feb. 2012). “Visual landmarks facilitate rodent spatial navigation in virtual reality environments.” eng. In: *Learning and Memory* 19.3, pp. 84–90 (cit. on p. 140).
- Yuste, Rafael (2015). “From the neuron doctrine to neural networks.” In: *Nature Reviews Neuroscience* 16.8, pp. 487–497 (cit. on p. 25).
- Zaremba, Jeffrey D., Anastasia Diamantopoulou, Nathan B. Danielson, Andres D. Grosmark, Patrick W. Kaifosh, John C. Bowler, Zhenrui Liao, Fraser T. Sparks, Joseph A. Gogos, and Attila Losonczy (2017). “Impaired hippocampal place cell dynamics in a mouse model of the 22q11.2 deletion.” In: *Nature Neuroscience* 20.11, pp. 1612–1623 (cit. on p. 55).
- Zhang, K (1996). “Representation of spatial orientation by the intrinsic dynamics of the head-direction cell ensemble: a theory.” In: *The Journal of neuroscience : the official journal of the Society for Neuroscience* 16.6, pp. 2112–26 (cit. on p. 30).
- Zhang, K, I Ginzburg, B L Mcnaughton, and T J Sejnowski (Feb. 1998). “Interpreting neuronal population activity by reconstruction: unified framework with application to hippocampal place cells.” eng. In: *Journal of neurophysiology* 79.2, pp. 1017–1044 (cit. on p. 66).
- Zhang, Kechen and Terrence J. Sejnowski (1999). “Neuronal tuning: To sharpen or broaden?” In: *Neural Computation* 11.1, pp. 75–84 (cit. on pp. 66, 141).
- Zhang, Sijie and Denise Manahan-Vaughan (2015). “Spatial olfactory learning contributes to place field formation in the hippocampus.” In: *Cerebral Cortex* 25.2, pp. 423–432 (cit. on pp. 49, 50).
- Zhao, Xinyu, Edward S. Lein, Aiqing He, Stanley C. Smith, Christopher Aston, and Fred H. Gage (2001). “Transcriptional profiling reveals strict boundaries between hippocampal subregions.” In: *Journal of Comparative Neurology* 441.3, pp. 187–196 (cit. on p. 17).
- Zhu, X. O. and M. W. Brown (1995). “Changes in neuronal activity related to the repetition and relative familiarity of visual stimuli in rhinal and adjacent cortex of the anaesthetised rat.” In: *Brain Research* 689.1, pp. 101–110 (cit. on p. 79).
- Zhu, X. O., M. W. Brown, and J. P. Aggleton (1995). “Neuronal Signalling of Information Important to Visual Recognition Memory in Rat Rhinal and Neighbouring Cortices.” In: *European Journal of Neuroscience* 7.4, pp. 753–765 (cit. on pp. 79, 80).
- Zinyuk, L., S. Kubik, Y. Kaminsky, A. A. Fenton, and J. Bures (2012). “Understanding hippocampal activity by using purposeful behavior: Place navigation induces place cell discharge in both task-relevant and task-irrelevant spatial reference frames.” In: *Proceedings of the National Academy of Sciences* 97.7, pp. 3771–3776 (cit. on p. 58).
- Ziv, Yaniv, Laurie D. Burns, Eric D. Cocker, Elizabeth O. Hamel, Kunal K. Ghosh, Lacey J. Kitch, Abbas El Gamal, and Mark J. Schnitzer (2013). “Long-term dynamics of CA1 hippocampal place codes.” In: *Nature Neuroscience* 16.3, pp. 264–266 (cit. on p. 38).
- Zoccolan, Davide (2015). “Invariant visual object recognition and shape processing in rats.” In: *Behavioural Brain Research* 285, pp. 10–33 (cit. on p. 84).
- Zugaro, Michaël B., Alain Berthoz, and Sidney I. Wiener (2001). “Background, But Not Foreground, Spatial Cues Are Taken as References for Head Direction Responses by Rat Anterodorsal Thalamus Neurons.” In: *The Journal of Neuroscience* 21.14, RC154–RC154 (cit. on pp. 75, 140).
- Zugaro, Michaël B, Lénaïc Monconduit, and György Buzsáki (Jan. 2005). “Spike phase precession persists after transient intrahippocampal perturbation.” In: *Nature neuroscience* 8.1, pp. 67–71 (cit. on p. 34).